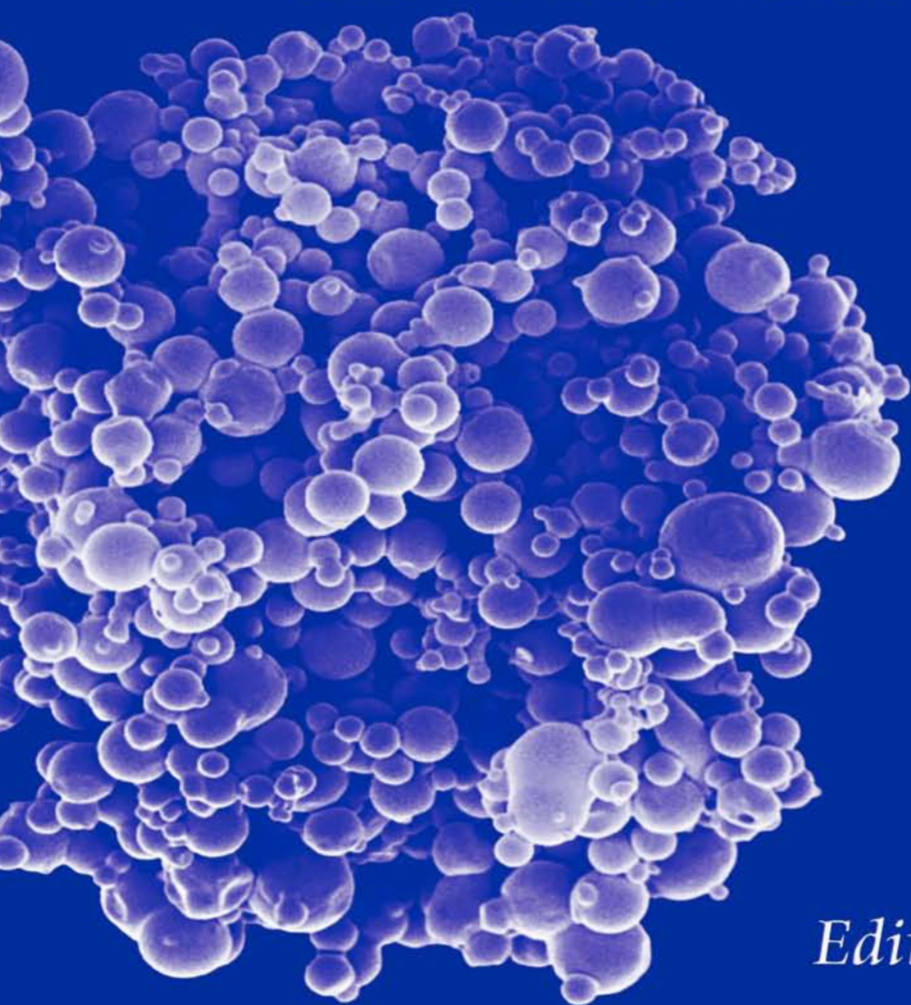# Liposome Technology

Third Edition

Volume I
Liposome Preparation
and Related Techniques

Edited by

Gregory Gregoriadis

Liposome Technology
Third Edition

Volume I
Liposome Preparation
and Related Techniques

Edited by

Gregory Gregoriadis

The School of Pharmacy
University of London
and
Lipoxen PLC
London, U.K.

informa

healthcare

Visit the Informa Web site at
www.informa.com

and the Informa Healthcare Web site at
www.informahealthcare.com

Dedicated to the memory of my parents,
Christos and Athena

Preface

The science and technology of liposomes as a delivery system for drugs and vaccines have evolved through a variety of phases that I have been privileged to witness from the very beginning. The initial observation (1) that exposure of phospholipids to excess water gives rise to lamellar structures that are able to sequester solutes led to the adoption of these structures (later to become known as liposomes) as a model for the study of cell membrane biophysics. Solute sequestration into liposomes prompted a few years later the development of the drug delivery concept (2,3) and, in 1970, animals were for the first time injected with active-containing liposomes (3,4). Subsequent work in the author's laboratory and elsewhere worldwide on drug- and vaccine-containing liposomes and their interaction with the biological milieu in vivo culminated in the licensing of a number of injectable liposome-based therapeutics and vaccines. The history of the evolution of liposomes from a structural curiosity in the 1960s to a multifaceted, powerful tool for transforming toxic or ineffective drugs into entities with improved pharmacological profiles today has been summarized elsewhere (5,6).

The great strides made toward the application of liposomes in the treatment and prevention of disease over nearly four decades are largely due to developments in liposome technology; earlier achievements were included in the previous two editions of this book (7,8). The avalanche of new techniques that came with further expansion of liposomology since

the second edition in 1992 has necessitated their inclusion into a radically updated third edition. Indeed, so great is the plethora of the new material that very little from the second edition has been retained. As before, contributors were asked to emphasize methodology employed in their own laboratories since reviews on technology with which contributors have no personal experience were likely to be superficial for the purpose of the present book. In some cases, however, overviews were invited when it was deemed useful to reconnoiter distinct areas of technology. A typical chapter incorporates an introductory section directly relevant to the author's subject with concise coverage of related literature. This is followed by a detailed methodology section describing experiences from the author's laboratory and examples of actual applications of the methods presented, and, finally, by a critical discussion of the advantages or disadvantages of the methodology presented vis-a-vis other related methodologies. The 55 chapters contributed have been distributed logically into three volumes. Volume I deals with a variety of methods for the preparation of liposomes and an array of auxiliary techniques required for liposome characterization and development. Volume II describes procedures for the incorporation into liposomes of a number of drugs selected for their relevance to current trends in liposomology. Volume III is devoted to technologies generating liposomes that can function in a "targeted" fashion and to approaches of studying the interaction of liposomes with the biological milieu.

It has again been a pleasure for me to undertake this task of bringing together so much knowledge, experience, and wisdom so generously provided by liposomologist friends and colleagues. It is to be hoped that the book will prove useful to anyone involved in drug delivery, especially those who have entered the field recently and need guidance through the vastness of related literature and the complexity and diversity of aspects of liposome use. I take this opportunity to thank Mrs. Concha Perring for her many hours of help with the manuscripts and Informa Healthcare personnel for their truly professional cooperation.

Gregory Gregoriadis

REFERENCES

1. Bangham AD, Standish MM, Watkins JC. Diffusion of univalent ions across the lamellae of swollen phospholipids. J Mol Biol 1965; 13:238.
2. Gregoriadis G, Leathwood PD, Ryman BE. Enzyme entrapment in liposomes. FEBS Lett 1971; 14:95.
3. Gregoriadis G, Ryman BB. Fate of protein-containing liposomes injected into rats. An approach to the treatment of storage diseases. Eur J Biochem 1972; 24:485.

4. Gregoriadis G. The carrier potential of liposomes in biology and medicine. New Engl J Med 1976; 295:704–765.
5. Gregoriadis G. "Twinkling guide stars to throngs of acolytes desirous of your membrane semi-barriers. Precursors of bion, potential drug carriers...". J Liposome Res 1995; 5:329.
6. Lasic DD, Papahadjopoulos D (Eds), Medical Applications of Liposomes, Elsevier. Amsterdam 1998.
7. Gregoriadis G. Liposome Technology. CRC Press, Boca Raton, Volumes I, II and III, 1984.
8. Gregoriadis G. Liposome Technology 2nd Edition. CRC Press, Boca Raton, Volumes I, II and III, 1992.

Acknowledgments

The individuals listed below in chronological order (1972–2006) worked in my laboratory as postgraduate students, senior scientists, research assistants, post-doctoral fellows, technicians, visiting scholars, and Erasmus or Sandwich students. I take this opportunity to express my gratitude for their contributions to the science and technology of liposomes and other delivery systems, as well as their support and friendship. I am most grateful to my secretary of 14 years, Concha Perring, for her hard work, perseverance, and loyalty.

Rosemary A. Buckland (UK), Diane Neerunjun (UK), Christopher D.V. Black (UK), Anthony W. Segal (UK), Gerry Dapergolas (Greece), Pamela J. Davisson (UK), Susan Scott (UK), George Deliconstantinos (Greece), Peter Bonventre (USA), Isobel Braidman (UK), Daniel Wreschner (Israel), Emanuel Manesis (Greece), Christine Davis (UK), Roger Moore (UK), Chris Kirby (UK), Jackie Clarke (UK), Pamela Large (UK), Judith Senior (UK), Ann Meehan (UK), Mon-Moy Mah (Malaysia), Catherine Lemonias (Greece), Hishani Weereratne (Sri Lanka), Jim Mixson (USA), Askin Tümer (Turkey), Barbara Wolff (Germany), Natalie Garçon (France), Volkmar Weissig (USA), David Davis (UK), Alun Davies (UK), Jay R. Behari (India), Steven Seltzer (USA), Yash Pathak (India), Lloyd Tan (Singapore), Qifu Xiao (China), Christine Panagiotidi (Greece), K.L. Kahl (New Zealand), Zhen Wang (China), Helena da Silva (Portugal), Brenda McCormack (UK), M. Yaşar Ozden (Turkey), Natasa Skalko (Croatia), John Giannios (Greece), Dmitry Genkin (Russia), Maria Georgiou (Cyprus), Sophia Antimisiaris (Greece), Becky J. Ficek (USA), Victor Kyrylenko (Ukraine), Suresh Vyas (India), Martin Brandl (Germany), Dieter Bachmann (Germany), Mayda Gursel (Turkey), Sabina Ganter (Germany), Ishan Gursel (Turkey), Maria Velinova (Bulgaria), Cecilia D'Antuono (Argentina),

Contents

Contributors

Mario Amacker   Pevion Biotech, Ltd., Bern, Switzerland

Shona Anderson   Department of Pharmaceutical Sciences, University of Strathclyde, Glasgow, Scotland, U.K.

Michel Bessodes   Unité de Pharmacologie Chimique et Génétique, Université René Descartes, Paris, France

Martin Brandl   Department of Pharmaceutics and Biopharmaceutics, Institute of Pharmacy, University of Tromsø, Breivika, Tromsø, Norway

Anthony Brownlie   Department of Pharmaceutical Sciences, University of Strathclyde, Glasgow, Scotland, U.K.

Tarquinus H. Bunch   Gilead Sciences, Inc., San Dimas, California, U.S.A.

Daan J. A. Crommelin   Department of Pharmaceutics, Utrecht Institute for Pharmaceutical Sciences, Utrecht University, Utrecht, and Octoplus, Leiden, The Netherlands

John H. Crowe   Section of Molecular and Cellular Biology, University of California, Davis, California, U.S.A.

Lois M. Crowe   Section of Molecular and Cellular Biology, University of California, Davis, California, U.S.A.

JingXia Cui   School of Pharmacy, Hebei Medical University, Shijiazhuang City, Hebei Province, P.R. China

YingJie Deng   School of Pharmacy, Shenyang Pharmaceutical University, Shenyang City, Liaoning Province, P.R. China

Crispin G. S. Eley   Gilead Sciences, Inc., San Dimas, California, U.S.A.

Abdelbary M. A. Elhissi   Department of Pharmaceutics, School of Pharmacy, University of London, London, U.K.

Patrick Garidel   Institute of Physical Chemistry, Martin Luther University Halle/Wittenberg, Halle/Saale, Germany

Marie Garinot   Unité de Pharmacologie Chimique et Génétique, Université René Descartes, Paris, France

Helmut Hauser   Lipideon Biotechnology AG, Uerikon, Switzerland

Michael J. Hope   Inex Pharmaceuticals Corporation, Burnaby, British Columbia, Canada

Ning Hu   Gilead Sciences, Inc., San Dimas, California, U.S.A.

Zhaohua Huang   Department of Biopharmaceutical Sciences, School of Pharmacy, University of California, San Francisco, California, U.S.A.

Fumiyoshi Ishii   Department of Pharmaceutical Sciences and Technology, Meiji Pharmaceutical University, Tokyo, Japan

Gerard M. Jensen   Gilead Sciences, Inc., San Dimas, California, U.S.A.

Andreas R. Krammer   Pevion Biotech, Ltd., Bern, Switzerland

Jürgen Lasch   Institute of Physical Chemistry, Martin Luther University Halle/Wittenberg, Halle/Saale, Germany

Chad Leidy   Section of Molecular and Cellular Biology, University of California, Davis, California, U.S.A.

ChunLei Li   ZhongQi Pharmaceutical Technology Co., Ltd., Shijiazhuang City, Hebei Province, P.R. China

Ulrich Massing   Clinical Research Unit, Tumor Biology Center at Albert Ludwigs University Freiburg, Freiburg, Germany

Christophe Masson   Unité de Pharmacologie Chimique et Génétique, Université René Descartes, Paris, France

Nathalie Mignet   Unité de Pharmacologie Chimique et Génétique, Université René Descartes, Paris, France

Kenichi Morigaki   Research Institute for Cell Engineering, National Institute of Advanced Industrial Science and Technology (AIST), Ikeda, Osaka, Japan

Barbara Mui   Inex Pharmaceuticals Corporation, Burnaby, British Columbia, Canada

Trishool Namani   Department of Materials, ETH, Zürich, Switzerland

Ann E. Oliver   Section of Molecular and Cellular Biology, University of California, Davis, California, U.S.A.

Regine Peschka-Süss   Pharmaceutical Technology and Biopharmacy, University of Freiburg, Freiburg, Germany

Xiaozhong Qu   Department of Pharmaceutical Sciences, University of Strathclyde, Glasgow, Scotland, U.K.

Josette Ricker   Section of Molecular and Cellular Biology, University of California, Davis, California, U.S.A.

Daniel Scherman   Unité de Pharmacologie Chimique et Génétique, Université René Descartes, Paris, France

Francis C. Szoka, Jr.   Department of Biopharmaceutical Sciences, School of Pharmacy, University of California, San Francisco, California, U.S.A.

Kevin M. G. Taylor   University College London Hospitals, Camden and Islington Pharmaceutical Services, and School of Pharmacy, University of London, London, U.K.

Nelly M. Tsvetkova   Section of Molecular and Cellular Biology, University of California, Davis, California, U.S.A.

Ijeoma Florence Uchegbu   Department of Pharmaceutical Sciences, University of Strathclyde, Glasgow, Scotland, U.K.

Peter Walde   Department of Materials, ETH, Zürich, Switzerland

Nicolaas J. Zuidam   Foods Research Centre, Unilever Research and Development, Vlaardingen, The Netherlands

Rinaldo Zurbriggen   Pevion Biotech, Ltd., Bern, Switzerland

Formation and Properties of Fatty Acid Vesicles (Liposomes)

Peter Walde and Trishool Namani

Department of Materials, ETH, Zürich, Switzerland

Kenichi Morigaki

Research Institute for Cell Engineering, National Institute of Advanced Industrial Science and Technology (AIST), Ikeda, Osaka, Japan

Helmut Hauser

Lipideon Biotechnology AG, Uerikon, Switzerland

INTRODUCTION

This chapter deals with the phase behavior of fatty acid-soap-water systems, particularly the region of the phase diagram in which fatty acid/soap vesicles are formed in excess water (>95 wt% water). In contrast to pH-insensitive diacyl phosphatidylcholine vesicles (conventional liposomes), which are thermodynamically and chemically stable over a relatively large pH range of 3 to 9, fatty acid/soap vesicles are pH sensitive. The thermodynamic stability of these vesicles is restricted to a rather narrow pH range that is close to pH 7, 8, or 9, depending on the fatty acid. The vesicles are characterized by a fatty acid to soap molar ratio close to 1. For the sake of simplicity, fatty acid/soap vesicles are just called fatty acid vesicles. On either side of the stable pH range, the lamellar fatty acid/soap phase (the fatty acid vesicles)

is in equilibrium with other phases; i.e., at the high pH boundary, the vesicles are in equilibrium with soap micelles, whereas at the low pH boundary they are in equilibrium with fatty acid oil droplets. This pH-sensitivity or instability is a property of fatty acid vesicles that is distinct from conventional phospholipid vesicles. Good use can be made of the limited pH stability of fatty acid vesicles. The release of compounds entrapped in the aqueous cavity of these vesicles can be readily triggered by small pH changes, e.g., by a small increase in pH that induces the vesicle–micelle transition.

Furthermore, routes of preparation of fatty acid vesicles, some properties of the resulting vesicles such as stability, the critical concentration of vesicle formation (CVC), the entrapment of water-soluble compounds, and possible applications of fatty acid vesicles are discussed.

The difference in properties between fatty acid vesicles and diacyl phospholipid vesicles can be rationalized in terms of different physicochemical properties of the two molecules. Although long-chain fatty acid and long-chain phospholipid molecules are both water-insoluble and have a preference of forming lamellar phases when dispersed in water at a temperature above the chain-melting transition temperature (T_m) and at the appropriate degree of deprotonation, they differ greatly in the details. While the monomer concentration of oleic acid in equilibrium with oleic acid vesicles is less than 1 mM, the monomer concentration in equilibrium with dipalmitoyl phosphatidylcholine bilayers is less than 10^{-10} M (1); in practical terms, therefore, it is negligible. Both molecules have cylindrical geometry or shape implying that the sum of the cross-sectional area of the hydrocarbon chain(s) is equal to the cross-sectional area of the polar group, and molecules fulfilling this condition are known to readily pack into lipid bilayers. However, the cross-sectional area of one fatty acid molecule in the liquid-crystalline state is about half of that of a phospholipid molecule ($0.50-0.60\,nm^2$). Hence, the tighter packing of fatty acid molecules is associated with a significantly higher surface potential relative to phospholipid bilayers. This surface potential of fatty acid/soap bilayers is responsible for the marked shift of the pK_a of 4.6 characteristic of a carboxyl group in aqueous solution to an apparent pK_a of 7 to 8.5 characteristic of a carboxyl group present at the fatty acid/soap bilayer interface. The relatively high surface potential resulting from the high packing density of fatty acid/soap molecules is also responsible for the fact that the fully ionized state of long-chain fatty acids is only obtained at a bulk pH greater than 11 (2,3), 6 to 7 pH units higher than the pK_a of a free carboxylic acid group present in aqueous solution. Assuming the distribution of ions between the bulk water phase and the lipid bilayer phase is governed by Boltzmann's law, the surface pH (pH_s) is given by the following equation: $pH_s = pH + (e\Psi_0)/(2.3\,kT)$, where e is the electronic charge, Ψ_0 the surface potential, T the absolute temperature, and k the Boltzmann constant (4). This equation predicts that a closely packed monolayer or bilayer of a negatively charged lipid with a surface potential of

$\Psi_0 = -200\,\text{mV}$ has a surface pH_s that is 3.5 pH units lower than the bulk pH and, therefore, the pK_a value will be increased accordingly. In this chapter, the difference in physicochemical properties between fatty acid and phospholipid vesicles is emphasized repeatedly. It is not a primary goal of this review to account for these differences quantitatively. However, from this introductory note it is clear that the differences observed in the properties of the two kinds of vesicles can be rationalized in terms of different hydrophobicities of single-chain fatty acids and double-chain phospholipids and in turn differences in surface-chemical properties of the two classes of lipids.

TERNARY PHASE DIAGRAMS OF SOAP, THE CORRESPONDING FATTY ACID, AND WATER

The aggregation behavior of mixtures of certain soaps, the corresponding fatty acids, and water has been studied in the past at a fixed temperature as a function of the relative amounts of soap, fatty acid, and water. The results obtained from such studies are usually represented in ternary phase diagrams, e.g., for sodium (or potassium) octanoate–octanoic acid–water at 20°C (5,6); for potassium oleate–oleic acid–water at 37°C (5); for sodium hexadecanoate–hexadecanoic acid–water at 70°C (7).

Sodium Octanoate–Octanoic Acid–Water

The most intensively investigated soap–fatty acid–water system is probably that of sodium octanoate–octanoic acid–water at 20°C. The ternary phase diagram of this three-component system (Fig. 1) defines the different phases observed over the complete compositional range of the three components. In each corner of the triangle, one of the three compounds is present in pure form (100 wt%). All samples containing a fixed amount of one of the three components lie on a line within the triangle that is parallel to one of the sides of the equilateral triangle, i.e., parallel to the side that is opposite to the corner representing that particular component. For example, all samples containing 10 wt% sodium octanoate lie on a line that is parallel to the water–octanoic acid side and that crosses the water–sodium octanoate side at 10% of its length. All samples containing 30 wt% octanoic acid are on a line that is parallel to the water–sodium octanoate side and that crosses the sodium octanoate–octanoic acid side at the 30% point. The crossing point of the two lines specified above for 10 wt% sodium octanoate, 30 wt% octanoic acid corresponds to a sample that contains 10 wt% sodium octanoate, 30 wt% octanoic acid, and 60 wt% water. All possible mixtures of sodium octanoate–octanoic acid–water have, therefore, their fixed position within the triangle.
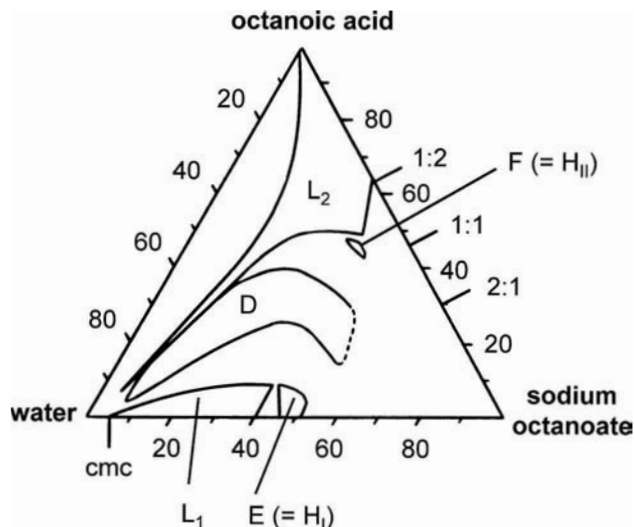
Figure 1 Ternary phase diagram of sodium octanoate–octanoic acid–wate[r]
L_1: normal micellar phase; L_2: inverted micellar phase; E ($= H_I$): normal h[exagonal]
phase; F ($= H_{II}$): inverted hexagonal phase; D: lamellar liquid crystalline p[hase; the]
ratios 1:2, 1:1, and 2:1 indicate molar ratios of sodium octanoate:octan[oic acid.]
Source: The diagram is a simplified version of Figure 1 in Ref. 6; see text fo[r details.]
Abbreviation: cmc, critical concentration for micelle formation.

In the following, some of the phases formed at thermodynami[c equili-]
brium at 20°C in the system sodium octanoate–octanoic acid–w[ater are]
briefly discussed, based on the simplified diagram shown in Figur[e 1. For]
a more detailed phase diagram and an extensive discussion, see (6)[.]

L_1 is an isotropic liquid phase containing normal micelles in [dynamic]
equilibrium with nonassociated, monomeric octanoate (or octano[ic acid]
molecules present in water. The critical concentration for micelle fo[rmation]
(CMC) is about 5 wt% (approximately 400 mM). At the border o[f this]
phase (40.5 wt% sodium octanoate corresponding at a maximum wa[ter con-]
tent to 13.6 moles water per mole sodium octanoate), there are just [enough]
water molecules to completely hydrate both the sodium ions (prob[ably two]
H_2O molecules per ion) and the carboxylate ions (probably five $H_2[O$ mole-]
cules per ion).

L_2 is another isotropic liquid phase. It contains inverted (als[o called]
reverse or reversed) micelles. The two regions E and F are liquid-cr[ystalline]
hexagonal phases. E is a normal hexagonal phase (H_I), i.e., rod-lik[e aggre-]
gates within an aqueous environment. The diameter of the rod-like ag[gregates]
ranges between 21 Å and 25 Å. F is most likely an inverted hexagon[al phase]
(H_{II}), i.e., water-rods surrounded by surfactant molecules in such a [way that]
the polar head groups point toward the water and the hydropho[bic]

toward the apolar octanoic acid environment. The thickness of the water channel is about 9.5 Å (6).

D is a lamellar liquid crystalline phase. The water content in this region of the phase diagram varies approximately between 20 wt% and 90 wt% and the mole fraction of octanoic acid—defined as (moles octanoic acid)/(moles octanoic acid + moles sodium octanoate)—is approximately between 0.3 and 0.7. In other words, the composition varies between one octanoic acid: two sodium octanoate and two octanoic acid:one sodium octanoate. At water content between 65% and 90%, the samples appear grayish-blue and flow easily (5), corresponding to a dispersion of vesicles. The octanoic acid mole fraction in this region varies approximately between 0.38 and 0.6. The bilayer thickness is approximately 20 Å and the mean area per polar head group is approximately 27 Å^2. There is a substantial amount of sodium octanoate (and octanoic acid) in the aqueous regions between the bilayers. Octanoic acid/octanoate bilayer formation is understood on simple electrostatic and geometric considerations: the octanoic acid molecules that are localized between the octanoate molecules lead to an elimination of the electrostatic repulsions between the charged octanoate head groups. This brings the head groups in closer contact (possibly stabilized by an intermolecular hydrogen bond), leading to the formation of more or less cylindrical acid/soap dimers. These cylinders pack into bilayers (8). Essentially, the phase diagram of sodium (or potassium) octanoate–octanoic acid–water at 20°C is similar to the system sodium octanoate–decanol–water (6,9).

Potassium Oleate–Oleic Acid–Water

Octanoic acid is a rather short-chain fatty acid, containing just eight carbon atoms. The characteristics of the phase diagram of longer chain fatty acid–soap–water systems, however, seem to be similar (6). Figure 2 is a simplified representation of the ternary phase diagram for potassium oleate–oleic acid–water at 25°C (6). Again, there is a micellar phase (L$_1$) close to the water corner, in the presence of an excess amount of oleate over oleic acid. Due to the longer hydrophobic chain (18 carbon atoms), the CMC [≤ 1 mM = 0.35 wt%,(10)] is considerably lower than in the case of octanoate (see above). The inverted micellar phase (L$_2$) is localized toward the oleic acid corner. Furthermore, there is again a normal hexagonal phase (H$_I$) and an inverted hexagonal phase (H$_{II}$, formed in approximately 1:1 oleic acid:oleate mixtures at water content below 45 wt%, not shown in Fig. 2). The lamellar liquid crystalline phase (D) is present toward the water corner, mainly centered around mixtures containing equimolar amounts of oleic acid and oleate. Most of the phase boundaries in Figure 2 are only tentatively assigned (indicated as dashed lines). The properties of samples containing 1:1 mixtures of oleic acid and potassium oleate have been investigated to some extent as a function of water content and temperature (11).
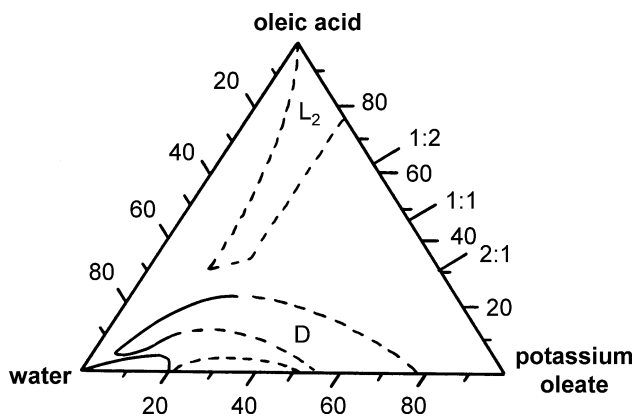
Figure 2 Simplified ternary phase diagram of potassium oleate–oleic acid–water at 25°C. See Figure 1 and text for details. *Source*: Adapted from Ref. 6.

In the water-free 1:1 crystals, the oleic acid content is 46.8 wt%. These crystals melt at 47°C and decompose to potassium oleate crystals and oleic acid if heated above the melting temperature. Upon adding water, the chain-melting transition temperature decreases to about 22°C at 20 wt% water and 11°C at 30 wt% water (6).

Above 60 wt% water and above the chain-melting transition temperature of 11°C, a lamellar liquid-crystalline phase is present (D in Fig. 2). It contains an ordered array of lipid bilayers with intercalated water layers. The bilayer thickness is about 46 Å (11,12). At very high water content (>92 wt%) and above the chain-melting transition temperature, closed bilayers exist, corresponding to unilamellar (11) and most likely multilamellar *vesicles* (liposomes). The mean head area per lipid is about 33 Å^2 (11).

General Conditions for Fatty Acid Vesicle Formation

In a number of studies, it has been shown that aqueous fatty acid–soap systems contain regions within the phase diagrams, in which dispersed vesicles exist above the corresponding fatty acid–soap chain-melting transition temperature. The vesicles form from short-chain (<14 C-atoms), as well as long-chain fatty acids (>14 C-atoms), if approximately equimolar amounts of the fatty acid and the soap are present. This has been shown not only in the cases of octanoic acid/octanoate (13) and oleic acid/oleate (3,10,13–18), but also for decanoic acid/decanoate (3,13,19,20), dodecanoic acid/dodecanoate (13), tetradecanoic acid/tetradecanoate (13), hexadecanoic acid/hexadecanoate (13), linoleic acid/linoleate (14–17,21), myristoleic acid/myristoleate (22), palmitoleic acid/palmitoleate (22), and (R)-2-methyl-dodecanoic acid/(R)-2-methyl-dodecanoate (23). The vesicles formed are

usually called fatty acid/soap vesicles *or just* fatty acid vesicles (or fatty acid liposomes). Because dilute equimolar mixtures of fatty acids and soaps have a pH that is close to pH 7, fatty acid/soap vesicles only form at an intermediate pH (pH 7–9). This is in clear contrast to vesicles (liposomes) formed from conventional phosphatidylcholines.

TITRATION CURVES

One convenient way of studying in more detail the formation of fatty acid/soap vesicles at high water content (usually >95 wt% water) is the use of titration curves (3,19–21,24). These experiments are conducted typically by adding various amounts of hydrochloric acid (HCl) to a fully ionized soap solution and measuring the pH values after equilibration. Figure 3A shows the titration curve of oleic acid/sodium oleate (total concentration 80 mM).

The amount of added HCl corresponds approximately to the composition of oleic acid (degree of protonation) at each point of the titration curve. The titration curve shows two inflection points that are assigned to transitions between different types of aggregates (vide infra). At point A in Figure 3A, the solution is clear. Because the concentration is higher than the CMC of sodium oleate [approximately 1 mM (10)], micelles in equilibrium with monomers are present. At point B, the solution becomes slightly turbid, indicating the formation of larger aggregates (vesicles). There is a pH plateau between points B and C, where the turbidity of the solution is increased. At point C, the pH starts to decrease again. At point D, the solution appears milky white and a small pH plateau is observed between points D and E. Upon further addition of HCl from point E, the solution starts to separate into two macroscopic phases (aqueous and oil) and the pH value decreases rapidly. In a titration experiment, one obtains a series of samples with a constant water composition (approximately 97.8 wt% in the case of Fig. 3A) but varied ratios of oleic acid and sodium oleate. In the case of Figure 3A, at least three distinctive aggregation types are observed with the increasing amounts of added HCl. Micelles are present at a high ionization degree of the carboxylic acid. Lamellar bilayers (vesicles) are observed in the intermediate protonation range (approximately 0.2–0.55), as independently confirmed by various analytical techniques, for instance, electron microscopy. The dominant aggregation species at higher protonation degrees are oil droplets. Cistola et al. (3) have interpreted the appearance of pH plateaus in titration curves as the transitions between different types of aggregates by applying the Gibbs phase rule. The Gibbs phase rule depicts the relation between the number of components (C), the number of phases (P), and the number of independent variables (F) as $F = C - P + 2$. Assuming that aggregation species such as micelles and bilayers are independent phases in addition to the aqueous phase, it is possible to calculate the degree of freedom of the chemical system. For example, a fatty acid–soap

(A)

(B)

(C)
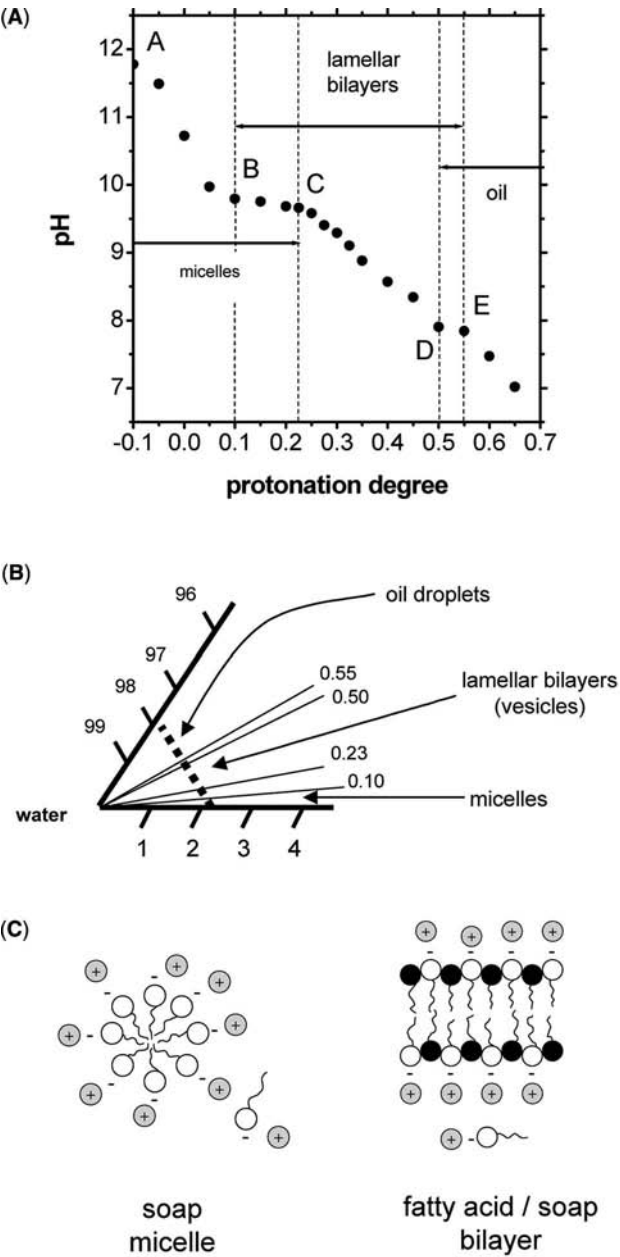
Figure 3   (*Caption on facing page*)

aqueous system contains three components (fatty acid, soap, water) and the phase rule predicts three degrees of freedom for a system that contains two phases (e.g., aqueous, micelles) ($F = 3 - 2 + 2 = 3$). At constant temperature and pressure, there is one remaining degree of freedom (e.g., pH value). If two distinctive types of aggregates are coexisting, on the other hand, the number of phases would be three (e.g., aqueous, micelles, bilayers) and the phase rule predicts no degree of freedom at constant temperature and pressure. In this way, the invariance of pH values in the plateau regions can be correlated to the coexistence of two types of aggregates. Therefore, in the titration curve in Figure 3A the two plateau regions (B–C and D–E) correspond to the conditions where micelles/bilayers and bilayers/oil droplets are coexisting, respectively.

If one neglects the fact that the titration curve experiments described above include the presence of additional $Na^+(aq)$ (arising from the initially added NaOH) and various amounts of $Cl^-(aq)$ ions (from the added HCl), then all samples analyzed in a titration curve experiment are on a specific line within the phase diagram shown in Figure 3B. This line is parallel to the oleic acid–oleate line and crosses the water–oleate 2.2% and the water–oleic acid line at 97.8% of its length (Fig. 3B).

Figure 3C illustrates schematically the different types of aggregates formed at high pH (micelles) and at intermediate pH (bilayers). Please note that the micelles do not need to be spherical; they may also be cylindrical or disc-like. Moreover, although the application of Gibbs phase rule to the titration curve predicts that bilayers (vesicles) are the only aggregation form or type within the region between C and D in Figure 3A, recent electron spin resonance (ESR) measurements have indicated that a portion of oleic acid molecules are *not* forming the bilayer structure (24). It may be that some of the oleic acid molecules are embedded within the hydrophobic part of the membranes in such a way that the carboxylic acid headgroup is not in direct contact with water, leading to the formation of vesicles with partially swollen bilayers.

Figure 3 (*Figure on facing page*) (**A**) Titration curve for 80 mM oleic acid/oleate. (**B**) Water-rich corner of the ternary phase diagram of sodium oleate–oleic acid–water, indicating the line (*dashed*) on which the titration curve data presented in Figure 3A are localized. (**C**) Schematic representation of a soap micelle (high pH) and a fatty acid/soap bilayer fragment at intermediate pH [as part of the shell(s) of self-closed vesicles]. Depending on the chain length of the soap molecules, the micelle may be more or less spherical (short-chains) or expected to be cylindrical (long-chains). Surfactants with empty head groups represent the negatively charged soap molecules; surfactants with filled head groups represent fatty acid molecules. Shown are also the counterions, which are expected to bind to some extent to the surface of the aggregates (Gouy–Chapman double layer), see (25).

PREPARATION OF FATTY ACID VESICLES

Fatty acid vesicles are colloidal dispersions of lamellar fatty acid/soap bilayers. The formation of these vesicles can be achieved along various pathways. The general principles underlying fatty acid vesicle formation are basically the same as in the case of phospholipid vesicles (conventional liposomes). Therefore, similar approaches as in the case of conventional liposomes are often used for the preparation of fatty acid vesicles. However, there are also certain unique characteristics of the fatty acid/soap systems. Fatty acid vesicles always form from mixtures of protonated fatty acids and ionized soaps, and their ratio is essential for their self-assembly into bilayers. As observed in corresponding titration experiments (Fig. 3A), for every specific fatty acid/soap system there is a rather narrow range of the protonation-to-ionization ratio within which stable bilayers form. Therefore, vesicles are usually prepared using a high-capacity buffer solution in which the degree of fatty acid protonation is optimum for bilayer formation (approximately 0.5).

In practice, fatty acid vesicles can be formed starting from various initial states, including monomer solutions, micelles, and lamellar bilayers (Fig. 4). One of the simplest (and most popular) methods is to hydrate fatty acid (and/or soap) molecules with a suitable buffer solution and disperse the formed lamellar bilayer mechanically (on a laboratory scale, usually just shaking) (10). Alternatively, vesicles have been prepared by pH adjustment of alkaline aqueous soap solutions (3) or by injecting a concentrated solution of monomers or micelles into a buffered solution (26). Either of these preparation techniques generally results in multilamellar vesicles with a polydisperse size distribution. Therefore, a sizing-down procedure is usually necessary to obtain vesicles that are homogeneous with respect to size distribution and lamellarity. As in the case of conventional phospholipid vesicles, large unilamellar vesicles (LUV with diameters above 100 nm) and small unilamellar vesicles (with diameters below 100 nm) are obtained in most cases by extrusion through polycarbonate membranes (10,23,26) or by sonication.

In the following, experimental details are described for the preparation of oleic acid vesicles, as an example, by using three different methods at room temperature (10,26).

Preparation of oleic acid vesicles by dispersing a dry film of sodium oleate in a buffer solution of intermediate pH. Sodium oleate (0.24 mmol) is first dissolved in 3 mL of methanol. This methanolic solution is then added to a 100 mL round-bottomed flask, and the methanol is removed under reduced pressure with a rotatory evaporator. The oleate film formed is dried overnight at high vacuum and then dispersed by vortexing in buffer by adding 3 mL of 0.2 M *Tris*/HCl (pH 8.5). The pH of the multilamellar vesicle suspension is measured and if necessary readjusted to pH 8.5 by adding HCl. The final concentration of oleate + oleic acid is 80 mM.
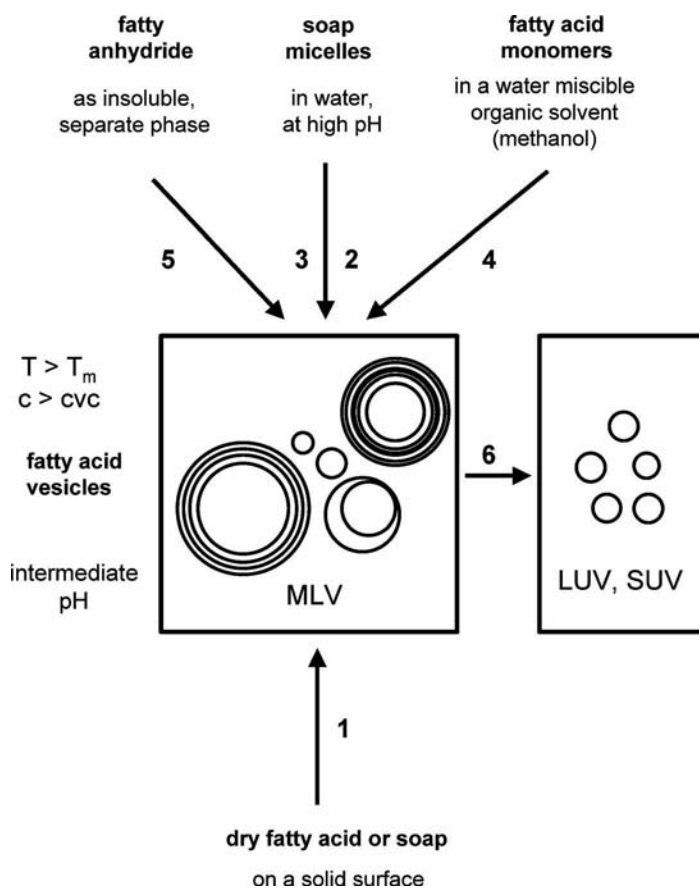
Figure 4 Schematic representation of different pathways for the formation of fatty acid vesicles at a temperature above the chain-melting transition temperature of the hydrated fatty acid/soap mixtures. 1. Hydration with a buffer solution of an intermediate pH. 2. Addition of strong acid (HCl) to an alkaline micellar soap solution. 3. Addition of soap micelles into a buffer solution of intermediate pH. 4. Addition of fatty acid monomers into a buffer solution of intermediate pH. 5. Hydrolysis of water-insoluble, non-bilayer forming fatty anhydrides by a strong base (NaOH) or by an appropriate concentrated buffer solution of intermediate pH. 6. Extrusion or sonication of MLV. *Abbreviations*: T, temperature; T_m, chain-melting transition temperature; C, concentration; CVC, critical concentration for vesicle formation; MLV, multilamellar vesicles; LUV, large unilamellar vesicles; SUV, small (sonicated) unilamellar vesicles. *Source*: From Refs. 10, 13 and 26.

Preparation of oleic acid vesicles by pH adjustment of an alkaline oleate solution to yield a suspension with an intermediate pH. Sodium oleate (0.24 mmol) is dissolved in 3 mL of 0.05 M *Tris*/HCl (pH 9.0), resulting in

a transparent micellar solution of approximately pH 10.9. The pH is then adjusted with 1 M HCl to pH 8.5. The final concentration of oleate + oleic acid is 80 mM.

   Preparation of oleic acid vesicles by adding an alkaline oleate solution to a buffer solution of intermediate pH. Sodium oleate is first dissolved in distilled water at a concentration of 80 mM. Then 0.062 mL of this micellar solution is added to 2.438 mL 0.2 M *Tris*/HCl, pH 8.5 under stirring. The vesicle formation and equilibration of the system is not immediate (26). The final concentration of oleic acid + oleate is 2 mM.

   It should be noted that in all three examples described, the type and concentration of the buffer species could be varied, as well as the total concentration of oleic acid and the pH. The pH needs to be within the pH range of vesicle formation; the oleic acid concentration needs to be above the CVC (Table 1) and should not exceed concentrations that lead to the formation of other phases (Fig. 3B). For other fatty acids, the conditions have to be adopted accordingly.

PROPERTIES OF FATTY ACID VESICLES

Because fatty acid vesicles are composed of single-chain amphiphiles that have a weakly acidic head group, some of the properties of this type of vesicles are very different from the properties of the liposomes formed from conventional phosphatidylcholines.

Vesicle Stability

Fatty acid vesicles are thermodynamically stable above the chain-melting transition temperature of the hydrated fatty acid/soap mixtures only within a certain—relatively narrow—intermediate pH range (Fig. 3) (Table 1). If the pH is too high, the transformation of vesicles into micelles occurs. If the pH is too low, oil droplets form. There are pH regions of coexistence of vesicles (bilayers) and micelles as well as vesicles (bilayers) and oil droplets (Fig. 3).

   An extension of the vesicle stability to *more alkaline pH* values (up to pH 11) can be achieved by coadding to the fatty acid/soap mixture a fatty alcohol [e.g., dodecanol added to dodecanoic acid/dodecanoate (13); nonanol added to nonanoic acid/nonanoate (27); monoolein/oleate (31)]. Also see the discussion above about the similarity between the phase diagram of sodium octanoate–octanoic acid–water and the phase diagram of sodium octanoate–decanol–water.

   An extension of the pH regions to a more acidic pH can be achieved by coadding to the fatty acid/soap mixture a negatively charged surfactant with a high pK_b, e.g., sodium dodecylbenzenesulfonate (SDBS, $pK_b \sim 15$

Table 1 Experimental Conditions for the Formation of Fatty Acid Vesicles

Fatty acid	T_m (°C)	CVC ≈ [monomer] (mM)	pH range	References
Octanoic acid		~150	7.5	13,27
Nonanoic acid		85	~7	27
Decanoic acid	15–22	10–30	6.4–7.8	11,20
Dodecanoic acid	30–34	~23	7.0–8.5	11,13
Tetradecanoic acid	43		~9	11,13
cis-9-Tetradecenoic acid (= myristoleic acid)		~4	~8.5	22
cis-9-Hexadecenoic acid (= palmitoleic acid)		–	~8.5	22
cis-9-Octadecenoic acid (= oleic acid)	8–13	< 1	8–9.5	3,11,14–17, 24,28
cis-cis-9,12-Octadecadienoic acid (= linoleic acid)		< 1.7	8–9	14–17,21
(R)-2-Methyl-dodecanoic acid	~8		7.5–8.8	23

Note: The following are given if known: (a) the approximate melting temperature of the hydrated fatty acid/soap systems (T_m)—the chain-melting transition temperatures of the hydrated fatty acid/soap bilayers are considerably lower than the melting temperatures of the corresponding fatty acids; (b) the CVC and the approximate free monomer concentration coexisting with the vesicles (monomer)—the CVC values and the free monomer concentration depend on the pH, (19,20) and are only approximate in order to indicate the concentration range; and (c) the approximate pH range for the formation of the fatty acid vesicles (pH range)—the pH-range of vesicle formation depends on the total fatty acid concentration (20). The upper and lower limits are rather uncertain because a distinction between the "vesicle only" regions (between point C and point D in Fig. 3A) from the coexistence regions (vesicles and micelles or vesicles and oil droplets) is difficult (see text).
Abbreviations: CVC, critical concentration for vesicle formation; T_m, chain melting transition temperature.
See also (29,30).

or higher, with a $pK_a \sim -1$ or lower of the corresponding acid). This has been demonstrated at least in the case of decanoic acid vesicles, where addition of SDBS at a molar ratio of decanoic acid:SDBS 1:1 allowed the preparation of unilamellar vesicles at pH 4.3 (20). The roles of the fatty alcohol or the alkylsulfonate can be seen in a bilayer stabilization through the formation of mixed charged-uncharged dimers (13,27,28), soap (R1-COO-)-alcohol (R²-OH), or sulfonate (R³-SO₃⁻)-fatty acid (R1-COOH). The dimers may be stabilized through hydrogen bonds, as proposed in the case of fatty acid (R1-COOH)-soap (R1-COO-) dimers.

Because fatty acid vesicles are often prepared in the presence of high concentrations of buffer species, the type of buffer ions used may also be of

importance for the stability of the vesicles through a possible interact
the vesicles (24). A physical stabilization of fatty acid vesicle membr
be achieved by coembedding cholesterol within the bilayer membra
Furthermore, fatty acid methyl (18) or ethyl (32) esters can also
up by the vesicle membranes, as shown in the case of oleic acid vesi

Below the chain-melting transition temperature of the hydra
acid/soap mixtures, precipitation (crystallization) is observed (3,
stable vesicle dispersions can be formed. Furthermore, the presence
amounts of divalent cations (like Ca^{2+}, Mg) leads to the precipitatio
fatty acid/soap aggregates (33).

Soap Monomer Solubility and Critical Concentration
for Vesicle Formation

Fatty acids have a much higher monomer solubility compared with
tional diacylphospholipids. This is especially the case if the hydr
chain is relatively short. The presence of monomers becomes non-n
(Table 1). For example, the free monomer concentration for fatty a
cles composed of decanoic acid and sodium decanoate at pH 7
20 mM, (19,20), as determined by ultrafiltration experiments (Fig.
high monomer concentrations have direct consequences on the ves
paration strategies (such as the minimum lipid concentration requi
as well as for the vesicle stability and transformation. Below a criti
centration, no bilayer formation is observed (Table 1).
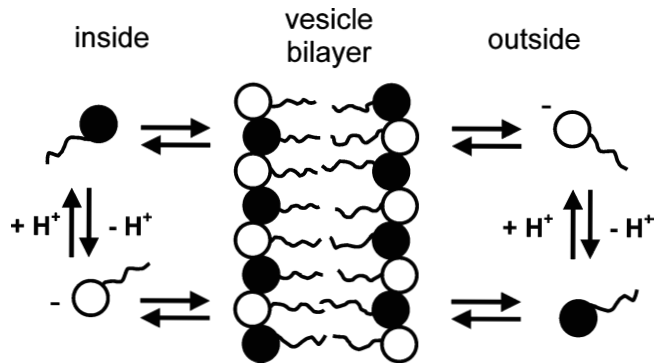
Figure 5 Schematic representation of the bilayer-monomer equilibrium a
inside as well as outside the fatty acid vesicles. The exchange of the surfacta
cules between the bilayer and the bulk phase (or between the bilayer and t
trapped volume) is expected to be fast as a dilution of the vesicles below th
concentration of vesicle formation leads to a complete disintegration of th
within seconds (short-chains) or minutes (long-chains).

Entrapment of Water Soluble Compounds

Entrapment of water soluble molecules, including enzymes (34), in the internal aqueous volume of fatty acid vesicles is possible, but very often the separation of nonentrapped molecules from the vesicles either by size exclusion chromatography (gel filtration), dialysis, or centrifugation is technically difficult because of the high monomer concentration existing in equilibrium with the vesicles. In the case of a separation of the vesicles from the nonentrapped substances by gel filtration, the elution buffer needs to be saturated with monomeric fatty acids (20,23). This is particularly important if vesicles from short-chain fatty acids are used. At least the following water-soluble compounds have been entrapped inside fatty acid vesicles: glucose (14,15,17), potassium hexacyanoferrate (10), arsenazo III (10,20,23,32), terbium(III) chloride (TbCl$_3$) (32,35), dipicolinic acid (32,35), polynucleotide phosphorylase (34), Chromobacterium viscosum lipase (32), ferritin (36).

APPLICATIONS OF FATTY ACID VESICLES AND CONCLUSIONS

Since their discovery in 1973 (14), fatty acid vesicles have been considered as model compartments for the precursor structures, called protocells, that may have preceded the first cells at the origin of life (13,22,34,37,38).

In contrast to conventional phospholipid vesicles, which are built from contemporary, chiral double-chain amphiphiles, fatty acid vesicles are made of simple single-chain surfactants. One may even think that fatty acids were synthesized during prebiotic times on Earth, or somewhere else (37). Along this line of research, different aspects related to the formation of fatty acid vesicles and their reproduction have been investigated. The hydrolysis of water-insoluble oleic anhydride leads to the formation of two oleic acid molecules for each anhydride, and if the pH of the aqueous solution corresponds to the intermediate pH for bilayer formation, then more and more bilayers (vesicles) form as the hydrolysis reaction proceeds (10). Under certain conditions, a kind of vesicle reproduction is observed (10,23,34). The concentration of bilayers increases with time. In combining the chemical formation of fatty acids (oleic acid from oleic anhydride) and the simultaneous, competitive chemical destruction of the fatty acid (oxidation of oleic acid to 9,10-dihydroxystearic acid), a chemical model of the homeostatic behavior of a protocell model has been achieved (39). Another way of increasing the amount of bilayers is to add to fatty acid vesicles a micellar solution of the corresponding soap. By doing so, the size of the initially present vesicles is only slightly increased, while there is an increase in the number of vesicles and particularly an increase in the speed with which a transient equilibrium state is reached. Without preadded vesicles, the formation of vesicles and the achievement of equilibrium is a very slow process. This experimental finding has been called ''matrix effect'' (21,26,36,40,41),

because the preadded vesicles act as a kind of matrix. This principle has been applied to rather sophisticated experimental systems within the field of prebiotic chemistry, explaining the origin of the first cellular compartments (22,42).

It has also been found that clay particles (montmorillonite) accelerate the formation of fatty acid vesicles from soap micelles (22). The clay particles thereby often get encapsulated by the vesicles.

The interaction of fatty acid vesicles with flat solid surfaces (glass) containing adsorbed hydrocarbons showed that LUV can aggregate and fuse into giant vesicles by a process that is not known in detail but seems to occur on the surface of glass (43).

Possible applications of fatty acids in cosmetics, medicine, and food technology seems to be largely unexplored. In an attempt to develop a liposomal system containing paramagnetic manganese(III) mesoporphyrin for an enhanced absorption by the gastrointestinal tract, it was found that manganese(III) mesoporphyrin preferentially interacts with oleic acid vesicles, with an apparently optimal embedding within the oleic acid vesicle membranes (44). Oleic acid containing emulsion systems have indeed been found in the past to increase the absorption efficiency of orally administered drugs (studies with carboxyfluorescein-containing oleic acid systems administered to rats) (45).

Because the horny layer (*stratum corneum*) of the human skin contains no phospholipids, but rather fatty acids, cholesterol, and ceramides, non-phospholipidic bilayer-forming amphiphiles are used as model systems. These systems include mixtures of fatty acids and soaps to mimic the barrier properties of this upper-most layer of the skin; oleic acid/oleate and palmitic acid/palmitate mixtures have indeed been investigated in this context (46,47). The total fatty acid concentration in these cases, however, is considerably higher than in the case of the dispersed vesicle systems.

In summary, there are a number of properties of fatty acid vesicles that clearly distinguish them from conventional phospholipid vesicles. Depending on the applications one is looking for, these differences may be of advantage or of disadvantage. Although the vesicle (bilayer) stability is limited to an (fatty acid-specific) intermediate pH range of 7 to 9, this pH region can be extended to the alkaline as well as to the acidic regions by coaddition of an alcohol (to increase the stability toward high pH) or a sulfonated surfactant (to increase the stability toward low pH). On the other hand, a fixed pH region of vesicle existence allows an unloading of trapped solutes into the bulk medium by a simple increase in pH (vesicle–micelle-transition). Therefore, fatty acid vesicles are a particular type of pH-sensitive vesicles. The strong pH-dependency of fatty acid aggregate formation allows different types of transformations that may be controlled in part by local fatty acid concentration and local pH changes, e.g., the transformations observed in giant oleic acid vesicles during the hydrolysis of oleic anhydride (48,49).

REFERENCES

1. Smith R, Tanford C. The critical micelle concentration of L-α-dipalmitoyl-phoshatidylcholine in water and in water/methanol solutions. J Mol Biol 1972; 67:75–83.
2. Hauser H, Dawson RMC. The binding of calcium at lipid–water interfaces. Eur J Biochem 1967; 1:61–69.
3. Cistola DP, Hamilton JA, Jackson D, Small DM. Ionization and phase behavior of fatty acids in water: application of the Gibbs phase rule. Biochemistry 1988; 27:1881–1888.
4. Gennis RB. Biomembranes: Molecular Structure and Function. New York: Springer–Verlag, 1989.
5. Ekwall P, Mandell L. Solutions of alkali soaps and water in fatty acids. I. Region of existence of the solutions. Kolloid Z Z Polymere 1969; 233:938–944.
6. Fontell K, Mandell L. Phase equilibria and phase structure in the ternary systems sodium or potassium octanoate-octanoic acid-water. Colloid Polym Sci 1993; 271:974–991.
7. Skurtveit R, Sjoblom J, Højland H. Emulsions under elevated temperature and pressure conditions. I. The model system water–hexadecanoic acid–sodium hexadecanoate–decane at 70°C. J Colloid Interface Sci 1989; 133:395–403.
8. Mitchell DJ, Ninham BW. Micelles, vesicles and microemulsions. J Chem Soc Faraday Trans 2 1981; 77:601–629.
9. Ekwall P. Composition, properties and structures of liquid crystalline phases in systems of amphiphilic compounds. In: Brown GH, ed. Advances in Liquid Crystals. New York: Academic Press, 1975:1–142.
10. Walde P, Wick R, Fresta M, Mangone A, Luisi PL. Autopoietic self-reproduction of fatty acid vesicles. J Am Chem Soc 1994; 116:11649–11654.
11. Cistola DP, Atkinson D, Hamilton JA, Small DM. Phase behavior and bilayer properties of fatty acids: hydrated 1:1 acid-soaps. Biochemistry 1986; 25:2804–2812.
12. Small DM. The Physical Chemistry of Lipids; Handbook of Lipid Research. Vol. 4. New York: Plenum Press, 1986.
13. Hargreaves WR, Deamer DW. Liposomes from ionic, single-chain amphiphiles. Biochemistry 1978; 17:3759–3768.
14. Gebicki JM, Hicks M. Ufasomes are stable particles surrounded by unsaturated fatty acid membranes. Nature 1973; 243:232–234.
15. Gebicki JM, Hicks M. Preparation and properties of vesicles enclosed by fatty acid membranes. Chem Phys Lipids 1976; 16:142–160.
16. Hicks M, Gebicki JM. Microscopic studies of fatty acid vesicles. Chem Phys Lipids 1977; 20:243–252.
17. Hicks M, Gebicki JM. A quantitative relationship between permeability and the degree of peroxidation in ufasome membranes. Biochim Biophys Res Commun 1978; 80:704–708.
18. Bittman R, Blau L. Permeability behavior of liposomes prepared from fatty acids and fatty acid methyl esters. Biochim Biophys Acta 1986; 863:115–120.
19. Morigaki K, Walde P, Misran M, Robinson BH. Thermodynamic and kinetic stability. Properties of micelles and vesicles formed by the decanoic acid/decanoate system. Colloids Surf. A: Physicochem Eng Aspects 2003; 213:37–44.

20. Namani T, Walde P. From decanoate micelles to decanoic acid/dodecylbenzene-sulfonate vesicles. Laugmuir 2005; 21:6210–6219.
21. Rogerson HL, Robinson BH, Bucak S, Walde P. Kinetic studies of the interaction of fatty acids with phosphatidyl choline vesicles (liposomes). Colloids surf B Bio Interfaces 2006; 48(1):24–34.
22. Hanczyc MM, Fujikawa SM, Szostak JW. Experimental models of primitive cellular compartments: encapsulation, growth, and division. Science 2003; 302:618–622.
23. Morigaki K, Dallavalle S, Walde P, Colonna S, Luisi PL. Autopoietic self-reproduction of chiral fatty acid vesicles. J Am Chem Soc 1997; 119:292–301.
24. Fukuda H, Goto A, Yoshioka H, Goto R, Morigaki K, Walde P. Electron spin resonance study of the pH-induced transformation of micelles to vesicles in an aqueous oleic acid/oleate system. Langmuir 2001; 17:4223–4231.
25. Evans DF, Wennerström H. The Colloidal Domain: Where Physics, Chemistry, and Biology Meet. 2d ed. New York: Wiley-VCH, 1999.
26. Blöchliger E, Blocher M, Walde P, Luisi PL. Matrix effect in the size distribution of fatty acid vesicles. J Phys Chem B 1998; 102:10383–10390.
27. Apel CL, Deamer DW, Mautner MN. Self-assembled vesicles of monocarboxylic acids and alcohols: conditions for stability and for encapsulation of biopolymers. Biochim Biophys Acta 2002; 1559:1–9.
28. Haines TH. Anionic lipid headgroups as a proton-conducting pathway along the surface of membranes: a hypothesis. Proc Natl Acad Sci U S A 1983; 80:160–164.
29. Walde P, Morigaki K. Formation and transformation of fatty acid/soap vesicles. In: Robinson BH, ed. Self-Assembly. Amsterdam: IOS Press, 2003:443–453.
30. Monnard PA, Deamer DW. Preparation of vesicles from nonphospholipid *amphiphiles*. Methods Enzymol 2003; 372:133–151.
31. Borné J, Nylander T, Khan A. Vesicle formation and other structures in aqueous dispersions of monoolein and sodium oleate. J Colloid Interface Sci 2003; 257:310–320.
32. Vonmont-Bachmann PA, Walde P, Luisi PL. Lipase-catalyzed reactions in vesicles as an approach to vesicle self-reproduction. J Liposome Res 1994; 43:1135–1158.
33. Monnard P-A, Apel CL, Kanavarioti A, Deamer DW. Influence of ionic inorganic solutes on self-assembly and polymerization processes related to early forms of life: implications for a prebiotic aqueous medium. Astrobiology 2002; 2:139–152.
34. Walde P, Goto A, Monnard PA, Wessicken M, Luisi PL. Oparin's reactions revisited: enzymatic synthesis of poly(adenylic acid) in micelles and self-reproducing vesicles. J Am Chem Soc 1994; 116:7541–7547.
35. Cheng Z, Luisi PL. Coexistence and mutual competition of vesicles with different size distributions. J Phys Chem B 2003; 107:10940–10945.
36. Berclaz N, Müller M, Walde P, Luisi PL. Growth and transformation of vesicles studied by ferritin labeling and cryotransmission electron microscopy. J Phys Chem B 2001; 105:1056–1064.
37. Deamer D, Dworkin JP, Sandford SA, Bernstein MP, Allamandola LJ. The first cell membranes. Astrobiology 2002; 2:371–381.
38. Luisi PL, Walde P, Oberholzer T. Lipid vesicles as possible intermediates in the origin of life. Curr Opin Colloid Interface Sci 1999; 4:33–39.

39. Zepik HH, Blöchliger E, Luisi PL. A chemical model of homeostasis. Angew Chem Int Ed 2001; 40:199–202.
40. Rasi S, Mavelli F, Luisi PL. Matrix effect in oleate micelles–vesicles transformation. Origins Life Evol Biosphere 2004; 34:215–224.
41. Rasi S, Mavelli F, Luisi PL. Cooperative micelle binding and matrix effect in oleate vesicle formation. J Phys Chem B 2003; 107:14068–14076.
42. Chen IA, Szostak JW. A kinetic study of the growth of fatty acid vesicles. Biophys J 2004; 87:988–998.
43. Morigaki K, Walde P. Giant vesicle formation from oleic acid/sodium oleate on glass surfaces induced by adsorbed hydrocarbon molecules. Langmuir 2002; 18: 10509–10511.
44. Dong P, Choi P, Schmiedl UP, Nelson JA, Starr FL, Ho RJY. Interaction of manganese-mesoporphyrin with oleic acid vesicles. Biochemistry 1995; 34: 3416–3422.
45. Engblom J, Engström S, Fontell K. The effect of the skin penetration enhyncer Azone® on fatty acid–sodium soap–water mixtures. J Control Release 1995; 33: 299–305.
46. Norlén L, Engblom J. Structure-related aspects on water diffusivity in fatty acid– soap and skin model systems. J Control Release 2000; 63:213–226.
47. Oba N, Sugimura H, Umehara Y, Yoshida M, Kumira T, Yamaguchi T. Evaluation of an oleic acid-water-in-oil-water-type multiple emulsion as potential drug carrier *via* the enteral route. Lipids 27:701–705.
48. Wick R, Walde P, Luisi PL. Light microscopic investigations of the autocatalytic self-reproduction of giant vesicles. J Am Chem Soc 1995; 117:1435–1436.
49. Wick R. Untersuchungen an Riesenvesikeln als chemische Mikroreaktoren und Modelle für biologische Zellen. Dissertation ETH-Zürich, Nr. 11711, 1996.

2

The Preparation of Lipid Vesicles (Liposomes) Using the Coacervation Technique

Fumiyoshi Ishii

*Department of Pharmaceutical Sciences and Technology,
Meiji Pharmaceutical University, Tokyo, Japan*

INTRODUCTION

The preparation techniques of liposomes were classified broadly into several categories according to the basic modes of dispersion, e.g., mechanical dispersion, detergent solubilization, and solvent dispersion (1). Further research to improve the techniques was anticipated to encapsulate sufficient amounts of materials stably and in a reproducible fashion with the possibility of application on an industrial scale, in order to use the liposomes as delivery tools of therapeutic agents. We have explored various new techniques of liposomal preparation. In our extensive research of colloidal formulations for therapeutic agents, we took unique approaches in applying colloidal techniques used for the preparation of microparticulate carriers other than liposomes, e.g., microcapsules or lipid emulsions.

We have already introduced the microencapsulation vesicle (MCV) method in a previous edition of the Liposome Technology series (2). The MCV method was devised by applying methods and apparatuses of preparing microcapsules, while its theoretical basis was that of lipid emulsions (2,3). The MCV method was considered in parallel with several methods using double emulsion techniques (1,4). However, the MCV method had the

advantage of being able to easily control the preparation conditions, such as the kind of organic solvent, the intensity and time of mechanical agitation, and the ambient temperature of each emulsification (2,3,5). These features allowed the optimization of the preparation conditions to control the size or encapsulation efficiency of the drug-loaded liposomes. Various preparatory conditions and their effects on such physicochemical properties of liposomes also produced useful information that elucidated how the liposomes were formed during the two-step emulsification process (6).

In this chapter, we offer a unique perspective on liposome preparation by applying a coacervation (phase separation) technique that had been commonly used to prepare microcapsules in agrochemical and other fields. We investigate phospholipid–water–alcohol systems using various alcohols with different miscibilities with water. The studies demonstrate the possibility of applying the technique to encapsulate materials susceptible to harsh conditions, such as heat or extreme mechanical agitation. Moreover, these findings expanded the understanding of the colloid formation of phospholipids in water–alcohol systems, which produced a versatile platform for possible new liposomal preparation techniques for specific demands. This review summarizes the preparation condition and some physicochemical properties of the liposomes prepared by a coacervation method (7,8).

METHODS

Analysis of Phosphatides

Refined egg-yolk phosphatides (PL-100E) used in this study were kindly provided by QP Co., Ltd. The phospholipid compositions of the phosphatides were determined by the thin-layer chromatography flame-ionization detection method described in our previous paper (7,9). Briefly, a standard solution of various phospholipids such as phosphatidylcholine, phosphatidylethanolamine, lysophosphatidylcholine, and sphingomyelin was dissolved in chloroform. The refined egg-yolk phosphatides were analyzed using thin-layer chromatography with flame-ionization detection (TLC-FID), employing an Iatroscan MK-5, Iatron Laboratories Inc., Tokyo, Japan. TLC was performed on a chromarod, 0.9 mm in diameter and 153 mm in length, consisting of a 75-μm-thick silica gel layer sintered onto a quartz support. Then, the chromarod, to which 1 μL of the sample dissolved in chloroform had been applied, was passed through the FID. The lipid compositions of the refined egg-yolk phosphatides used were mainly 80.7% phosphatidylcholine, 14.4% phosphatidylethanolamine, 0.5% sphingomyelin, 0.9% lysophosphatidylcholine, and other neutral lipids (0.5% triglyceride and 3.0% cholesterol). Methanol, ethanol, 1-propanol, and 2-propanol, which were selected as a lipid solvent, were of reagent grade. Deionized double-distilled water or saline solutions containing various

electrolytes (sodium chloride, ammonium chloride, magnesium chloride, calcium chloride, and sodium sulfate) were used as a nonsolvent of lipid.

Preparation of the Phase Diagram

A triangular phase diagram of the coacervation system was elaborated to optimize the coacervation conditions. Fifty different phospholipid–alcohol solutions containing between 0.1% and 50% (w/v) phospholipid were prepared. Water was added dropwise to the phospholipid–alcohol solutions of various concentrations, causing the formation of coacervated droplets under agitation at constant temperature (20°C).

The mixture was equilibrated in a glass test tube for five minutes with mixing and for one hour without mixing at 20°C. The procedure was repeated until a phase change was noted, that is, until the desired amount of water had been added. The positions of the various phases produced on transition from a clear solution to complete turbidity change were examined. The formation of coacervates was then observed microscopically at room temperature.

Preparation of Liposomes (Lipid Vesicles)

A visking dialysis tube was washed several times with distilled water and left to soak in distilled water before use. Thirty milliliters of the coacervation system prepared according to the optimum coacervation conditions obtained by the phase diagram was pipetted into the dialysis tube, which was double-tied at each end, and placed in 900 mL of distilled water at various constant temperatures with constant stirring at 150 rpm. The dialysis tube containing lipid vesicles was then dialyzed three times with distilled water for one hour.

Observation of Liposomes by Freeze-Fracture Electron Micrographs

Freeze-fracture electron micrographs were prepared as described previously (3). Briefly, lipid vesicle preparations were mixed with 25% (v/v) glycerol solution and then quickly frozen in Freon slush at −170°C. The samples were fractured in a freeze-etching apparatus (Model JFD-9000, JEOL, Japan) at −120°C and replicated with platinum–carbon shadowing. Replicated samples were transferred to flamed 200-mesh grids and observed in a transmission electron microscope (Model JEM-1200EX II, JEOL, Japan).

Observation of Liposomes by Scanning Electron Micrographs

Scanning electron micrographs were obtained using the specific malachite green fixation technique described in our previous paper (10). Briefly, pieces of qualitative filter paper (Whatman 2) were immersed in the lipid vesicle suspension and then removed rapidly. Lipid vesicles adsorbed on the filter paper were fixed

by immersion for 24 hours at 4°C in 1% (v/v) glutaraldehyde and 1% (w/v) malachite green–mixed buffer solution (NaH_2PO_4-Na_2HPO_4, pH 7.4). After fixation, the lipid vesicles were briefly washed in buffer solution and reacted for eight hours with cold 1% (w/v) osmium tetroxide buffered with phosphate. All samples were subsequently dehydrated in a graded ethanol series. After critical-point drying with liquid carbon dioxide, the fixed lipid vesicles were mounted on a sample stage with double-sided adhesive tape, vacuum coated with gold to a thickness of about 300 Å, and viewed in a scanning electron microscope (Model JSM-T200, JEOL, Japan).

Determination of Particle Sizes of Lipid Vesicles

Particle sizes of lipid vesicles were determined by measuring their diameters on scanning electron micrographs. For each preparation, at least 300 particles were measured in three separate experiments.

RESULTS AND DISCUSSION

Preparation of the Phase Diagram

In simple coacervation, it is important that the lipid solvents such as methanol, ethanol, 1-propanol, and 2-propanol are freely miscible with water or saline solutions as a nonsolvent. It was found that when water was added to these low-molecular-weight alcohols containing phospholipid, phase separation (coacervation) occurred in the systems at an adequate concentration. First, we examined the effects of the kind of alcohol on coacervation by triangular phase diagram, varying the mixing ratio of phospholipid–water–alcohol systems in detail.

Figures 1–4 show each triangular diagram of the phase boundaries of the coacervate system of phospholipid, various alcohols, and water at 20°C. In these figures, the number and types of phase were examined and the percentage composition at which a phase change occurred was calculated. Figure 1 shows the phase diagram of the methanol–phospholipid–water system. The phase diagram presented in this figure is mainly divided into three fields. The viscous gel phase field and the coacervation field are represented by (V) and (C), respectively. The other field (S) indicates lipid solution in aqueous alcohol (methanol). As shown in Figure 1, an increase in the phospholipid concentration in methanol can easily induce coacervation when less water is added. Moreover, an increase in the percentage composition of water from that composition led to the enhancement of viscosity of the system. The further addition of water to that viscous gel phase converted that phase into a suspension.

The ternary phase diagram of the phospholipid–ethanol–water system is shown in Figure 2. Areas (S) and (C) represent the region of lipid solution
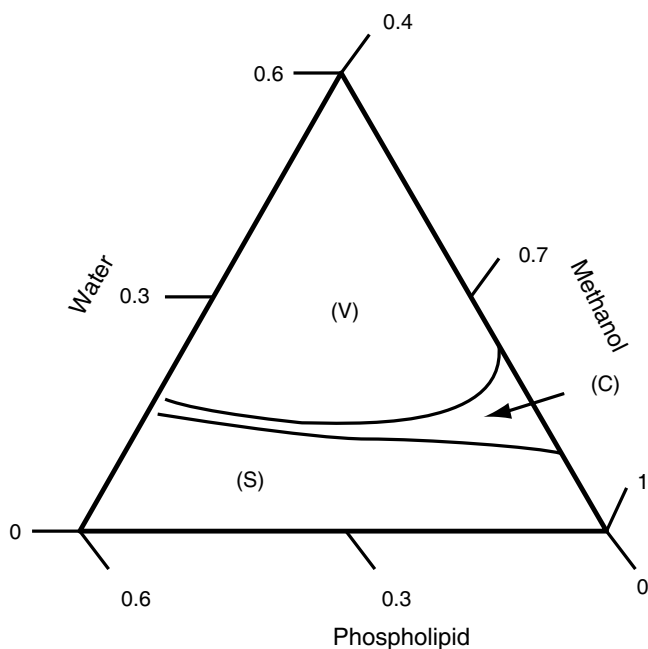
Figure 1 Ternary diagram of the phase boundaries in the phospholipid–methanol–water system: (S) a region of lipid solution in aqueous alcohol; (C) coacervating region; (V) viscous gel phase region.

in aqueous ethanol and the coacervating region, respectively. Then, in the ethanol system, the aggregation area (A) of precipitated phospholipids is observed. As shown in Figure 2, the percentage composition of water of the coacervation area was approximately the same as in Figure 1 when methanol was used as the solvent for phospholipid. Composition of more than 5% of water induced the coacervation for the phospholipids–ethanol–water system. The increase in water content from that percentage composition to the 20% composition of water caused the separation of coacervate precipitation from the suspension.

Figures 3 and 4 show ternary phase diagrams for the 1-propanol–phospholipid–water and 2-propanol–phospholipid–water systems, respectively. In both propanol systems, the coacervation areas lay in a field with a relatively high proportion of water. This is because these alcohols have higher hydrophobicity than ethanol or methanol, which possess affinity for phospholipids (11). Therefore, a large volume of water is required to achieve coacervation in the propanol systems.

For the appearance of coacervate in the phospholipids–alcohol–water system, requirements such as the formation or solvation of colloids and
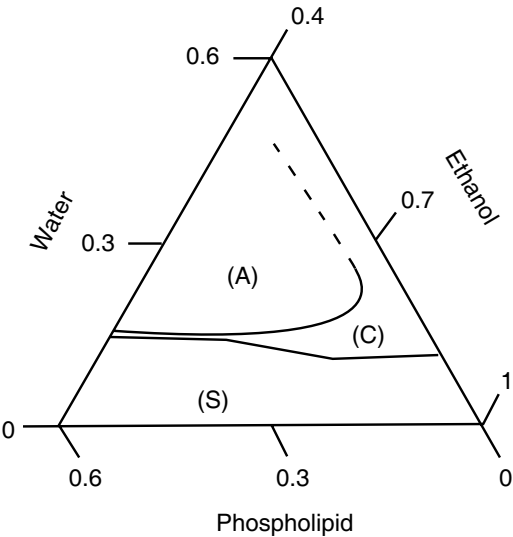
Figure 2 Ternary diagram of the phase boundaries in the phospholipid–ethanol–water system: (S) a region of lipid solution in aqueous alcohol; (C) coacervating region; (A) aggregation region.
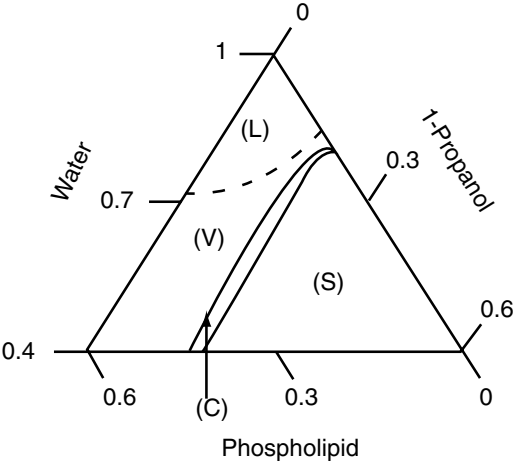
Figure 3 Ternary diagram of the phase boundaries in the phospholipid–1-propanol–water system: (S) a region of lipid solution in aqueous alcohol; (C) coacervating region; (V) viscous gel phase region; (L) liposome suspension region.
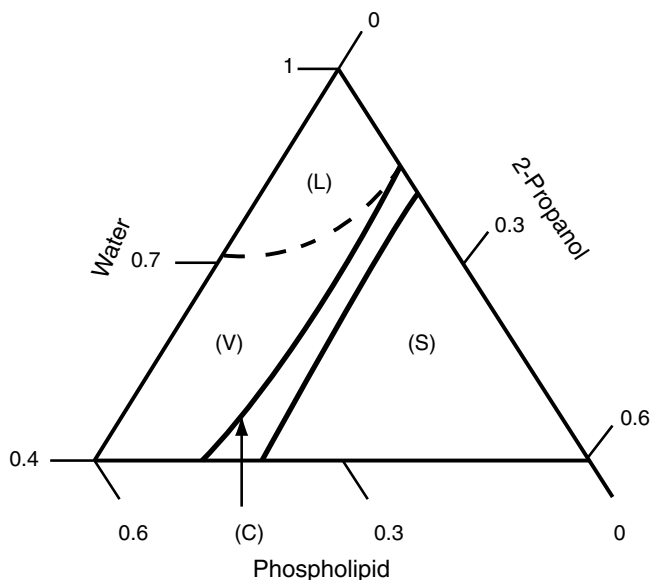
Figure 4 Ternary diagram of the phase boundaries in the phospholipid–2-propanol–water system: (S) a region of lipid solution in aqueous alcohol; (C) coacervating region; (V) viscous gel phase region; (L) liposome suspension region.

suppression of electric repulsion between colloids are needed. When water is added to the alcohol solution containing the phospholipid, the solubility of the phospholipid for the alcohol is decreased with an increase in polarity of the system, and the dissociation of the choline residue of the phospholipid might be promoted. In the coacervating region in the ternary diagrams, it seems that the phospholipid molecules solvated with many alcohol molecules form an association of colloids orientating those head groups toward the water phase (12,13). Furthermore, when water was added into the coacervate phase, the extraction of the alcohol molecules for the water phase by the partition between water and the phospholipid might cause the lamella of the coacervate to produce spherical vesicles (14). Moreover, the vesicles were dispersed in that system by the increase in repulsion among the vesicles as a consequence of the increase in the polarity of the system.

Differences in phase behavior among the alcohols used in this study might be due to the differences in the water content and to the dissociation condition of choline residue, at the point of coacervation in the diagrams. When propanol is used as a solvent for phospholipid, dissociation and repulsion of the polar residues facilitate the organization of phospholipids, as coacervation only occurs in the region with a high percentage of water composition in the system. Furthermore, three-dimensional (3-D) lamella

binding with water form a gel structure owing to the high solubility of phospholipid for the portions of propanol at that point of the ternary phase diagram. On the other hand, the phase separation occurs in the low dissociation of polar residues, because of the low solubility of phospholipid for methanol. In this condition, because the organization of the phospholipid in the continuous phase is insufficient to construct 3-D lamella structure (11), those molecules might take on a random structure.

Ethanol molecules orientated themselves toward the glycerol residue of phospholipid when those were added to the phospholipid bilayer dispersed in water (15). In this study, when only ethanol was used as a solvent, fluidized precipitation of phospholipid was observed. Ethanol was thought to be optimum for the preparation of liposome by the coacervation method with phospholipid used in this study. Furthermore it is also considered that the ethanol stabilizes the lamella with fluidity because ethanol has a peculiar inclination of orientation toward the glycerol residue of the phospholipid molecule (16).

Size Control of Liposomes

At a fixed concentration of phosphatides in the total mixture, the particle size of the lipid vesicles prepared by the coacervates produced from ethanol systems varied with the volume of water added. Figure 5 shows the effect of the percent ratio of water as a poor solvent for lipids in the phospholipid–ethanol–water system on the mean diameter of the resulting lipid vesicles. As seen in Figure 5, an increase in the volume of water in the system resulted in a decrease in particle size of the lipid vesicles. This was because the increase in the volume of water produced an increase in hydrophobic bonding among the lipid molecules. By addition of an appropriate volume of water as a poor solvent for lipids, the mean diameter of the resulting lipid vesicles could be controlled within the range of 200 to 2000 nm. We have found that the formation and the mean diameter of the lipid vesicles depend significantly upon the phospholipid–ethanol–water ratio. Furthermore, it was found that the lipid vesicles prepared in the phospholipid–methanol–water system and phospholipid–1-propanol–water system could be controlled within the particle size range of 100 to 1000 nm and the range of 50 to 300 nm, respectively.

Observation of the Inner Structure of Liposomes

The most important characteristics of lipid vesicles are generally their lamellarity and size. Lamellarity is the number of lipid bilayers surrounding the inner aqueous space. Negative-stain electron microscopy is not suitable for the determination of droplet size or estimation of the lamellarity of the original particles because of vesicle distortion during specimen preparation (17). On the other hand, freeze-fracturing reveals some unique aspects of the internal lamellae when cross-fracturing occurs between nonpolar lipid
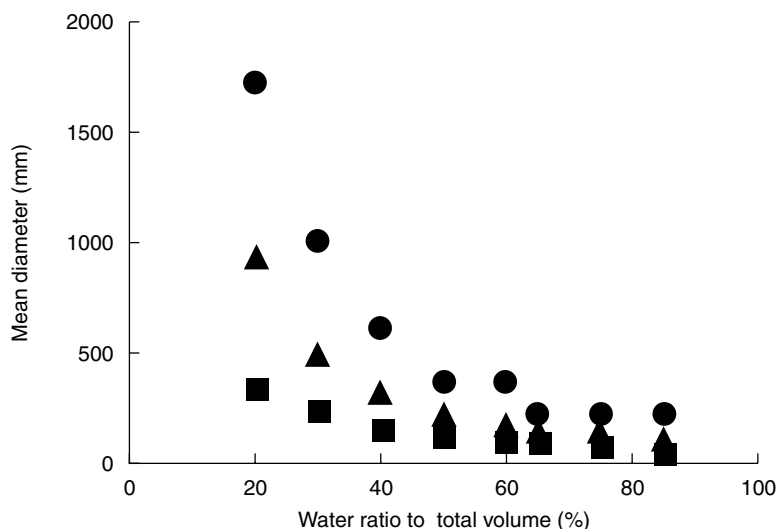
Figure 5 Effect of added water on the particle size of lipid vesicles in the phospholipid–various alcohol–water systems: (▲) phospholipid–methanol–water; (●) phospholipid–ethanol–water; (■) phospholipid–1-propanol–water.

layers. Figure 6 shows freeze-fracture micrographs of vesicles prepared by the coacervation technique. The majority of the vesicles formed using methanol as a solvent appear to be large and unilamellar, ranging in diameter from 100 to 1000 nm, as shown in the micrographs (Fig. 6A).

Although it is easy to obtain fractures exposing the inner surface membrane, it is difficult to obtain good fractures exposing the multilamellar vesicles. As illustrated in Figure 6B, when the vesicles are prepared using ethanol as a solvent, concentric lamellae of multilamellar vesicles are observed. Because cross-fracturing always occurs between nonpolar lipid layers (18), the fracture view of the internal lamellae supports an uneven number of lipid layers. Perette et al. (19) reported similar results due to the formation of a proliposome mixture containing lipid, ethanol, and water.

Figures 6C and 6D show the electron micrographs of lipid vesicles prepared using 1-propanol and 2-propanol, respectively. Relatively homogeneous preparations yield unilamellar vesicles with diameters ranging from 50 to 300 nm.

The findings shown in Figure 6 indicate the importance of solvent hydrophilicity and the phospholipid–alcohol–water ratio with respect to the formation and structure of lipid vesicles. In the coacervation technique, we can control the size and lamellarity of the lipid vesicles merely by using different low-molecular-weight alcohols as a lipid solvent. Furthermore, the
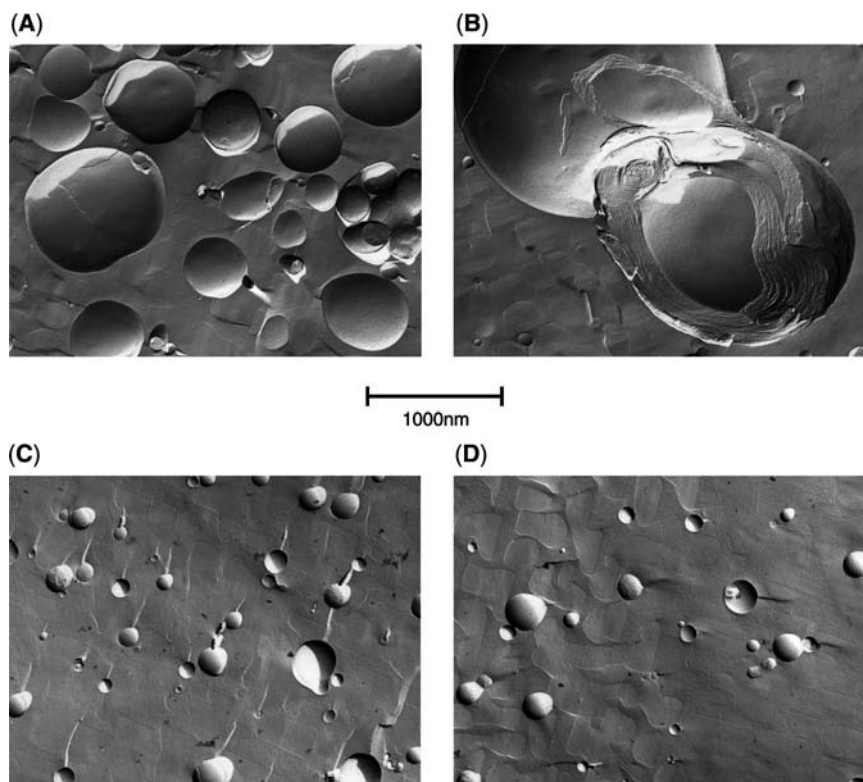
Figure 6 Freeze-fracture electron micrographs of lipid vesicles prepared in various systems: **(A)** phospholipid–methanol–water; **(B)** phospholipid–ethanol–water; **(C)** phospholipid–1-propanol–water; **(D)** phospholipid–2-propanol–water.

vesicles prepared using methanol and ethanol may be larger than those prepared using propanol.

Observation of Outer Surface of Liposomes

The scanning electron microscopy can be used to examine the homogeneity of the surface topography of the lipid vesicles, in contrast with freeze-fracture electron micrographs. Previously, we reported a specific fixation technique using malachite green, which adheres to phospholipid components (10). Using this technique, complete images of lipid vesicles can be obtained by scanning electron microscopy. Figure 7 shows typical scanning electron micrographs of lipid vesicles prepared using various low-molecular-weight alcohols as a lipid solvent. All of the vesicles were spherical particles with smooth surfaces. In particular, as shown in Figure 7, highly homogeneous
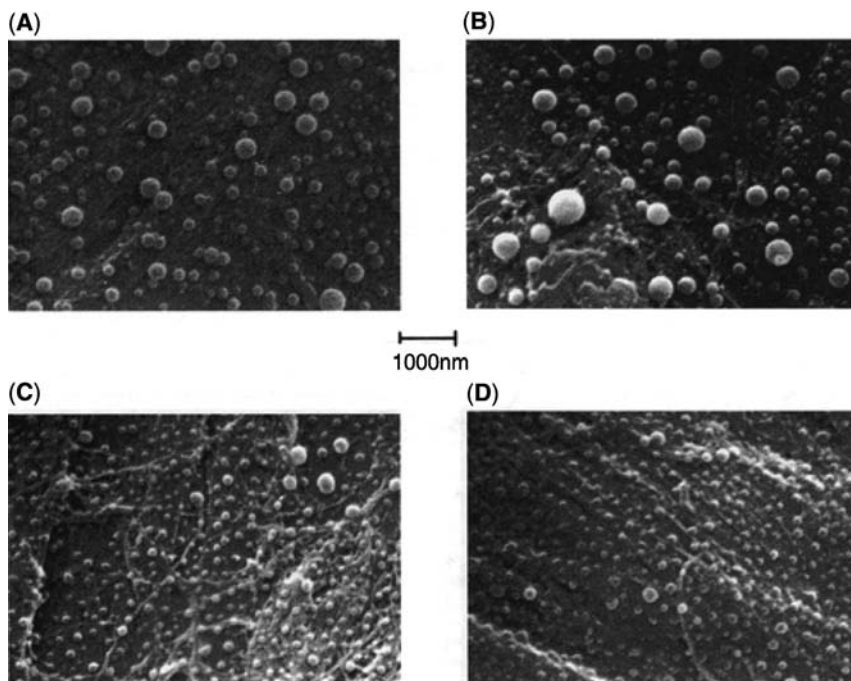
Figure 7 Scanning electron micrographs of lipid vesicles fixed using the malachite green technique: **(A)** phospholipid–methanol–water; **(B)** phospholipid–ethanol–water; **(C)** phospholipid–1-propanol–water; **(D)** phospholipid–2-propanol–water.

populations of vesicles were produced using 1-propanol (Fig. 7C) or 2-propanol (Fig. 7D) as the lipid solvent, in comparison with methanol (Fig. 7A) or ethanol (Fig. 7B).

CONCLUSIONS

We found that the coacervation technique can be used for the preparation of lipid vesicles of the required size and lamellarity by varying the type of lipid solvent employed. Coacervation is a unique way of forming various types and sizes of lipid vesicles spontaneously without the need for special equipment or modification of the lipid components. The procedure does not use solvents that give rise to pharmaceutically unacceptable residues and does not involve sonication steps, which are difficult to scale up.

This well-characterized system may be used quantitatively as a biological model membrane for studies on the fusion of membranes, the functional reconstitution of membrane-bound proteins, and the permeability of low-molecular-weight materials such as ions and amino acids, and can

be valuable as a drug carrier for encapsulation and sustained and controlled release of various drugs within the body. The coacervation method is a simple, reproducible method for the mass production of liposomes as the carriers for drug delivery systems or gene delivery systems.

REFERENCES

1. New RRC. Preparation of liposomes. In: New RRC, ed. Liposomes—A Practical Approach. New York: Oxford University Press, 1990:36–90.
2. Ishii F. Production and size control of large unilamellar liposomes by emulsification. In: Gregoriadis G, ed. Liposome Technology. Vol. 1. 2d ed. Boca Raton, FL: CRC Press, 1992:111–121.
3. Ishii F, Takamura A, Ogata H. Preparation conditions and evaluation of the stability of lipid vesicles (liposomes) using the microencapsulation technique. J Dispersion Sci Technol 1988; 9:1–15.
4. Kim S, Martin GM. Preparation of cell-size unilamellar liposomes with high captured volume and defined size distribution. Biochim Biophys Acta 1981; 646:1–9.
5. Nagasaka Y, Ishii F. Preparation conditions of liposomes using a novel device for liposome production based on microencapsulation method. Material Technol 2000; 18:363–369.
6. Nii T, Takamura A, Mohri K, Ishii F. Factors affecting physicochemical properties of liposomes prepared by hydrogenated purified egg yolk lecithins by the microencapsulation vesicle method. Colloids Surf B Biointerfaces 2003; 27: 323–332.
7. Ishii F, Takamura A, Ishigami Y. Procedure for preparation of lipid vesicles (liposomes) using the coacervation (phase separation) technique. Langmuir 1995; 11:483–486.
8. Saegusa K, Ishii F. Triangular phase diagrams in the phospholipid–water–alcohol system for the preparation of lipid vesicles (liposomes) using the coacervation technique. Langmuir 2002; 18:5984–5988.
9. Ishii F, Nagasaka Y. Interaction between erythrocytes and free phospholipids as an emulsifying agent in fat emulsions or drug carrier emulsions for intravenous injections. Colloids Surf B: Biointerfaces 2004; 37:43–47.
10. Ishii F, Takamura A, Noro S. Observation of liposomes by scanning electron microscope. Membrane 1982; 7:307–308.
11. Chiou J, Krishna PR, Kamaya H, Ueda I. Alcohols dehydrate lipid membranes: an infrared study on hydrogen bonding. Biochim Biophys Acta 1992; 1110: 225–233.
12. Rottenberg H. Probing the interactions of alcohols with biological membranes with the fluorescent probe Prodan. Biochemistry 1992; 31:9473–9481.
13. Rowe ES. Thermodynamic reversibility of phase transitions. Specific effects of alcohols on phosphatidylcholines. Biochim Biophys Acta 1985; 813:321–330.
14. Klemm WR. Biological water and its role in the effects of alcohol. Alcohol 1998; 15:249–267.
15. Barry JA, Gawrisch K. Direct NMR evidence for ethanol binding to the lipid-water interface of phospholipid bilayers. Biochemistry 1994; 33:8082–8088.

16. Vierl U, Lobbecke L, Nagel N, Cevc G. Solute effects on the colloidal and phase behavior of lipid bilayer membranes: ethanol-dipalmitoylphosphatidylcholine mixtures. Biophys J 1994; 67:1067–1079.
17. Johnson SM, Bangham AD, Hill MW, Korn ED. Single bilayer liposomes. Biochim Biophys Acta 1971; 233:820.
18. Verkleij AJ, de Gier J. In: Knight CG, ed. Liposomes. Amsterdam: Elsevier/North-Holland Biomedical Press, 1981:83–103.
19. Perette S, Golding M, Williams WP. A simple method for the preparation of liposomes for pharmaceutical applications: characterization of the liposomes. J Pharm Pharmacol 1991; 43:154–161.

3

Preparation of Liposomes and Oily Formulations by Freeze-Drying of Monophase Solutions

ChunLei Li

ZhongQi Pharmaceutical Technology Co., Ltd., Shijiazhuang City, Hebei Province, P.R. China

YingJie Deng

School of Pharmacy, Shenyang Pharmaceutical University, Shenyang City, Liaoning Province, P.R. China

JingXia Cui

School of Pharmacy, Hebei Medical University, Shijiazhuang City, Hebei Province, P.R. China

INTRODUCTION

Freeze-drying (also known as lyophilization) has been a standard practice employed to manufacture many pharmaceutical products. The overwhelming majority of these products are lyophilized from simple aqueous solutions. Typically, water is the only solvent that must be removed from the solution via the freeze-drying process. However, there are still many instances where pharmaceutical products are manufactured via a process that requires freeze-drying from organic cosolvent systems (1).

The cosolvent system that has been most extensively investigated is the tertiary butyl alcohol (TBA)/water combination. Freeze-drying using

TBA/water cosolvent systems was first evaluated by Kasraian and DeLuca in 1995 (2,3). In the subsequent years, the growing interest in using TBA in freeze-drying has led to a series of investigations on TBA/water combination (4–8). It has been found that freeze-drying using TBA/water cosolvent systems may offer many advantages over simple drying from an aqueous solution, which may include increased drug wetting or solubility, increased sublimation rates and hence decreased drying time, increased predried bulk solution or dried product stability, decreased reconstitution time, and possible enhancement of sterility assurance of the predried bulk solution (1).

It should be noted, though, that there are additional uses for the technique of the freeze-drying from TBA/water cosolvent systems other than the optimization of the freeze-drying process. Observations from our laboratory has shown that freeze-drying of TBA/water cosolvent systems can be used to prepare submicron liposomes of narrow size distribution (9) and oil solution formulations of hydrophilic drugs. Based on our work, it is found that both hydrophilic and hydrophobic species can be simultaneously dissolved in TBA/water cosolvent system with an appropriate volume ratio to form an optically clear monophase solution. Lyophilization of the resulting monophase solution will obtain a homogenous codispersion of hydrophilic and hydrophobic species. Further treatment of this kind of solid dispersions will result in the formation of liposomes and oil solution formulations. In this chapter, we will mainly discuss two novel technologies developed in our laboratory.

PREPARATION OF LIPOSOMES

The superiority of liposomes as drug carriers has been widely recognized (10). To realize the industrial-scale production of liposomes, a great many preparation methods have been developed (11). Although some of these methods have been successfully used for the production of liposomes on a large scale, they still suffer from one or more deficiencies including the use of pharmaceutically unacceptable solvents, an additional sizing process, multiple-step drug entrapment procedure, the need for special equipments, and lack of accepted and easy-to-perform technology for sterilization.

A novel procedure is presented here for the preparation of sterile and pyrogen-free submicron liposomes of narrow size distribution. The procedure is based on the initial formation of an optically clear solution by dissolving liposome-forming lipids and water-soluble carrier materials such as sucrose in TBA/water cosolvent systems, which is then lyophilized to remove solvents after sterilization by filtration through 0.22-μm pores. On addition of water, the lyophilized product will spontaneously form homogenous submicron liposomes.

Experimental Section

Lipids and Chemicals

Soybean phosphatidylcholine (SPC, purity of more than 92%), soybean phosphatidylserine (SPS, purity $>90\%$), hydrogenated SPC (HSPC, purity of more than 95%), and soybean phosphatidylglycerol (SPG, purity of more than 95%) were kind gifts from Degussa (Freising, Germany). 1,2-dipalmitoyl-SN-glycero-3-phosphocholine (DPPC) was purchased from Sigma (St. Louis, MO, U.S.A.). Cholesterol was purchased from Shenyang Medicines Company (Shenyang, China). All other chemicals were of analytical reagent grade.

Liposome Preparation

SPC was dissolved in TBA and water-soluble carrier materials such as sucrose were dissolved in water. These two solutions were mixed in an appropriate ratio to get a third monophase solution. After filtration through 0.22-µm pores, the monophase solution was filled into the 10-mL freeze-drying vials with a fill volume of 2 mL.

A laboratory freeze-drier (FD-1, Beijing Bioking Technology Company, China) was used. The freeze-drying process was as follows: (i) freezing at $-40°C$ for eight hours; (ii) primary drying at $-40°C$ for 48 hours; (iii) secondary drying at 25°C for 10 hours. The chamber pressure was maintained at 20 Pa during the drying process.

Lyophilized products were reconstituted by addition of equal volume of water and gentle shaking, which led to the formation of the aqueous suspensions of liposomes.

Size Measurements

The average diameter and size distribution of the liposomes were measured using a submicron particle analyzer—Zetasizer Nano ZS (Malvern, Southborough, United Kingdom).

Thermal Analysis and X-Ray Diffraction

Differential scanning calorimetry was carried out with Perkin-Elmer 7 series thermal analysis system, which was equipped with mechanical cooling. Diffraction data were collected by D/max 2400 Diffractometer (9).

Results and Discussion

The Formation of Monophase Solution

Based on our investigation, the ternary phase diagram of SPC, TBA, and water mixtures could be divided into at least three main regions, corresponding to a clear solution of SPC in aqueous TBA, the suspension of stacked hydrated lipid bilayers in excess aqueous TBA, and the suspension of heterogeneous liposomes (9).

For the phospholipids (PLs) that are insoluble in pure TBA (such as SPS and SPG), monophase solutions can also be obtained by dissolving PLs in the cosolvent systems. However, an additional insoluble region might be found in the corresponding ternary phase diagram.

Here, it is important to note the different solubility characteristics of different PLs. For natural PLs with low phase-transition temperatures (T_m), their solubility in cosolvents is almost independent of temperature. Therefore, during the cooling process, the ternary mixtures can maintain the isotropic status. However, it is not the case for PL with a high T_m such as DPPC and HSPC, whose solubility in cosolvents decreases markedly with the decreasing temperature. Accordingly, the appearance of lipid precipitates is inevitable during the cooling process, which might lead to the heterogeneity of final liposome suspensions. In all, the usage of natural PL with a low T_m might be a rational choice provided that our method is used.

The Cooling of Monophase Solution

According to the phase diagram of TBA/water mixtures, cooling the mixtures with a TBA/water volume ratio ranging from 1:1 to 1:2 resulted in the formation of solid TBA hydrates and eutectic A in turn (2). Thus, two peaks can be found in the relevant DSC thermograms. When the TBA/water mixtures were supplemented with sucrose or SPC, the resulting diagram still had two peaks, but the peak positions changed with the change of the components of mixtures. Inclusion of SPC in the frozen solutions led to the altered position of TBA hydrate peak and inclusion of sucrose induced the position change of eutectic A peak, which implies that during the cooling process SPC accumulated in the TBA-rich phase, and sucrose existed in the water-rich phase. Because SPC possesses strong affinity to TBA and sucrose has excellent solubility in water, it is reasonable to draw the above conclusion.

The Lyophilized Powder

Other work has proved that solid-state PLs obtained from lyophilization spontaneously form highly structured stacked lamellae (12). But, using X-ray diffraction technology, we found that there were no detectable stacked lamellae or large unilamellar vesicles (LUVs) in the lyophilized products. Although during the cooling and drying process, vesicles or stacked lamellae cannot be formed as in traditional method, we still believe that PLs will self-aggregate and rearrange themselves to form specific lamellar structures. Usually, only four kinds of lamellae can be formed: unclosed stacked lamellae, closed stacked lamellae [multilamellar vesicles (MLVs)], closed separate bilayers (LUVs), and unclosed separate bilayers [phospholipid bilayer fragments (PBFs)]. Based on our results, it may be the only possibility that PLs form PBFs. Why freeze-drying could induce the formation of PBFs will be discussed in detail in a later section.

In fact, the final lyophilized products should be regarded as solid dispersions, in which tiny PBFs were uniformly dispersed in amorphous matrix such as dry sucrose glass.

The Formation of Liposomes

On addition of water, the lyophilized products could spontaneously form liposome suspensions. The size and size distribution of final liposome preparations are strongly dependent on the following factors.

Lipid Composition: For the purpose of achieving submicron and monodisperse liposome preparations, only PLs with a low T_m can be employed. Our method is not applicable to the synthetic PLs with high T_m. Furthermore, inclusion of a small fraction of charged PLs (e.g., SPS) in the formulation could significantly decrease the vesicle size. Reconstruction of the solid dispersion with SPC:SPS:sucrose equal to 9:1:50 (w/w/w) can lead to the formation of liposomes with a volume mean size of 75.7 nm. In contrast, if the formulation did not contain SPS, the liposome size increased to 131.6 nm.

Types of Carriers: Water-soluble carriers with different molecular weights can be used in our method with equal ease, but different carriers might exert different influence on the final liposome preparations. When disaccharides such as sucrose and trehalose are used as carriers, the size of final liposomes is usually in the range of 100 to 200 nm, provided that sugar/lipid weight ratio is less than two. However, when water-soluble polymers such as PEG-8000 were employed, liposomes in the micron range will be obtained, which could be easily observed in optical microscope.

The Carrier/Lipid Ratio: The carrier/lipid ratio might play an important role in the uniformity of final liposome preparations. It is found that the increasing sucrose/lipid ratio resulted in smaller size and narrower size distribution. Accordingly, we may control the uniformity and size of resulting liposome preparation by carefully adjusting the carrier/lipid ratio.

The Possible Liposome Formation Mechanism

A different liposome preparation method often involves a different liposome formation mechanism; hence, it is desirable to put forward a model to expound why this method results in the formation of submicron and monodisperse liposome preparations.

In the study, the TBA/water volume ratio of initial solutions ranges from 1:1 to 1:2 and the SPC concentration is less than 20 mg/mL. Under this circumstance, we detected no particles in the monophase solutions using a submicron particle analyzer, whose detection range is from 0.6 to 6000 nm. Therefore, SPC might be dispersed in the cosolvents in the form of single molecule.

Upon cooling, first solid TBA hydrate will crystallize from the system. Because the crystallization of solid TBA hydrate results in the formation of new ice–water interface, SPC will preferably adhere to the surface of solid TBA hydrate to drop the surface tension (13). Perhaps due to the adherence of SPC on the surface of solid TBA hydrate, the crystallization behavior of TBA hydrate has been modified, resulting in the altered peak position on DSC thermograms. Then, as the temperature is continually lowered, more lipid-rich solid TBA hydrate will crystallize and the unfrozen bulk solution becomes a concentrated sucrose solution, which has high water content. Owing to the existence of noncrystallizing solute, sucrose, the bulk solution will thoroughly solidify to form sucrose glass when the temperature is lowered to a point. Therefore, the frozen solution is a dispersion of lipid-rich solid TBA hydrate in sucrose glass.

During the solvent removal process, SPC on the surface of TBA hydrates will arrange themselves to form PBFs, in which the head groups orient toward sucrose and are further stabilized by sucrose (14), and the aryl chain regions may orient toward the center of bilayer and are stabilized by hydrophobic interactions among them.

On addition of water, the PBFs might spontaneously curve and seal to form liposome suspensions. A schematic representation of this model can be found in Figure 1.

In accordance with this model, if the aggregation and fusion between different PBFs are effectively inhibited, the polydispersity index and size of liposomes will directly relate to the uniformity and size of solid TBA hydrate.

Quick calculation has shown that if the solid TBA hydrate has a volume equivalent spherical diameter of 150 to 400 nm, each PBF may contain enough lipids to form an entire liposome, ranging from 100 to 200 nm (9). Based on our observation, this size range of solid TBA hydrate may be formed if the freezing process is well controlled.

In our method, sucrose may serve many functions. Firstly, during cooling of initial solutions, high viscosity of sucrose solutions may inhibit the appearance of large solid TBA hydrate, which forces the formation of tiny PBFs. Secondly, it might prevent the fusion of different PBFs during the drying process and in dry status. Thirdly, on addition of water, sucrose might prevent the aggregation and fusion of different PBFs, which also guarantees the formation of monodisperse liposome preparation. These might be true because the hydration of a lyophilized product with a low sucrose/lipid ratio achieves a heterogeneous liposome preparation, which may be indicative of the fusion of different PBFs. Moreover, Crowe et al. (14–16) have showed that liposomes (about 100 nm in diameter) are stable during lyophilization in the presence of 2 g sucrose/g lipid. This appears to correspond to the amount of sucrose necessary to achieve monodisperse liposome preparation in our method.

Figure 1 Schematic representation of the liposome formation process. (**A**) T... genous solution of SPC and sucrose in TBA/water mixture. (**B**) Solid TBA... surrounded by SPC. (**C**) **Rearrangement of SPC to form PBFs.** (**D**) Liposome f... on addition of water. *Note:* sucrose is not shown. *Abbreviations:* SPC, soybean ... tidylcholine; TBA, tertiary butyl alcohol; PBFs, phospholipid bilayer fragmen...

This liposome formation model can be used to expound almos... phenomena associated with the novel method. Perhaps it is just... PEG8000 cannot inhibit the fusion of different PBFs that lipos... the micron range will be obtained on hydration of PL/PEG solid... sions. For negatively charged PLs such as SPS, it can effectively... the increase of solid TBA hydrate size through electrostatic repulsi... adhesion on the surface of TBA hydrate, thus leading to the form... small-size liposomes.

The Preparation of Drug-Containing Liposomes

Usually, there are two kinds of approaches for loading drugs into lip... namely, passive loading and active loading. If the drug of interest h...

solubility in TBA/water and good affinity to PLs due to hydrophobic interaction or electrostatic interaction or both interactions, it is reasonable to encapsulate the drug by passive loading approach, which involves the formation of a dispersion of PLs and drug in carrier materials.

If the drug can be loaded in response to some gradients, it is desirable to adopt the active loading method. When active loading is used in combination with our method, a three-component liposome treatment system can be provided, which is composed of dry dispersions for forming empty liposomes, buffer for exterior pH adjustment, and the drug. In fact, sometimes a two-component system can also be used, which includes a dispersion of drug, internal buffer such as citric acid and lipids in carrier materials, and a pH-adjustment buffer solution.

When our method is used, the stability problems related to drug retention during shelf time will be resolved because the liposome formation and the drug loading can be performed just prior to clinical use (under the situation that the loading efficiency and capability are acceptable).

The Comparison of Our Method with Other Methods

Here our method is compared with two relevant liposome preparation methods: Evans' method (17) and ethanol injection technology.

Evans' method was reported in the 1970s and involved the freeze-drying of the solution of PLs in TBA to form liposomes. The main difference between Evans' method and ours is that our method results in the formation of monodisperse liposome preparations in the range of 100 to 200 nm, but Evans' method produces heterogeneous large MLVs in micron range. Usually the optimal liposome size for parenteral administration is between about 100 and 300 nm, because this size range of liposomes gives uniform and predictable drug-release rate and stability in the bloodstream. Furthermore, liposomes with a size of less than 150 nm are useful in targeting tumor tissue, hepatocytes, and ischemic myocardial tissue (18–20).

In addition, Evans' method is only suitable for lipophilic drugs that can be dissolved in TBA in a therapeutically effective amount, and our method can be used to load many drugs irrespective of whether they are lipophilic or not. Furthermore, because the water-soluble substances such as citric acid can be included in the final lyophilized product, active loading of drugs into liposomes is possible using our method. Active loading is a very important means that has led to three commercially available liposomal products: Daunoxome®, Doxil®/Caelyx®, and Myocet®.

Alcohol injection method is a robust technology in comparison with other liposome preparation methods and has been developed by two pharmaceutical companies: Alza and Polymun. Alza's production procedure involves the extrusion of the heterogeneous liposomes (21). In contrast, Polymun uses a cross-injection module to produce uniform liposomes (22). On the liposome formation, ethanol could be removed by cross-flow

dialysis. Alcohol injection method possesses many advantages such as simplicity and energy conservation, but if a dry product is preferable due to problems associated with aqueous liposome preparations, our method may provide an option.

SOLUBILIZATION OF HYDROPHILIC DRUGS IN OIL

The advent of modern biotechnology has afforded the ready availability of a wide range of biological molecules (e.g., polypeptides) as therapeutic agents. But these hydrophilic molecules are usually hard to formulate due to their liability to hydrolysis and inability to cross cellular membranes and other biological barriers (23).

To address these two problems, various approaches have been tested with varying degrees of success, of which solubilization of hydrophilic molecules in pharmaceutically acceptable hydrophobic solvent might be a rational design. Now, two solubilization approaches have been developed, which involve the formation of hydrophobic ion–paired complexes (24–28) and dehydrated hydrophile/amphiphile complexes (29,30), respectively.

The HIP process is composed of the binding of stoichiometric amount of ionic detergents to oppositely ionic compounds and the solubilization of the resulting HIP complexes that display altered solubilizing properties (26). Most of the work to date on HIP complexes have focused on basic drugs and anionic detergents. Because cationic detergents are relatively toxic, it is almost impossible to extend this approach to acidic compounds. In addition, this approach is not applicable to neutral macromolecules, and certainly not to small hydrophilic molecules.

In contrast, the second method does not need the strong ionic interaction between the components, and it can be used to solubilize almost all hydrophilic species in oil irrespective of their molecular shape, size, and charge. This method consists of a multistep preparation procedure, which involves the formation of MLVs, the conversion of MLVs to small unilamellar vesicles (SUVs), and the lyophilization of the mixtures of SUVs and hydrophilic species followed by reconstruction with oil phase (30). Accordingly, this method is complicated and hard to scale up in comparison with the HIP process.

Here we present a simple, flexible, and novel solubilization procedure, which involves the dissolution of amphiphiles (e.g., PLs) and hydrophilic molecules in TBA–water cosolvent systems followed by freeze-drying, followed by reconstruction with oil phase.

Experimental Section

Materials

SPC, with more than 92% purity, was a kind gift from Degussa (Freising, Germany). Sodium ursodeoxycholate was generously provided by Tianjin

Pacific Pharmaceutical Co. Ltd. (Tianjin, China). Caprylic/capric triglyceride (MCT) was kindly provided by Condea Chemie GmbH (Witten, Germany). Medium-chain partial glycerides (MCM) were obtained from Karlshamns AB (Karlshamn, Sweden). Polysorbate 80 was a product of Croda (Singapore). Calcein was purchased from Sigma (St. Louis, MO, U.S.A.). Thymopentin (TP5) is a product of Chengdu Diao group (Chengdu, China). Insulin (27.6 IU/mg) was obtained from Xuzhou Wanbang Biochemical Company (Xuzhou, China). All other chemicals were of analytical reagent grade.

The Preparation of Oily Formulations

First, lipophilic substances (e.g., SPC) and hydrophilic substances (e.g., model drugs) were dissolved in TBA and purified water, respectively. Monophase solution can be obtained by mixing above solutions in an appropriate ratio. After filtration through 0.22-μm pores, the isotropic solution was filled into the 10-mL freeze-drying vials with a fill volume of 1 mL and lyophilized in a laboratory FD-1 (Beijing Bioking Technology Company, China).

The freeze-drying process was performed as described above. After lyophilization, 1-mL oil phase was added to the freeze-drying vial, resulting in the formation of an optically clear oil solution.

The Studies on the Solubilization Procedure

To determine whether the monophase solution contained tiny micelles, a submicron particle analyzer—Zetasizer Nano ZS (Malvern, Southborough, United Kingdom)—was used, whose detection range is from 0.6 to 6000 nm.

The total amount of residual solvents was determined by thermogravimetric analysis (TGA). The residual levels of TBA were measured using gas chromatography method described by Gogineni et al. (31). Thus, the weight percentage of water in the lyophilized cakes can be calculated by subtraction of the residual level of TBA from the total amount of residual solvents.

To determine whether effective solubilization has been achieved, the absorption value of final preparation was determined using a UV–visible spectrophotometer. The detection wavelength was usually set at 400 nm. If the final preparation was optically clear and its absorption value was not significantly different to that of control solution, it was regarded that effective solubilization has been realized.

To investigate the factors that may affect the solubilization, formulations with different amphiphile/drug ratios and different amphiphile–oil phase combinations were prepared.

The Main Formulations Used in this Study

The formulations could be divided into two groups. For type 1 formulations, SPC was used as "masking agent" and oil phase was composed of MCT. But in the case of type 2 formulations, the oil phase comprised

MCM and polysorbate 80 (9:1, w/w) and both SPC and bile salt were used as ''masking agents.'' Here a small fraction of polysorbate 80 was used to increase the self-emulsification properties of oil solutions.

Analysis of Model Drugs

Before analysis, the oil-based formulations were mixed with purified water and vortexed for 30 sec to form emulsions. The emulsions were centrifuged at 50,000 g for 30 min using CS120GX ultracentrifuge (Hitachi Koki Co., Japan) to obtain component phases.

The calcein concentrations in all component phases were determined using a fluorescence spectrophotometer (930, Shanghai Analytic Instrument Company, China). The excitation wavelength and emission wavelength were set at 400 nm and 530 nm, respectively. To explore whether a fraction of drugs were released in liposome-entrapped form from type 1 formulation, a method first described by Oku et al. (32) was employed.

A stability-indicating reversed-HPLC method was used to determine the long-term stability of TP5 oil solution (33).

For the analysis of insulin, two different HPLC methods were used, which can be found in Ref. 34.

In Vivo Studies

Animals: The animal models employed for testing oily formulations of insulin were Wistar rats (male, weighing about 0.25 kg) and New Zealand albino rabbits (male, weighing about 2 kg), which were provided by the pharmacological laboratory of Shenyang Pharmaceutical University. The study protocol was approved by the Institutional Animal Care and Use Committee (Shenyang Pharmaceutical University, China).

Hypoglycemic Effect of Insulin in Nondiabetic Rabbits: At least 10 days before the dosing, an indwelling catheter was inserted into a carotid artery for blood sampling. Before experiments, rabbits were fasted for 18 h. Nondiabetic rabbits were injected subcutaneously into the neck region with a single injection of insulin aqueous solution and oil solution (type 1 formulation), respectively.

Oral Insulin Absorption in Diabetic Rats: Diabetes was induced by intravenous injection of 36 mg/kg of tetraoxypyrimidine in male Wistar rats. The rats were considered to be diabetic if the basal glucose levels were more than 10 mM. Three days after the induction of diabetes and 24 hours before experiment, a catheter was implanted in the carotid artery and a fine plastic cannula was surgically inserted into the duodenum of the rat. With the intention of determining the efficacy of oil-based formulation, a type 2 formulation and insulin aqueous solution were intraduodenally

administrated to two groups of fasted rats at a dose of 8 mg/kg. In addition, control oil solution was administrated to the control group. To roughly estimate relative bioavailability of insulin, insulin aqueous solution was subcutaneously injected to a group of rats at a dose of 2 mg/kg.

Blood Sampling and Glucose Analysis: Blood samples were collected from carotid artery before the administration and at different times after dosing. The plasma glucose level at zero time was taken as 100% glucose level. The plasma glucose level was determined by the glucose-oxidase method.

Statistical Analysis: The results in both figures are shown as the mean values of plasma glucose levels $\pm$ standard deviations of animals of individual groups ($n = 8$, for diabetic rats; $n = 6$, for nondiabetic rabbits). In Figure 2, the hypoglycemic effect of different formulations at each time point was compared using a series of two independent sample t tests. In Figure 3, the hypoglycemic effect of different formulations in rats at each time point was examined using one-way, analysis of variance. Post-hoc comparisons of the means of individual groups were performed using Turkey's Honestly Significant Difference test. In both cases, a p value of less than 0.05 was considered to be statistically significant.
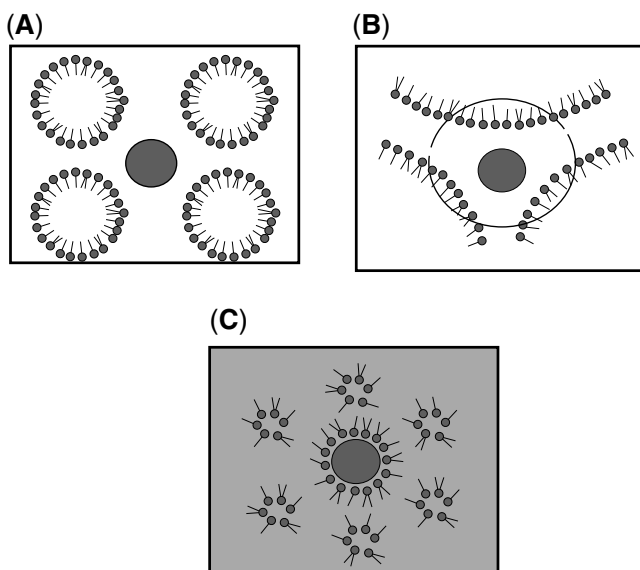
Figure 2 (**A**) Schematic representation of the solubilization process for the oil-based formulations, showing the solution of hydrophilic drugs and micelles. (**B**) Codispersion of hydrophilic drugs and amphiphiles after solvent removal and (**C**) the formation oil solution on addition of oil.
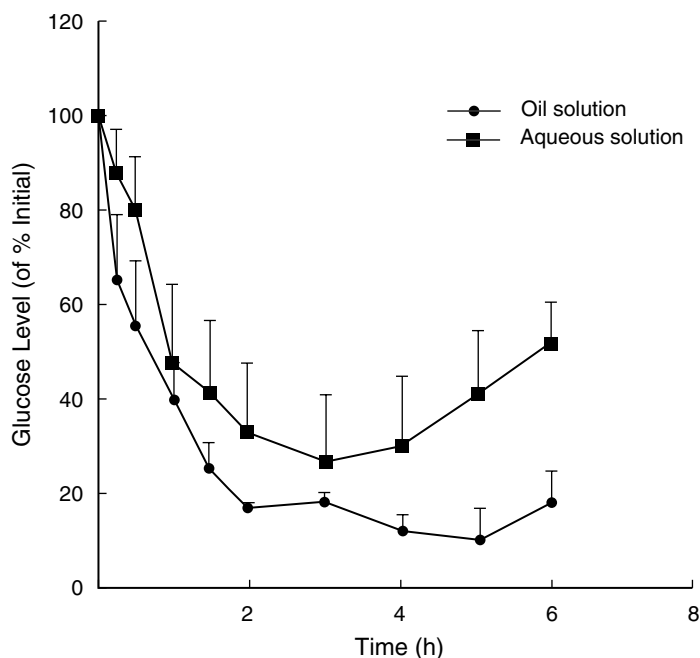
Figure 3 Plasma glucose levels obtained in rabbits following SC injection of insulin oil solution (type 1 formulation) and insulin aqueous solution (0.25 mg/kg) (mean ± sd, $n = 6$); $p < 0.05$, oil solution versus aqueous solution. *Abbreviations*: sd, standard deviation; SC, subcutaneous.

Results and Discussion

Factors Affecting Solubilization

Formation of Monophase Solution: As described in previous work, the ternary phase diagram of SPC/TBA/water can be divided into three main regions corresponding to a clear monophase solution, the suspension of stacked hydrated lipid bilayers, and the suspension of heterogeneous liposomes (9). In our method, the hydrophilic drugs are preferably dissolved in the isotropic solution phase to facilitate sterilization by filtration through 0.22-μm pores and guarantee the uniformity of final preparations.

If SPC and bile salt are simultaneously used as "masking agents" and the molar ratio of bile salt to SPC is more than 1, an isotropic micellar solution can be easily achieved and it is not necessary to refer to the three phase diagram of SPC/TBA/water.

The Optimum Combination of Oil and Amphiphile: Although there is no restriction on the nature of solubilized materials, the correct choice of

amphiphile and oil is still crucial to the success of solubilization. Our data show that if SPC is used as a "masking agents," both MCM and MCT can be employed. In contrast, if SPC and bile salt are simultaneously used as "masking agents," it is necessary to adopt MCM as oil medium and sodium citrate as solubilization aid.

Ratio of Amphiphile to Hydrophilic Drug: To realize solubilization, there must be enough amphiphiles to mask the hydrophilicity and polarity of hydrophilic drugs. Otherwise, a turbid suspension rather than oil solution will be formed. The absorption value of the final preparation can be used to determine whether effective solubilization has been achieved. As a rule, the absorption value of the formulation decreases with the increasing amount of amphiphiles, if the concentration of hydrophiles in oil is same. When the amount of amphiphiles reaches a threshold level, optically clear solution will be achieved, revealing the complete dissolution of hydrophiles in oil.

The Possible Solubilization Mechanism

In this study, when only SPC was used as the masking agent, the concentration of SPC in monophase solution was more than 50 mg/mL. Under this condition, SPC can self-aggregate to form tiny micelles with diameters of about 10–30 nm, which can be detected by submicron particle analyzer. Therefore, in the monophase solution, SPC might adopt the correct orientation with respect to hydrophilic drugs, namely with the hydrophilic head groups toward hydrophilic drugs, and with the hydrophobic tails directed away from hydrophilic drugs. When monophase solution was subjected to freeze-drying, the orientation between SPC and hydrophilic drugs was maintained, but the interactions between them may be further enhanced after solvent removal. The loose structure in the lyophilized product permitted the rapid permeation of oil. Therefore, on addition of oil phase, driven by the need to mask the hydrophilic drugs and the head groups from oil, SPC was forced to form a protective sheath between oil and hydrophilic drugs, leading to the formation of reverse micelle–like structures. A schematic representation of this solubilization mechanism can be found in Figure 4.

When SPC and bile salt are employed as "masking agents" simultaneously, the amphiphiles can spontaneously aggregate to form detectable mixed micelles. The solubilization process is similar to what is described in Figure 4.

Based on the above analysis, there are reverse micelle–like structures in the oil solutions. But this structure is different from reverse micelle and is without microemulsion due to the lack of internal water pool. Our data show that the residual TBA levels were 0.8% or less and the residual water levels were less than 2% in the lyophilized products. Accordingly, the calculated W_0 (the molar ratio of water to amphiphile) was about 0.8; however, the reverse micelles usually have a W_0 value of 2.0 or higher (35), which may mean that in our method the head groups of amphiphiles
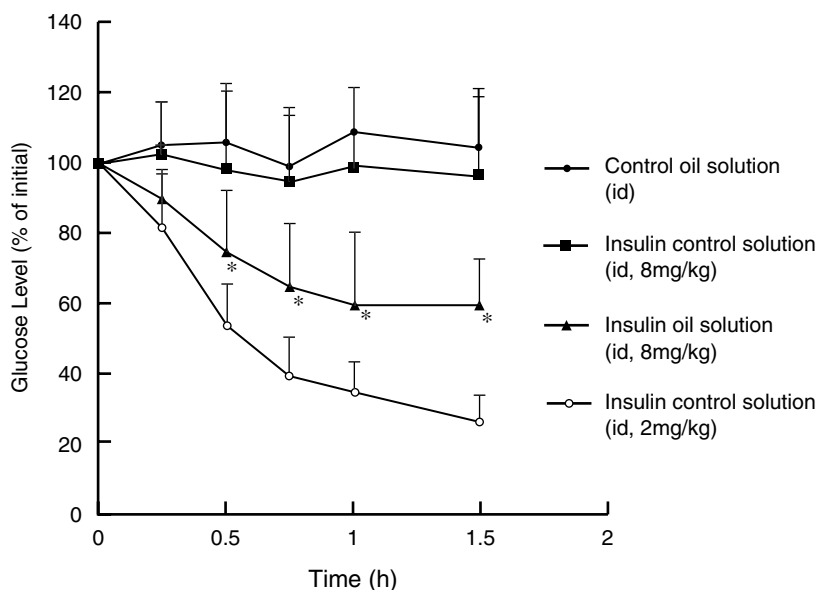
Figure 4 Plasma glucose levels achieved in rats following duodenal administration of control oil solution, insulin control solution (aqueous solution, 8 mg/kg), and insulin oil solution (type 2 formulation, 8 mg/kg), and SC injection of insulin control solution (2 mg/kg) (mean $\pm$ sd, $n = 8$); $p < 0.05$, oil solution aqueous solution. *Abbreviations*: sd, standard deviation; SC, subcutaneous.

are interacting directly with hydrophilic drugs. Thus, this specific structure is named ''anhydrous reverse micelles.''

Why is sodium citrate indispensable when bile salt is used as a ''masking agent?'' It might be related to the molecular shape of bile salt. Bile salt has a critical packing parameter of less than 1/3, and it can form micelles easily in water. However, it is hard to form a reverse micelle–like structure without the aid of sodium citrate.

The Release of Model Drug Calcein from Oil-Based Formulations

Two different calcein oil solution formulations were used to determine drug release behavior when the oily formulations were exposed to water. As described in Experimental Section, the oil used in formulation 1 was MCT, and in formulation 2, the oil phase was composed of polysorbate 80 and MCM.

Because formulation 2 was made of surfactants—including bile salt, SPC, medium-chain partial glycerides, and polysorbate 80—it was a self-emulsifying drug delivery system. When formulation 2 is in contact with water, gentle shaking can lead to the formation of an oil-in-water emulsion.

To determine the release of calcein from oil phase, formulation 2 was diluted with water in a volume ratio ranging from 1:2 to 1:16. After centrifugation, the resulting emulsions were fractionated into three component phases—oil, supernatant, and clear micellar phase. The calcein level in the supernatant liquid was determined by fluorescence intensity analysis. It was found that about 75% of calcein was released into the aqueous phase independent of dilution folds. The result shows that on exposure to water, the anhydrous reverse micelles were destroyed, resulting in the release of calcein.

On the contrary, formulation 1 is not so easily emulsified. However, it is interesting to note that after exposure to water, calcein could be released both in the free form (about 50%) and in the liposome-encapsulated form (over 30%). To prove this, the emulsions obtained by diluting formulation 1 with water were subjected to centrifugation. After centrifugation, the emulsions were fractionated into three component phases—oil, supernatant, and precipitate. The suspensions obtained by resuspending the precipitates contained obvious multilamellar vesicles that could be observed using optical microscope. Fluorescence analysis also supported the in situ formation of liposomes. It was shown that the fluorescence intensity of the suspension before and after addition of $CoCl_2$ had no obvious changes, revealing that the calcein was entrapped in the internal aqueous space of the lipid vesicles—liposomes.

Long-Term Stability of Oil-Based Thymopentin Formulation

TP5 is a synthetic 5-amino acid peptide (RKDVY) (36). Because it is liable to hydrolysis, no liquid preparations are commercially available. However, when it was solubilized in oil, the stability of TP5 was greatly enhanced. Oil-based formulation of TP5 was physically and chemically stable at room temperature for at least 12 months. No significant changes in appearance were observed during the course of the stability study. To determine the chemical stability of TP5, the HPLC method was used. It was found that there were no detectable degradation products of TP5 after storage at room temperature for one year. Therefore, it is concluded that when TP5 is solubilized in oil, the stability problems associated with aqueous phase could be resolved.

Hypoglycemic Effect of Insulin in Nondiabetic Rabbits

To determine whether oil-based formulation can be used as sustained drug delivery system, nondiabetic rabbits were injected subcutaneously into the neck region with a single injection of insulin aqueous solution and oil solution (type 1 formulation).

Figure 2 clearly shows the hypoglycemic effect of these two different formulations. After administration of insulin aqueous solution (0.25 mg/kg), glucose levels began to fall immediately, reaching a minimum in all six of the rabbits after 3 hours, and then starting to rise gradually back to the baseline level.

Similarly, the administration of insulin oil solution resulted in a rapid fall in blood glucose level. However, in the latter case, glucose levels appeared to be continuously decreased throughout the experiment period. The hypoglycemic effect of oil solution at 0.25, 0.5, 4, 5, and 6 hours was significantly different to that of insulin aqueous solution ($p < 0.05$) at the same time durations.

Why did oil solution induce the enhanced and prolonged hypoglycemic effect? It might be due to the specific drug release mechanism of oily formulations. After SC injection, oil solution was in contact with physiological fluid, which led to the release of insulin from oil phase. Based on our results, insulin could be released both as a free drug and in the liposome-encapsulated form. The rapid release of free insulin from oil might be responsible for the rapid fall of glucose levels after dosing. On the other hand, liposomal insulin might be relevant to the prolonged action of oily formulation.

Oral Absorption of Insulin in Diabetic Rats

As shown in Figure 3, the administration of control oil solution without insulin to rats did not cause any modification in blood glucose levels during the experimental period, indicating that the rats were not stressed by the administration procedure and blood sampling. The administration of insulin control solution at a dose of 8 mg/kg also had no obvious influence on the glucose level. The same figure shows that the administration of insulin oil solution (type 2 formulation, 8 mg/kg) resulted in gradual decrease of blood glucose levels. The plasma glucose levels were significantly different ($p < 0.05$) from those of control group at 0.5, 0.75, 1, and 1.5 hours post-administration. These results clearly prove the ability of insulin oil solution to enhance the oral absorption of insulin.

Why does insulin oil solution enhance the oral absorption of insulin? The excipients in the type 2 formulation may play important roles. Bile salt and monoglycerides (or diglycerides) are physiological permeation enhancers, and they may promote the transport of insulin across intestinal mucosa. Moreover, some mechanisms associated with lipid absorption may serve certain functions in oral insulin delivery (37).

CONCLUDING REMARKS

A novel technology has been developed by which water-soluble substances can be solubilized in the absence of water into oils. The formation of anhydrous reverse micelles might play an important role in the solubilization and the resulting oil solutions are physically and chemically stable. Two types of formulations are developed. On exposure to water, a substantial amount of drug can be released from type 1 formulations in the liposome-entrapped form; therefore, type 1 formulations can be used as lipid depot drug delivery systems. In contrast, type 2 formulations are self-emulsifying drug delivery systems and might find application in oral delivery of peptides/proteins.

REFERENCES

1. Teagarden DL, Baker DS. Practical aspects of lyophilization using non-aqueous co-solvent systems. Eur J Pharm Sci 2002; 15:115.
2. Kasraian K, DeLuca PP. Thermal analysis of the tertiary butyl alcohol-water system and its implications on freeze-drying. Pharm Res 1995; 12:484.
3. Kasraian K, DeLuca PP. The effect of tertiary butyl alcohol on the resistance of the dry product layer during primary drying. Pharm Res 1995; 12:491.
4. Wittaya-Areekul S, Nail SL. Freeze-drying of tert-butyl alcohol/water cosolvent systems: effects of formulation and process variables on residual solvents. J Pharm Sci 1998; 87:491.
5. Oesterle J, Franks F, Auffret T. The influence of tertiary butyl alcohol and volatile salts on the sublimation of ice from frozen sucrose solutions: implications for freeze-drying. Pharm Dev Technol 1998; 3:175.
6. Nuijen B, et al. Pharmaceutical development of a parenteral lyophilized formulation of the novel antitumor agent aplidine. PDA J Pharm Sci Technol 2000; 54:193.
7. Wittaya-Areekul S, et al. Freeze-drying of tert-butanol/water cosolvent systems: a case report on formation of a friable freeze-dried powder of tobramycin sulfate. J Pharm Sci 2002; 91:1147.
8. Van Drooge DJ, Hinrichs WL, Frijlink HW. Incorporation of lipophilic drugs in sugar glasses by lyophilization using a mixture of water and tertiary butyl alcohol as solvent. J Pharm Sci 2004; 93:713.
9. Li C, Deng Y. A novel method for the preparation of liposomes: freeze drying of monophase solutions. J Pharm Sci 2004; 93:1403.
10. Maurer N, Fenske DB, Cullis PR. Developments in liposomal drug delivery systems. Expert Opin Biol Ther 2001; 1:923.
11. Walde P, Ichikawa S. Enzymes inside lipid vesicles: preparation, reactivity and applications. Biomol Eng 2001; 18:143.
12. Buboltz JT, Feigenson G. A novel strategy for the preparation of liposomes: rapid solvent exchange. Biochim Biophys Acta 1999; 1417:232.
13. Wang W. Lyophilization and development of solid protein pharmaceuticals. Int J Pharmaceut 2000; 203:1.
14. Crowe JH, Crowe LM. Preservation of liposomes by freeze-drying. In: Gregoriadis G, ed. Liposome Technology. Boca Raton: CRC Press, Inc., 1993:chap 14.
15. Crowe JH, Crowe LM. Factors affecting the stability of dry liposomes. Biochim Biophys Acta 1988; 939:327.
16. Crowe LM, et al. Prevention of fusion and leakage in freeze-dried liposomes by carbohydrates. Biochim Biophys Acta 1986; 861:131.
17. Evans JR, Fildes FJT, Oliver JE. Process for preparing freeze-dried liposome compositions. US Pat. 4311712, 1982.
18. Drummond DC, et al. Optimizing liposomes for delivery of chemotherapeutic agents to solid tumors. Pharmacol Rev 1999; 51, 691.
19. Scherphof G, Kamps JA. The role of hepatocytes in the clearance of liposomes from the blood circulation. Prog Lipid Res 2001; 40:149.
20. Baldeschwieler JD. Liposomal targeting of ischemic tissue. US Pat. 5527538, 1996.

21. Slater JL, Colbern GT, Working PK. Liposome-entrapped topoisomerase inhibitors. US Pat. 6465008, 2002.
22. Wagner A, et al. The cross-flow injection technique: an improvement of the ethanol injection method. J Liposome Res 2002; 12:259.
23. Fix JA. Strategies for delivery of peptides utilizing absorption-enhancing agents. J Pharm Sci 1996; 85:1282.
24. Meyer JD, et al. Generation of soluble and active subtilisin and alpha-chymotrypsin in organic solvents via hydrophobic ion pairing. Int J Pept Protein Res 1996; 47:177.
25. Kendrick BS, et al. Hydrophobic ion pairing as a method for enhancing structure and activity of lyophilized subtilisin BPN' suspended in isooctane, Arch Biochem Biophys 1997; 347:113.
26. Meyer JD, Manning MC. Hydrophobic ion pairing: altering the solubility properties of biomolecules. Pharm Res 1998; 15:188.
27. Claffey DJ, et al. Long chain arginine esters: a new class of cationic detergents for preparation of hydrophobic ion-paired complexes. Biochem Cell Biol 2000; 78:59.
28. Zhou H, et al. Hydrophobic ion pairing of isoniazid using a prodrug approach. J Pharm Sci 2002; 91:1502.
29. New RRC, Kirby CJ. Solubilization of hydrophilic drugs in oily formulations. Adv Drug Deliver Rev 1997; 25:59.
30. Kirby CJ. Oil-based formulations for oral delivery of therapeutic peptides. J Liposome Res 2000; 10:391.
31. Gogineni PV, Crooks PA, Murty RB. Gas chromatographic determination of residual levels of tert-butanol from lyophilized liposomal formulations. J Chromatogr 1993; 620:83.
32. Oku N, Kendall DA, Macdonald RC. A simple procedure for the determination of the trapped volume of liposomes. Biochim Biophys Acta 1982; 691:332.
33. Lee ML, Stavchansky S. Isothermal and nonisothermal decomposition of thymopentin and its analogs in aqueous solution. Pharm Res 1988; 15:1702.
34. Li CL, Deng YJ. Oil-based formulations for oral delivery of insulin. J Pharm Pharmacol 2004; 56:1101.
35. Luisi PL, et al. Reverse micelles as hosts for proteins and small molecules. Biochim Biophys Acta 1988; 947:209.
36. Gonser S, Weber E, Folkers G. Peptides and polypeptides as modulators of the immune response: thymopentin—an example with unknown mode of action. Pharm Acta Helv 1999; 73:265.
37. Nordskog BK, et al. An examination of the factors affecting intestinal lymphatic transport of dietary lipids. Adv Drug Deliver Rev 2001; 50:21.

4

Formation of Large Unilamellar Vesicles by Extrusion

Barbara Mui and Michael J. Hope

Inex Pharmaceuticals Corporation, Burnaby, British Columbia, Canada

INTRODUCTION

The sequential passage of liposomes through filters of a defined pore size to generate large unilamellar vesicles (LUV) with a mean diameter reflecting the diameter of the filter pore was first described 25 years ago (1). In the 1970s, making LUV was an arduous process, often taking several days and severely limiting the rate at which some areas of model membrane research could advance. However, this changed in the mid-1980s with the introduction of robust, practical, high-pressure equipment that greatly simplified LUV production (2). Using the devices described in this chapter, extrusion can be applied to a wide variety of lipid species and mixtures, it works directly from multilamellar vesicles (MLV) without the need for sequential size reduction, process times are on the order of minutes, and it is only marginally limited by lipid concentration compared to other methods. Manufacturing issues related to the removal of organic solvents or detergents from final preparations are eliminated and the equipment has been scaled for bench volumes (0.1–10 mL) through to preclinical (10 mL–1 L) and clinical (>l L) applications employing relatively low-cost equipment, especially at the research and preclinical levels (3).

LARGE UNILAMELLAR VESICLES AND EXTRUSION

It is relatively straightforward to make MLV because they usually form spontaneously when bilayer-forming lipid mixtures are hydrated in excess water. Unfortunately, unprocessed MLV have limited uses in research because of their large diameters, heterogeneity of size (typically 0.5–10 μm), multiple internal compartments, low-trap volumes, and inconsistencies from preparation to preparation. Approximately 10% of the total lipid in a typical MLV preparation is present in the outer monolayer of the external bilayer (2). A more desirable model system is the one in which a single bilayer encloses an aqueous space to form a vesicle with a sufficiently large radius that approximately 50% of the total membrane lipids are present in the outer monolayer, a typical definition of an LUV, and which better represents the macroscopic lipid bilayer structures of plasma membranes or large organelle membranes.

Until extrusion methodologies were developed, making LUV was a complex process. Common size reduction techniques, such as the use of ultrasound or microfluidization, tend to generate significant populations of "limit size" vesicles in which the radius of curvature of the bilayer is at a maximum and as much as 70% of the total lipid is located in the outer monolayer. These small unilamellar vesicles not only have very small trapped volumes, limiting their usefulness, but are also subject to significant lipid packing constraints that can make the vesicles physically unstable (4). Reverse-phase evaporation methods were also common in the 1980s and usually involved the formation of aqueous/organic emulsions followed by solvent evaporation to produce liposome populations with large trapped volumes and improved trapping efficiencies (5). However, these methods are restricted by lipid solubility in solvent or solvent mixtures; moreover, removal of residual solvent can be tedious. Detergent dialysis techniques are also subject to similar practical difficulties associated with lipid solubility and complete removal of detergent.

The extrusion technique employs nitrogen gas to apply moderate pressures, typically 100–800 lb/in^2 (where 1 lb/in^2 = 6895 Pa) to force liquid crystalline MLV through polycarbonate filters with defined pore sizes. The majority of laboratories specializing in liposome research, particularly as applied to drug delivery, use a heavy-duty device commercially available from Northern Lipids (6). The Extruder is an easy-to-use, robust stainless steel unit, which can operate up to pressures of 800 lb/in^2 (Fig. 1). A quick-fit sample port assembly allows for the rapid and convenient cycling of preparations through the device; the simplicity of the process means that the equipment requires virtually no maintenance and has an unlimited life-span in the average laboratory setting. The sequential use of large to small pore filters (1) to reduce back pressure is not necessary for the majority of lipid samples, and MLV can be extruded directly through filter pore sizes

Figure 1 A research scale extrusion device (Lipex^{TM} Extruder) manufactured by Northern Lipids (Vancouver, BC, Canada) has a 10-mL capacity and can be operated over a wide range of temperatures when used in combination with a circulating water bath. The quick-release sample port at the top of the unit allows for the rapid cycling of sample through the filters.

as small as 30 nm. The equipment is also fitted with a water-jacketed, sample holding barrel that enables the extrusion of lipids with gel–liquid crystalline phase transitions above room temperature, an important feature because gel-state lipids will not extrude.

Other devices on the market include systems built around syringes fitted with filter holders, such as those supplied by Avanti Polar Lipids (7) and Avestin (8). These are best suited to making small volume preparations of LUV (typically < 1 mL) and where low lipid concentrations are acceptable; one example consists of two Hamilton syringes connected by a filter holder, allowing for back-and-forth passage of the sample (9). Using this technique, a dilute suspension of liposomes (composed of liquid crystalline lipid) can be passed through the filters to reduce vesicle size. This method, however, is limited by the back pressure that can be tolerated by the syringe and filter holder, as well as the pressure that can be applied manually.

The preferred filters for reducing the mean diameter of liposome preparations are those made of polycarbonate in which straight-through,

cylindrical pores have been formed by chemical etching along ion tracks, such as the Nuclepore^{TM} brand membranes (10). Other filter materials can be used, but the polycarbonate type has proven to be reliable, inert, durable, and easy to apply to filter supports without damage. Pore density influences extrusion pressure. In our experience, there is usually little variation between filters from the same manufacturer. However, occasionally users may notice changes in vesicle diameter prepared using filters from different batches from the same supplier or between filters in which the pores are created using different manufacturing processes. Tortuous path-type filters do not have well-defined pore diameters like the straight-through type, and back pressure tends to be higher when using these filters for liposome extrusion. However, adequate size reduction can still be achieved.

MECHANISM OF EXTRUSION

A few studies have been published where the biophysical aspects of extrusion have been considered (11–14). As liposomes are squeezed through the cylindrical pores, they are subject to considerable shear-induced tensions in the bilayer, it has been proposed that these lead to membrane instabilities within the pore or at the pore exit, resulting in vesicles blebbing off from the larger MLV structures (11,14). This model predicts that the radius of extruded vesicles will decrease as the flow rate through the filters pores is increased, which appears to be the case, especially at relatively low lipid concentrations. However, flow rate is dependent on the applied pressure; in a recent publication, Patty and Frisken conclude that shear forces experienced in the pores may be less important than the pressure differential across the filter in determining vesicle size (14).

Although the precise biophysical mechanism of vesicle formation during extrusion may be debatable, it is clear that as the concentric layers of a typical MLV squeeze into the filter pore under pressure a process of membrane rupture and resealing occurs. The practical consequence of this is that any solute trapped inside an MLV or large liposome prior to size reduction will leak out during the extrusion cycle. Therefore, when specific solutes are to be encapsulated, extrusion is nearly always performed in presence of medium containing the desired final solute concentration and external (unencapsulated) solute is removed only when sizing is complete. However, vesicles that have been sized to 100 nm can be passed through filters with pore diameters greater than or equal to 200 nm with minimal effect. This is an important point in the field of liposomal drug delivery because it enables the processing of final formulations through sterile filtration cartridges.

Cycling an MLV preparation through filters with 100-nm pores produces a homogeneous population of vesicles with a mean diameter of approximately 100 nm usually after about 10 passes (Fig. 2). Lamellarity
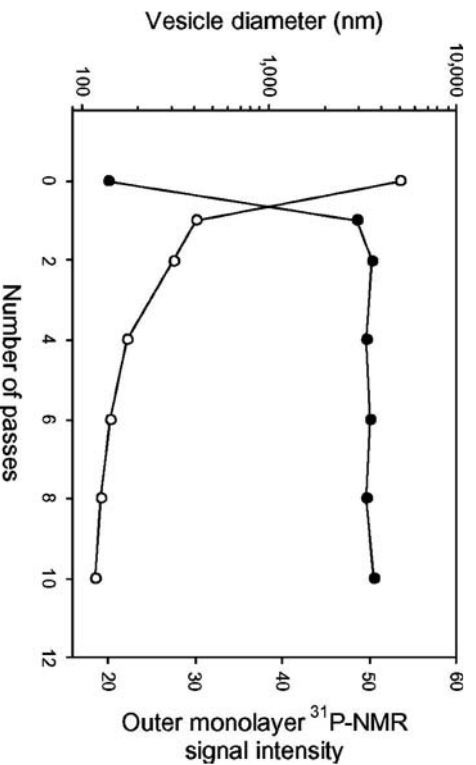
Figure 2 Vesicle size reduction and increased phospholipid present in the monolayer. MLV (100 mg egg PC/mL) prepared in 150 mM NaCl, 20 mM pH 7.4 were extruded through two stacked 100-nm pore-sized filters. (○) Mean diameter determined by quasi-elastic light scattering. (●) The percentage phospholipid present in the outer monolayer determined using ^{31}P-NMR. *Abbr* NMR, nuclear magnetic resonance; PC, phosphatidylcholine.

of a liposome preparation can be determined by using ^{31}P-nuclear resonance (NMR) to monitor the phosphorus signal at the outer monolayer compared to the total signal. Adding an in able paramagnetic or broadening reagent to the external med decrease the intensity of the initial ^{31}P-NMR signal by an amount tional to the fraction of lipid exposed to the external medium (2,15). the first five passes through two (stacked) polycarbonate filters with pore sizes, egg phosphatidylcholine (egg PC) MLV rapidly decrease whilst a concomitant increase in phospholipid detectable at the in with the external medium is observed (Fig. 2). These data are consist the large multilamellar structure, in which the majority of the associated with internal bilayers, rupturing, and resealing into prog smaller vesicles with fewer and fewer internal lamellae, until appro 50% of the phosphorous signal is accounted for in the outer mo indicating that the vesicle population largely consists of single vesicles (LUV). Between 5 and 10 cycles, there is no further change mean size or outer monolayer signal intensity.

A common practice introduced by Mayer et al. (16) is to subjec to freeze-thaw cycles prior to extrusion, which increases the propo unilamellar vesicles in preparations sized through filters with a p greater than 100 nm. It is important to note, however, that the thawi

occur at temperatures above the gel–liquid crystalline phase tran
the lipids used unless cholesterol is included in the lipid mixture (
estimated that as much as 90% of vesicles passed through a filter wit
size of 200 nm are unilamellar if prepared from frozen and thawe
lamellar vesicles (15). The freezing and thawing cycle has been s
cause internal lamellae of MLVs to separate and vesiculate, which p
reduces the number of closely associated bilayers forced throug
together, thus reducing the formation of oligolamellar vesicles.
fracture electron microscopy and cryo-electron microscopy give
qualitative indication of lamellarity than ^{31}P-NMR signal intensity r
ments. Figure 3A is a freeze-fracture micrograph of an egg PC multi
liposome that has cross-fractured, thus demonstrating the close ap
and large number of internal bilayers associated with a typical MLV. F
is a cryo-electron micrograph of egg PC/cholesterol vesicles sized th
100-nm pore-size filter; approximately 20% of the vesicles in this po
contain one to two internal lamellae, which are clearly visible us
visualization technique. Another key advantage of the extrusion te
is the ability to process liposomes at very high lipid concentrations.
is a freeze-fracture micrograph of egg PC vesicles sized to 100 nm a
centration of 400 mg/mL, a solution that no longer flows as a li
behaves as a semisolid paste.

The rupture and resealing process can also give rise to oval- or
shaped vesicles, as demonstrated by Mui et al. (18), who showed that th
deformation is largely dictated by osmotic force. As vesicles are s
through the pores, they elongate and lose internal volume through
membrane rupture to accommodate the increase in surface area to volu

(A)   **(B)**
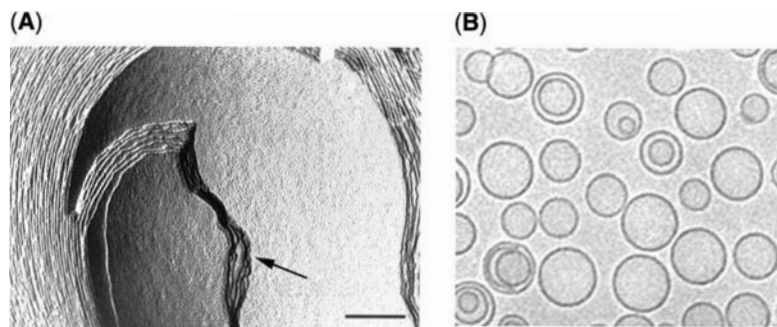
Figure 3 Vesicle lamellarity visualized by freeze-fracture and cryo-electron
copy. (**A**) The close apposition and multiple internal bilayers seen in cross
(*arrow*) of MLVs composed of egg PC. (**B**) Egg PC/cholesterol vesicles t
been extruded through 100-nm pore-size filters are predominantly unilar
visualized by cryo-electron microscopy. The bars represent 100 nm. *Abb*
PC, phosphatidylcholine.
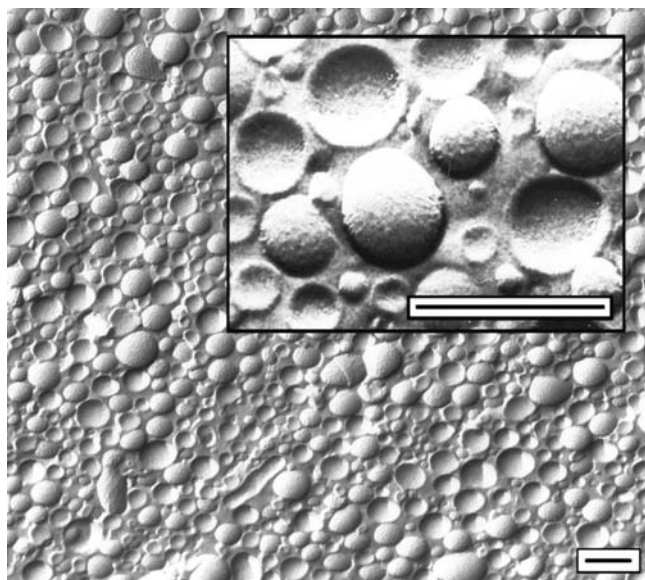
Figure 4 Freeze-fracture micrograph of egg phosphatidylcholine vesicles prepared at 400 mg/mL in 150 mM NaCl, 20 mM HEPES, pH 7.4 by extrusion through 100-nm pore-size filters. The insert is a magnified view of the vesicles. Bar represents 200 nm.

associated with the nonspherical morphology. Upon exiting the pore, the membrane wants to adopt a sphere—thermodynamically the lowest energy state for the bilayer—but the required increase in trapped volume is opposed by osmotic force. Therefore, in the presence of impermeable or semipermeable solutes (e.g., common buffers and salts) oval- or sausage-shaped vesicles are produced, whereas vesicles made in pure water are spherical (Fig. 5A and B).

Sausage-like and dimpled vesicle morphology is observed when extrusion occurs even in solutions of relatively low osmolarity such as 10 mM NaCl. It should be noted that these vesicle morphologies have only been observed employing cryo-electron microscopy techniques where vesicles are visualized through thin films of ice in the absence of cryo-protectants. Freeze-fracture methods do not reveal sausage-like morphology under the same conditions, which may be due to the very high concentrations of membrane permeable glycerol (25% v/v) used as a cryo-protectant affecting the osmotic gradient. Rounding-up of vesicles is readily achieved by simply lowering the ionic strength of the external medium (18).
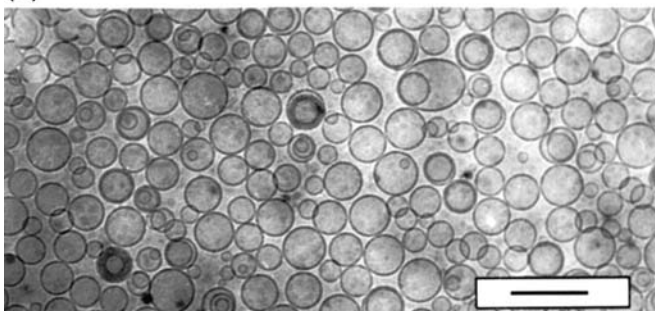
EXTRUSION AND LIPID COMPOSITION

Perhaps the most important compositional factor in liposome extrusion is the gel–liquid crystalline phase transition temperature (T_c) of the membrane

(A)
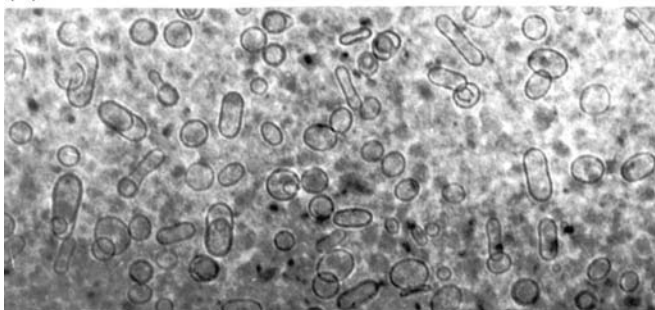
(B)

Figure 5 Cryo-electron microscopy of extruded egg phosphatidylcholine/cholesterol vesicles made in (**A**) 150 mM NaCl, 20 mM HEPES, pH 7.4, or (**B**) distilled water. Bar represents 200 nm.

lipid. Nayar et al. (17) conducted an extensive study on temperature and extrusion of MLV composed of distearoyl PC (DSPC) and DSPC/cholesterol (55:45 mole ratio). At an applied pressure of 500 lb/in^2 the flow rate of liposomes through a 25-mm Nuclepore filter with a pore size of 100 nm was recorded as a function of temperature. MLV composed of DSPC alone could only be extruded above 55°C (the T_c for DSPC); at lower temperatures, pressures as high as 800 lb/in^2 did not result in extrusion. However, above 55°C extrusion proceeds rapidly and the rate is no longer temperature dependent. Surprisingly, in the presence of cholesterol (which abolishes the cooperative gel-liquid crystalline transition), the rate of extrusion below T_c is still very slow (0.06 mL/min at 40°C), whereas at 65°C, the extrusion rate is 200-fold higher. Similar effects were also observed for other saturated lipids. These results indicate that lipids in the gel state cannot be extruded at medium pressure and that extrusion rates at temperatures below the gel-liquid phase transition are prohibitively slow, even in the presence of cholesterol. It is reasonable to conclude that the inability to extrude below the phase transition temperature is most likely related to the much higher

viscosity of gel-state membranes and their decreased deformability (19). The observation that cholesterol slightly facilitates extrusion below T_c but reduces extrusion rates above T_c correlates with the ability of cholesterol to decrease membrane viscosity below T_c and increase viscosity above T_c. When saturated systems are extruded at temperatures at which the phospholipid is normally in a liquid-crystalline state, size reduction and the formation of unilamellar vesicles proceeds normally; however, users should be aware of some stability issues discussed below.

Liposomes composed from long-chain saturated lipids can be unstable when cooled below their T_c. For example, small vesicles produced by extrusion of DSPC or diarachidoyl PC (DAPC). DAPC through filters with a pore size of 30 nm are metastable. The vesicles aggregate and fuse when incubated at 4 or 20°C. This is likely due to the gel–liquid crystalline phase transition, which is associated with a large decrease in molecular surface area as lipid enters the gel state. This reduced surface area (which can be as much as 40%–50%) is expected to destabilize vesicles. These effects can be observed by freeze-fracture when vesicles are prepared above T_c then cooled to below T_c prior to cryo-fixing. Angular fracture planes are observed but not when cholesterol is present, consistent with its ability to prevent phospholipid from forming a cooperative, all-*trans*. gel-state configuration, thus reducing changes in surface area as the temperature is decreased (17).

For all practical purposes, extrusion of saturated systems is limited to lipids with a T_c below 100°C. Successful extrusion of PCs with chain lengths ranging from 14 to 22 carbons has been achieved, the latter (dibehenoyl PC) extrudes at 100°C (unpublished observation). Because of the high viscosity associated with the membranes of long-chain saturated lipids, especially if extrusion occurs at or near the T_c, back pressure tends to be high and extrusion rates slow.

The majority of liposomes used either in drug delivery or as tools of membrane research are composed of phosphoglycerides or sphingomyelin and in our experience all liquid–crystalline, bilayer-forming phospholipids (in isolation or as complex mixtures) are amenable to the extrusion technique. The rate of extrusion, or the operational pressure required to force liposomes through filters, varies with charge, acyl composition, pH, ionic strength, and the presence of interacting ions such as Ca^{2+} or Mg^{2+}. However, these factors do not usually prevent extrusion.

We (and others) have found that there is an advantage to extruding some liposome preparations in the presence of ethanol. Most lipids commonly used to prepare liposomes dissolve in this solvent and MLV form spontaneously when the alcohol/lipid dispersion is diluted with buffer to a final ethanol concentration in the range of 10% to 25% (v/v). Not only is this ethanol/aqueous mixture readily extruded, but the alcohol also facilitates the passage of lipid through the filter pores, resulting in lower back pressure and enhanced flow rate. The vesicles generated tend to exhibit

an even more homogeneous size distribution around the pore size than is observed in the absence of alcohol. Furthermore, ethanol is one of the few organic solvents acceptable in the manufacturing process of pharmaceutical products and its miscibility with water means that it is very easily removed from vesicle preparations by gel filtration, dialysis, or tangential flow.

APPLICATIONS

The introduction of extrusion has had the greatest impact on the development of liposomal drug delivery technology. Homogeneous vesicle populations with diameters from 70 to 150 nm are required to maximize the accumulation of liposomal drugs at disease sites following intravenous administration (20). Vesicles of this size are small enough not only to circulate without becoming trapped in tissue microvasculature but also to extravasate through pores and gaps in the vascular endothelium associated with tumors and areas of inflammation (21,22). Furthermore, vesicles in the 70- to 150-nm range have good drug carrying capacity, but are small enough to pass through sterilizing filters without damage or loss of contents.

Finally, the extrusion process can be readily incorporated into a scaled-up manufacturing process to generate large volumes of formulation for industrial and medical applications. Pumps are typically employed in large-scale processes rather than the nitrogen gas pressure employed at bench scale. Filter surface area is a critical factor and each formulation tends to have a maximum volume that can be extruded through a given membrane surface area before pores clog and back pressure starts to build. Prefiltering all solutions through 50-nm pore-size filters can help increase the volumes that can be processed before clogging occurs and filters have to be changed.

REFERENCES

1. Olson F, Hunt CA, Szoka FC, Vail WJ, Papahadjopoulos D. Preparation of liposomes of defined size distribution by extrusion through polycarbonate membranes. Biochimica Et Biophysica Acta 1979; 557:9–23.
2. Hope MJ, Bally MB, Webb G, Cullis PR. Production of large unilamellar vesicles by a rapid extrusion procedure. Characterization of size distribution, trapped volume and ability to maintain a membrane potential. Biochim Biophys Acta 1985; 812:55–65.
3. Mui BL, Chow L, Hope MJ. Extrusion technique to generate liposomes of defined size. In: Duzgunes N, ed. Methods in Enzymology, Liposomes Part A. San Diego: Elsevier, 2003:367.
4. Hope MJ, Bally MB, Mayer LD, Janoff AS, Cullis PR. Generation of multi-lamellar and unilamellar phospholipid vesicles. Chem Phys Lipids 1986; 40: 89–107.

5. Szoka F, Olson F, Heath T, Vail W, Mayhew E, Papahadjopoulos D. Preparation of unilamellar liposomes of intermediate size (0.1–0.2 mumol) by a combination of reverse phase evaporation and extrusion through polycarbonate membranes. Biochim Biophys Acta 1980; 601:559–571.

6. www.northernlipids.com

7. www.avantilipids.com

8. www.avestin.com

9. MacDonald RC, MacDonald RI, Menco BP, Takeshita K, Subbarao NK, Hu LR. Small-volume extrusion apparatus for preparation of large, unilamellar vesicles. Biochim Biophys Acta 1991; 1061:297–303.

10. www.whatman.com

11. Clerc SG, Thompson TE. A possible mechanism for vesicle formation by extrusion. Biophys 1994; 67:475–477.

12. Gompper G, Kroll DM. Driven transport of fluid vesicles through narrow pores. Phys Rev E Stat Phys Plasmas Fluids Relat Interdiscip Topics 1995; 52:4198–4208.

13. Hunter DG, Frisken BJ. Effect of extrusion pressure and lipid properties on the size and polydispersity of lipid vesicles. Biophys J 1998; 74:2996–3002.

14. Patty PJ, Frisken BJ. The pressure-dependence of the size of extruded vesicles. Biophys J 2003; 85:996–1004.

15. Mayer LD, Hope MJ, Cullis PR. Vesicles of variable sizes produced by a rapid extrusion procedure. Biochim Biophys Acta 1986; 858:161–168.

16. Mayer LD, Hope MJ, Cullis PR, Janoff AS. Solute distributions and trapping efficiencies observed in freeze-thawed multilamellar vesicles. Biochim Biophys Acta 1985; 817:193–196.

17. Nayar R, Hope MJ, Cullis PR. Generation of large unilamellar vesicles from long chain saturated phosphatidylcholine by extrusion techniques. Biochim Biophys Acta 1989; 986:200–206.

18. Mui BL, Cullis PR, Evans EA, Madden TD. Osmotic properties of large unilamellar vesicles prepared by extrusion. Biophys J 1993; 64:443–453.

19. Cullis PR, de Kruijff B. Lipid polymorphism and the functional roles of lipids in biological membranes. [Review]. Biochimica Et Biophysica Acta 1979; 559:399–420.

20. Allen TM, Cullis PR. Drug delivery systems: entering the mainstream. Science 2004; 303:1818–1822.

21. Hobbs SK, Mosky WL, Yuan F, et al. Regulation of transport pathways in tumor vessels: role of tumor type and microenvironment. Proc Natl Acad Sci USA 1998; 95:4607–4612.

22. Klimuk SK, Semple SC, Scherrer P, Hope MJ. Contact hypersensitivity: a simple model for the characterization of disease-site targeting by liposomes. Biochim Biophys Acta 1999; 1417:191–201.

5

Preparation of Liposomes for Pulmonary Delivery Using Medical Nebulizers

Kevin M. G. Taylor

University College London Hospitals, Camden and Islington Pharmaceutical Services, and School of Pharmacy, University of London, London, U.K.

Abdelbary M. A. Elhissi

Department of Pharmaceutics, School of Pharmacy, University of London, London, U.K.

INTRODUCTION

The delivery of drugs to the respiratory tract offers considerable advantages over alternative routes of administration. Pulmonary administration is particularly appropriate for drugs having a local action in the respiratory tract, resulting in rapid localized drug action. Moreover, the large alveolar surface area, high vascularity and thinness of the alveolar epithelium, reduced extracellular enzyme levels compared to the gastrointestinal tract, and the evasion of first-pass hepatic metabolism by the absorbed drug offer the potential for pulmonary administration of systemically active materials.

Although the onset of inhaled-drug action is rapid, the duration of activity is often short-lived due to the rapid removal of drug from the lung or metabolism, necessitating frequent dosing. Consequently, controlled drug delivery systems have been researched as a means of prolonging drug residence within the airways. A major advantage of liposomes as pulmonary drug delivery systems is that they can be prepared from phospholipids that

are endogenous to the lungs as components of lung surfactant. It is assumed that pulmonary-delivered vesicles will thus be biocompatible, and that the relevant apparatus for safe and effective processing exists in the lung (1).

A wide range of liposome-associated materials have been administered to the airways of both animals and humans. These include antiasthma (2,3) and antimicrobial compounds (4,5), antioxidants (6), cytotoxic drugs (7–9), peptides and proteins (10,11), and recombinant genes for gene therapy (12). Together, such studies have demonstrated that drug encapsulation in liposomes prior to administration can produce modulated absorption, resulting in localized drug action in the respiratory tract, a prolonged drug presence in circulation, and decreased systemic adverse effects.

Liposomes are a relatively unstable colloidal system. Physical instability is manifested in vesicle aggregation and fusion, which are associated with changes in vesicle size and loss of entrapped hydrophilic materials. Chemical instability, particularly ester bond hydrolysis, and oxidation of unsaturated acyl bonds accelerates liposome breakdown and alters drug-release characteristics. To overcome instability problems, liposomes may be freeze-dried, though freezing may cause phase-transition changes, osmotic stress, and the expansion of bilayers due to ice formation (13), leading to bilayer disruption, fusion, and vesicle aggregation, resulting in loss of entrapped material (14) and changes in liposome size distribution (15). Such effects may be minimized by the inclusion of cryoprotectants (e.g., disaccharide sugars) within the liposome formulations (14). As an alternative to freeze-drying, proliposome approaches to liposome formation have been described as a means of enhancing stability. Proliposomes may be of two types: particulate-based proliposomes comprise soluble, free-flowing carrier particles coated with phospholipids (16,17), whilst alcohol-based proliposomes comprise a concentrated alcoholic solution of phospholipids (18). Both these types of proliposomes generate liposomes on addition of an appropriate aqueous phase.

Liposome Delivery to the Airways

A major function of the airways, resulting from their tortuous structure, is to prevent inhaled material from depositing in the deep lung. The ability of a particle to access the peripheral airways depends principally on its aerodynamic size. Reaching the respiratory bronchioles or alveoli generally requires the size to be less than about 5 to 6 μm, with particles less than 2 μm preferable for alveolar deposition (19). Thus, control of the size of aerosols is critical for effective inhalation therapy. It is also necessary to consider the distribution of sizes about the mean, changes in the size of formulations as they pass through the humid airways, and pathophysiological changes in the airways resulting from disease.

Currently, drug delivery to the human respiratory tract is achieved by three principal types of devices.

Pressurized Metered Dose Inhalers

Pressurized metered dose inhalers (pMDIs) comprise solutions or suspensions of the drug in liquefied propellants, traditionally chlorofluorocarbons (CFCs), and the increasingly used nonozone-depleting hydrofluoroalkanes (HFAs). Phospholipids dissolved in CFCs will spontaneously form vesicles on contact with an aqueous environment, such as occurs in the airways (20). However, the HFA replacements for CFCs, such as propellant 134a, are very poor solvents for phospholipids (21). Consequently, future approaches to formulation of liposomes into pMDIs are likely to involve the suspension of freeze-dried or spray-dried vesicles in propellants.

Dry-Powder Inhalers

These disperse the drug into the patient's airstream as a fine powder during inhalation. Often carrier lactose particles are included in formulations to allow adequate deaggregation of drug powder into fine "inhalable" particles. Freeze-dried (22) and spray-dried (23) liposomes can be successfully aerosolized using such devices. Alternatively, two proliposome approaches to producing fine "liposome" particles have been investigated. Firstly, by micronizing a blend of phospholipids, lactose, and the drug (24); secondly, by spray-drying an ethanolic solution of phospholipids and the carrier (25). Proliposomes so produced have the potential for delivery from dry-powder inhalers (DPIs).

Nebulizers

The third type of inhalation device, nebulizers, are the most suitable for delivering liposomes in the early stages of research, because formulation of nebulizer fluids is relatively easy and large-dose volumes can be administered. In jet nebulizers (also called air-jet and air-blast nebulizers), compressed gas is used to convert a liquid into a spray. A small proportion of the generated primary aerosol has a size sufficiently small for inhalation and leaves the nebulizer directly. The remaining large droplets impact on strategically positioned baffles or the walls of the nebulizer chamber and are recycled into the reservoir fluid. The aerosol output from a jet nebulizer comprises aerosolized droplets and solvent vapor, which saturates the outgoing air. This causes the solute concentration to increase and liquid temperature to decrease with time (26). The suitability of such nebulizers for delivering liposomes has been shown to be formulation-dependent. Significant losses of entrapped drug may occur as liposomes and liposome aggregates are broken up during passage through the nebulizer (27,28).

Ultrasonic nebulizers generate aerosols through high-frequency vibrations of a piezoelectric crystal, which generate cavitation bubbles and capillary waves in the fluid, producing a fountain of liquid at the surface, which subsequently yields aerosol droplets (29). Excess energy is converted

to heat, which may inactivate sensitive materials, such as proteins (30). Consequently, these devices have not been extensively investigated for liposome delivery because the increase in temperature may induce fusion of liposomes and loss of entrapped drug.

Vibrating-mesh nebulizers have recently become commercially available. These devices aerosolize fluid by passing it through vibrating mesh or a plate having multiple apertures (31). Such nebulizers have been shown to efficiently deliver materials such as small, linear plasmid DNA without degrading them (32). This compares favorably with jet nebulizers, which substantially degrade DNA (33).

METHODOLOGY

Nebulizers

Many nebulizers have been used in these studies, varying in design and mode of operation:

Jet Nebulizers

Cirrus® (Intersurgical, U.K.)
Hudson® (Henleys Medical Supplies, U.K.)
Pari LC® (Pari GmbH, Germany)
Pari LC Plus® (Pari GmbH, Germany)
Pari LC Star® (Pari GmbH, Germany)
Respirgard II® (Marquest, U.S.A.)
Sidestream Durable® (Medic-Aid Ltd, U.K.)
   Jet nebulizers were used with compressed air at variable flow rate or with a Pari Master® compressor (Pari GmbH, Germany).

Ultrasonic Nebulizers

Liberty® (Clement Clarke International, U.K.)
Medix Electronic® (Medix Ltd, U.K.)
Omron U1® (Omron Healthcare, U.K.)

Vibrating-mesh Nebulizers

Aeroneb Pro (Large mesh) (Nektar, U.S.A.)
Omron NE U22® (Omron Healthcare, U.K.)

Preparation of Liposomes

Multilamellar and Reverse-Phase Evaporation Liposomes

Multilamellar liposomes (MLVs) were prepared from phospholipids alone or with equimolar quantities of cholesterol (Chol), by dissolving them in chloroform in a round-bottomed flask, and then removing the chloroform

at reduced pressure on a rotary evaporator at 40°C. Aqueous phase was added at a temperature above the main phospholipid phase-transition temperature (T_c) to hydrate the lipid film, followed by mechanical agitation to form vesicles. Reverse-phase evaporation vesicles (REVs) were prepared by dissolving the lipid components in chloroform/diethylether (1:1) in a long-necked round-bottomed flask, and then adding the aqueous phase to give an organic to aqueous phase volume ratio of 6:1. The flask was sealed under nitrogen and sonicated for four to six minutes above the T_c to produce an emulsion. Slow removal of organic solvent using a rotary evaporator resulted in production of REVs. The mean liposome size was reduced, where appropriate, by repeated extrusion through polycarbonate membrane filters (Nucleopore Inc., U.S.A.) held in 25-mm holders. Materials entrapped in the liposomes include sodium cromoglicate (cromolyn sodium), salbutamol sulphate (albuterol sulphate), and lactate dehydrogenase (LDH). Free drug was removed by dialysis or ultracentrifugation, and the volume median diameter (VMD) and size distribution of liposomes were measured using laser Fraunhofer diffraction analysis' Coulter Counter or photon correlation spectroscopy.

Freeze-Dried Liposomes

Liposome dispersions were added to glass-drying vessels and frozen in a freezer at −20°C. The vessels were then attached to a freeze-drier (Edwards Micro Modulyo, Edwards Ltd, U.K.) and dried for 12 hours. The freeze-dried samples were stored in vacuum-sealed vessels at 1 to 5°C in darkness, until required. Prior to use, the freeze-dried liposome samples were rehydrated with deionized water at ambient temperature followed by two minutes vortex mixing to thoroughly redisperse the liposomes.

Particulate-Based Proliposomes

The method was adapted from Ref. (16). A pear-shaped glass flask containing sucrose particles (300–500 μm) was attached to a modified rotary evaporator under vacuum at 40°C. A solution (60 mg/mL) of soyPC and cholesterol (1:1 mole ratio) in chloroform was added portion-wise via a feed-line with chloroform been removed under vacuum at 40°C.

Alcohol-Based Proliposomes

The method was adapted from Ref. (18). Briefly, 100 μL of an isotonic sodium chloride or sucrose solution containing 5 mg salbutamol sulphate was added to a proliposome formulation [50 mg SoyPC/cholesterol (1:1) dissolved in 60 mg ethanol at 70°C for one minute] followed by mild mixing for one minute. The dispersion was made up to 5 mL with the appropriate isotonic solution and was hand-shaken vigorously for one minute to produce the final liposome dispersion.

Production and Characterization of Aerosols
Produced by Nebulizers

Measurement of Aerosol Size

Aerosol size was measured by laser diffraction (Malvern 2600c, Malvern Instruments, U.K.). The liposomes under study (5 mL) were added to the reservoir of the nebulizer. The nebulizer mouthpiece was clamped 25 mm from the center of the laser beam, and adjusted so that the emitted aerosol traversed the beam at a distance of 5 mm from the 63-mm lens. Nebulization was continued for 5 or 10 minutes or until aerosol production ceased.

Characterization of Liposomes Deposited in Impingers

The aerosol released from each nebulizer was collected by directing the aerosol into a two-stage (twin) impinger (TI) (34) also called the Single Stage Glass Impinger (USP) or a multistage liquid impinger (MSLI). These devices are routinely used for characterizing inhalation aerosols (Fig. 1A and B). Aerosols were drawn through these devices at 60 L/min by means of a vacuum pump for a specified time and the stages assayed for both free and entrapped drug, where appropriate, and the size of deposited liposomes measured by laser diffraction analysis.

RESULTS AND DISCUSSION

Delivery of Conventional Liposomes by Jet Nebulizers

The effectiveness of inhaled drug delivery depends on the ability of the drug to reach its target site within the lung; this may be the respiratory bronchioles for bronchodilator drugs such as salbutamol, or the alveoli for systemically active agents. The site of drug deposition depends fundamentally on the aerosol particle size. Table 1 shows the size of aerosols produced from MLVs that were delivered from a Hudson jet nebulizer, which produces aerosols in the range of 2 to 6 μm for deposition in the respiratory airways. At low gas flow rates, which produce large aerosol droplets, and high flow rates, which generate smaller aerosols, the size distribution was unaffected by the presence of liposomes of varying sizes, including those in the liquid crystalline and gel states, and those containing cholesterol.

Studies with latex spheres have indicated that even relatively large, rigid particles can be delivered from jet nebulizers (35). However, liposomes are more delicate structures and may be degraded by the shearing action associated with droplet production from a bulk liquid (27,28). When MLVs having a VMD of 5 μm were nebulized in four jet nebulizers of different designs, there was a time-dependent reduction in the size of vesicles in the reservoir, the reduction being greatest for EggPC liposomes (Fig. 2).

(A)
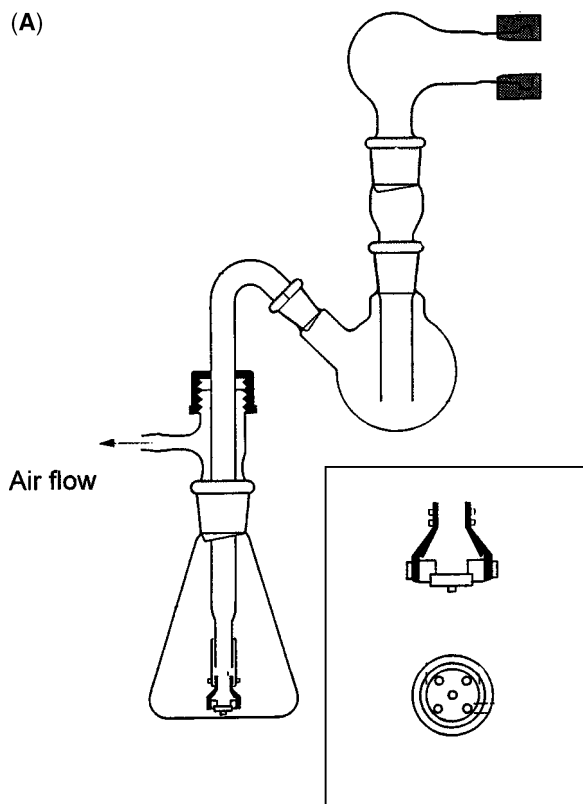
Figure 1 (*Continued on next page*) Impingers for aerosol characterization. (**A**) Two-stage impinger, (**B**) multistage liquid impinger. *Source*: From Ref. 34.

The ambient temperature exceeded the T_c of EggPC. As a result, EggPC bilayers are relatively fluid, which makes them more susceptible to disruption by the shearing action of the driving gas flow than the more rigid bilayers of dipalmitoylphosphatidyl choline (DPPC) Chol liposomes. The extent of size reduction was determined by the nebulizer used. There was some relationship between vesicle size reduction and the size of the aerosol emitted from a nebulizer, as seen in the Respirgard II nebulizer, which produced the smallest aerosol droplets (VMD = 1.5 μm) and also gave the greatest vesicle instability (36). This association might be predicted because the production of smaller droplets is generally associated with higher shear forces and increased droplet recycling. Recycling of liposomes that are too large to be included in the aerosol output of the nebulizer is likely to continue until they are processed into a size small enough to be included in the secondary aerosol emitted from the nebulizer. However, for Sidestream,

(B)

Stage 1

Stage 2

Stage 3

Stage 4

Stage 5 (filter)

Outlet
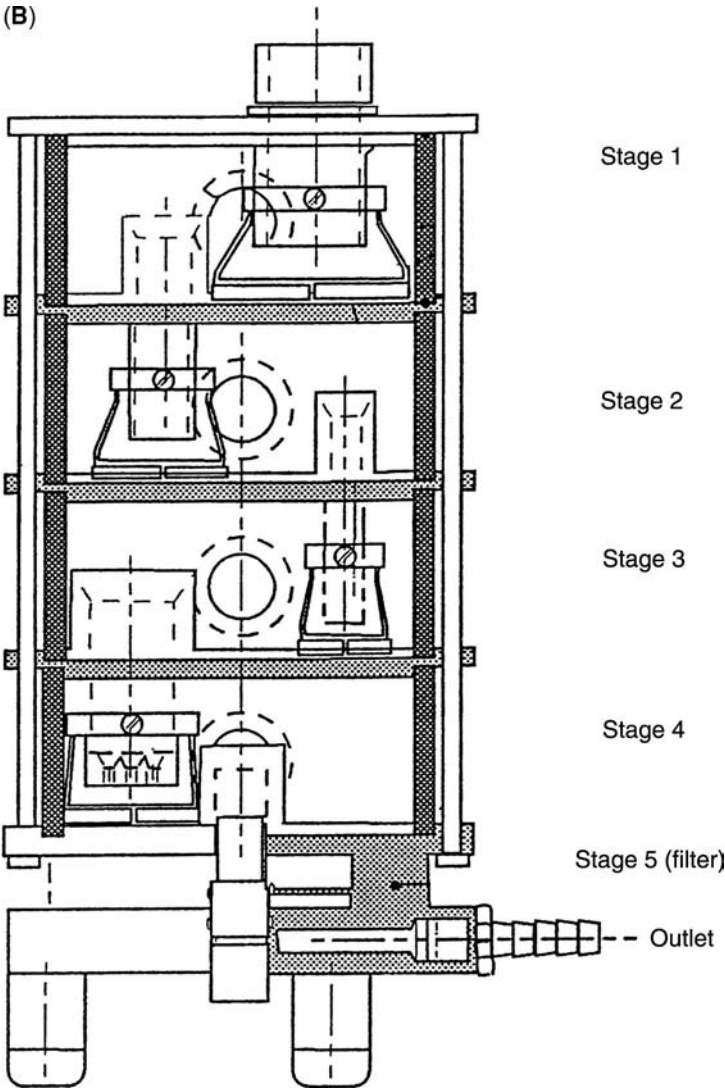
Figure 1 (*Continued from previous page*)

Pari LC, and Cirrus, there was no clear relationship between aerosol size and vesicle disruption. Thus, the size of the aerosol is not the sole factor determining vesicle disruption. The design features of particular nebulizers that govern the droplet size selectivity, including dimensions of the jet orifice(s) and the design of baffles that recycle large aerosol droplets, should also be considered (37).

Table 1 Mean Size Characteristics of Aerosols Produced by Nebulizing Liposomes (40 mg/mL) in a Hudson Jet Nebulizer ($n = 3$)

Formulation	Mean vesicle size (µm)	Flow rate (L/min)	Mean aerosol size (µm)	90% less than (µm)
Water		6	5.2	10.5
		10	2.7	6.5
EggPC	3.6	6	4.9	10.3
		10	3.0	7.2
EggPC/Chol (1:1)	6.2	6	5.0	10.9
		10	2.9	7.1
DPPC	3.8	6	5.0	10.7
		10	2.9	7.2
EggPC	0.9	6	5.0	10.4
		10	2.8	6.7
DPPC	0.9	6	4.9	10.8
		10	2.9	7.0
EggPC	0.1	6	5.0	10.5
		10	2.8	6.6

Abbreviations: DPPC, dipalmitoylphosphatidyl choline; Chol, cholesterol.

Size reduction is usually associated with loss of drugs that are incorporated into the aqueous compartments of liposomes (Table 2). The mean size of EggPC/Chol MLVs and REVs was reduced during nebulization with considerable loss of the entrapped hydrophilic drug sodium cromoglicate. This loss was markedly reduced when liposomes were reduced in mean size by extrusion prior to nebulization. For extruded formulations, deposition of liposome-entrapped drug was predominantly in stages 3 and 4 and in the filter of the MSLI (Fig. 3), i.e., they were carried in aerosol droplets having a median diameter less than 3.6 µm and hence would be predicted to deposit in the "respiratory" airways of man.

Liposome entrapment may provide protection of labile materials during the process of nebulization (38,39). The model protein LDH was significantly degraded during nebulization in a range of nebulizers, particularly jet nebulizers (Table 3). However, when the protein was entrapped in dimyristoylphosphatidyl choline (DMPC) liposomes (median size 150–170 nm) prior to nebulization, the protein was protected against loss of activity. Increased stability probably results from physical protection of the protein by the liposomal bilayers, which may be enhanced by a direct interaction of LDH with the bilayers.

Delivery of Conventional Liposomes by Ultrasonic Nebulizers

Ultrasonic nebulizers are inefficient at delivering high-viscosity fluids (40) and some suspensions (35) and, in contrast to jet nebulizers, may increase
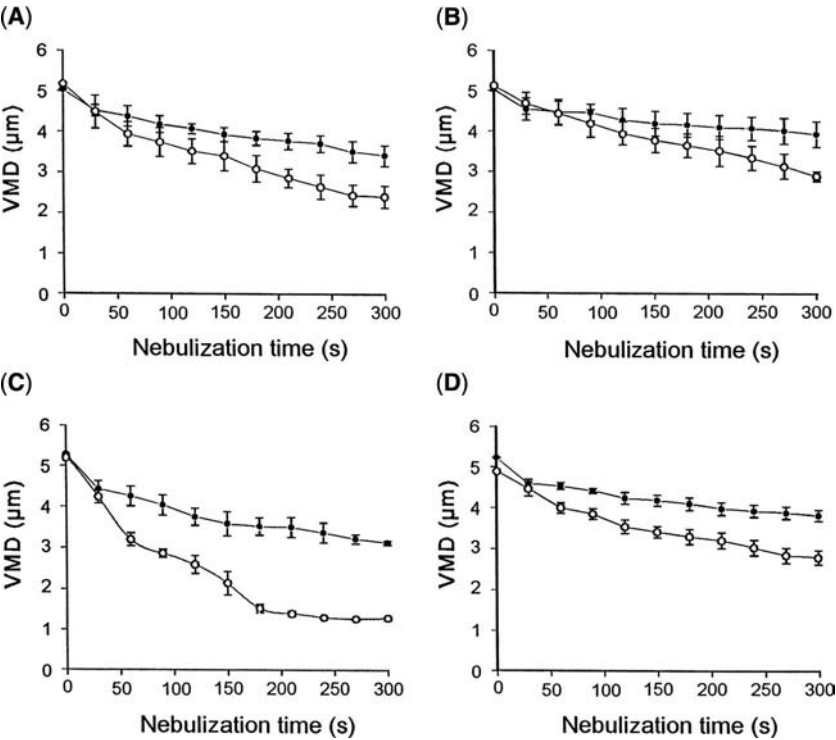
Figure 2 Mean (±S.E.) vesicle size of (○) EggPC and (●) DPPC/Chol liposomes during nebulization in (**A**) Pari LC, (**B**) Sidestream, (**C**) Respirgard II and (**D**) Cirrus jet nebulizers. *Abbreviations*: DPPC, dipalmitoylphosphatidyl choline; Chol, cholesterol; VMD, volume median diameter. *Source*: From Ref. 36.

Table 2 The Effect of Jet Nebulization on Liposomal Formulations of Sodium Cromoglicate (Mean ± S.E.; $n = 3$)

Formulation	Drug lost (%)	Mean size pre-nebulization (μm)	Mean size post-nebulization (μm)
EggPC/Chol (MLV)	50.8 ± 0.5	5.4	2.7
EggPC/Chol (REV)	31.9 ± 2.6	3.4	2.5
EggPC/Chol (REV) (extruded)	16.6 ± 2.4	1.2	1.1
DPPC/Chol (REV) (extruded)	14.2 ± 0.8	1.2	1.1

Abbreviations: MLV, multilamellar liposome; REV, reverse-phase evaporation vesicle; DPPC, dipalmitoylphosphatidyl choline; Chol, cholesterol.
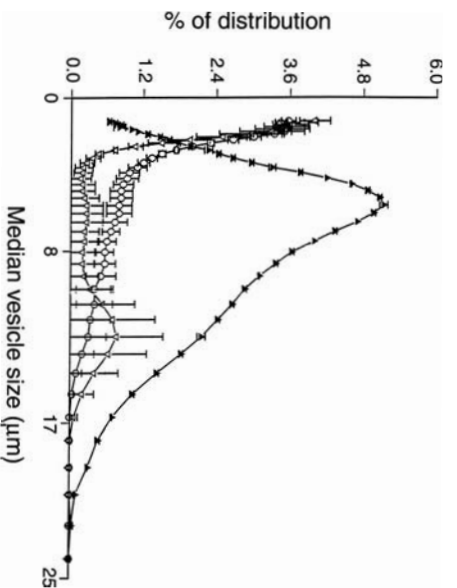*Source*: From Ref. 27.
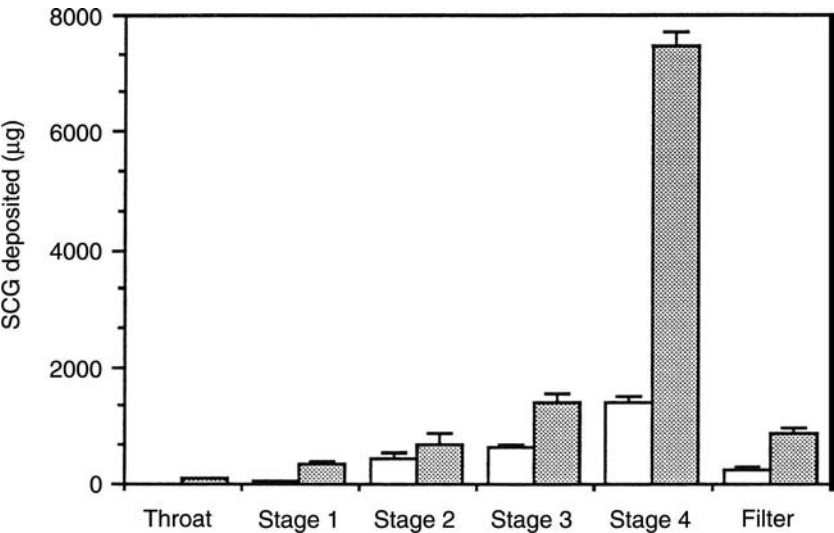
Figure 3 Deposition of free (□) and liposome entrapped (■) sodium cromoglicate in a multistage liquid impinger following jet nebulization of extruded dipalmitoyl-phosphatidyl choline/cholesterol reverse-phase evaporation vesicles (mean ± S.E.). *Abbreviation*: SCG, sodium cromoglicate G. *Source*: From Ref. 27.

the temperature of liquids during atomization. When EggPC liposomes were nebulized using an ultrasonic device, there was a marked reduction in size throughout nebulization (Fig. 4). Over 10 minutes, the mean size was reduced from 5.2 to 1 μm, with the production of a small subpopulation of vesicles having a mean size of approximately 13 μm, suggesting that after a prolonged time, when the reservoir temperature is at its highest, some aggregation and/or fusion of liposomes occurs. The reduction in size of the more rigid EggPC/Chol liposomes during nebulization was less marked, though a shift in the size distribution to a smaller mean size was still apparent (41).

Table 3 The Activity of LDH Before and After Nebulization (Mean ± S.D.)

Nebulizer	LDH		Liposomal LDH	
	% Pre-nebulization	% Post-nebulization	% Pre-nebulization	% Post-nebulization
Pari LC Plus (jet)	100 ± 2.8	24.2 ± 2.7	100 ± 9.6	101.0 ± 7.0
Pari LC Star (jet)	100 ± 2.0	61.7 ± 0.4	100 ± 4.9	91.1 ± 7.9
Omron U1 (ultrasonic)	100 ± 3.8	95.2 ± 2.9	100 ± 7.7	101.3 ± 8.0

Abbreviation: LDH, lactate dehydrogenase.
Source: From Refs. 38 and 39.

Figure 4 Changes in the size distribution of EggPC liposomes remaini... reservoir of the Medix Electronic ultrasonic nebulizer at $t = 0$ sec (●), t... (○) and $t = 600$ sec (▽) (mean ± S.E.). *Source:* From Ref. 41.

Aerosols collected in the throat and upper stage of the TI hav... median aerodynamic diameter (MMAD) greater than 6.4 μm (34) considered "nonrespirable." Any aerosol droplet penetrating to t... stage is considered the "useful" or "respirable" aerosol, having an... less than 6.4 μm. Such aerosols are predicted to deposit in the pe... regions of the lungs. During nebulization, the mean size of EggPC li... collected in the upper and lower stages indicated fractionation of the... in the impinger, with the smallest vesicles delivered in the aerosol... containing the smaller droplets. Initially on nebulization of EggP... liposomes, there was some evidence of vesicle aggregation in the low... though between 5 and 10 minutes, the mean size deposited in bot... was about 3.4 μm, which compares to the size of liposomes in the... reservoir of 3.8 and 4.1 μm at 5 and 10 minutes respectively, sugges... fractionation of these less "fluid" liposomes (41).

Nebulization of Rehydrated Freeze-Dried Liposomes

Liposomes freeze-dried without trehalose were rapidly reduced in s... ing the first half of nebulization with a jet nebulizer, compared to eq... non-freeze-dried liposomal formulations (Table 4). This reflects the i... mean size of the liposomes (approximately 7 μm) within the form... that was previously freeze-dried without cryoprotectant. The lar... caused an increased resistance to aerosolization, making the li... and/or its aggregates less suitable to be included within secondary... droplets; and they are prone to size reduction as a result of shearin...

Table 4 The Rate of Liposome Size Reduction Within a Pari LC Jet Nebulizer for Liposomes Freeze-Dried in the Absence or Presence of Trehalose, and of Non-Freeze-dried EggPC/Chol Liposome Formulations (Mean $\pm$ S.D.)

	The rate of liposome size reduction (nm/min)	
Liposomes	0–50% of nebulization	50–100% of nebulization
Initial size 2.5 μm (nonfreeze-dried)	184 ± 27	127 ± 25
Initial size 5 μm (nonfreeze-dried)	233 ± 30	46 ± 50
Initial size 1 μm (freeze-dried)	622 ± 36	156 ± 78
Initial size 2.5 μm (freeze-dried)	767 ± 11	64 ± 70
Initial size 1 μm (freeze-dried + trehalose)	58 ± 25	-1.3 ± 12
Initial size 2.5 μm (freeze-dried + trehalose)	66 ± 29	62 ± 25

Source: From Ref. 42.

the nebulizer (42). Inclusion of trehalose in freeze-dried formulations reduced vesicle size at the beginning of nebulization, such that the rate of size reduction of liposomes during nebulization was greatly reduced compared to preparations freeze-dried without trehalose. Thus, the presence of the cryoprotectant during freeze-drying permits jet nebulization of reconstituted vesicles, with minimal disruption of bilayers.

The size of liposomes deposited in the TI on nebulization of the formulation with an initial mean of liposome size of 1 μm did not significantly differ between the upper and lower stages. This was because the liposomal aerosol was produced from a population of liposomes with a relatively small mean size following reconstitution (1.61 μm) that was readily accommodated in nebulizer droplets. Larger liposomes freeze-dried with trehalose and those freeze-dried in the absence of trehalose are effectively fractionated, with the largest liposomes present in the largest aerosol droplets being deposited in the upper stage of the TI, whilst the smaller liposomes were collected in the lower stage.

Nebulization of Proliposomes

Particulate-Based Proliposomes

Hydration of particulate-based proliposomes in jet (Pari LC Plus) and ultrasonic (Liberty) nebulizers, and during one-minute shaking within a vibrating-mesh (Omron NE U22) nebulizer, together with the energy generated within devices for atomization, resulted in the ready production of MLVs in situ. Preliminary experiments showed that a short hand-shaking of dispersed proliposomes was necessary prior to their delivery from the

vibrating-mesh nebulizer to ensure that discrete liposomes were formed because the atomization process within this device was much less ''energetic'' than in jet or ultrasonic devices.

Nebulizing dispersions in all three types of devices resulted in size reduction of the aggregates/vesicles present (43). The mechanism of aerosol generation for jet and vibrating-mesh nebulizers ensured that liposomes formed in situ were aerosolized. However, with ultrasonic nebulizers, aerosol is formed at the fluid surface. Aerosols must be present at the surface and entrained into air passing across that surface it if they are to be delivered from the nebulizer. The results suggest that the size of both the vesicles and aggregates formed in the Liberty ultrasonic nebulizer was such that they were excluded from the emitted aerosol droplets.

The sizes of liposomes formed from proliposomes and delivered to both stages of the TI were very similar, even though they employ different operating principles: VMDs for the Pari Plus were 3.76 and 3.18 μm for upper and lower stages respectively, and for the Omron were 3.55 and 4.00 μm for upper and lower stages respectively. The results for the vibrating-mesh device suggest that in producing aerosols from hydrated proliposomes, liposomes are extruded through the apertures in the mesh plate to have a median diameter approximating the size of those apertures (approximately 3 μm). Phospholipid output from the nebulizer was in the order: Pari (jet) > Omron (mesh) >>> Liberty (ultrasonic) nebulizers (43). Both the jet and vibrating-mesh nebulizers were successful in depositing phospholipids, as liposomes, in the lower stage of the impinger (Fig. 5). This indicates that both jet and vibrating-mesh nebulizers could be combined with a proliposome formulation for the delivery of liposomal formulations of therapeutic agents to the peripheral airways. The ready formation in situ of an isotonic liposome formulation from proliposomes would seem to offer advantages over other formulation approaches.
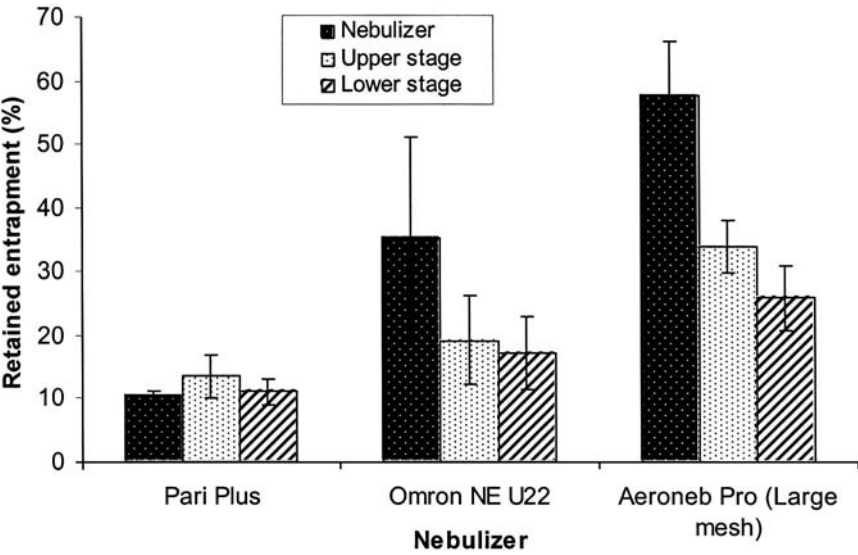
Alcohol-Based Proliposomes

Hydration of alcohol-based SoyPC/Chol proliposomes by manual shaking resulted in formation of oligolamellar vesicles and MLVs from all formulations. In general, vesicles with smaller mean sizes were preferentially delivered to the lower stage of the TI. When proliposomes were dispersed in isotonic sodium chloride solution, the rate of phospholipid output was greater from the Omron NE U22 and Aeroneb Pro vibrating-mesh nebulizers than for those redispersed in isotonic sucrose solutions. However, there was no difference in performance of the Pari jet nebulizer for the two dispersion media.

Liposomes generated from proliposomes that are dispersed in sodium chloride solutions had an entrapment efficiency of $62.1 \pm 3.1\%$ for salbutamol sulphate, which was much higher than for conventional MLVs, having the same phospholipid composition and concentration ($1.2 \pm 0.2\%$). Nebulization in all devices had a detrimental effect on liposome stability, resulting
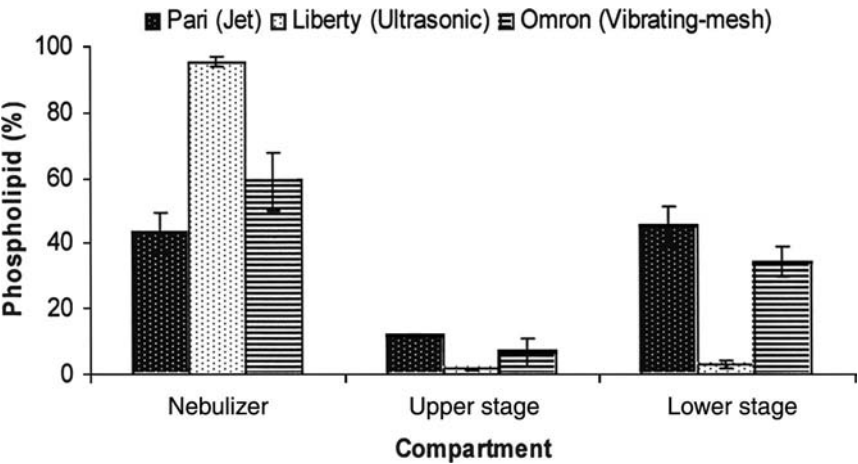
Figure 5 Phospholipid distribution in nebulizers and the two-stage impinger for particulate-based proliposomes delivered from jet, ultrasonic, and vibrating-mesh nebulizers (mean ± S.D.). *Source*: From Ref. 43.

Figure 6 Effect of nebulization on the retained entrapment of salbutamol sulphate in liposomes retained in nebulizers and delivered to the two-stage impinger for alcohol-based proliposomes (mean ± S.D.).

in significant loss of previously entrapped drug. However, vibrating-mesh nebulizers produced more retention of the entrapped drug within liposomes than the jet nebulizer (Fig. 6). The much lower drug retention for the jet nebulizer may be attributed to fluid recycling and high shearing forces within the device resulting in bilayer disruption. Contrastingly, in vibrating-mesh nebulizers, extrusion through mesh pores is less damaging to vesicle structures. In particular, the large apertures in the mesh (8 μm) of the Aeroneb Pro ensured that this nebulizer was particularly efficient at retaining more of the drug entrapped in delivered liposomes.

The entrapped doses delivered to the therapeutically relevant lower impinger stage were 239.2 ± 36.4, 263.1 ± 57.1, and 380.3 ± 139.2 μg for the Pari Plus, Aeroneb Pro (large mesh), and Omron NEU22 respectively. Such entrapped doses delivered to the lower airways would potentially provide a large reservoir for sustained release. Further work is required to reduce the unentrapped drug delivered to the airways, though this will provide an initial loading dose at the airways' surface, as has previously been shown for pulmonary-delivered liposomal sodium cromoglicate (2).

CONCLUSION

From a toxicological viewpoint, liposomes are an appropriate drug delivery system for administration to the lungs. Studies in both animals and humans have shown that liposomes can modulate the fate of pulmonary deposited materials, increasing their residence time within the airways and potentially decreasing systemic adverse effects.

Nebulization offers the simplest means, in terms of formulation, whereby liposomes can be delivered to the human respiratory tract. Nebulization may have adverse effects on liposome stability; however, proper consideration of both the formulation process and the nebulization device can minimize damage to delivered vesicles. Proliposome approaches to formulating systems that are stable to storage are a promising alternative to the more traditional freeze-drying approach. Particulate- and alcohol-based proliposomes are readily converted to isotonic liposome formulations, which can then be delivered from jet and vibrating-mesh nebulizers in aerosols of an appropriate size for peripheral lung deposition. The recently introduced vibrating-mesh nebulizers seem particularly appropriate for liposome delivery, creating less instability in nebulized liposomes and delivering, within aerosols, a large proportion of the formulation placed into the nebulizer reservoir.

REFERENCES

1. Taylor KMG, Farr SJ. Liposomes for drug delivery to the respiratory tract. Drug Dev Ind Pharm 1993; 19:123.
2. Taylor KMG, et al. The influence of liposomal encapsulation on sodium cromoglycate pharmacokinetics in man. Pharm Res 1989; 6:633.

3. Saari SM, et al. Regional lung deposition and clearance of [99mTc]-labelled beclomethasone-DLPC liposomes in mild and severe asthma. Chest 1998; 113:1573.
4. Gilbert BE. Liposomal aerosols in the management of pulmonary infections. J Aerosol Med 1996; 9:111.
5. Finlay WH, Wong JP. Regional lung deposition of nebulized liposome-encapsulated ciprofloxacin. Int J Pharm 1998; 167:121.
6. Suntres ZE, Shek PN. Liposomal α-tocopherol alleviates the progression of paraquat-induced lung damage. J Drug Targ 1995; 2:493.
7. Juliano RL, McCullough HN. Controlled delivery of an antitumour drug: localised action of liposome encapsulated cytosine arabinoside administered via the respiratory tract. J Pharmacol Exp Ther 1980; 214:381.
8. Koshkina NV, et al. Paclitaxel liposome aerosol treatment induces inhibition of pulmonary metastases in murine renal carcinoma. Clin Cancer Res 2001; 7:3258.
9. Verschraegen CF, et al. Clinical evaluation of the delivery and safety of aerosolized liposomal 9-nitro-20(S)-camptothecin in patients with advanced pulmonary malignancies. Clin Cancer Res 2004; 10:2319.
10. Liu F, et al. Pulmonary delivery of free and liposomal insulin. Pharm Res 1993; 10:228.
11. Gilbert BE, et al. Tolerance of volunteers to cyclosporine A—dilaurylphosphatidylcholine liposome aerosol. Am J Respir Crit Care Med 1997; 156:1789.
12. Caplen NJ, et al. Liposome-mediated CFTR gene transfer to the nasal epithelium of patients with cystic fibrosis. Nat Med 1995; 1:39.
13. Hauser H. Stabilising of liposomes during spray drying. In: Gregoriadis G, ed. Liposome Technology. Vol. 1. 2nd ed. New York: CRC Press, 1993:197.
14. Crowe LM, et al. Preservation of freeze-dried liposomes by trehalose. Arch Biochem Biophys 1985; 242:240.
15. Crowe LM, et al. Prevention of fusion and leakage in freeze-dried liposomes by carbohydrates. Biochim Biophys Acta 1986; 861:131.
16. Payne NI, et al. Proliposomes: a novel solution to an old problem. J Pharm Sci 1986; 75:325.
17. Payne NI, Browning I, Hynes CA. Characterization of proliposomes. J Pharm Sci 1986; 75:330.
18. Perrett S, Golding M, Williams P. A simple method for the preparation of liposomes for pharmaceutical applications: characterization of the liposomes. J Pharm Pharmacol 1991; 43:154.
19. Stahlhofen W, Gebhart J, Heyder J. Experimental determination of the regional deposition of aerosol particles in the human respiratory tract. Am Ind Hyg Assoc J 1980; 41:385.
20. Farr SJ, Kellaway IW, Carman-Meakin. Assessing the potential of aerosol-generated liposomes from pressurised pack formulations. J Contr Rel 1987; 5:119.
21. Byron PR, et al. Some aspects of alternative propellant solvency. Respir Drug Deliv 1994; IV:231.
22. Schreier H, et al. Formulation and in vitro performance of liposome powder aerosols. STP Pharm Sci 1994; 4:38.
23. Goldbach P, Brochart H, Stamm A. Spray drying of liposomes for a pulmonary administration. II. Retention of encapsulated materials. Drug Dev Ind Pharm 1993; 19:2623.

24. Desai TR, et al. A novel approach to the pulmonary delivery of liposomes in dry powder form to eliminate the deleterious effects of milling. J Pharm Sci 2002; 91:482.
25. Alves GP, Santana MHA. Phospholipid dry powders produced by spray drying processing: structural, thermodynamic and physical properties. Powder Technol 2004; 145:139.
26. Ferron GA, Kerrebijn KF, Weber J. Properties of aerosols produced with three nebulizers. Am Rev Respir Dis 1976; 114:899.
27. Taylor KMG, et al. The stability of liposomes to nebulisation. Int J Pharm 1990; 58:57.
28. Niven RW, Speer M, Schreier H. Nebulization of liposomes II. The effects of size and modelling of solute release profiles. Pharm Res 1991; 8:217.
29. Taylor KMG, McCallion ONM. Ultrasonic nebulizers. In: Swarbrick J, Boylan JC, eds. Encyclopaedia of Pharmaceutical Technology. 2nd ed. New York: Marcel Dekker, 2002:2840.
30. Cipolla DC, et al. Assessment of aerosol delivery systems for recombinant human deoxyribonuclease. STP Pharm Sci 1994; 4:50.
31. Dhand R. Nebulizers that use a vibrating mesh or plate with multiple apertures to generate aerosol. Respir Care 2002; 47:1406.
32. Smart J, Stangl R, Fritz E. TouchSpray technology: a preliminary in vitro evaluation of plasmid DNA of different size and topology. Respir Drug Deliv 2002; VII:529.
33. Schreier H, et al. Simulated lung transfection by nebulization of liposome DNA complexes using a cascade inpactor seeded with 2-CFSME$_o$-cells. J Aerosol Med 1998; 11:1.
34. Hallworth GW, Westmoreland DG. The twin impinger: a simple device for assessing the delivery of drugs from metered dose pressurised aerosol inhalers. J Pharm Pharmacol 1987; 39:966.
35. McCallion ONM, et al. Nebulisation of monodisperse suspensions of latex spheres in air-jet and ultrasonic nebulisers. Int J Pharm 1996; 133:203.
36. Bridges PA, Taylor KMG. Nebulisers for the generation of liposomal aerosols. Int J Pharm 1998; 173:117.
37. Bridges PA, Taylor KMG. Factors influencing the jet nebulisation of liposomes. Int J Pharm 2000; 204:69.
38. Khatri L, et al. An investigation into the nebulisation of lactate dehydrogenase solutions. Int J Pharm 2001; 227:121.
39. Khatri L, et al. The stability of liposome entrapped lactate dehydrogenase to nebulisation. J Pharm Pharmacol 2004; 56(suppl):S-41.
40. McCallion ONM, et al. Nebulization of fluids of different physicochemical properties with air-jet and ultrasonic nebulizers. Pharm Res 1995; 12:1682.
41. Leung KKM, Bridges PA, Taylor KMG. The stability of liposomes to ultrasonic nebulisation. Int J Pharm 1996; 145:95.
42. Bridges PA, Taylor KMG. The effects of freeze drying on the stability of liposomes to jet nebulisation. J Pharm Pharmacol 2001; 53:393.
43. Elhissi AMA, Taylor KMG. Delivery of liposomes generated from proliposomes using air-jet, ultrasonic, and vibrating-mesh nebulisers. Drug Deliv Sci Technol. 2005; 15:261.

6

Immunopotentiating Reconstituted Influenza Virosomes

**Rinaldo Zurbriggen, Mario Amacker, and Andreas R. Krammer**
Pevion Biotech, Ltd., Bern, Switzerland

INTRODUCTION

Common vaccines show, besides their prophylactic effect, quite often unfavorable side effects with symptoms such as pain, swelling, and inflammation. These effects can be traced back to the use of aluminum-based salts as adjuvant. During the last two decades, a variety of new adjuvants have been investigated to replace the widely used aluminum salts. However, only two new adjuvants were approved by regulatory authorities in the last 20 years. One of them is an immunopotentiating reconstituted influenza virosome, which is a potent adjuvant without showing any unfavorable effects . Additionally, virosomes stand apart from all other adjuvants by their capability as an antigen carrier. A wide variety of antigens including peptides, proteins, carbohydrates, and nucleic acids can be delivered by them.

The adjuvant capabilities of virosomes are independent of any inflammatory reaction in contrast to that of aluminum salts, which develop their effect by inducing a local inflammation (1,2). Virosomes cause an increased uptake of selected antigens into antigen-presenting cells (APC), which then present them to the immune system in a natural way. Moreover, they induce the synthesis and secretion of cytokines to further support the specific immune response against the antigen.

The antigen delivery by virosomes is identical to the natural pathway of antigen processing and presentation. The virosome-based vaccines stand
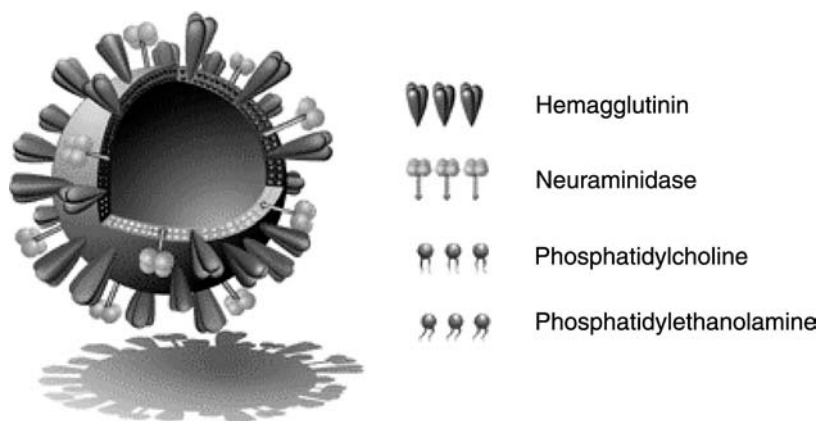
Figure 1 Immunopotentiating reconstituted influenza virosomes with functional viral envelope of glycoprotein.

out due to their excellent safety and side-effect profile, already proven in two marketed products.

Virosomes are spherical, unilamellar vesicles with a mean diameter of approximately 150 nm (Fig. 1) 1. Their base is a liposome comprising phosphatidylcholine, phosphatidylethanolamine, and lipids derived from the influenza virus. Phospholipids are virtually nonimmunogenic and have enjoyed a long history of use in human pharmaceutical preparations. The hemagglutinin (HA) and trace quantities of viral neuraminidase (NA) and phospholipids from the influenza virus are intercalated within the phospholipid bilayer, whereby the presence of HA is necessary to enhance the immunopotentiating effect to the antigen associated with virosomes (3). The influenza HA plays a key role in the mode of action of the virosomes. HA is a trimeric integral membrane protein (M_r 220 000) comprising an ectodomain of identical subunits, each of which contains two polypeptides, HA_1 and HA_2, linked by a disulfide bond (4). The two polypeptides arise from a proteolytic cleavage event and are essential for fusion activity of the virus with the endosomal membrane (5–7). HA_1 has a high affinity for sialic acid, which is present at relatively high concentrations on the surface of APC (e.g., macrophages and dendritic cells). Like influenza virus, virosomes bind to sialic acid residues on the cell surface and the entry of influenza virosomes into cells occurs through receptor-mediated endocytosis (8). At the low pH of the host cell endosome (approximately pH 5), a conformational change occurs in the HA, which is a prerequisite for fusion to occur. The HA_2 subunit of HA then mediates the fusion of virosomal and endosomal membranes.

The second influenza glycoprotein exposed on the virosome surface, the enzyme NA, is a tetramer composed of four equal, spherical subunits that are hydrophobically embedded in the membrane by a central stalk. The entire enzymatic activity takes place in the region of the head. NA catalyzes

the cleavage of *N*-acetylneuraminic acid (sialic acid) from bound sugar residues (9). In the mucus, this process leads to a decrease in viscosity and allows the influenza virus easier access to epithelial cells. In the area of the cell membrane, the same process leads to destruction of the HA receptor. The consequence of this is, first, that newly formed virus particles do not adhere to the host cell membrane after budding, and second, that aggregation of the viruses is prevented. NA therefore allows the influenza virus to retain its mobility. In terms of the virosome, these characteristics of NA can, in theory, be utilized in that, after coupling with HA, virosomes not taken up by phagocytosis could be cleaved off again and would therefore not be lost. Also, the reduction in viscosity of the mucus could be useful in connection with the development of a mucosal virosome vaccine.

MODE OF ACTION

Virosomes have the capability to deliver an antigen selectively to the major histocompatibility complex (MHC) class I or class II pathway and finally induce a humoral or cellular immune response (Fig. 2). The nature of the immune response elicited depends on whether the antigens are located on the surface or inside the virosome.

B-cell antigens linked onto the surface of virosomes elicit a humoral immune response. In contrast, antigen encapsulation into virosomes ensures a proper presentation of the antigens through the MHC I pathway because the antigen is delivered in a natural way into the cytosol of the APC.

The specific immune response against the antigen is boosted by a supplementary unspecific CD4+ immune response, which is evoked by virosomal influenza-specific glycoproteins (HA and NA).

In addition, upon receptor-mediated uptake, antigens containing and CD4 epitopes are degraded in endosomes of the cell and are therefore directed to the MHC II antigen presentation. By this mechanism, an antigen-specific helper immune response is induced, which potentiates both the cellular and humoral immune response.

Induction of a Humoral Immune Response

Virosomes are capable of inducing a highly specific humoral immune response. Antigens have to be crosslinked or adsorbed to the surface of virosomes in order to be recognized by naive B cells and to induce a solid antibody immune response. Alternatively, if the antigen is a membrane protein, it has to be integrated into the virosomal bilayer. T-cell helper antigens enter the APC by receptor-mediated endocytosis. Once in the endosome, the virosome fuses in a pH-dependent process with the endosomal membrane, which results in the processing of the antigens. The processed antigen fragments are then presented to the immune system by an MHC class II presentation. This mechanism was confirmed in vivo using streptavidin as a model antigen (10).
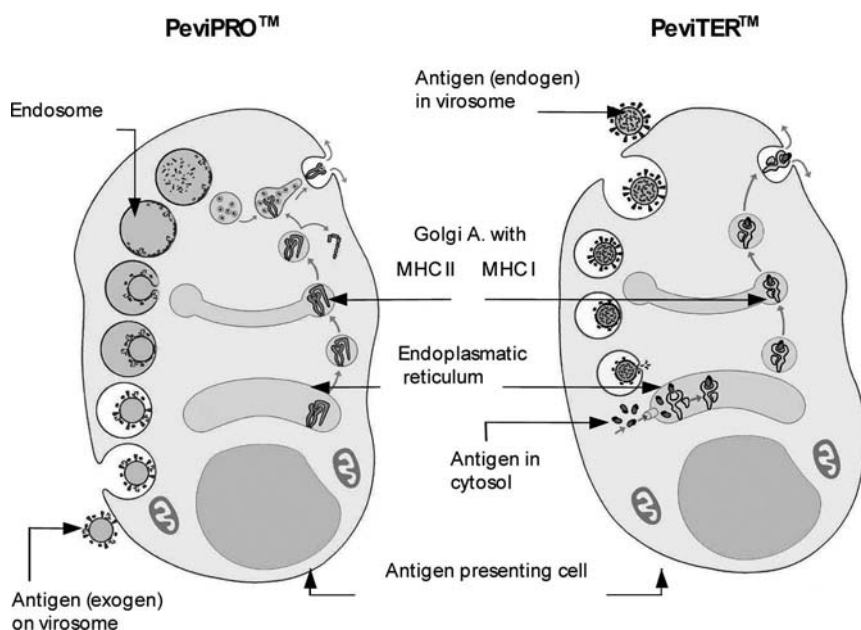
Figure 2 *Virosome-based antigen processing*: Putative interactions of virosomes with cells of the immune system are shown. Virosomes are taken up by antigen-presenting cells, particularly dendritic cells. Antigens on the virosome surface (PeviPRO^{TM}), as well as antigens derived from degraded virosomes, enter the MHC class II pathway, activating T helper cells. Antigens inside the virosomes (Pevi-TER^{TM}), through fusion of the virosomes with the endosomal membrane, access the cytosolic MHC class I presentation pathway, activating cytotoxic T lymphocytes. *Abbreviation*: MHC, major histocompatibility complex.

Strong Adjuvant Effect of Virosomes

Virosomes not only have a better side-effect profile than the conventional adjuvants but also show higher adjuvant potency than aluminum salts. The immunogenicity and protectivity of diphtheria or tetanus toxoid formulated either with aluminum or with virosomes were compared in mice. The two toxoids were either adsorbed to alumoxid or crosslinked to virosomes. Using an in vitro test, diphtheria toxin–neutralizing antibodies were tested. Diphtheria virosomes induced a significantly ($p = 0.002$) higher titer of diphtheria toxin–neutralizing antibodies than diphtheria-alum. Tetanus challenge experiments showed that the virosome-based tetanus vaccine induced a three fold higher titer of protective antibodies than the tetanus toxoid adsorbed to alum. Therefore, the virosome-based formulations appeared to be superior to the alum-based vaccines in terms of immunogenicity and protectivity (11).

Virosomes: A Carrier/Adjuvant for Difficult Immunogens

One of the biggest challenges is to direct the immune response only to epitopes within an antigen, which elicit neutralizing antibodies. Premium epitopes are already formed by peptides of 20 to 50 amino acids. However, so far no adjuvant has been able to elicit a reasonable immune response against peptide epitopes. Virosomes offer the opportunity to induce a peptide epitope–specific immune response. Vaccines using conformationally defined, proteolytically stable peptide B-cell epitopes would have a dramatic impact on medicinal chemistry. Synthetic peptide vaccines are currently under investigation to prevent malaria, HIV infection, schistosomiasis, foot-and-mouth disease, and influenza, among others. These synthetic, conformational B-cell epitopes would offer a number of advantages over conventional protein-based vaccines, including: (i) ease of handling and storage of small inherently stable molecules rather than proteins, (ii) ease of synthesis, (iii) avoidance of problems associated with materials produced in cells, and (iv) avoidance of other immune reactions associated with intact foreign proteins. The development of such synthetic peptide vaccines depends on a delivery system that presents these epitopes to the immune system in a natural way and does not destroy the conformation of the epitopes. The synthetic peptides should function by stimulating the immune system to produce antibodies that recognize the intact parasite.

This approach was validated in humans using the virosomal delivery system together with conformationally constrained malaria B-cell epitopes. We investigated the application of small three-dimensionally fixed antigens of the malarial parasite *Plasmodium falciparum* presented on virosomes as a model system. We focused on the central $(NPNA)_n$ repeat region of the circumsporozoite protein. Cyclic peptides of the NPNA repeats were formulated using virosomes and (for comparison) a multiple-antigen peptide (MAP). Both virosome and MAP formulations induced mimetic-specific humoral immune responses in mice, but only with the mimetic-virosome preparations; a significant fraction of the elicited antibodies cross-reacted with sporozoites (12). These results demonstrate that virosomes are a delivery system suitable for the efficient induction of antibody responses against conformationally defined epitopes. In contrast to liposomes, virosomes not only allow a particulate delivery of antigens but also enhance the immune response efficiently (Fig. 3).

Combined with combinatorial chemistry, this approach may have great potential for the rapid optimization of molecularly defined synthetic vaccine candidates against a wide variety of infectious agents.

The first vaccines with two virosome-formulated antimalaria peptide epitopes already entered clinical testing. Two virosome-formulated synthetic peptide vaccine components were administered alone and in combination to 46 healthy participants as a randomized, placebo-controlled blind study. After three vaccinations, the clinical data show that the peptide vaccine
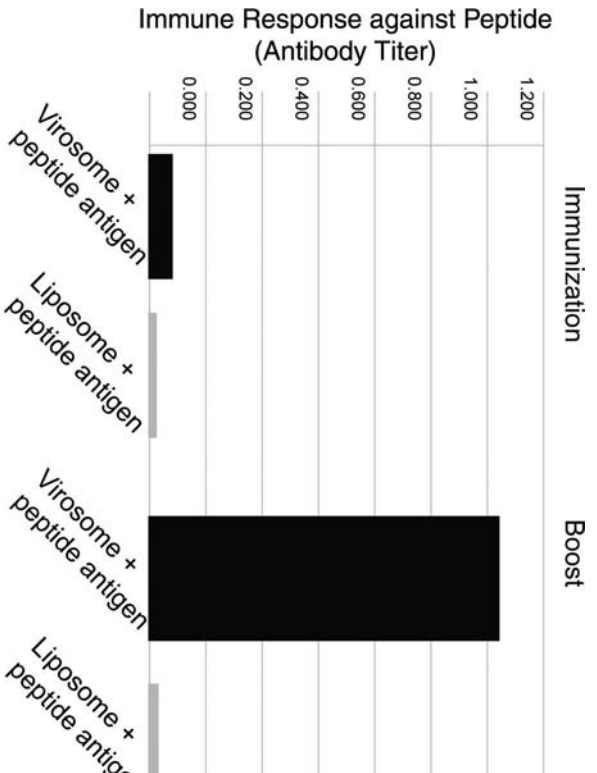
Figure 3 Mean enzyme linked immunosorbent assay immunoglobulin responses in mice immunized twice with small conformationally restricte... delivered either by virosomes or by liposomes.

Chart axis labels: Immune Response against Peptide (Antibody Titer) — values 0.000, 0.200, 0.400, 0.600, 0.800, 1.000, 1.200. Categories: Virosome + peptide antigen, Liposome + peptide antigen, Virosome + peptide antigen, Liposome + peptide antige... Groupings: Immunization, Boost.

components are well tolerated, safe, and highly immunogenic... confirms the preclinical data (12,13).

Induction of a Cellular Immune Response

Virosomes are capable of inducing not only a highly specific B-cell response but also a CD8 T-cell response. In contrast to the humoral r... CD8 antigens have to be encapsulated into the virosome. This will g... antigen to the MHC class I pathway. These antigens enter the... receptor-mediated endocytosis. Once in the endosome, the viroso... in a pH-dependent process with the endosomal membrane, which r... the release of the cytotoxic T-cell (CTL) epitopes into the cyto... T-cell epitopes are directed into the MHC class I antigen presentati... way, thereby leading to the induction of CD8+ T cells. It has alrea... shown in vitro that virosomes containing a synthetic peptide are... deliver the peptide antigen to the MHC class I presentation p... stimulating specific CTLs as well as rendering target cells susceptibl... gen-specific CTL-mediated lysis (14). To induce a CTL response,... CTL epitopes have to be delivered, but also T helper epitopes. Th... topes play a critical role in the induction of MHC class I-r... CTLs (15–18). The virosomal carrier is also able to trigger a...

response because T-helper epitopes are located on the influenza HA, the major component of virosomes. It has been demonstrated that a synthetic peptide enclosed in virosomes is able to induce a CTL immune response in mice (19). In addition, the use of virosomes helps to avoid the induction of tolerance, which has been observed under certain conditions after immunizing mice intraperitoneally with soluble peptide (20).

Synthetic peptide–based vaccines, which are designed to stimulate CD8+ CTLs, are an attractive approach to the treatment or prevention of infectious diseases and chronic diseases including cancer.

The proof of concept was demonstrated using peptide-loaded virosomes. Human leukocyte antigen (HLA)-A2 transgenic mice were immunized with hepatitis C virus Core132 peptide encapsulated in virosomes. Animals were immunized twice with either differen concentrations of the CD8 T-cell epitope or the carrier system alone as a negative control. The strength of the induced CTL response was dose dependent, with the highest dose giving the highest specific lysis of about 47% lysis at an E/T ratio of 33:1 (Fig. 4A). Neither in naive mice nor in mice immunized with empty virosomes could a substantial lysis of the target cells be detected. In addition, interferon γ (IFNγ) release was chosen as another indicator of T-cell response induced by virosome-formulated peptides. IFNγ release was quantified by enzyme-linked immunosorbent spot (ELISPOT) assay (Fig. 4B). The numbers of IFNγ-producing cells correlated well with the peptide-specific cytotoxicity, with higher numbers induced by higher amounts of peptide in the virosomal formulations (21).

This indicates that virosomes containing Core132 peptide efficiently induce specific cytotoxic and IFNγ-producing T cells in HLA-A2.1 transgenic mice. Those responses were dose dependent and even the lowest dose of 2 µg peptide per injection induced a CTL immune response.

We could already show that preexisting immunity to influenza virus, reflecting the situation in humans, affected neither the humoral immune response (11) nor the induction of IFNγ-producing CD8+ T cells by virosomes (21). On the contrary, it can be speculated that influenza-specific CD4+ T cells could provide help to raise a CTL response directed against the peptide encapsulated in the virosome. Such a phenomenon has been observed in vitro with human peripheral blood mononuclear cell (PBMC) where virosomes activated CD4+/CD45RO+ T cells and induced a cytokine profile consistent with Th1 stimulation (22).

VIROSOME-BASED VACCINES ON THE MARKET

Epaxal

The first liposomal vaccine for human use, a virosomal hepatitis A vaccine, was licensed in 1996 and is now registered in nearly all countries of the European Union, the Americas, and Asia. This vaccine contains formalin-inactivated and highly purified hepatitis A viruses (HAV) of strain
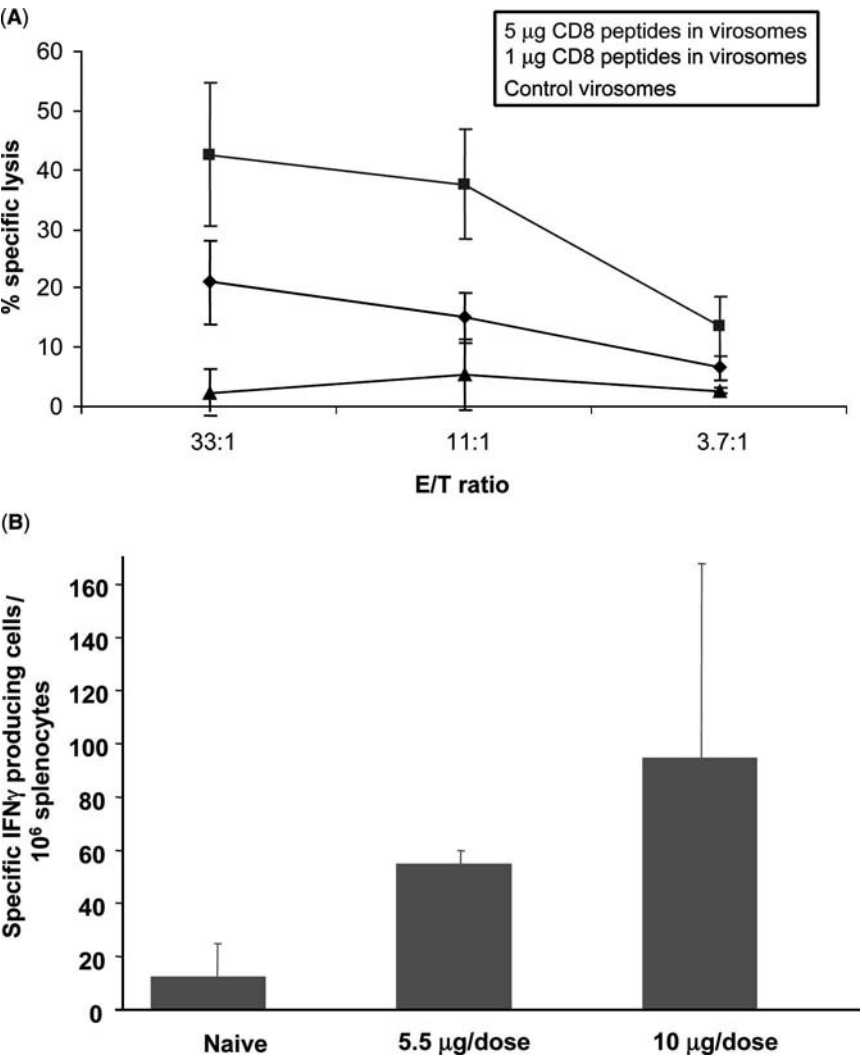
Figure 4 (**A**) HLA-A2 transgenic (HHD) mice were immunized twice subcutaneously at a three-week interval with empty or peptide-loaded virosomes. Spleen cells were isolated two weeks after the second immunization. After five days of in vitro restimulation with CD8 peptide, the stimulated spleen cells were used as effector cells against HHD transfected EL4 as target cells in a Cr-release assay with an E/T ratio starting at 33:1. Results show peptide mean specific lysis (lysis of target cells with peptide–lysis of target cells without peptide) of two to three individual mice ± standard deviation. (**B**) Interferon γ-producing cells in virosome-immunized HHD mice. HHD mice were immunized twice subcutaneously at a three-week interval with peptides encapsulated into virosomes. Spleen cells were isolated two weeks after the second immunization. The spleen cells were isolated and stimulated overnight with peptide or a control peptide (negative control). Shown are the mean values as derived from two to three individual mice ± standard deviation. *Abbreviation*: E/T, effector to target. *Source*: From Ref. 21.

RG-SB, cultured on human diploid cells, which are coupled to the virosome vesicle. The virosomal HAV vaccine is able to induce a very fast immune response because 10 days after immunization 100% of seroconversion has been observed (23). In addition to the excellent tolerability (Fig. 5) (24), a very good long-term protection could also be shown (25). In a placebo-controlled field trial, the HAV-virosome vaccine has proven its efficacy (26).

Inflexal

A trivalent, virosome-formulated influenza vaccine has shown a very good immunogenicity in all age groups and also excellent tolerability (27). The purified influenza membrane glycoproteins are incorporated into the lipid bilayer and are presented to the immune system in a natural way. The influenza HA physically stabilizes the virosomes, so they will maintain an appropriate particle size, allowing for efficient uptake by macrophages and other APC. Extensive clinical testing confirmed that this vaccine is safe and does not engender any antiphospholipid antibodies against the lipid components of the virosome (28). The virosome adjuvant represents the first alternative to the problematic old aluminum salts.
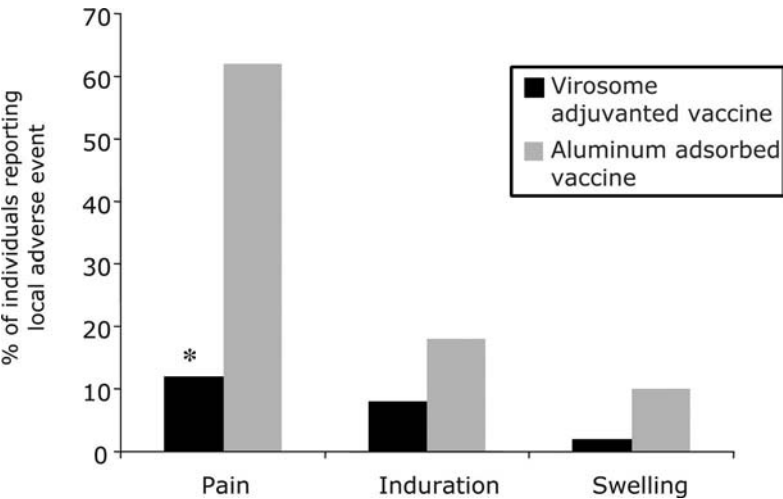
Figure 5 *Safety profile of virosomes*: Highly improved tolerability of the virosome-adjuvanted hepatitis A vaccine in comparison with an aluminum-adsorbed vaccine. ∗ indicates statistically significant less pain at site of injection with the virosome adjuvanted vaccine ($p < 0.001$). *Source*: From Ref. 24.

VIROSOMES FOR DRUG DELIVERY

Virosomes can be used for cell- and organ- or tissue-specific delivery of pharmaceutically active substances in the body. The unique properties of virosomes partially relate to the presence of HA in their membrane. This viral protein not only confers structural stability and homogeneity to virosomal formulations, but also significantly contributes to the fusion activity of virosomes, which induces the endolysosomal pathway. On the virosomal surface, ligands can be attached. This function is crucial for the targeted delivery of drugs. Therefore, virosomes selectively bind with their ligands to the target cell. Likewise, the virosomal HA promotes binding to the target cell and receptor-mediated endocytosis. In the endosome, the virosomal HA—triggered by an acidic environment—mediates membrane fusion, and therapeutically active substances escape from the endosome into the cytoplasm of the target cell. This concept has been validated in vivo. The cytotoxic drug doxorubicin was encapsulated into the virosomes. On their surface, monoclonal antibodies were cross-linked, mediating specific targeting of the carrier to cancer cells. Data showed that these virosome-formulated cytostatics were delivered to the target cells and dramatically reduced the tumor volume (29). The specificity of the targeting as well as the efficiency of cellular uptake can be highly modulated and adapted to the preferred conditions.

REFERENCES

1. Collier LH, Polakoff S, Mortimer J. Reactions and antibody responses to reinforcing doses of adsorbed and plain tetanus vaccines. Lancet 1979; 1(8131):1364–1368.
2. Gupta RK, Relyveld EH, Lindblad EB, Bizzini B, Ben-Efraim S, Gupta CK. Adjuvants—a balance between toxicity and adjuvanticity. Vaccine 1993; 11(3): 293–306.
3. Gluck R, Wegmann A. Virosomes, a new liposome-like vaccine delivery system. In: Lasic DD, Papahadjopoulos D, eds. Medical Applications of Liposomes. Amsterdam: Elsevier, 1998:75–115.
4. Wilson IA, Skehel JJ, Wiley DC. Structure of the haemagglutinin membrane glycoprotein of influenza virus at 3A resolution. Nature 1981; 289:366–373.
5. Klenk HD, Rott R, Orlich M, Blodorn J. Activation of influenza A viruses by trypsin treatment. Virology 1975; 68:426–439.
6. Durrer P, Galli C, Hoenke S, et al. H + -induced membrane insertion of influenza virus hemagglutinin involves the HA2 amino-terminal fusion peptide but not the coiled coil region. J Biol Chem 1996; 271:13417–13421.
7. Tsurudome M, Gluck R, Graf R, Falchetto R, Schaller U, Brunner J. Lipid interactions of the hemagglutinin HA2 NH2-terminal segment during influenza virus-induced membrane fusion. J Biol Chem 1992; 267:20225–20232.
8. Matlin KS, Reggio H, Helenius A, Simons K. Infectious entry pathway of influenza virus in a canine kidney cell line. J Cell Biol 1981; 91:601–613.

9. Air GM, Laver WG. The neuraminidase of influenza virus. Proteins 1989; 6: 341–356.
10. Zurbriggen R, Novak-Hofer I, Seelig A, Glück R. Virosome-adjuvanted hepatitis A vaccine: in vivo absorption and biophysical characterization. Prog Lipid Res 2000; 39(1):3–18.
11. Zurbriggen R, Glück R. Immunogenicity of virosome- versus alum-adjuvanted diphtheria and tetanus toxoid vaccines in influenza primed mice. Vaccine 1999; 17:1301–1305.
12. Moreno R, Jiang L, Moehle K, et al. Exploiting conformationally constrained peptidomimetics and an efficient human compatible delivery system in synthetic vaccine design. Chem Bio Chem 2002; 2:838–834.
13. Mueller MS, Renard A, Boato F, et al. Induction of parasite growth-inhibitory antibodies by a virosomal formulation of a peptidomimetic of loop I from domain III of *Plasmodium falciparum* apical membrane antigen 1. Infect Immun 2003; 71(8):4749–4758.
14. Hunziker IP, Grabscheid B, Zurbriggen R, Gluck R, Pichler WJ, Cerny A. In vitro studies of core peptide-bearing immunopotentiating reconstituted influenza virosomes as a non-live prototype vaccine against hepatitis C virus. Int Immunol 2002; 14:615–626.
15. Zinkernagel RM, Callahan GN, Klein J, Dennert G. Cytotoxic T cells learn specificity for self H-2 during differentiation in the thymus. Nature 1978; 271: 251–253.
16. Keene JA, Forman J. Helper activity is required for the in vivo generation of cytotoxic T lymphocytes. J Exp Med 1982; 155:768–782.
17. Bennett SR, Carbone FR, Karamalis F, Miller JF, Heath WR. Induction of a CD8+ cytotoxic T lymphocyte response by cross-priming requires cognate CD4+ T cell help. J Exp Med 1997; 186:65–70.
18. Toes RE, Ossendorp F, Offringa R, Melief CJ. CD4 T cells and their role in antitumor immune responses. J Exp Med 1999; 189:753–756.
19. Arkema A, Huckriede A, Schoen P, Wilschut J, Daemen T. Induction of cytotoxic T lymphocyte activity by fusion-active peptide-containing virosomes. Vaccine 2000; 18:1327–1333.
20. Aichele P, Brduscha-Riem K, Zinkernagel RM, Hengartner H, Pircher H. T cell priming versus T cell tolerance induced by synthetic peptides. J Exp Med 1995; 182:261–266.
21. Amacker M, Engler O, Kammer AR, et al. Peptide-loaded chimeric influenza virosomes for efficient in vivo induction of cytotoxic T cells. Int Immunol 2005; 17:695–704.
22. Schumacher R, Adamina M, Zurbriggen R, et al. Influenza virosomes enhance class I restricted CTL induction through CD4+ T cell activation. Vaccine 2004; 22:714–723.
23. Abrosch F, Glück R, Herzog C. Clinical and immunological studies with a new virosome based hepatitis A vaccine. Proceedings of 2nd European Congress Trop Medicine, Liverpool, 1998.
24. Holzer BR, Hatz C, Schmid-Sissolak D, Glück R, Althaus B, Egger M. Immunogenicity and adverse effects of inactivated virosome versus alum-adsorbed hepatitis A vaccine: a randomized controlled trial. Vaccine 1996; 14:982–986.

25. Bevier P, Farinelli T, Loutan L, Herzog C, Glück R. Long-term immunogenicity following immunization with a virosome hepatitis A vaccine. Abstracts of 5th International Conference on Travel Medicine, Geneva, 1997 (abstract No 127).
26. Mayorga O, Egger M, Zellmeyer M, Glück R, Herzog C, Frösner G. Efficacy of a virosome formulated hepatitis A vaccine in an endemic region in Nicaragua: a randomized plazebo-controlled trial. Abstract of 37th ICAAC, Toronto, 1997 (abstract No H-4).
27. Conne P, Gauthey L, Vernet P, et al. Immunogenicity of trivalent subunit versus virosome-formulated influenza vaccines in geriatric patients. Vaccine 1997; 15:1675–1679.
28. Cryz SJ, Que JU, Glück R. A virosome vaccine antigen delivery system does not stimulate an antiphospholipid antibody response in humans. Vaccine 1996; 14:1381–1383.
29. Waelti E, Wegmann N, Schwaninger R, et al. Targeting her-2/neu with antirat Neu virosomes for cancer therapy. Cancer Res 2002; 62(2):437–444.

7

Lipoplexes in Gene Therapy Under the Considerations of Scaling Up, Stability Issues, and Pharmaceutical Requirements

Patrick Garidel

Institute of Physical Chemistry, Martin Luther University Halle/Wittenberg, Halle/Saale, Germany

Regine Peschka-Süss

Pharmaceutical Technology and Biopharmacy, University of Freiburg, Freiburg, Germany

INTRODUCTION

The identification of unknown functional genes has induced the propagation of new and modern medical treatments like gene vaccination and gene therapy. These novel therapies try to cure illnesses at the genetic level (genotype) and not by treating symptoms (phenotype). Although gene therapy as a treatment for diseases still holds great promises, the progress in developing effective clinical protocols has been slow over the last 15 years (1). A critical point lies in the development of safe and efficient gene transfer systems. In addition, efforts need to be undertaken with regard to difficulties encountered during the manufacturing and industrial production of stable gene delivery systems as well as with patient compliance. The first clinically approved study for somatic gene therapy started in September 1990 (2). In the intervening 15 years, approximately 1000 gene therapy clinical trials have been initiated worldwide [according to statistics published in *The Journal of Gene Medicine*, 2006; (3)]. More than 60% of the clinical trials were

performed in the United States, whereas about 30% were in Europe and the remaining studies took place in Asia and Australia. Most of the trials are performed in early clinical phases (phase I and phase I/II, approximately 84%), 13% in phase II, and only 3% in late clinical phases (phase II/III and phase III).

The conclusions from the results of the first clinical trials were that gene therapy has the potential for treating a broad range of human diseases. However, with the tragic case of Jesse Gelsinger in 1999, the high hopes for gene therapy were instantaneously destroyed. Jesse Gelsinger suffered from a mild form of a rare inherited nitrogen metabolism disorder (ornithine transcarbamylase deficiency). He was involved in a phase I clinical trial that was testing an engineered adenovirus (AV) vector as a gene transfer vehicle carrying a gene intended to correct the defect and thus to cure the disease. It was found that his death was caused by an acute respiratory system collapse with subsequent multiorgan failure that was induced, at least in part, by the patient's immune system's response to the engineered viral vector (4–7).

From the very beginning, it was known that using viral vectors as gene transfer systems represents a certain risk. This is also obvious from the cases observed in Alain Fischer's clinical trial, where young patients with a severe combined immunodeficiency syndrome (SCID) were treated. Although it was found that the SCID patients appear to have benefitted from the experimental gene therapy procedure, an undesired gene insertion due to the viral vector was observed and has been suspected to be the cause of a rare leukemia (8–12). On the contrary, the first commercially manufactured gene therapy product became available on the Chinese market in January 2004 (13). Thus, China became the first country to approve the commercial production of a gene therapy product. The Chinese company Shenzhen SiBiono GenTech (Shenzhen, China) obtained a drug license from the State Food and Drug Administration of China for its recombinant Ad-p53 gene therapy for head and neck squamous cell carcinoma. The drug is sold under the brand name Gendicine. This first commercially available gene therapy drug is based on an adenoviral vector.

As can be seen in Table 1, cancer is by far the largest indication area for gene therapy. Almost 75% of the above-mentioned clinical trials use viral transfer systems, whereas about 25% of the trials are performed with nonviral systems. At the beginning of the century (2000), about 15% to 20% of the trials were carried out via lipofection (transfection using lipid–DNA systems), whereas currently only 10% use lipid-DNA complexes as gene delivery systems (Table 2).

In gene therapy, a pharmaceutical sequence is transferred by viral or nonviral vector systems. The latter includes chemicals [lipids, polymers, and protein plasmid DNA (pDNA) condensation] as well as physical transfection methods (electroporation, jet gun, etc.) or naked DNA. The advantages and disadvantages of these transfection systems have been described in a number of papers (1,14). Common challenges encountered

Table 1 Indications Addressed by Gene Therapy Clinical Trials

Indications addressed	Percentage
Cancer diseases	66
Monogeneic diseases	10
Vascular diseases	8
Infectious diseases	7
Other diseases	3
Gene marking	5
Healthy volunteers	1

Source: Adapted from *The Journal of Gene Medicine*, 2006.

in nonviral and viral gene therapies are summarized in Table 3. However, a number of efforts are being undertaken in both fields to overcome the drawbacks, e.g., the development of safer viral transfection systems or the production of these systems under good manufacturing practice (GMP) conditions (15–23). The transfection efficiency of nonviral systems has also increased considerably by using new lipids or polymers combined with DNA condensation agents (1,14,24–30).

This paper is focused on the use of liposome–DNA complexes (so called lipoplexes) in gene therapy. The following issues will be discussed— manufacturing and stabilisation of liposomes, plasmids, and lipoplexes with special consideration of the required industrial and pharmaceutical aspects. Quality control of the involved materials, liposomes, DNA, and the final product lipoplex with regard to these aspects is also very important. Additionally, biophysical methods are presented for the elucidation of the lipid–DNA structures, and the relation of these structures with respect to transfection efficiency is also briefly discussed.

Table 2 Vectors Used in Gene Therapy Clinical Trials

Vectors	Percentage
Retrovirus	27
Adenovirus	26
Adeno-associated virus	3
Pox virus	7
Vaccina virus	4
Herpes simplex virus	3
Others	5
Naked/plasmid DNA	15
Lipofection	10

Source: Adapted from *The Journal of Gene Medicine*, 2006.

Table 3 Viral vs. Nonviral Transfection Systems

Viral	Nonviral (lipids, polymer, and naked DNA)
(+) Very efficient	(−) Less efficient
(+) Transfection of dividing and non-dividing cells	(−) Limited transfection of non-dividing cells
(−) Immunogenetic	(+) Low immunogenetic and toxic
(−) Potentially mutagenetic	(+) Biodegradable systems (e.g., lipids)
(−) Low viral titers	(+) Targeted delivery
(−) Limited loading capacity	(+) No known limitation in DNA size
(−) Repeat dosing difficult	(+) Can deliver different forms of DNA (e.g., CCC, OC, linear form)
(−) Complicated manufacturing	(+) Repeat dosing possible
	(+) "Relatively" simple manufacturing

Note: Advantages (+), disadvantages (−).

LIPOSOME FORMATION

Various methods have been described in the literature for the preparation of liposomes, and variations and adaptations thereof are still being developed. The most relevant preparation methods are: (i) hand-shaken multilamellar vesicles, (ii) ethanol injection vesicles, (iii) sonicated small, mostly unilamellar vesicles, (iv) freeze-dried rehydration vesicles, (v) reverse-phase evaporation vesicles, (vi) high-pressure homogenization vesicles, (vii) detergent depletion–producing unilamellar and oligolamellar vesicles, and (viii) extrusion procedures. Protocols for each of these techniques can be found in Lasch et al. (31) and the references cited therein.

Depending on the method used, the size, morphology, and lamellarity of the liposomes produced can be quite different [for more information see Refs. (32–46)]. This has an important impact with regard to the preparation and stability of lipid–DNA complexes (Peschka-Süss and Garidel, unpublished results) and their transfection efficiency (1,14,28,47).

However, not all of the above-mentioned methods are suitable for up-scaling and the industrial production of large amounts of liposomes of defined size. Methods in which organic solvents are used require an additional step in the manufacturing procedure to completely remove the organic solvent (44). The methods involving detergent removal (39) have the advantage that unilamellar liposomes with an extremely small size distribution are generated. However, for the special requirements of industrial manufacturing, these methods are often time consuming and expensive (e.g., detergent costs).

Liposomes of a defined size can also be obtained by using the extrusion technique (48–50). This technique allows the manufacturing of liposomes for industrial purposes (see below). An additional important point to consider is the sterilization procedure of the liposomal formulation.

Various options are available for sterilization, such as steam and dry heat, gas (formalin and hydrogen peroxide), ionization radiation, and sterile filtration. For the preparation of sterile liposomes, however, some of these operations are not applicable because of the degradation of the lipids and changes in liposome morphology. Gamma irradiation (with 25 kGy as recommended by the regulatory authorities) as a sterilization procedure is not suited because of its highly destructive action on lipids (51–56).

The most suitable sterilization technique for liposome dispersions is sterile filtration through a 0.2-μm filter membrane. When the filtration procedure is performed at temperatures above the main phase transition temperature of the lipids, even vesicles larger than about 1–2 μm can be filtered because of increased lipid membrane flexibility in the liquid crystalline phase. However, it remains to be shown that the morphology and size of the liposomal dispersion is not altered during sterile filtration. Alternatively, preparation of the liposomes may be performed under aseptic conditions in a Class A environment. This procedure is well established in the biopharmaceutical industry for the production, filling, and finishing required during the manufacturing process. Analytical assays for the characterization of liposomal dispersions have been described in the past and are summarized in Table 4 [for more details see Refs. (50,57,59–65)].

PLASMID PRODUCTION

The active ingredient in nonviral gene drugs is the naked or complexed pDNA. With regard to applicability in clinical trials, it is of great importance to supply even early studies with the required amounts of high-purity pDNA, manufactured under GMP conditions (66–68). Efforts are currently being undertaken to develop industrial scale processes for the production of pDNA with batch yields from grams to kilograms, while meeting the appropriate quality standards requested by the national health agencies. According to international regulations, it is expected that greater than 90% of the content must be in the covalently closed circular (ccc) form. The other plasmid topological forms reduce homogeneity and should be removed by separation processes (Fig. 1). Additionally, impurities related to the *Escherichia coli*–producing cells (genomic DNA, RNA, proteins, and endotoxins) should also be removed. For clinical trials, pDNA has to be made available with regard to pharmaceutical considerations (see below).

Fermentation

A standard *E. coli* host strain for manufacturing pDNA does not exist. The quality of the produced pDNA is dependant on the host. Therefore, the most suitable host–plasmid combination has to be evaluated on a case-by-case basis. However, over the last few years a number of experiments in the field of molecular cloning and DNA techniques were performed

Table 4 Characterization Assays for Liposomal Formulations

Basic assays	Methodology
pH	pH meter
Osmolarity	Osmometer
Lipid concentration	Lipid phosphorus content, HPLC, enzymatic assays, HPTLC
Lipid composition	TLC, HPLC
Cholesterol concentration	HPLC, HPTLC, enzymatic assay
Lipid hydrocarbon chain composition	GC
Residual organic solvent	GC
Heavy metals	NMR
Chemical stability	
Lipid hydrolysis	HPLC, HPTLC
Lipid hydrocarbon chain oxidation	Lipid peroxides, conjugated dienes, fatty acid composition (GC), TBA method
Free fatty acid concentration	HPLC
Cholesterol oxidation	HPLC, TLC
Physical stability	
Appearance, color, clarity	Pharmacopoeia methods
Vesicle size distribution submicron range	DLS, SLS, microscopy, HPSEC, turbidity
Micron range	Light obscuring method, light microscopy, laser diffraction, SLS, Coulter counter
Lamellarity	Electron microscopy
Zeta potential	Electrophoretic mobility
Thermotropic phase behavior	DSC, NMR, FTIR, fluorescence spectroscopy, Raman spectroscopy
Phase separation	DSC, NMR, FTIR, fluorescence spectroscopy, Raman spectroscopy, ESR, turbidity, AFM
Microbiological assay	
Sterility	Pharmacopoeia methods
Endotoxin	Pharmacopoeia methods (LAL)

Abbreviations: HPLC, high-performance liquid chromatography; HPTLC, high-performance thin-layer liquid chromatography; TLC, thin-layer chromatography; GC, gas chromatography; NMR, nuclear magnetic resonance; TBA, thiobarbituric acid; DLS, dynamic light scattering; SLS, static light scattering; HPSEC, high-performance size-exclusion chromatography; DSC, differential scanning calorimetry; FTIR, Fourier transform infrared spectroscopy; ESR, electron paramagnetic spin relaxation spectroscopy; AFM, atomic force microscopy; LAL, limulus amebocyte lysate assay.
Source: Adapted from Refs. 57, 58.
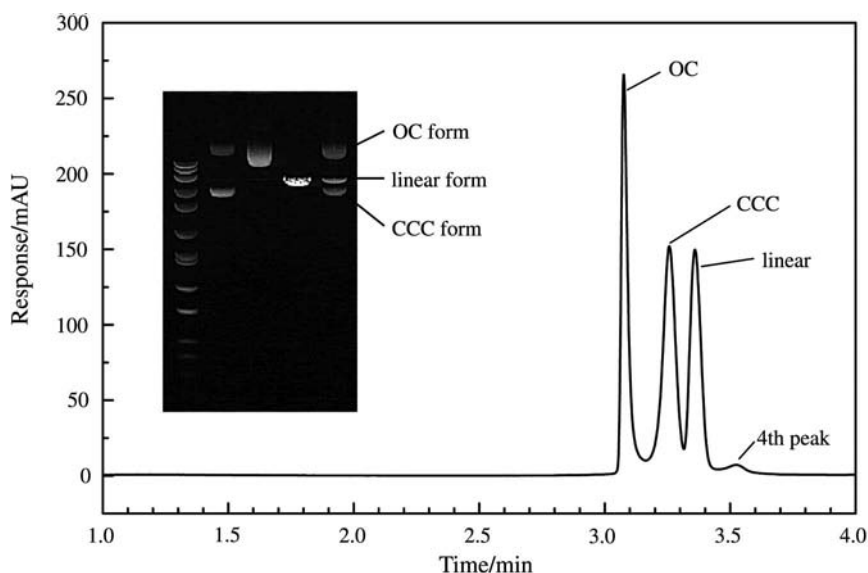
Figure 1 High-performance liquid chromatogram of a mixture of various pDNA topomers. Insert: agarose gel showing the identification of various topomers (DNA stained with ethidium bromide). *Abbreviations*: OC, open circular; CCC, covalently closed circular.

using *E. coli* K12 (69,70), because it is a safe strain that is well characterized for plasmid production (71–73).

The fermentation process itself strongly influences the yield and homogeneity of pDNA. Initially, batch processes with culture media containing complex nitrogen sources were used for pDNA manufacturing. In order to increase the plasmid yields, high-cell-density cultivation processes have been developed. It could be demonstrated that by the development of optimized culture media (without complex or animal-derived compounds and antibiotics) and by the establishment of sophisticated feeding regimes, plasmid titers of up to 1 g/L of culture broth are possible [for more details see Ref. (74)].

The parallel cultivation of a number of different *E. coli* hosts (e.g., NM522, DH5, DH5-α, DH1, JM110, and JM101) harboring the same plasmid showed significant difference in pDNA quality with respect to the plasmid isoforms produced (75).

Currently, industrial processes are available for the pharmaceutical production of pDNA under GMP, which are scalable up to 4000 L for the production of a few kilograms of pDNA [for more information see Ref. (74)] (75). Careful selection of the optimal host and plasmid combination, as well as the development of a rational production pathway, enables pDNA yields with concentrations higher than 1000 mg/L of fermentation broth. Figure 2 shows a

Plasmid DNA titer (mg/L)

700
600
500
400
300
200
100
0

0 5 10 15 20 25 30 35 40 45

Time (h)

─■─ pDNA(mg/L) ── start feed ─◆─ DCW (g/L) ···▲··· spec.pDNA (mg/g)
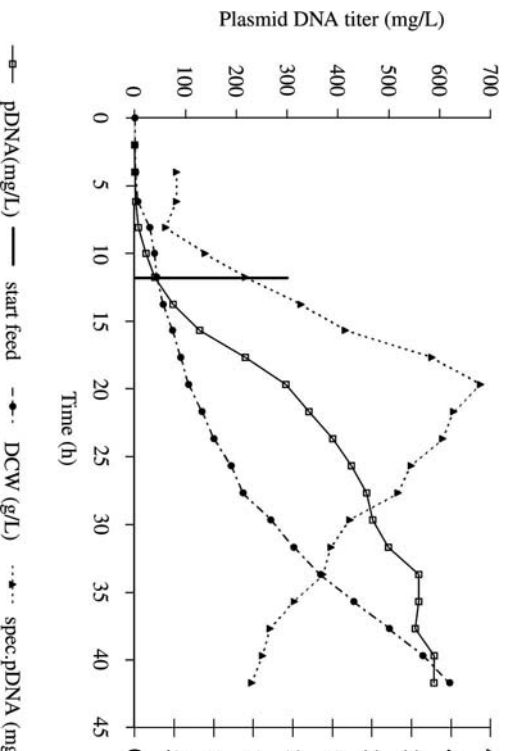
Figure 2 Example of a high-cell-density fermentation of *Escherichia coli* f... facturing of plasmid DNA. A fed-batch fermentation was carried out at ... 20 L. Feeding of the culture medium was carried out in order to maintain growth rate of $\mu = 0.1\,h^{-1}$. The fermentation titer of the plasmid was around 6... more than 90% of which was present in its supercoiled conformation.

high-cell-density fermentation of *E. coli* for the manufacturing of pla... the example presented, a fed-batch fermentation was carried out at a 20... Feeding of the culture medium was carried out to maintain a specifi... rate of $\mu = 0.1\,h^{-1}$. The fermentation titer of the plasmid was 600 mg/L, more than 90% of which was present in a supercoiled confo...

Purification

As described previously, supercoiled multimeric plasmids are of p... interest for pharmaceutical purposes because they contain multipl... of a therapeutic gene and can therefore be more efficient vectors.

pDNA is not necessarily a homogeneous product because of i... nature. Different plasmid topologies such as the CCC form, the ope... (OC) form, or the linear form are known. These basic forms can also multimeric shapes, denoted as concatamers.

A standard purification process consists of alkaline cell lysi... lysis using lysozyme, RNA removal by RNase, extraction and prec... with organic solvents, and ultracentrifugation in density gradien... processes, however, are more adapted for the laboratory scale. T... extremely time consuming, use toxic reagents (e.g., phenol and Cs... in most cases are not scaleable to the levels required for industrial ceutical manufacturing.

Chromatographic purification techniques have recently become available for the fast and efficient purification of large amounts of pDNA under GMP requirements (70,76–83). It is preferable to avoid the use of enzymes or organic solvents during large-scale manufacturing of pDNA.

An industrial manufacturing process for pDNA typically consists of the following steps: cell lysis, clarification, purification, polishing, formulation, and the fill-and-finish step [for more details see Ref. (70)].

Plasmid Stability and Quality Control

Walther et al. (84) have recently reported stability data of naked pDNA stored for one year. Depending on the storage temperature and formulation, the relative stability of plasmids can be quite different. By means of capillary gel electrophoresis, they were able to show that stable storage conditions at $-80°C$ prevent an increase in OC plasmid, preserving the CCC form. But in long-term storage of plasmid formulation at $4°C$, a rapid decline of the CCC form and an increase of the OC isomer and linear DNA were observed. Examination of transfection efficiency of plasmid formulations stored for 1, 2, and 13 months at $-80°C$ in jet-injected xeno-transplanted colon carcinoma showed similar results, thus indicating the stability and integrity of the stored DNA formulation (84). Various guidelines [see Ref. (70) and references cited therein] address the production and quality control of pDNA. Agarose gel electrophoresis has been used for the analysis of the quality, quantity, and identity of pDNA for a number of years. However, more sensitive methods are currently available. Anion exchange high-performance liquid chromatography (AIEX-HPLC) is a robust and sensitive method for the determination of the quality (with regard to the percentage of plasmid in the CCC form) and the quantity of DNA (75,85). For the analysis of different plasmid forms and identification of restriction fragments, high-performance capillary electrophoresis is the method of choice because of its extreme high resolution and accuracy. Restriction digestion maps can also be generated by using chip-based technologies, which allow a higher throughput of samples.

A number of papers describing various methods for the characterization of pDNA are available (86–98). The major assays currently in use as quality control assay are summarized in Table 5.

THE FORMATION OF LIPID–DNA COMPLEXES

The interaction of cationic liposomes with anionic DNA is driven by the electrostatic attraction between the positive charges of the vesicle and the negative charges of the phosphate backbone of the DNA. Upon mixing of the two agents, neutralization of the negative charge of the DNA results in condensation of the lipid with the DNA. Still, the resulting structure of

Table 5 Quality Control Tests and Assays for Plasmid DNA

Test	Assay
Appearance	Visual inspection
Color	Color test according to United Sates Pharmacopeia
Turbidity	Nephelometry
Plasmid identity	Restriction enzyme digest and agarose gel electrophoresis, sequencing
DNA homogeneity	Agarose gel electrophoresis, capillary gel electrophoresis
DNA concentration	UV (A_{260} in 1 mM Tris Cl, pH 8.5)
Presence of bacterial host DNA	Agarose gel electrophoresis, blot hybridization
Presence of protein	BCA colorimetric assay
Presence of RNA	HPLC
Presence of endotoxin	LAL assay (according to USP)
Absence of microorganisms	Bioburden assay (according to USP)

Abbreviations: BCA, Bradford colorimetric assay; HPLC, high-performance liquid chromatography; LAL, Limulus amebocyte lysate; USP, United States Pharmacopeia; UV, ultraviolet.
Source: From Ref. 70.

the lipid/DNA complex depends on the lipid and buffer composition as well as the lipid-to-plasmid ratio. Additionally, the formation of lipoplexes is strongly dependent on the liposome preparation method itself (99), as well as on the mixing procedure used to form lipid/DNA complexes. Today, it is known that the order of combining lipid and DNA has a very critical effect on the physical properties (100) and even on the biological activity of liposomes. Kennedy et al. (101) studied this effect in detail and showed that the fundamental differences were dependent upon their mode of preparation and the ionic strength of the preparation medium. It has been reported in numerous studies that lipid/DNA aggregates can be very heterogeneous in size (1). Taking into account the fact that there is no standard method for the preparation of lipoplexes, this is not surprising. The correlation between size (100–102), lamellarity (47), and structure (103) of the lipoplexes and their biological activity still is not understood.

The optimal ratio of lipid/DNA has to be evaluated carefully and depends on the cell model used for transfection. For example, in Figure 3, transfection efficiencies of varying lipid/DNA ratios were evaluated in different cells. Smooth muscle cells from rat (A-10 SMC), human smooth muscle cells (HASMC), and human aorta endothelium cells (HAEC) were transfected with DC-30/DNA 5:1 (m:m) using a green fluorescent protein (GFP) plasmid. Transfected cells were quantified by flow cytometry. Not only the number of cells transfected, but also the optimal lipid/DNA ratio was found to be significantly related to cell type.
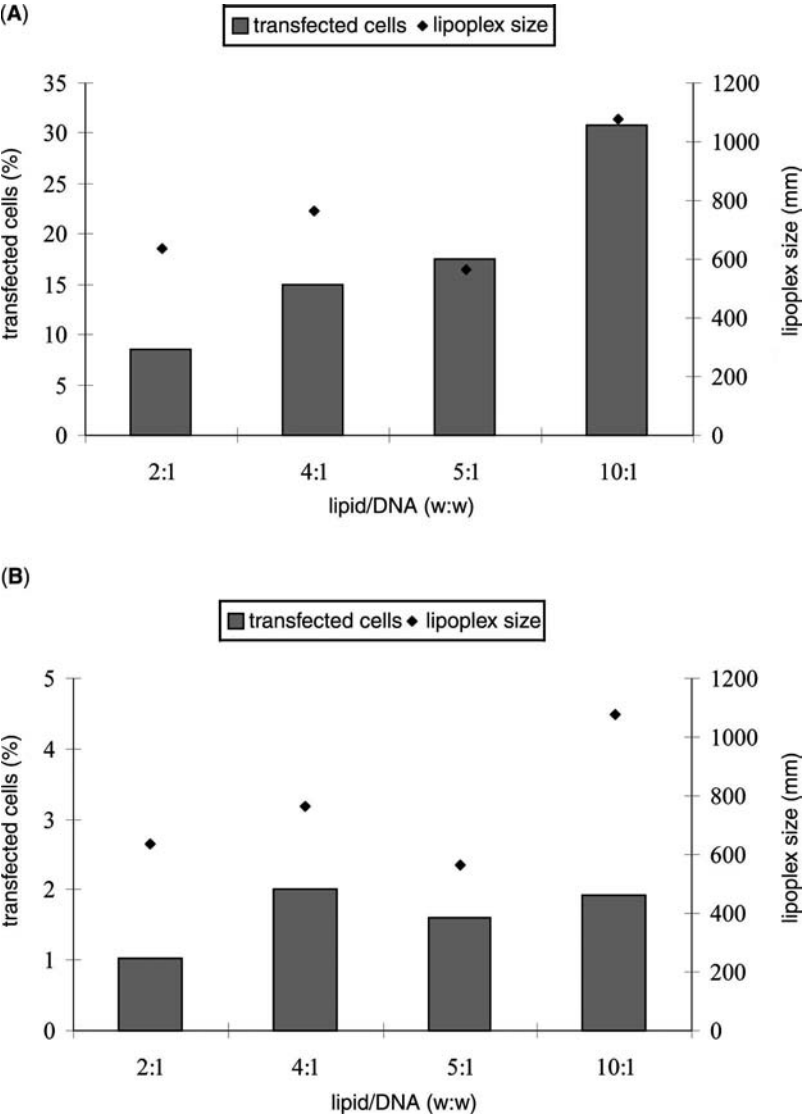
Figure 3 (*Continued on next page*) Transfection efficiencies of DC-30 with varying lipid/DNA(pGFP) ratios (m/m) (**A**) A-10 smooth muscle cells (SMC) (rat SMC, cell line), (**B**) human aorta smooth muscle cells, (**C**) human aorta endothelial cells. *Source*: From Ref. 104.

 In most cases, the reproducibility of transfection results has been unsatisfactory and does not meet the requirements of quality control for drug manufacturing. The urgent need of a reproducible method of lipid/DNA complex preparation is obvious, but very little has been reported in this field.

(C)
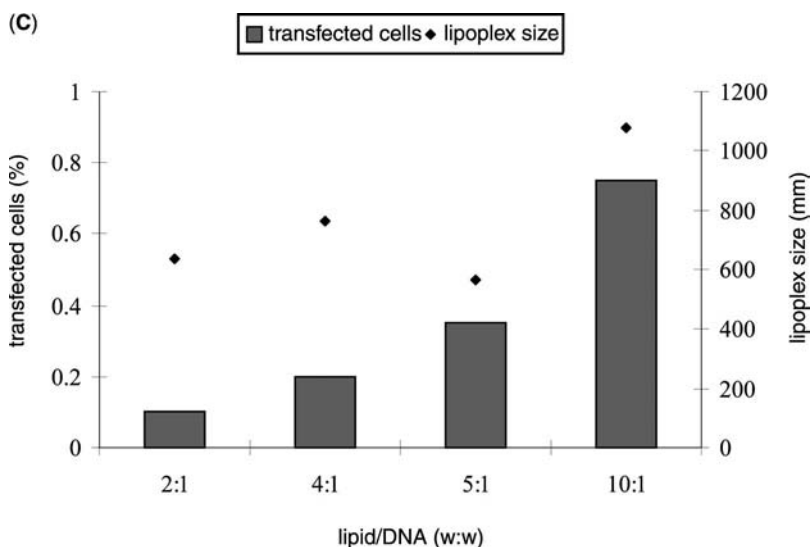
Figure 3 (*Continued from previous page*)

To assure reproducibility of preparation conditions and the quality of the resulting lipoplex, especially with respect to industrial manufacturing, a scale-up process was developed as follows (105). Lipid and plasmid solutions were diluted separately to the desired concentrations. Different media were then tested. The appropriate lipid dispersion was pumped once through an 800 nm polycarbonate membrane using a peristaltic pump. To achieve simultaneous mixing of lipid and DNA at a constant flow rate, both preparations were mixed via a Y-connector. This way, the problem of the order of mixing with regard to irreproducible products was eliminated. The lipoplex dispersion was collected in an appropriate reservoir and then analyzed.

BIOPHYSICAL CHARACTERIZATION OF LIPOPLEXES

The beginning of gene therapy using lipofection was governed by more or less modest reproducibility of the transfection results. This was mainly due to the large heterogeneity and product quality of the lipoplexes used, thus making comparison between various studies very difficult. Nowadays, it is known that the particle size, zeta potential, lipid composition, lipid-to-DNA ratio, hydration properties, buffer, etc. are all critical parameters for the successful transfection as well as stability of the lipoplexes (106–111).

Because of this, a number of biophysical studies were initiated in order to better understand the relation between the lipoplex structure, morphology, and bioactivity [e.g., (112–114)]. Additionally, such studies were also initiated for a more precise characterization of a potential pharmaceutical product.

Audouy and Hoekstra (115) have reviewed some important aspects for the successful in vivo application of cationic lipid–based gene delivery systems with respect to the need of a better understanding of fundamental and structural parameters that govern transfection efficiency. This includes issues of cationic lipid/DNA complex formation (with or without helper lipid), stability towards biological fluids, complex target-membrane interaction and translocation, and gene integration into the nucleus (116–118).

Electron Microscopy

Using electron microscopic techniques, like cryo-transmission electron microscopy and/or freeze fracture electron microscopy, it was possible to show that different lipoplex morphologies were formed (105,119,120).

So called spaghetti-and-meatball structures were described by Sternberg (121,122). Other extremely condensed structures were also observed. This depends on the positive-to-negative charge ratios during condensation as well as, e.g., the ionic strength of the formulation (107,110).

Figure 4 shows cryo-TEM images of some lipoplex structures obtained by condensing DC-30 [composed of 30 wt% DC-Chol and 70 wt% dioleoyl-phosphatidylethanolamine (DOPE)] at a 5:1 weight-to-weight ratio with pDNA (∼6 kbp) in 25 mM NaCl and 250 mM sucrose at pH 7.4. As can be seen in the extremely condensed structures, the DNA seems to be completely integrated in the lipoplex (105).

This is confirmed by investigation of these structures using atomic force microscopy (AFM) (data not shown).

Atomic Force Microscopy

AFM can also be used for the visualization of lipoplexes. This method is a noninvasive technique and allows the analysis of lipoplexes in solution under native conditions. AFM images showed that lipoplexes were formed from extensively fused and apparently homogeneous lipid particles incorporating the DNA (123–125). Depending on the mixing procedure, the condensation effect and incorporation of the DNA into the lipoplex structure is more or less pronounced.

Fluorescence Spectroscopy

The phase behavior and fluidity of the lipid in the cationic lipid–DNA complex is also of interest because this seems to be a factor influencing the transfection intensity (1,14). The measurement of fluorescence anisotropy is an appropriate method to characterize membrane fluidity within a defined system (e.g., lipoplex or liposome) and is used to elucidate structure–activity relationships (126,127).

Madeira et al. (128) used the fluorescence resonance energy transfer (FRET) technique for the elucidation of the formation of cationic lipid–DNA complexes. FRET technique allows the determination of the distance

(A)

(B)
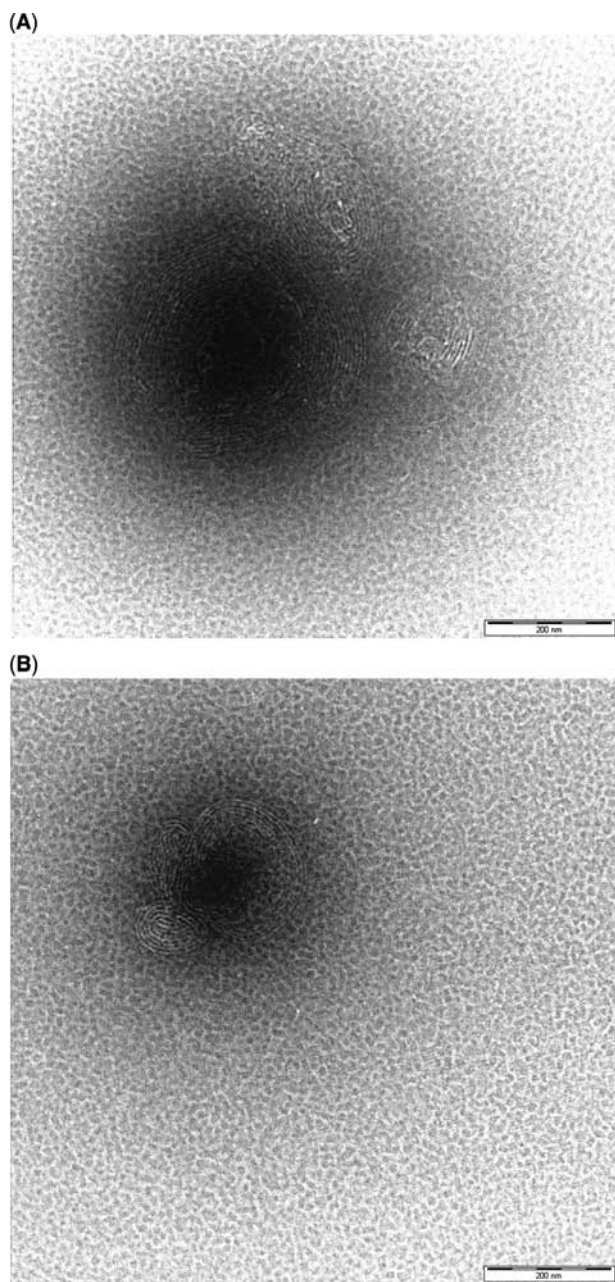
Figure 4 Cryo-transmission electron microscopy images (**A**) and (**B**) of DC-30 (30 wt% DC-Chol and 70 wt% DOPE) at a 5:1 weight-to-weight ratio with DNA (∼6 kbp) in 25 mM NaCl, 250 mM sucrose at pH 7.4 prepared on a large scale.

between the fluorescent intercalator on the DNA and a membrane dye on the lipid. Additionally, from these data, the encapsulation efficiencies can be evaluated (128).

Fluorescence methods are also used to examine the distribution of lipoplexes within the tissue. Using a fluorescent oligonucleotide as a marker, information concerning the cytoplasmic release of the genetic material can be addressed (129).

X-Ray and Neutron Scattering Methods

X-ray is a powerful method for the characterization of submolecular structures. From in vitro transfection results, it was observed that lipoplexes containing DOPE, instead of DOPC as a helper lipid, show higher transfection efficiencies (130,131). However, this is not observed when comparing in vitro and in vivo results (1,14,115,132). Using X-rays, it was found that when DNA is mixed with cationic liposomes composed of DOPC/DOTAP, the result is a topological phase transition into more or less condensed lipid–DNA complexes, which adopt a multilamellar structure (L_α^c). This L_α^c structure is composed of a DNA monolayer sandwiched between cationic lipid bilayers (133).

A columnar inverted hexagonal H_{II}^c liquid crystalline phase in these lipoplexes was also detected using synchrotron small angle X-ray diffraction. With replacing the zwitterionic DOPC lipid by DOPE, it was observed that the structural transition from the lamellar to the hexagonal phase could be forced. Additionally, it was found that this phase transition can also be triggered by variations of external parameters or electrostatic interactions. Figure 5 shows the thermal-induced phase transition of DC-40:DNA 1:13 wt/wt in 139 mM NaCl at pH 7 as a function of temperature (Garidel and Funari, unpublished results, DC40:40 wt% DC-Chol:DOPE 40:60 wt%). At room temperature, the ratio of the reflex position corresponds to 1:2:3:4, which represents a lamellar phase. In Figure 5, the first two orders are shown. At about 49°C a phase transition and new peaks are observed. A hexagonal phase is given by the peak position rations: $1:\sqrt{3}2:\sqrt{7}$. The appearance of these new reflections is marked by a star in Figure 5. Even at higher temperature (59°C) both phases coexist; in the example presented, a full transition to the hexagonal phase is not observed under the experimental conditions used.

The reason for the adaptation of an inverted hexagonal phase using DOPE lies in the geometrical structure and thus packing parameter of the lipid. DOPC has a more or less rectangular shape, whereas DOPE adopts a conical shape. Thus, the structural transition is mainly controlled by the spontaneous curvature of the lipid monolayer (134). Further investigations using these systems have revealed that lipoplexes that form lamellar structures bind stably to the negatively charged model membranes. These lipoplexes also show weak transfection efficiency. This is in contrast to the unstable binding complexes, which are seen when lipoplexes that form
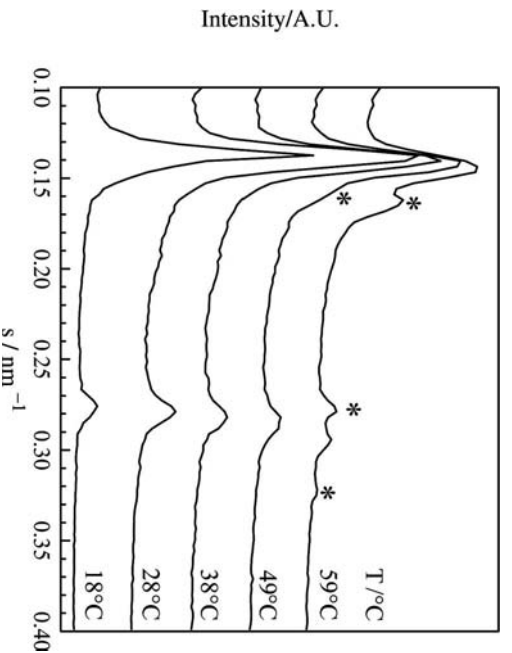
Figure 5 Small-angle X-ray diffraction scattering of DC-40:DNA 1:1 139 mM NaCl at pH 7 as a function of temperature, DC-40:40 wt% DC-60 wt% DOPE (*asterisks*) scattering reflexes of the H_{II}^c-phase. *Source:* Ga Funari, unpublished results.

hexagonal structures bind with negatively charged membranes. In to the former, these lipoplexes show a higher efficiency for tran It was also noted that the latter lipoplexes (H_{II}^c) rapidly fuse with th membrane and as a consequence the DNA is released in the cy [for more details see **Refs.** (1,14,135–138)]. One possible explanatio large differences in transfection efficiency of these two structures ma ferent cell internalization pathways [for more details see **Refs.** (139–

It was also reported that PEG lipids are able to stabilize the phase of lipoplexes, whereas their acyl-chain length dependent trans the complex enables eadaptation of the hexagonal phase. This wa from X-ray as well as cryo-electron microscopic investigation Neutron scattering can also be used for analyzing structural prop lipoplexes (143).

Calorimetry

Differential scanning calorimetry (DSC) has been used extensively determination of transition temperatures as well as enthalpy between various lipid phases, primarily the gel-to-liquid crystalli transition. Additionally, changes of the phase behavior because binding of external compound to membranes as well as the extent action, can elegantly be analyzed by DSC (144). Thus, the degree o cationic lipid binding can be followed (127,145–147).

Based on DSC data, a complete phase diagram describing the composition of the lipid mixture as a function of temperature can be constructed by analyzing heat-capacity curves. The phase diagram and the shape of the coexisting lines delimit coexisting regions from pure phase regions (146).

The thermodynamic factors governing the assembly of cationic lipids with DNA are also investigated by means of isothermal titration calorimetry (ITC). In this experiment, cationic vesicles are titrated to DNA (or vice versa) under isothermal conditions, and the enthalpy changes are registered as a function of lipid titrated to DNA. The interactions can imply electrostatic binding as well as structural changes upon binding (101,148–150), which can be monitored. Stoichiometry data upon binding are also derived from the ITC titration curve.

Particle Size Measurements and Particle Size Homogeneity

Various methods are available for the determination of lipoplex size and homogeneity (Table 4). For in process control, photon correlation spectroscopy (PCS) is the most valuable and economical method. From PCS measurements, it is obvious that lipoplex size strongly depends on the preparation and mixing protocol of liposomes with DNA, as well as on external parameters [for more details see Refs. (27,28,105)].

Infrared Spectroscopy and Circular Dichroism

Infrared spectroscopy is an established method used to monitor the thermotropic phase behavior of lipids. Additionally, information concerning the arrangement (hexagonal or orthorhombic) of the acyl chains of the lipids can be derived. Infrared spectroscopy is an elegant method for the investigation of structural changes induced by the interactions of external partners with lipids (151,152). By analyzing infrared spectra from the lipoplexes as well as the pure compounds, Pohle et al. (153) were able to show that the structure of the DNA in the lipoplex show deviations from the B-form DNA structure (153). Furthermore, two additional water bands were observed in the infrared spectra, arising at positions different from those known for lipid- and DNA-bound water. These two bands are indicative of two distinct states of hydration in lipoplexes. A phase with headgroup interdigitation was also detected.

Information with regard to DNA structure can also be obtained from circular dichroism measurements (154–158).

LIPOPLEX ANALYSIS

Due to the fact that lipoplexes are the condensation products of DNA and cationic liposomes, all analytical assays utilized for the analysis of the individual components (Tables 4 and 5) can be used. An example of this is the measurement of the size of lipoplexes by dynamic light scattering, and the surface charge characteristics by zeta potential. The heterogeneity of

lipoplexes can be assessed by flow-field flow fractionation, as was shown by Lee et al. (159). Electrophoresis assays are used for the characterization of the DNA quality (57).

The interaction between DNA and the cationic-charged liposomes may be determined using the PicoGreen dye exclusion technique (159,160). This assay determines the DNA accessibility in the lipoplex for the double-stranded DNA-binding reagent PicoGreen. The total amount of DNA in the lipoplex formulation can also be determined (161). First, the complete lipoplex formulation is solubilized by, e.g., heparin sodium salt, inducing a decomplexation of DNA and lipid, and in a second step, the total amount of free and thus dye-accessible DNA is quantified via the PicoGreen assay. Other fluorescence assays for assessing lipid–DNA binding affinity have been described in the literature (128,162).

Lipid composition is usually quantified via high-performance liquid chromatography (HPLC) after extraction of the lipids in an organic phase (e.g., chloroform:methanol 1:1 v/v) (163). Meyer et al. (164) have proposed a direct method for lipid quantification, which does not require lipid extraction from the liposomal formulation prior to sample analysis. The lipoplexes are directly analyzed via RP-HPLC. Detection limits in the range of 0.5–1 µg were described, dependent on the lipid analyzed. These methods can be adapted as is the case in process control and product control methods used for the preparation of lipoplexes at a larger industrial scale.

LYOPHILIZATION OF LIPOPLEXES

It is currently well established that the application of the freeze-drying technique, also termed lyophilization, to liposomal formulation considerably improves the stability of the product (35,165–170).

During the process of lyophilization, the aqueous phase freezes and the water (ice) is removed by sublimation. As a consequence, the sample is dried (171).

The prime reason for using this method is the belief that drying enhances chemical stability, primarily because water removal prevents hydrolysis of the lipids. Additionally, other chemical and physical degradation processes are retarded because of lowering the molecular mobility in the solid phase.

However, as has also been observed for other biomolecules, lyophilization can also harm the product. In the case of liposomes, the bilayer membranes can be damaged during the freeze-drying cycle by mechanical stress caused by high pressures on the vesicle membranes when exposed to the formation of ice crystals. Additionally, freezing induces an increase in solute concentration, e.g., buffer salt phase separation, and as a consequence dramatic pH shifts that may in turn chemically degrade the lipids. Vesicle fusion and aggregation were also observed.

Therefore, protective agents are usually added to the formulation. These are the so-called cryo- and lyoprotectants. Cryoprotectants are substances (e.g., glycerol) that are used to protect from the effects of freezing, largely by preventing large ice crystal formation, whereas lyoprotectants stabilize the biomolecules in the dried state. Carbohydrates are favored as excipients, because of the fact that they are chemically innocuous and can be easily vitrified during freezing. A variety of sugars—including sucrose, glucose, fructose, trehalose, etc.—have been reported to act as protectants during dehydration/hydration of liposomes (172–175).

The glass temperature of most disaccharides and higher oligomeric sugars is above $-30°C$, making these substances attractive to use as freeze-drying excipients.

However, it is also known that some carbohydrates such as mannitol and lactose can phase separate from a frozen solution in the form of crystalline phases, dependent on the processing conditions employed. They can even crystallize within dried products (173–175). As reported by Maden and Boman (172), cryoprotectants are able to decrease vesicle fusion and vesicle leakage caused during the freeze–thaw and the freeze-drying process. Owing to the nature of the cryoprotectants being noneutectic and thus not crystallizing, an amorphous frozen matrix is formed upon cooling.

In general, the freezing process for formulations containing cryoprotectants occurs very quickly upon cooling to the freezing point depression. This effect, known as supercooling, decreases the exposure of vesicles to high concentrations of solute caused by slow ice crystallization and results in a more uniform frozen matrix. As described by Jennings (176), solutes that act as cryoprotectants typically undergo a transition from a viscous gel to a hard glass with less molecular mobility upon freezing. This is referred to as the glass transition temperature. A critical point to be considered for the successful lyophilization of bioproducts is that the product temperature remains below the glass transition temperature during primary drying to avoid "shrinkage" or product collapse (177).

The collapse temperatures for a number of disaccharides fall between $-30°C$ and $-35°C$. The use of cryoprotectants with high collapse temperatures allows faster rates of freeze-drying at higher product temperatures (178,179).

It was reported that nonreducing disaccharide sugars, such as sucrose and trehalose, may affect the stability of liposomes during freezing and freeze-drying. We found that a combination of 25 mM NaCl and 250 mM sucrose had a very stabilizing effect on the size of the educt (liposomes) and product (lipoplexes), both before and after lyophilization (Fig. 6). The protective effect of sugars during lyophilization appears to be sugar specific, because the monosaccharides glucose and fructose have less effect (172). Biophysical studies have revealed that disaccharides may directly interact with the phospholipid membrane, possibly via hydrogen bonding, and this may be a reason for stabilization (172).
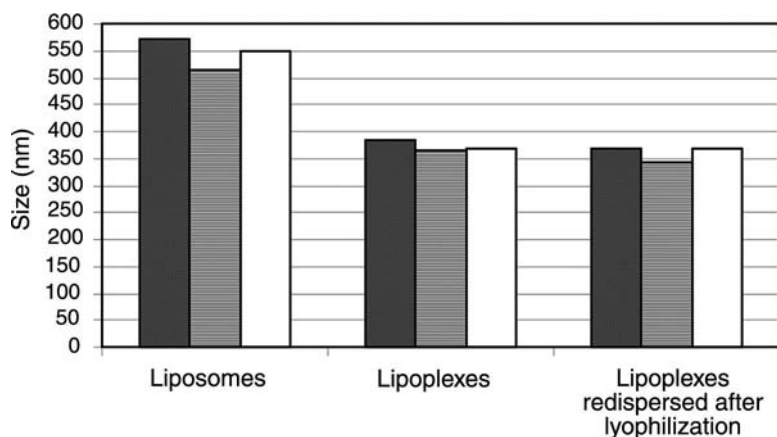
Figure 6 Sizes of liposomes (DC-30) before mixing with DNA (pGFP), lipoplexes after large-scale preparation, and lipoplexes redispersed after lyophilization. Data are shown for three independent batches manufacturers under identical conditions.

As has been previously described, the size of the lipid–DNA complexes is a critical parameter with respect to transfection efficiency. During the formation of lipoplexes, aggregation is often encountered, thus making it impossible to produce a more or less homogeneous liquid product. However, as described in the previous section, depending on the mixing process it is possible to produce stable lipoplexes in solution for at least a few days. Under the prospect of drug development, the lipoplexes need to be stabilized under ambient conditions over a much longer period of time ($\sim$3 years for a solid dosage form). As described above, lyophilization is a valuable option for this goal and thus enables the production of large lipoplex batches under pharmaceutical conditions and product stability requirements. The main principles and techniques used for the lyophilization of liposomes can be transferred to the lyophilization of lipoplexes. However, the process and the formulations must be adapted for their use with lipoplexes, primarily because it was reported that aggregation to an even greater extent may occur during their lyophilization. Allison and Anchordoquy (180) have reported that the aggregation of lipoplexes typically occurs during the freezing step of the lyophilization process. However, the presence of high amounts of sugars is capable of maintaining particle size. They found that glass formation is not the mechanism by which sugars protect lipid/DNA complexes during freezing. Instead, the data presented by Allison and Anchordoquy (180) suggest that phase separation of individual particles within the unfrozen fraction is the cause for the stabilization of lipoplexes with regard to aggregation during freezing (particle isolation hypothesis). An additional factor, the relatively low surface tension of mono- and disaccharides, allows

phase-separated particles to remain dispersed within the unfrozen excipient solution, which preserves particle size and transfection rates during freezing [for more details see Allison et al. (180,181)]. Such effects have in recent years been extensively investigated by a number of groups (182–195).

Thus, lyophilization is a valuable method for the long-term stabilization of lipoplexes, and a stability of two years was reported for lipid/ DNA complexes as lyophilisates (see Chapter 8).

LONG-TERM STABILITY

It is known that lipoplexes in liquid formulation cannot be stored for long periods of time without aggregation and loss of transfection efficiency (182). Early clinical trials were performed with preparations that were freshly prepared before injection (196). Since then, preparations with prolonged stability have been developed, all of which remain stable from several hours up to a few days. For instance, polyethylenglycol-ligands have been coupled to DNA-transfection systems to sterically stabilize the complexes and to prevent them from aggregating (197,198). Unfortunately, interaction with the cells and, consequently, transfection efficiency seem to be less effective (199).

Freeze drying has been suggested as a useful method for stabilization and storage of polyplexes (200), but the first tests turned out to produce large, irregularly shaped particles when applied to lipoplexes, resulting in a loss of transfection activity (191). New developments have, however, shown that these problems were for the most part eliminated by choosing the correct formulation and lyophilization process (see below). Spray drying resulted in stable respirable dry-powder systems for respiratory gene delivery (201). An improved storage form for lipoplexes might be as a lyophilized product. The advantages are obvious: the absence of liquid prevents not only hydrolysis but also increasing aggregation of the lipoplex. Furthermore, the product is easy to handle after simple rehydration prior to application [one vial application (105)]. However, both the freezing and drying throughout the process may induce damages to the product and have to be carefully considered. Influences on lipoplex size primarily occur during freezing (181). A slow cooling period was reported to be more harmful than fast freezing (202) (see preceding chapter).

It was recently shown that when process as well as formulation development is considered, lyophilization is a suitable storage form for lipoplexes (105). Clement et al. (104,105) reported 18 months/4°C to 8°C lipoplex stability data of freeze-dried lipoplexes. The lipoplex size was in the range of 350 nm and was not altered during storage over a period of 18 months at 4°C to 8°C. In addition, the bioactivity was not altered upon storage. It was also shown that the process used for the production of lipoplexes leads to reproducible product characteristics (Fig. 6). Different batches of lipoplexes were lyophilized, and the physical stability as well as bioactivity

was constant within the range of the standard deviations of the methods used. Lipoplex size before and after lyophilization was in the range of 360 ± 30 nm for three independent batches manufactured under identical conditions (Fig. 6). The lipoplex size was always smaller than the liposome size used for the preparation, indicating the strong condensation effect upon DNA binding (104).

An additional study investigating the stability of freeze-dried lipoplexes during prolonged storage was presented by Molina et al. (185). They analyzed the lipoplex stability effect of various formulations containing glucose, sucrose, or trehalose, which were stored for a period of two years at $-20°C$, $4°C$, $22°C$, $40°C$, or $60°C$. Simultaneously, the physicochemical characteristics like size, zeta potential, ethidium bromide accessibility, CCC DNA content, as well as the ability of vector formulations to transfect COS-7 cells at different time intervals were all analyzed. In addition, Molina et al. (185) utilized a fluorescence assay to assess levels of reactive oxygen species in the dried cake after storage. Results from this stability study show that a progressive degradation of lipid/DNA complexes occurs in terms of transfection rates, particle size, dye accessibility, and supercoil content, even when samples are stored at low temperatures (e.g., $-20°C$). Furthermore, Molina et al. presented preliminary results on the quantification of free radicals in rehydrated formulations and emphasized the importance of developing strategies to prevent the formation of reactive oxygen species during prolonged storage in the dried state [for more details see Ref. (185)].

IN VITRO TESTS

A lot of studies are being undertaken to understand the structures of lipoplexes and in optimizing transfection results in vitro, but even predicting the physical structure of the lipoplexes does not automatically result in a correlation with biological activity (203). In the 1990s, application of lipoplexes seemed to be limited due to the serum-associated reduction in transfection efficiency. The influence of serum still is a major focus of research (132,204–206). Serum-resistant formulations were generated by increasing the charge ratio (132). Furthermore, lipoplex size (102,205,207) and the lamellarity of liposomes used for preparation of lipoplexes (47) were found to be a major determinant of transfection efficiency. We found that lipoplex size is not necessarily always correlated with transfection efficiencies, although trends might be seen as demonstrated in Figure 7. Smooth muscle cells from rat (A-10 SMC) and HASMC were transfected with DC-30/pGFP 5:1 (w:w). Transfection efficiency seemed to increase with lipoplex size in A-10 SMC, whereas this trend was less expressed in HASMC. In the case of HASMC, it could be seen that transfection efficiency was related to the number of times, the cells have been split in culture before being used in the experiments (splitting passage) (Fig. 8).
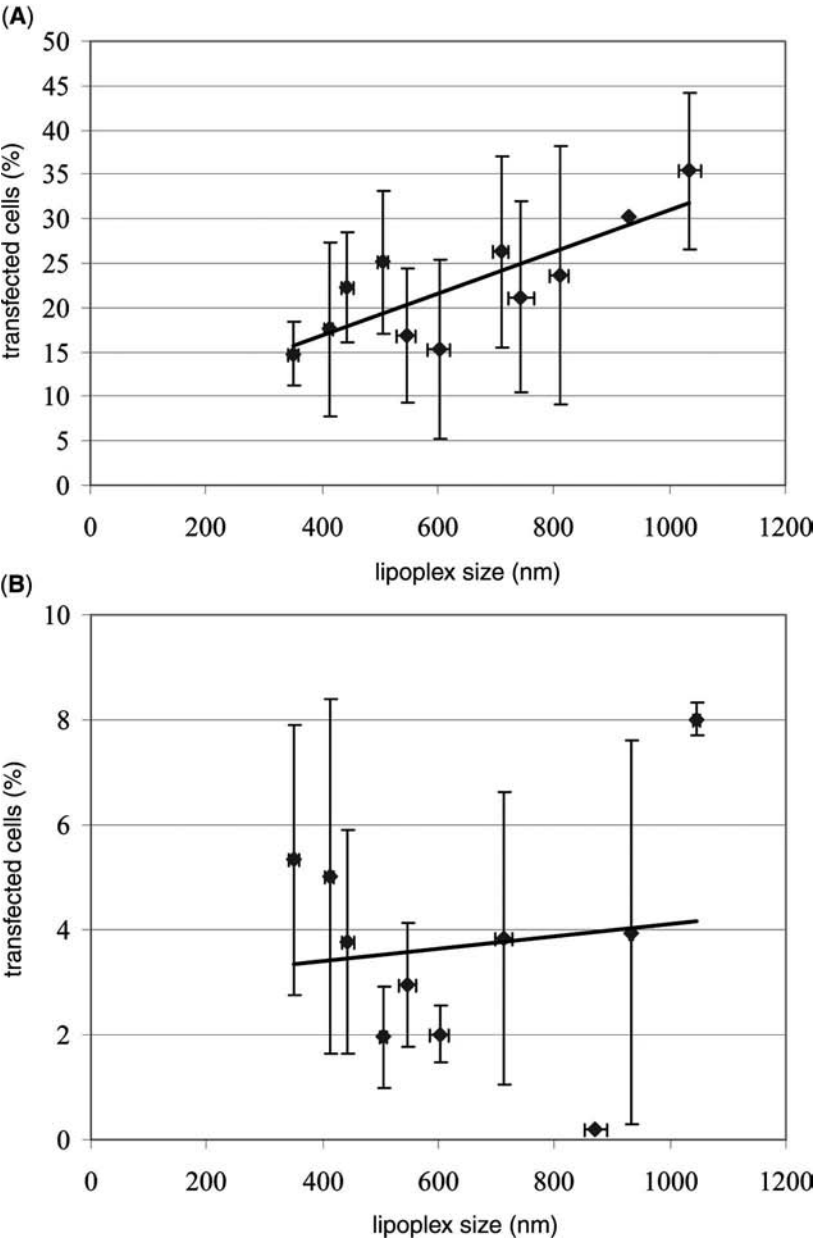
Figure 7 Correlation between lipoplex size and biological activity (103). DC-30/ DNA (pGFP) lipoplexes of different sizes were used for transfection in (**A**) A-10 smooth muscle cells (SMC) (rat SMC, cell line) and (**B**) human aorta smooth muscle cells. *Source*: From Ref. 104.
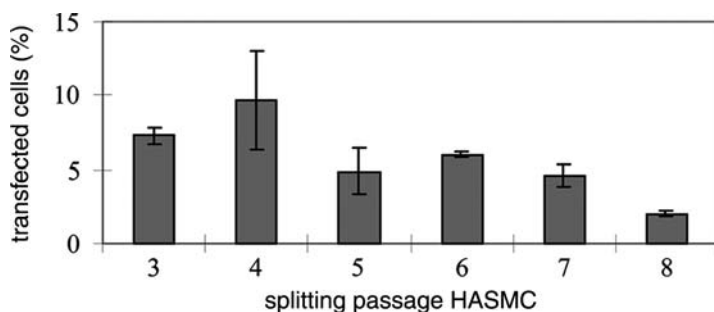
Figure 8 Transfection efficiency of DC-30/pGFP 4:1 (w:w) in human aorta smooth muscle cells (HASMC) relative to the cultivation passage.

Best results were achieved in the fourth passage, whereas efficiency was significantly reduced upon further cultivation.

However, after administration of lipoplexes in vivo, interactions with biophysiological fluid, target tissue, and the extracellular environment will further influence and alter lipoplex structure and transfection ability. Clinical studies showed that lipoplexes with optimal physicochemical characteristics for cystic fibrosis (CF) become inactive in vivo as a result of destabilization upon interaction with CF sputum (208). Numerous in vivo application studies have been reported: pulmonal (197,209), cardiovascular (210,211), brain (212), tumoral (213–215). Whereas local administration appeared to be a promising approach, systemic application did not fulfill the expectations or hopes that had been raised. The required knowledge of the optimal conditions for in vivo transfection is still poor, as in vitro results are not necessarily related to in vivo results (115).

Interactions between plasma lipoproteins and lipoplexes are still poorly characterized, but might be a limiting factor for in vivo transfection efficiency (216). Efficiency and toxicity is highly related to either the transfection reagent or the type of cell (28,217).

When developing a gene-delivery production process that is intended to be used for large-scale production, it is most important to establish a reproducible biological assay to be used for quality control of the produced preparations. Therefore, a cell model should be chosen which is easy to handle and as robust as possible. Such a cell assay should be used for the quality control of various batches. Therefore, we combined quality aspects such as robustness with a preferable association to the target of the lipoplex. Different cell models for the treatment of cardiovascular diseases were studied (HASMC, HAEC, and a stable, well-established rat smooth muscle cells line, A-10 SMC) for practicability. Cytotoxicity also should be considered by evaluating the transfection efficiency of various gene-transfer reagents (28,218–222). In our studies, the batches produced were also
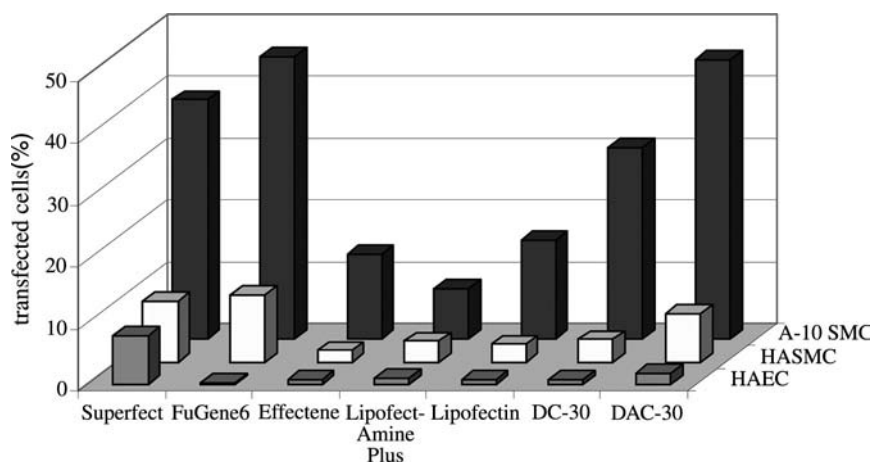
Figure 9 Transfection efficiencies obtained with optimized conditions of each transfection agent in A-10 smooth muscle cells (SMC), human aorta smooth muscle cells (HASMC), and human aorta endothelial cells (HAEC).

evaluated for their influence on cytotoxicity. It could be shown that transfection was in general consistently toxic for the individual cell types. High cell viability could be observed in A-10 SMC, whereas for HASMC the cell viability was affected. Different parameters of the manufacturing process, such as pretreatment of the lipid and lyophilization, did not significantly influence lipoplex characteristics and thus cell viability. Measured toxicity was therefore not attributed to the manufacturing process, but more likely to the sensitivity of the individual cell types to the gene transfer system.

Finally, it should be noted that in vitro transfection efficiencies have to be optimized with each transfection system in every cell type. Figure 9 shows how tremendously the results can differ according to the different materials used, in this case the transfection systems and the cells. Still, optimization in cell culture can only be a first and preliminary step in the development of a gene-transfer drug. With regard to quality control of an industrially produced product, it is of great importance to establish and validate an appropriate bioassay, such as transfection in cell culture, that is robust and reliable for the evaluation of reproducibility of the manufacturing process.

PHARMACEUTICAL CONSIDERATIONS AND GUIDELINES FOR PHARMACEUTICAL DEVELOPMENT

The marketing of a gene-based therapeutic requires the approval by the appropriate regulatory authorities [European medicines agency (EMEA), Food and Drug Administration, etc.]. It has to be shown that there is scientific evidence that the therapy is safe and effective for its intended application.

Additionally, it must also be demonstrated that the processes and controls used in manufacturing are properly controlled and validated to ensure the quality of the product.

Several sources of information, guidelines, or directives are available (e.g., Pharmacopeia, ICH guideline, EMEA notes, etc.). To make sure that the most recent version of guidelines are consulted, Table 6 summarizes the most important web sites where this type of information can be obtained. The textbook of Grimm et al. (223) gives an excellent introduction and overview of what has to be considered with the viewpoint of pharmaceutical development.

Various lipid-based (nongene) products are currently available on the market, such as e.g., Doxil®, Caelyx®, DaunoXome®, and Ambisome®. Thus, it has been shown that these products can be manufactured under the aspects of industrial and pharmaceutical requirements.

A draft guideline for industry (August 2002) from the U.S. Department of Health and Human Service, Food and Drug Administration, and Center for Drug Evaluation and Research with the title "Liposome drug products. Chemistry, manufacturing, and controls; human pharmacokinetics and bioavailability; and labeling documentation" (224) (www.fda.gov/cder/guidance) summarizes the current thinking of the FDA on this topic. This draft guidance gives recommendations on the unique aspects of liposome drug products. Liposome drug products are defined in this case as "drug products containing drug substances (active pharmaceutical ingredients) encapsulated in liposomes. A liposome is a microvesicle composed of a bilayer of lipid amphipathic molecules enclosing an aqueous compartment. Liposome drug products are formed when a liposome is used to encapsulate a drug substance within the lipid bilayer or in the interior aqueous space of the liposome" (224).

However, this draft guidance does not provide recommendations on, e.g., drug–lipid complexes. These drug–lipid complexes are formed by mixing a drug with lipids in such a way that the product does not result in the creation of liposomes.

It is recommended that applicants intending to submit an new drug application for a drug–lipid complex can consult the appropriate review division in CDER for additional guidance if necessary (224).

The regulation of the European Union (EU) Directive 2001/20/EC on Good Clinical Practice in Clinical Trials (www.europa.eu.int) covers the aspects of the conduct within the EU of human clinical trials with medicinal products, including gene therapy agents.

The directive 2001/83/EC, European Note for guidance on the quality, preclinical, and clinical aspects of gene transfer medicinal products (CPMP/BWP/3088/99), which can be downloaded (http://www.eudra/org/emea.html), gives an account of the opinions of the European Agency for the Evaluation of Medicinal Products. This note considers general

Table 6 Most Important Internet Addresses for Pharmaceutical Guidelines and Regulations

Guidelines	Internet Address
Center for Drug Evaluation and Research MaPP	www.fda.gov/cder/map.htm
Code of Federal Regulations (United States)	www.gpoaccess.gov/cfr/index.html
Bundesanzeiger	www.bundesanzeiger.de
Bundesinstitut für Arzneimittel und Medizinprodukte	www.bfarm.de/de/index.php
European Commission, Enterprise and Industry DG, Directorate F—Consumer goods	http://pharmacos.eudra.org/
EC Directives and Regulations (Medical Products for Human Use)	http://pharmacos.eudra.org/F2/eudralex/vol-1/home.htm
EC Guidelines (Pharmaceutical Legislation: Notice to Applicants)	http://pharmacos.eudra.org/F2/eudralex/vol-2/home.htm
EC Guidelines (Medicinal Products for Human Use: Quality, Biotechnology, Safety, Environment and Clinical Guidelines)	http://pharmacos.eudra.org/F2/eudralex/vol-3/home.htm
EC Guidelines (Medicinal Products for Human and Veterinary Use: Good Manufacturing Practice)	http://pharmacos.eudra.org/F2/eudralex/vol-4/home.htm
EC Guidelines (Pharmaceutical Legislation: Veterinary Medicinal Products)	http://pharmacos.eudra.org/F2/eudralex/vol-5/home.htm
EC Guidelines (Notice to Applicants: Veterinary Medicinal Products)	http://pharmacos.eudra.org/F2/eudralex/vol-6/home.htm
EC Guidelines (Guidelines: Veterinary Medicinal Products)	http://pharmacos.eudra.org/F2/eudralex/vol-7/home.htm
EMEA Guidelines	www.emea.eu.int
FDA Guidelines of CBER (Biologics)	www.fda.gov/cber/publications.htm www.fda.gov/cber/reading.htm
FDA Guidelines of CBER (Human Drugs)	www.fda.gov/cber/guidance/index.htm
ICH Guidelines (International Conference on Harmonisation of Technical Requirements for Registration of Pharmaceuticals for Human Use)	www.ich.org
PIC	http://21cfrpart11.com/files/library/reg_guid_docs/pics_guid.pdf
PIC/S	http://www.picscheme.org/
WHO (Guidelines, Certification, Scheme, International Pharmacopeia)	www.who.int/medicies/library/docseng frm_a_to_z.shtml

aspects with regard to production, purification, product characterization and consistency, and routine batch control of the final processed product. Additionally, specific considerations are given for individual gene-transfer strategies. The chapter "non viral vectors for delivery of transgenes (e.g., liposomes, receptor-mediated ligands)" looks at aspects that should be considered, such as physicochemical and biological characterization of the product, bio-distribution of the lipid–DNA complex, and stability of the product. The use of cationic liposomes to determine surface properties such as the surface charge of the liposomes and complexes is explicitly mentioned. The quality of the components and their purity has to be addressed (225). Additionally, the biannual meeting reports from the Gene Therapy Expert Group should be consulted on the web pages of the EMEA.

The World Health Organization mentioned in its meeting report (226) that: "Although it was initially presumed that DNA would be stable and DNA vaccines would not need any cold chain when shipped to its location of use, it has become clear that during storage at 4°C the monomeric cccDNA is reduced and may be damaged. This may not be a factor for stability during storage at −20°C." Information can also be found on the web pages of national regulatory organizations. In Germany the web site from the Paul-Ehrlich Institute (227) is a valuable site. Another web site to recommend is the Euregenethy 2 (228). Euregenethy 2 is a network of scientists focusing on the ethical, efficacy, safety, and regulatory issues related to clinical gene transfer in order to facilitate and help with the harmonization of these issues. The main objectives of the network are:

  i. Fostering interactions between all interested parties involved in gene therapy development.
 ii. Following up on evolving technologies in order to foster broad circulation of validated key information.
iii. Increase both public accountability and acceptance of genetic modified organism mediated interventions.
 iv. Anticipation of challenging scientific issues, which will attract interest and/or raise concerns.

Various papers deal with the regulatory aspects of gene therapy, but in most cases viral systems are considered (229–239).

These few examples of information presented above should allow one to get a general overview of what has to be considered and where information can be obtained for further reading.

CONCLUSIONS

Over the last several years, large efforts were undertaken to improve the delivery of genes via viral and nonviral transfer systems. In 2004, the first gene therapeutic was launched in China. However, the success of a drug also

depends on its pharmaceutical development. Issues like stability, up-scaling, batch-by-batch reproducibility, process robustness, etc. have to be addressed. Other important points are the efficacy and safety for the patient and the environment. Economical aspects also need to be taken into account.

This paper briefly describes the points to consider in the development and production of lipid–DNA complexes under industrial and pharmaceutical requirements.

ACKNOWLEDGMENTS

REFERENCES

1. Huang L, Hung MC, Wagner E, eds. Nonviral Vectors for Gene Therapy. London: Academic Press, 1999.
2. Blaese RM, Culver KW, Miller AD, et al. Lymphocyte-directed gene therapy for ADA SCID: initial trial results after 4 years. Science 1995; 270:475.
3. www3.interscience.wiley.com/cgi-bin/home
4. Teichler ZD. US gene therapy in crisis. Trends Genet 2000; 16:272.
5. Somia N, Verma IM. Gene therapy: trials and tribulations. Nat Rev Genetics 2000; 1:91.
6. Dettweiler U, Simon P. Points to consider for ethics committees in human gene therapy trials. Bioethics 2001; 15:491.
7. Grilley BJ, Gee AP. Gene transfer: regulatory issues and their impact on the clinical investigator and the good manufacturing production facility. Cytotherapy 2003; 5:197.
8. Cavazzana-Calvo M, Lagresle C, Hacein-Bey-Abina S, Fischer A. Gene therapy for severe combined immunodeficiency. Ann Rev Med 2005; 56:585.
9. Fischer A, Le Deist F, Hacein-Bey-Abina S, et al. Severe combined immunodeficiency. A model disease for molecular immunology and therapy. Immunol Rev 2005; 203:98.
10. Cavazzana-Calvo M, Fischer A. Efficacy of gene therapy for SCID is being confirmed. Lancet 2004; 18:2181.
11. Fischer A, Hacein-Bey-Abina S, Cavazzana-Calvo M. Thérapie génique du déficit immunitaire combine sévère lie a l'X: efficacité et complications. MS Md Sci 2004; 20:115.
12. Hacein-Bey-Abina S, von Kalle, C, Schmidt M, et al. A serious adverse event after successful gene therapy for X-linked severe combined immunodeficiency. N Engl J Med 2003; 348:255.
13. Pearson S, Jia H, Kandachi K. China approves first gene therapy. Nat Biotech 2004; 22:3.

14. Rolland A, Sullivan SM, eds. Pharmaceutical Gene Delivery Systems. Basel, New York: Marcel Dekker, 2003.

15. Farson D, Harding TC, Tao L, et al. Development and characterization of a cell line for large-scale, serum-free production of recombinant adeno-associated viral vectors. J Gene Med 2004; 6:1369.

16. Zhao Y, Azam S, Thorpe R. Comparative studies on cellular gene regulation by HIV-1 based vectors: implications for quality control of vector production. Gene Ther 2005; 12:311.

17. Vera M, Prieto J, Strayer DS, Fortes P. Factors influencing the production of recombinant SV40 vectors. Mol Ther 2004; 10:780.

18. McTaggart S, Al-Rubeai M. Retroviral vectors for human gene delivery. Biotech Adv 2002; 20:1.

19. Yang S, Delgado R, King SR, et al. Generation of retroviral vector for clinical studies using transient transfection. Hum Gene Ther 1999; 10:123.

20. Kanda T, Yajima M, Ahsan N, Tanaka M, Takada K. Production of high-titer Epstein–Barr virus recombinants derived from Akata cells by using a bacterial artificial chromosome system. J Virol 2004; 78:7004.

21. Smith RH, Ding C, Kotin RM. Serum-free production and column purification of adeno-associated virus type 5. J Virol Meth 2003; 114:115.

22. Harris JD, Stuart BG, Dickson JG. Novel tools for production and purification of recombinant adeno-associated viral vectors. Meth Mol Med 2003; 76:255.

23. Kumar M, Bradow BP, Zimmerberg J. Large-scale production of pseudotyped lentiviral vectors using baculovirus GP64. Hum Gene Ther 2003; 14:67.

24. Svahn MG, Lundin KE, Ge R, et al. Adding functional entities to plasmids. J Gene Med 2004; 6(suppl):S36.

25. Tranchant I, Thompson B, Nicolazzi C, Mignet N, Scherman D. Physicochemical optimisation of plasmid delivery by cationic lipids. J Gene Med 2004; 6(suppl):S24.

26. Ewert K, Slack NL, Ahmad A, et al. Cationic lipid DNA complexes for gene therapy: understanding the relationship between complex structure and gene delivery pathways at the molecular level. Curr Med Chem 2004; 11:133.

27. Lenter MC, Garidel P, Pelisek J, Wagner E, Ogris M. Stabilized nonviral formulations for the delivery of MCP-1 gene into cells of the vasculoendothelial system. Pharm Res 2004; 21:683.

28. Kiefer K, Clement J, Garidel P, Peschka-Süss R. Transfection efficiency and cytotoxicity of nonviral gene transfer reagents in human smooth muscle and endothelial cells. Pharm Res 2004; 21:1009.

29. Walker GF, Fella C, Pelisek J, et al. Toward synthetic viruses: endosomal pH-triggered deshielding of targeted polyplexes greatly enhances gene transfer in vitro and in vivo. Mol Ther 2005; 11:418.

30. Boeckle S, von Gersdorff K, van der Piepen S, Culmsee C, Wagner E, Ogris M. Purification of polyethylenimine polyplexes highlights the role of free polycations in gene transfer. J Gene Med 2004; 6:1102.

31. Lasch J, Weissig V, Brandl M. Preparation of liposomes. In: Torchilin, Weissig, eds. Liposomes. 2nd ed. New York: Oxford University Press, 2003 (chap.1).

32. Wassef NM, Alving CR, Richards RL. Liposomes as carriers for vaccines. Immunomethods 1994; 4:217.
33. Endruschat J, Henschke K. Bench scale manufacture of multilamellar liposomes using a newly developed multistage pressure filtration device. Int J Pharmaceut 2000; 196:151.
34. Zawada Z. A single-step method of liposome preparation. Cell Mol Biol Lett 2004; 9:603.
35. Li C, Deng Y. A novel method for the preparation of liposomes: freeze drying of monophase solutions. J Pharm Sci 2004; 93:1403.
36. Kim NH, Park HM, Chung SY, Go EJ, Lee HJ. Immunoliposomes carrying plasmid DNA: preparation and characterization. Arch Pharm Res 2004; 27:1263.
37. Pellequer Y, Ollivon M, Barratt G. Formulation of liposomes associated with recombinant interleukin-2: effect on interleukin-2 activity. Biomed Pharmacother 2004; 58:162.
38. Giovagnoli S, Blasi P, Vescovi C, et al. Unilamellar vesicles as potential capreomycin sulfate carriers: preparation and physicochemical characterization. AAPS Pharm Sci Tech 2003; 4:E69.
39. Schubert R. Liposome preparation by detergent removal. Meth Enzymol 2003; 367:46.
40. Wagner A, Vorauer-Uhl K, Kreismayr G, Katinger H. The crossflow injection technique: an improvement of the ethanol injection method. J Liposome Res 2002; 12:259.
41. Wagner A, Vorauer-Uhl K, Katinger H. Liposomes produced in a pilot scale: production, purification and efficiency aspects. Eur J Pharm Biopharm 2002; 54:213.
42. Yamashita Y, Oka M, Tanaka T, Yamazaki M. A new method for the preparation of giant liposomes in high salt concentrations and growth of protein microcrystals in them. Biochim Biophys Acta 2002; 1561:129.
43. Kikuchi H, Suzuki N, Ebihara K, et al. Gene delivery using liposome technology. J Controlled Rel 1999; 62:269.
44. Vemuri S, Rhodes CT. Preparation and characterization of liposomes as therapeutic delivery systems: a review. Pharmaceut Acta Helvetiae 1995; 70:95.
45. VemuriS, Rhodes CT. Development and characterization of a liposome preparation by a pH-gradient method. J Pharm Parmacol 1994; 46:778.
46. Dao HN, McIntyre JC, Sleight RG. Large-scale preparation of asymmetrically labeled fluorescent lipid vesicles. Anal Biochem 1991; 196:46.
47. Zuidam NJ, Hirsch-Lerner D, Margulies S, Barenholz Y. Lamellarity of cationic liposomes and mode of preparation of lipoplexes affect transfection efficiency. Biochim Biophys Acta 1999; 1419:207.
48. Mui B, Chow L, Hope MJ. Extrusion technique to generate liposomes of defined size. Meth Enzymol 367, 3; 2003:14.
49. Janoff AS. Liposomes, Rational Design. Basel, New York: Marcel Dekker, 1999.
50. Torchilin VP, Weissig V. Liposomes. 2nd ed. Oxford University Press: Oxford, 2003.

51. Zuidam NJ, Lee SS, Crommelin DJ. Gamma-irradiation of non-frozen, frozen, and freeze-dried liposomes. Pharm Res 1995; 12:1761.

52. Stensrud G, Passi S, Larsen T, et al. Toxicity of gamma irradiated liposomes. 1. In vitro interactions with blood components. Int J Pharm 1999; 178:33.

53. Stensrud G, Monkkonen J, Karlsen J. Toxicity of gamma irradiated liposomes. 2. In vitro effects on cells in culture. Int J Pharm 1999; 178:47.

54. Tardi C, Drechsler M, Bauer KH, Brandl M. Steam sterilisation of vesicular phospholipid gels. Int J Pharm 2001; 217:161.

55. Turanek J, Kasna A, Zaluska D, Neca J. Preparation of sterile liposomes by proliposome-liposome method. Meth Enzymol 2003; 367:111.

56. Zuidam NJ, Lee SS, Crommelin DJ. Sterilization of liposomes by heat treatment. Pharm Res 1993; 10:1591.

57. Lottspeich F, Zorbas H, eds. Bioanalytik. Heidelberg, Berlin: Spektrum Verlag, 1998.

58. Zuidam NJ, van Winden E, de Vrueh R, Crommelin DJA. Stability, storage, and sterilisation of liposomes. In: Torchilin, Weissig, eds. Liposomes. 2nd ed. New York: Oxford University Press, 2003 (chap. 5).

59. Lang JK. Quantitative determination of cholesterol in liposome drug products and raw materials by high-performance liquid chromatography. J Chromatogr A 1990; 507:157.

60. Lasic DD, Papahadjopoulos D. Medical Applications of Liposomes. Amsterdam: Elsevier, 1998.

61. Waterhouse DN, Madden TD, Cullis PR, Bally MB, Mayer LD, Webb MS. Preparation, characterization, and biological analysis of liposomal formulations of vincristine. Meth Enzymol 2005; 391:40.

62. Perjesi P, Kim T, Zharikova AD, et al. Determination of clodronate content in liposomal formulation by capillary zone electrophoresis. J Pharm Biomed Anal 2003; 31:929.

63. Duffy CF, Gafoor S, Richards DP, Admadzadeh H, O'Kennedy R, Arriaga EA. Determination of properties of individual liposomes by capillary electrophoresis with postcolumn laser-induced fluorescence detection. Anal Chem 2001; 73:1855.

64. Pacholski ML, Cannon DM Jr., Ewing AG, Winograd N. Static time-of-flight secondary ion mass spectrometry imaging of freeze-fractured, frozen-hydrated biological membranes. Rapid Commun Mass Spectrom 1998; 12:1232.

65. Vossen RC, van Dam-Mieras MC, Hornstra G, Zwaal RF. Continuous monitoring of lipid peroxidation by measuring conjugated diene formation in an aqueous liposome suspension. Lipids 1993; 28:857.

66. Points to consider on plasmid DNA vaccines for preventive infectious disease indications. CBER US FDA, www.fda.gov.

67. Middaugh CR, Evans RK, Montgomery DL, Casimiro DR. Analysis of plasmid DNA from a pharmaceutical perspective. J Pharm Sci 1998; 87:130.

68. Guidance for industry–guidance for human somatic cell therapy and gene therapy. CBER, US FDA, www.fda.gov.

69. Neidhardt FC, ed. *Escherichia coli* and *Salmonella typhimurium*. 2nd ed. Vols. I and II, Washington, D.C.: ASM Press, 1996.

70. Schleef M, ed. Plasmids for Therapy and Vaccination. Weinheim: Wiley-VCH, 2001.

71. Schleef M, Schmidt T, Animal-free production of ccc-supercoiled plasmids for research and clinical applications. J Gene Med 2004; 6(suppl):S45.
72. Schmidt T, Schleef M, Friehs K, Flaschel E. Hochzelldichtefermentation zur Gewinnung von Plasmid-DNA für Gentherapie und genetische Impfung. Bioforum 1999; 22:174.
73. Voß C, Schmidt T, Schleef M, Friehs K, Flaschel E. Production of supercoiled multimeric plasmid DNA for biopharmaceutical application. J Biotech 2003; 105:205.
74. www.boehringer-ingelheim.at.
75. Werner RG, Urthaler J, Kollmann F, Huber H, Necina H, Konopitzky K. pDNA–from process science to commercial manufacture. Pharm Technol 2002, No. 0523.
76. Urthaler J, Schegl R, Podgornik A, Strancar A, Jungbauer A, Necina R. Application of monoliths for plasmid DNA purification development and transfer to production. J Chromatogr A 2005; 1065:935.
77. Zöchling A, Hahn R, Ahrer K, Urthaler J, Jungbauer A. Mass transfer characteristics of plasmids in monoliths. J Sep Sci 2004; 27:819.
78. Ferreira GNM, Monteiro GA, Prazeres DMF, Cabral JMS. Downstream processing of plasmid DNA for gene therapy and DNA vaccine applications. Trends Biotechnol 2000; 18:380.
79. Levy MS, O'Kennedy RD, Ayazi-Shamlou P, Dunnill P. Biochemical engineering approaches to the challenges of producing pure plasmid DNA. Trends Biotechnol 2000; 18:296.
80. Strancar A, Podgornik A, Barut M, Necina R. Short monolithic columns as stationary phases for biochromatography. Adv Biochem Eng Biotechnol 2002; 49:76.
81. Stadler J, Lemmens R, Nyhammar T. Plasmid DNA purification. J Gene Med 2004; 6:S54.
82. Durland RH, Eastman EM. Manufacturing and quality control of plasmid-based gene expression systems. Adv Drug Del Rev 1998; 30:33.
83. Prazeres DMF, Ferreira GNM, Monteiro GA, Cooney CL, Cabral JMS. Large-scale production of pharmaceutical-grade plasmid DNA for gene therapy: problems and bottlenecks. Trends Biotechnol 1999; 17:169.
84. Walther W, Stein U, Voss C, Schmidt T, Schleef M, Schlag PM. Stability analysis for long term storage of naked DNA: impact on nonviral in vivo gene transfer. Anal Biochem 2003; 318:230.
85. Prazeres DMF, Schluep T, Cooney C. Preparative purification of supercoiled plasmid DNA using anion-exchange chromatography. J Chromatogr A 1998; 806:31.
86. Schmidt T, Friehs K, Schleef M, Voss C, Flaschel E. Quantitative analysis of plasmid forms by agarose and capillary gel electrophoresis. Anal Biochem 1999; 274:235.
87. Gut IG. DNA analysis by MALDI-TOF mass spectrometry. Hum Mutat 2004; 23:437.
88. Chen L, Ren J. High-throughput DNA analysis by microchip electrophoresis. Combinat Chem High Throughput Screen 2004; 7:29.
89. Righetti PG, Gelfi C, D'Acunto MR. Recent progress in DNA analysis by capillary electrophoresis. Electrophoresis 2002; 23:1361.

90. Gao Q, Shi Y, Liu S. Multiple-channel microchips for high-throughput DNA analysis by capillary electrophoresis. Fresenius J Anal Chem 2001; 371:137.

91. Diogo MM, Queiroz JA, Prazeres DMF. Chromatography of plasmid DNA. J Chromatogr A 2005; 1069:3.

92. Kepka C, Lemmens R, Vasi J, Nyhammar T, Gustavsson PE. Integrated process for purification of plasmid DNA using aqueous two-phase systems combined with membrane filtration and lid bead chromatography. J Chromatogr A 2004; 1057:115.

93. Gustavsson PE, Lemmens R, Nyhammar T, Busson P, Larsson PO. Purification of plasmid DNA with a new type of anion-exchange beads having a non-charged surface. J Chromatogr A 2004; 1038:131.

94. Eon-Duval A, Burke G. Purification of pharmaceutical-grade plasmid DNA by anion-exchange chromatography in an RNase-free process. J Chromatogr B 2004; 804:327.

95. Lemmens R, Olsson U, Nyhammar T, Stadler J. Supercoiled plasmid DNA: selective purification by thiophilic/aromatic adsorption. J Chromatogr B 2003; 784:291.

96. Ljunglöf A, Bergvall P, Bhikhabhai R, Hjorth R. Direct visualisation of plasmid DNA in individual chromatography adsorbent particles by confocal scanning laser microscopy. J Chromatogr A 1999; 844:129.

97. Iuliano S, Fisher JR, Chen M, Kelly WJ. Rapid analysis of a plasmid by hydrophobic-interaction chromatography with a non-porous resin. J Chromatogr A 2002; 972:77.

98. Thwaites E, Burton SC, Lyddiatt A. Impact of the physical and topographical characteristics of adsorbent solid-phases upon the fluidised bed recovery of plasmid DNA from Escherichia coli lysates. J Chromatogr A 2002; 943:77.

99. Goncalves E, Debs RJ, et al. The effect of liposome size on the final lipid/DNA ratio of cationic lipoplexes. Biophys J 2004; 86:1554.

100. Rakhmanova VA, Pozharski EV, et al. Mechanisms of lipoplex formation: dependence of the biological properties of transfection complexes on formulation procedures. J Membr Biol 2004; 200:35.

101. Kennedy MT, Pozharski EV, et al. Factors governing the assembly of cationic phospholipid-DNA complexes. Biophys J 2000; 78:1620.

102. Almofti MR, Harashima H. Lipoplex size determines lipofection efficiency with or without serum. Mol Membr Biol 2003; 20:35.

103. Congiu A, Pozzi D, et al. Correlation between structure and transfection efficiency: a study of DC-Chol-DOPE/DNA complexes. Colloids Surf B Biointerfaces 2004; 36:43.

104. Kiefer K. Entwicklung einer nicht-viralen upscalebaren Formulierung zur Transfektion humaner vaskulärer Endothelzellen und glatter Muskelzellen. Ph.D. Thesis, Albert-Ludwigs-Universität Freiburg, 2003.

105. Clement J, Kiefer K, Kimpfler A, Garidel P, Peschka-Süss R. Large scale production of lipoplexes with long shelf-life. Eur J Pharm Biopharm 2005; 59:35.

106. Kerner M, Meyuhas O, Hirsch-Lerner D, Rosen LJ, Min Z, Barenholz Y. Interplay in lipoplexes between type of pDNA promoter and lipid composition

determines transfection efficiency of human growth hormone in NIH3T3 cells in culture. Biochim Biophys Acta 2001; 1532:128.

107. Meidan VM, Cohen JS, Amariglio N, Hirsch-Lerner D, Barenholz Y. Interaction of oligonucleotides with cationic lipids: the relationship between electrostatics, hydration and state of aggregation. Biochim Biophys Acta 2000; 1464:251.

108. Meidan VM, Glezer J, Amariglio N, Cohen JS, Barenholz Y. Oligonucleotide lipoplexes: the influence of oligonucleotide composition on complexation. Biochim Biophys Acta 2001; 1568:177.

109. Simberg D, Danino D, Talmon Y, et al. Phase behavior, DNA ordering, and size instability of cationic lipoplexes. Relevance to optimal transfection activity. J Biol Chem 2001; 276:47453.

110. Weisman S, Hirsch-Lerner D, Barenholz Y, Talmon Y. Nanostructure of cationic lipid-oligonucleotide complexes. Biophys J 2004; 87:609.

111. Simberg D, Weisman S, Talmon Y, Barenholz Y. DOTAP (and other cationic lipids): chemistry, biophysics, and transfection. Crit Rev Therapeut Drug Carrier Sys 2004; 21:257.

112. Eastman SJ, Siegel C, Tousignant J, Smith AE, Cheng SH, Scheule RK. Biophysical characterization of cationic lipid: DNA complexes. Biochim Biophys Acta 1997; 1325:41.

113. Zuidam NJ, Barenholz Y. Characterization of DNA-lipid complexes commonly used for gene delivery. Int J Pharm 1999; 183:43.

114. Zuidam NJ, Barenholz Y. Electrostatic and structural properties of complexes involving plasmid DNA and cationic lipids commonly used for gene delivery. Biochim Biophys Acta 1998; 1368:115.

115. Audouy S, Hoekstra D. Cationic lipid-mediated transfection in vitro and in vivo. Mol Membr Biol 2001; 18:129.

116. Chesnoy S, Huang L. Structure and function of lipid-DNA complexes for gene delivery. Ann Rev Biophys Biomol Struct 2000; 29:27.

117. de Lima MC, Simoes S, Pires P, Gaspar R, Slepushkin V, Duzgunes N. Gene delivery mediated by cationic liposomes: from biophysical aspects to enhancement of transfection. Mol Membr Biol 1999; 16:103.

118. Lin AJ, Slack NL, Ahmad A, et al. Structure and structure-function studies of lipid/plasmid DNA complexes. J Drug Targeting 2000; 8:13.

119. Gustfasson J, Arvidson G, Karlsson G, Almgren M. Complexes between cationic liposomes and DNA visualised by cryo-TEM. Biochim Biophys Acta 1995; 1235:305.

120. Xu Y, Hui SH, Frederik P, Szoka FC. Physicochemical characterisation and purification of cationic lipoplexes. Biophys J 1999; 77:341.

121. Sternberg B. Ultrastructural morphology of cationic liposome DNA complexes for gene therapy. In: Lasic DD, Papahadjopoulos D, eds. Medical Application of Liposomes. Amsterdem: Elsevier, 1998:395–427 (chapter 5.4).

122. Sternberg B, Hong K, Zheng W, Papahadjopoulos D. Ultrastructural characterization of cationic liposome-DNA complexes showing enhanced stability in serum and high transfection activity in vivo. Biochim Biophys Acta 1998; 1375:23.

123. Oberle V, Bakowsky U, Zuhorn IS, Hoekstra D. Lipoplex formation under equilibrium conditions reveals a three-step mechanism. Biophys J 2000; 79:1447.

124. Almofti MR, Harashina H, Shinohara Y, Almofti A, Baba Y, Kiwada H. Cationic liposome mediated gene delivery: biophysical study and mechanism of internalisation. Arch Biochem Biophys 2003; 410:246.

125. Oberle V, Bakowsky U, Hoekstra D. Lipoplex assembly visualized by atomic force microscopy. Meth Enzymol 2003; 373:281.

126. Regelin AE, Fankhaenel S, Gurtesch L, Prinz C, von Kiedrowski G, Massing U. Biophysical and lipofection studies of DOTAP analogs. Biochim Biophys Acta 2000; 1464:151.

127. Hirsch-Lerner D, Barenholz Y. Hydration of lipoplexes commonly used in gene delivery: follow-up by laurdan fluorescence changes and quantification by differential scanning calorimetry. Biochim Biophys Acta 1999; 1461:47.

128. Madeira C, Loura LM, Aires-Barros MR, Fedorov A, Prieto M. Characterization of DNA/lipid complexes by fluorescence resonance energy transfer. Biophys J 2003; 85:3106.

129. Uyechi LS, Gagne L, Thurston G, Szoka FC Jr. Mechanism of lipoplex gene delivery in mouse lung: binding and internalization of fluorescent lipid and DNA components. Gene Ther 2001; 8:828.

130. Hui SW, Langner M, Zhao Y, Ross P, Hurley E, Chan K. The role of helper lipids in cationic liposome-mediated gene transfer. Biophys J 1996; 71:590.

131. Farhood H, Serbina N, Haung L. The role of dioleoyl phosphatidylethanolamine in cationic liposome mediated gene therapy. Biochim Biophys Acta 1995; 1235:289.

132. Yang JP, Huang L. Overcoming the inhibitory effect of serum on lipofection by increasing the charge ratio of cationic liposome to DNA. Gene Ther 1997; 4:950.

133. Koltover I, Salditt T, Safinya CR. Phase diagram, stability, and overcharging of lamellar cationic lipid-DNA self-assembled complexes. Biophys J 1999; 77:915.

134. Smisterova J, Wagenaar A, Stuart MC, et al. Molecular shape of the cationic lipid controls the structure of cationic lipid/dioleylphosphatidylethanolamine-DNA complexes and the efficiency of gene delivery. J Biol Chem 2001; 276: 47615.

135. Koltover I, Salditt T, Radler JO, Safinya CR. An inverted hexagonal phase of cationic liposome-DNA complexes related to DNA release and delivery. Science 1998; 281:78.

136. Harries D, May S, Gelbart WM, Ben-Shaul A. Structure stability, and thermodynamics of lamellar DNA-lipid complexes. Biophys J 1998; 75:159.

137. Huebner SR. Struktur und Entstehung von Komplexen aus Kationischen Lipiden und DNS. Ph.D. Thesis, Technische Universität München, 2000.

138. Hanulová M, Uhríková D, Devínsky F, Lacko I, Funari SS, Balgavý P. The structure of aggregate DNA – unilamellar DPPC liposomes – Ca2+: SAXD study. HASYLAB Annu Rep 2004; 1:824.

139. Barron LG, Uyechi LS, Szoka FC Jr. Cationic lipids are essential for gene delivery mediated by intravenous administration of lipoplexes. Gene Ther 1999; 6:1179.

140. Lasic DD. Structure and structure-activity relationships of lipid-based gene delivery systems. In: Huang L, Hung MC, Wagner E, eds. Nonviral Vectors for Gene Therapy. London: Academic Press, 1999.

141. Prasad TK, Gopal V, Madhusudhana Rao N. Structural changes in DNA mediated by cationic lipids alter in vitro transcriptional activity at low charge ratios. Biochim Biophys Acta 2003; 1619:59.

142. Shi F, Wasungu L, Nomden A, et al. Interference of poly(ethaylene glycol)-lipid analogues with cationic lipid mediated delivery of oligonucleotides; role of lipid exchangeability and non-lamellar transitions. Biochem J 2002; 366:333.

143. Natali F, Castellano C, Pozzi D, Castellano CA. Dynamic properties of an oriented lipid/DNA complex studied by neutron scattering. Biophys J 2005; 88:1081.

144. Blume A, Garidel P. Lipid model membranes and biomembranes. In: Gallagher PK, series ed. The Handbook of Thermal Analysis and Calorimetry. Kemp RB, ed. From Macromolecules to Man. 1st ed. Amsterdam: Elsevier, 1999; 4:109–173.

145. Wang J, Guo X, Xu Y, Barron L, Szoka FC Jr. Synthesis and characterization of long chain alkyl acyl carnitine esters. Potentially biodegradable cationic lipids for use in gene delivery. J Med Chem 1998; 41:2207.

146. Zantl R, Baicu L, Artzner F, Sprenger I, Rapp G, Rädler JO. Thermotropic phase behavior of cationic lipid-DNA complexes compared to binary lipid mixtures. J Phys Chem B 1999; 103:10300.

147. Subramanian M, Holopainen JM, Paukku T, et al. Characterisation of three novel cationic lipids as liposomal complexes with DNA. Biochim Biophys Acta 2000; 1466:289.

148. Elouahabi A, Thiry M, Pector V, Ruysschaert JM, Vandenbranden M. Calorimetry of cationic liposome-DNA complex and intracellular visualization of the complexes. Meth Enzymol 2003; 373:313.

149. Pozharski E, MacDonald RC. Thermodynamics of cationic lipid-DNA complex formation as studied by isothermal titration calorimetry. Biophys J 2002; 83:556.

150. Pector V, Backmann J, Maes D, Vandenbranden M, Ruysschaert JM. Biophysical and structural properties of DNA-diCi4-amidine complexes. Biol Chem 2000; 275:29533.

151. Hübner W, Blume A. Interactions at the lipid-water interface. Chem Phys Lipids 1998; 96:229.

152. Garidel P, Blume A, Hübner W. A Fourier transform infrared spectroscopic study of the interaction of alkaline earth cations with the negatively charged phospholipid 1,2-dimyristoyl-sn-glycero-3-phosphoglycerol. Biochim Biophys Acta 2000; 1466:245.

153. Pohle W, Selle C, Gauger DR, Zantl R, Artzner F, Rädler JO. FTIR spectroscopic characterization of a cationic lipid-DNA complex and its components. Phys Chem Chem Phys 2000; 2:4642.

154. Boffi F, Bonincontro A, Bordi F, et al. Two-step mechanism in cationic lipoplex formation as observed by dynamic light scattering, dielectric relaxation and circular dichroism methods. Phys Chem Chem Phys 2002; 4:2708.

155. Pasternack RF. Circular dichroism and the interactions of water soluble porphyrins with DNA. Chirality 2003; 15:329.

156. Norden B, Kurucsev T. Analysing DNA complexes by circular and linear dichroism. J Mol Recog 1994; 7:141.

157. Woody RW. Circular dichroism. Meth Enzymol 1995; 246:34.
158. Gray DM, Ratliff RL, Vaughan MR. Circular dichroism spectroscopy of DNA. Meth Enzymol 1992; 211:389.
159. Lee H, Williams SKR, Allison SD, Anchordoquy TJ. Analysis of self-assembled cationic lipid-DNA gene carrier complexes using flow-field-flow fractionation and light scattering. Anal Chem 2001; 73:837.
160. Haque KA, Pfeiffer RM, Beerman MB, Struewing JP, Chanock SJ, Bergen AW. Performance of high-throughput DNA quantification methods. BMC Biotech 2003; 3:20.
161. Whlean JA, Russell NB, Whelan MA. A method for the absolute quantification of cDNA using real-time PCR. J Immunol Meth 2003; 278:261.
162. Geall AJ, Blagbrough IS. Rapid and sensitive ethidium bromide fluorescence quenching assay of polyamine conjugate-DNA interactions for the analysis of lipoplex formation in gene therapy. J Pharm Biomed Anal 2000; 22:849.
163. Tsai JT, Furstoss KJ, Michnick T, Sloane DL, Paul RW. Quantitative physical characterization of lipid-polycation-DNA lipopolyplexes. Biotechnol Appl Biochem 2002; 36:13.
164. Meyer O, Roch O, Elmlinger D, Kolbe HV. Direct lipid quantitation of cationic liposomes by reversed-phase HPLC in lipoplex preparation process. Eur J Pharm Biopharm 2000; 50:353.
165. Glavas-Dodov M, Fredro-Kumbaradzi E, Goracinova K, et al. The effects of lyophilization on the stability of liposomes containing 5-FU. Int J Pharm 2005; 291:79.
166. Liu S, O'Brien DF. Stable polymeric nanoballoons: lyophilization and rehydration of cross-linked liposomes. J Am Chem Soc 2002; 124:6037.
167. Zou Y, Priebe W, Perez-Soler R. Lyophilized preliposomal formulation of the non-cross-resistant anthracycline annamycin: effect of surfactant on liposome formation, stability and size. Cancer Chemother Pharmacol 1996; 39:103.
168. Ohsawa T, Miura H, Harada K. A novel method for preparing liposome with a high capacity to encapsulate proteinous drugs: freeze-drying method. Chem Pharm Bull 1984; 32:2442.
169. van den Besselaar AM, Witteveen E, Schaefer-van Mansfeld H, Meeuwisse-Braun J, Strebus A. Accelerated degradation test of lyophilized recombinant tissue factor-liposome preparations. Thrombosis Haemostasis 1995; 73:392.
170. Rabinovici R, Rudolph AS, Vernick J, Feuerstein G. Lyophilized liposome encapsulated hemoglobin: evaluation of hemodynamic, biochemical, and hematologic responses. Crit Care Med 1994; 22:480.
171. Tang X, Pikal MJ. Design of freeze-drying processes for pharmaceuticals: practical advice. Pharm Res 2004; 21:191.
172. Madden TD, Boman N. Lyophilisation of liposomes. In: Janoff AS, ed. Liposome, Rational Design. Basel, New York: Marcel Dekker, 1999:261–282 (chap. 11).
173. Franks F. Freeze-drying of bioproducts: putting principles into practice. Eur J Pharm Biopharm 1998; 45:221.
174. Van Winden ECA. Freeze drying of liposomes: theory and practice. Meth Enzymol 2003; 367:99.
175. Rambhatla S, Ramot R, Bhugra C, Pikal MJ. Heat and mass transfer scale-up issues during freeze drying: II. Control and characterization of the degree of supercooling. AAPS Pharm Sci Tech 2004; 5:e58.

176. Jennings TA. Lyophilization Introduction and Basic principles. Denver, Colorado: Interpharm Press, 1999.
177. Cameron P, ed. Good Pharmaceutical Freeze-Drying Practice. Buffalo, Grove: Interpharm Press, 1997.
178. Aso Y, Yoshioka S. Effect of freezing rate on physical stability of lyophilized cationic liposomes. Chem Pharm Bull 2005; 53:301.
179. van Winden EC, Zhang W, Crommelin DJ. Effect of freezing rate on the stability of liposomes during freeze-drying and rehydration. Pharm Res 1997; 14:1151.
180. Allison SD, Anchordoquy TJ. Mechanisms of protection of cationic lipid-DNA complexes during lyophilisation. J Pharm Sci 2000; 89:682.
181. Allison SD, Molina MC, Anchordoquy TJ. Stabilization of lipid/DNA complexes during the freezing step of the lyophilization process: the particle isolation hypothesis. Biochim Biophys Acta 2000; 1468:127.
182. Lai E, van Zanten JH. Evidence of lipoplex dissociation in liquid formulations. J Pharm Sci 2002; 91:1225.
183. Armstrong TK, Girouard LG, Anchordoquy TJ. Effects of PEGylation on the preservation of cationic lipid/DNA complexes during freeze-thawing and lyophilisation. J Pharm Sci 2002; 91:2549.
184. Cortesi R, Esposito E, Nastruzzi C. Effect of DNA complexation and freeze-drying on the physicochemical characteristics of cationic liposomes. Antisense Nucl Acid Drug Dev 2000; 10:205.
185. Molina MC, Armstrong TK, Zhang Y, Patel MM, Lentz YK, Anchordoquy TJ. The stability of lyophilized lipid/DNA complexes during prolonged storage. J Pharm Sci 2004; 93:2259.
186. Armstrong TK, Anchordoquy TJ. Immobilization of nonviral vectors during the freezing step of lyophilisation. J Pharm Sci 2004; 93:2698.
187. Zhang Y, Anchordoquy TJ. The role of lipid charge density in the serum stability of cationic lipid/DNA complexes. Biochim Biophys Acta 2004; 1663:143.
188. Zhang Y, Garzon-Rodriguez W, Manning MC, Anchordoquy TJ. The use of fluorescence resonance energy transfer to monitor dynamic changes of lipid-DNA interactions during lipoplex formation. Biochim Biophys Acta 2003; 1614:182.
189. Choosakoonkriang S, Wiethoff CM, Koe GS, Koe JG, Anchordoquy TJ, Middaugh CR. An infrared spectroscopic study of the effect of hydration on cationic lipid/DNA complexes. J Pharm Sci 2003; 92:115.
190. Lengsfeld CS, Anchordoquy TJ. Shear-induced degradation of plasmid DNA. J Pharm Sci 2002; 91:1581.
191. Molina MC, Allison SD, Anchordoquy TJ. Maintenance of nonviral vector particle size during the freezing step of the lyophilization process is insufficient for preservation of activity: insight from other structural indicators. J Pharm Sci 2001; 90:1445.
192. Choosakoonkriang S, Wiethoff CM, Anchordoquy TJ, Koe GS, Smith JG, Middaugh CR. Infrared spectroscopic characterization of the interaction of cationic lipids with plasmid DNA. J Biol Chem 2001; 276:8037.
193. Anchordoquy TJ, Koe GS. Physical stability of nonviral plasmid-based therapeutics. J Pharm Sci 2000; 89:289.
194. Anchordoquy TJ, Girouard LG, Carpenter JF, Kroll DJ. Stability of lipid/DNA complexes during agitation and freeze-thawing. J Pharm Sci 1997/1998; 87:1046.

195. Anchordoquy TJ, Carpenter JF, Kroll DJ. Maintenance of transfection rates and physical characterization of lipid/DNA complexes after freeze-drying and rehydration. Arch Biochem Biophys 1997; 348:199.

196. Nabel GJ, Nabel EG. Direct gene transfer with DNA-liposome complexes in melanoma: expression, biologic activity, and lack of toxicity in humans. Proc Natl Acad Sci USA 1993; 90:11307.

197. Eastman SJ, Lukason MJ, Tousignant JD, et al. A concentrated and stable aerosol formulation of cationic lipid: DNA complexes giving high-level gene expression in mouse lung. Hum Gene Ther 1997; 8:765.

198. Hong K, Zheng W, Baker A, Papahadjopoulos D. Stabilization of cationic liposome-plasmid DNA complexes by polyamines and poly(ethylene glycol)-phospholipid conjugates for efficient in vivo gene delivery. FEBS Lett 1997; 400:233.

199. Harvie P, Wong FM, Bally MB. Use of poly(ethylene glycol)-lipid conjugates to regulate the surface attributes and transfection activity of lipid-DNA particles. J Pharm Sci 2000; 89:652.

200. Talsma H, Cherng J. Stabilization of gene delivery systems by freeze-drying. Int J Pharm 1997; 157:233.

201. Seville PC, Kellaway IW, Birchall JC. Preparation of dry powder dispersions for non-viral gene delivery by freeze-drying and spray-drying. J Gene Med 2002; 4:428.

202. Zelphati O, Nguyen C, Ferrari M, et al. Stable and monodisperse lipoplex formulations for gene delivery. Gene Ther 1998; 5:1272.

203. Ferrari ME, Rusalov D, Enas J, Wheeler CJ. Trends in lipoplex physical properties dependant on cationic lipid structure, vehicle and complexation procedure do not correlate with biological activity. Nucl Acids Res 2001; 29:1539.

204. Son KK, Patel DH. Cationic liposome and plasmid DNA complexes formed in serum-free medium under optimum transfection condition are negatively charged. Biochim Biophys Acta 2000; 1466:11.

205. Turek J, Dubertret C, Jaslin G, Antonakis K, Scherman D, Pitard B. Formulations which increase the size of lipoplexes prevent serum-associated inhibition of transfection. J Gene Med 2000; 2:32.

206. Simberg D, Weisman S, Talmon Y, Faerman A, Shoshani T, Barenholz Y. The role of organ vascularization and lipoplex-serum initial contact in intravenous murine lipofection. J Biol Chem 2003; 278:39858.

207. Ross PC, Hui SW. Lipoplex size is a major determinant of in vitro lipofection efficiency. Gene Ther 1999; 6:651.

208. Sanders NN, Van Rompaey E, De Smedt SC, Demeester J. Structural alterations of gene complexes by cystic fibrosis sputum. Am J Respir Crit Care Med 2001; 164:486.

209. Hyde SC, Gill DR, Higgins CF, et al. Correction of the ion transport defect in cystic fibrosis transgenic mice by gene therapy. Nature 1993; 362:250.

210. Nabel EG, Plautz G. Recombinant gene expression in vivo within endothelial cells of the arterial wall. Science 1989; 244:1342.

211. Stephan DJ, Yang ZY. A new cationic liposome DNA complex enhances the efficiency of arterial gene transfer in vivo. Hum Gene Ther 1996; 7:1803.

212. Schwartz B, Benoist C, Abdallah B, et al. Lipospermine-based gene transfer into the newborn mouse brain is optimized by a low lipospermine/DNA charge ratio. Hum Gene Ther 1995; 6:1515.
213. Nomura T, Nakajima S. Intratumoral pharmacokinetics and in vivo gene expression of naked plasmid DNA and its cationic liposome complexes after direct gene transfer. Cancer Res 1997; 57:2681.
214. Clark PR, Stopeck AT, Ferrari M, Parker SE, Hersh EM. Studies of direct intratumoral gene transfer using cationic lipid-complexed plasmid DNA. Cancer Gene Ther 2000; 7:853.
215. Mohr L, Yoon SK, Eastman SJ, et al. Cationic liposome-mediated gene delivery to the liver and to hepatocellular carcinomas in mice. Hum Gene Ther 2001; 12:799.
216. Tandia BM, Lonez C, Vandenbranden M, Ruysschaert JM, Elouahabi A. Lipid mixing between lipoplexes and plasma lipoproteins is a major barrier for intravenous transfection mediated by cationic lipids. J Biol Chem 2005; 280:12255.
217. Uchida E, Mizuguchi H, Ishii-Watabe A, Hayakawa T. Comparison of the efficiency and safety of non-viral vector-mediated gene transfer into a wide range of human cells. Biol Pharm Bull 2002; 25:891.
218. Nagahiro I, Mora BN, Boasquevisque CH, Scheule RK, Patterson GA. Toxicity of cationic liposome-DNA complex in lung isografts. Transplantation 2000; 69:1802.
219. Zhang JS, Liu F, Huang L. Implications of pharmacokinetic behaviour of lipoplex for its inflammatory toxicity. Adv Drug Del Rev 2005; 57:689.
220. Romoren K, Thu BJ, Bols NC, Evensen O. Transfection efficiency and cytotoxicity of cationic liposomes in salmonid cell lines of hepatocyte and macrophage origin. Biochim Biophys Acta 2004; 1663:127.
221. Dass CR. Cytotoxicity issues pertinent to lipoplex-mediated gene therapy in-vivo. J Pharm Pharmacol 2002; 54:593.
222. Axel DI, Spyridopoulos I, Riessen R, Runge H, Viebahn R, Karsch KR. Toxicity, uptake kinetics and efficacy of new transfection reagents: increase of oligonucleotide uptake. J Vascular Res 2000; 37:221.
223. Grimm W, Harnischfeger G, Tegtmeier M. Stabilitätsprüfung in der Pharmazie Theorie und Praxis. Aulendorf: Cantor Verlag, 2004.
224. Draft guidance for industry (August 2002) from the U.S. Department of Health and Human Service, Food and Drug Administration, Center for Drug Evaluation and Research, "Liposome drug products. Chemistry, manufacturing, and controls; human pharmacokinetics and bioavailability; and labelling documentation," www.fda.gov/cder/guidance.
225. Note for guidance on the quality, preclinical and clinical aspects of gene transfer medicinal product. Committee for proprietary medicinal products (CPMP), http://www.emea.eu.int/.
226. WHO report of the WHO clinical gene transfer monitoring group, WHO consultation, Geneva, May 16–17, 2002, http://www.who.int/biologicals/Meeting-Reports/Gene-Therapy.htm.
227. www.pei.de
228. www.euregenethy.org/

229. Ledley FD. Pharmaceutical approach to somatic gene therapy. Pharm Res 1996; 13:1595.
230. Ledley FD. Nonviral gene therapy: the promise of genes as pharmaceutical products. Hum Gene Ther 1995; 6:1129.
231. Cohen-Haguenauer O, Rosenthal F, Gansbacher B, et al. Opinion paper on the current status of the regulation of gene therapy in Europe. Hum Gene Ther 2002; 13:2085.
232. Cohen-Haguenauer O. Gene therapy: regulatory issues and international approaches to regulation. Curr Opin Biotech 1997; 8:361.
233. Cohen-Haguenauer O. Gene therapy in Europe. Transfusion Sci 1996; 17:185.
234. Cohen-Haguenauer O. Safety and regulation at the leading edge of biomedical biotechnology. Curr Opin Biotech 1996; 7:265.
235. Blaese M, Blankenstein T, Brenner M, et al. European School of Oncology position paper. Gene therapy for the medical oncologist. Eur J Cancer 1995; 31A:1531.
236. Cohen-Haguenauer O. Overview of regulation of gene therapy in Europe: a current statement including reference to US regulation. Hum Gene Ther 1995; 6:773.
237. Cohen-Haguenauer O. Regulation of gene therapy in Europe: a current statement including reference to US regulation. Eur J Cancer 1994; 30A:1193.
238. Manilla P, Rebello T, Afable C, et al. Regulatory considerations for novel gene therapy products: a review of the process leading to the first clinical lentiviral vector. Hum Gene Ther 2005; 16:17.
239. Robertson JS, Cichutek K. From research data to clinical trials. In: Schleef M, ed. Plasmids for Therapy and Vaccination. Weinheim: Wiley-VCH, 2001:255–260 (chap. 13).

8

Synthesis and Advantages of Acid-Labile Formulations for Lipoplexes

**Marie Garinot, Christophe Masson, Nathalie Mignet,
Michel Bessodes, and Daniel Scherman**
*Unité de Pharmacologie Chimique et Génétique,
Université René Descartes,
Paris, France*

INTRODUCTION

The discovery of drug delivery systems that could carry a biologically active molecule to a targeted tissue and release its payload at the right time and position to mediate an effective therapeutic response has been the subject of intensive research activity. Among available drug delivery tools, liposomes offer many advantages (1). Strategies developed to improve liposome-mediated drug delivery include the enhancement of biodistribution (e.g., stability in the bloodstream, targeting specific tissues or cells) and facilitation of site-specific delivery (2). Indeed, an ideal carrier should transport its cargo to a specific tissue and then deliver it efficiently. Even though the development of sterically stabilized liposomes (namely "stealth liposomes") (3) and the use of targeting ligands have considerably improved systemic transport efficacy (4), a therapeutically relevant targeted liposome-mediated drug delivery system has not yet been developed. One expected property would be a site-specific destabilization of the liposome, inducing the release of the biologically active molecule where and when necessary to get an optimal biological response.

In the case of gene therapy, DNA is the biologically active molecule to be transported. Many delivery systems have been envisioned: viruses (5), physical techniques (6), and synthetic carrier systems (7). Among nonviral strategies, cationic lipid–mediated gene transfer looks very promising: DNA-cationic lipids particles (namely lipoplexes) are very efficient for in vitro transfection and have been extensively studied during the two last decades (8). Unfortunately, lipoplexes suffer from a lack of systemic stability after intravenous administration (short plasma half-lives mainly due to rapid clearance by the reticular endothelial system). Rapid removal from the circulation limits the accumulation of the particles around the targeted sites and thus avoids efficient and tissue-specific in vivo gene transfer (9). DNA release and traffic to the nucleus is another recognized barrier to efficient transfection (10). Even if the mechanisms occurring between internalization of lipoplexes and DNA expression within the nucleus are still far from known today, it is generally assumed that a triggered system that could help DNA release from the lipoplexes within the endosome could improve gene transfer efficacy.

Many chemical and physicochemical approaches have been devised to form particles that can be triggered to release their content in a controlled manner, ideally both spatial and temporal. These systems are made of lipids (or a mixture thereof) that, in response to a given change in neighborhood conditions, develop a propensity to form leaky or nonlamellar structures. Several triggers were envisioned: enzymatic activity, pH, redox potential, temperature, and light. These approaches have their advantages and draw-backs and have been extensively reviewed (11). More particularly, pH decrease is implicated in many physiological (endocytosis pathway) and pathological processes (tumor growth, inflammation, and myocardial ischemia) (12). Therefore, numerous pH-triggered systems have been designed and studied over the past three decades (13). Among them, one of the most popular strategies consists of the use of pH-sensitive liposomes. The inclusion of lipids with fusogenic properties results in the formation of so-called "fusogenic" liposomes, which undergo a phase transition under acidic conditions. Such particular systems are able to interact and promote fusion or destabilization of target membranes (e.g., endosomal membrane) and have been described to release efficiently the encapsulated material into the cytoplasm. The first pH-sensitive liposome system was introduced by Yatvin et al. (14). This was composed of phosphatidylcholine and *N*-palmitoyl homocysteine. Since then, a variety of pH-sensitive liposomes that feature a surfactant with a pH-titratable carboxylate group and a fusogenic lipid such as dioleylphosphatidylethanolamine (DOPE) have been described (15). More recently, the use of novel pH-sensitive lipids [oleyl alcohol–based formulations (16), imidazole derivatives (17), gemini surfactants (18), etc.] or of fusogenic peptides/proteins (19) and association of pH-sensitive polymers with liposomes have been reported (20). All these approaches are

well documented and rely on a quite similar mechanism: an acid-induced modification of the ionic balance within the particle promotes its destabilization and the release of its content.

This chapter will focus on another kind of pH-triggering, based on the degradation of the particle constituents. In contrast to ''pH-sensitive,'' this kind of system will be named ''pH-labile'' in this report. Such particles are prepared with pH-degradable lipids, i.e., lipids including an acid-cleavable bond. Interestingly, no charge is required to get the pH-triggered effect, unlike most pH-sensitive liposomes that are based on the protonation of a negatively charged surface. This strategy is thus rather different from former pH-sensitive systems and opens new areas of investigations.

More precisely, pH-labile lipids have been developed by our group in order to improve cationic lipid–mediated gene transfer. We tried to address two major issues using such systems. Both pH-labile cationic lipids and pH-labile polyethylene glycol (PEG)ylated lipids were envisioned for this purpose. This is to address two different stages where pH degradation could intervene: promote targeted gene delivery to solid tumors and inflammatory tissues (weakly acidic tissues) where degradation of the shielding PEG would reinitiate electrostatic membrane interactions and later facilitate lipoplex destabilization within the acidic endosomal compartments and cargo release in the cytosol. Several parameters had to be considered for the choice of the pH-labile function: It must be stable under physiological conditions but highly labile at lower pH, and subtle changes in pH must induce a rapid cleavage of the linkage. Furthermore, the sensitivity of the linkage must be easily adjustable, without changing linker nature or chemical route (because the optimal sensitivity for both tumor- and endosome-specific degradation is unknown, which creates the need to synthesize and compare lipids with various sensitivities).

Among documented acid-labile functional groups, orthoesters appeared as one of the most suitable function. They are commonly used as acid-labile protecting groups for diols, especially for carbohydrate chemistry (21). Polymers built with orthoesters motifs have been used for controlled drug release for several decades (22). Surprisingly, orthoesters had never been used as pH-labile linkage for drug delivery purposes until recently (23–26). Orthoester function consists of a carbon atom linked to three ''alkoxy'' groups. We envisioned a cyclic system, inspired from the well-documented use of orthoesters as protective groups: acid-catalyzed protection of a 1,2 or 1,3 diol with a trimethylorthoester affords, respectively, a five- or six-membered cyclic orthoester. Exocyclic methoxy group can be replaced by any other alkoxy group under acid catalysis (''trans-orthoesterification''). Such kind of strategy has a major asset: acid sensitivity can be easily modulated depending on the size of the ring (typically five- or six-membered) and the nature of the substituant on the ''central'' carbon atom. For instance, orthoformates (H-substituted) are more stable than orthoacetates (Me-substituted).

This chapter will successively describe examples and applications of formulations based on pH-labile cationic lipids and PEG lipids, both containing an orthoester linker.

METHODOLOGY

Acid-Sensitive Lipoplexes Based on pH-Degradable Cationic Lipids

Generalities

As mentioned in the introduction, we have chosen the orthoester linkage for its unique properties of hydrolysis in acidic media, which are closely related to structure and substitution pattern (27). The rationale here is to obtain pH-degradable lipoplexes, which would release their cargo at the lower pH occurring in endosomes. We have synthesized two cationic lipids, differentiated by the structure of the cationic head, as degradable analogs of compounds commonly used in our group. Both compounds bore the orthoester hydrolysable linker between the double alkyl chains and the polar cationic head (25). Lipoplexes formulated with this type of compound are expected to collapse following acid hydrolysis, hopefully inducing endosomal escape and release of their content into the cytoplasm.

Chemistry

Compounds *3* and *4* have been synthesized as analogs of stable cationic lipids *1* and *2* (Scheme 1). In a first step, the lipophilic moieties have been prepared from either dioctadecylamine or ditetradecylamine, which has been condensed with butyrolactone. The orthoester synthon 6 was obtained by reaction of N-protected 1-amino-propanediol with trimethyl orthoacetate, under *p*-toluene sulfonic acid (PTSA) catalysis. The resulting alcohols *5a* and *5b* were reacted with *6* to give the protected orthoester lipids *7a* and *7b*, which were hydrolyzed to the free amines *8a* and *8b* in alkaline medium. (Scheme 2).

The cationic heads were prepared independently. For compound *3*, spermine was protected as the tetra-trifluoroacetamide by reaction with trifluoroacetic anhydride. This was alkylated with *tert*-butyl bromoacetate, followed by deprotection with trifluoroacetic acid (TFA) to give a mixture from which compound *9* was isolated by column chromatography (Scheme 3).

For compound *4*, N-(3-aminopropyl)-1,3-propanediamine and 3-amino propanol were condensed to each other after six steps of protection and functionalization, to give the ramified protected cationic head *10*. The synthetic pathway is outlined in Scheme 4.

Compounds *3* and *4* were obtained by condensation of lipids *8a* and *8b* with, respectively, *9* and *10*, followed by deprotection of the trifluoroacetamide groups in alkaline media. Salification was securely obtained through
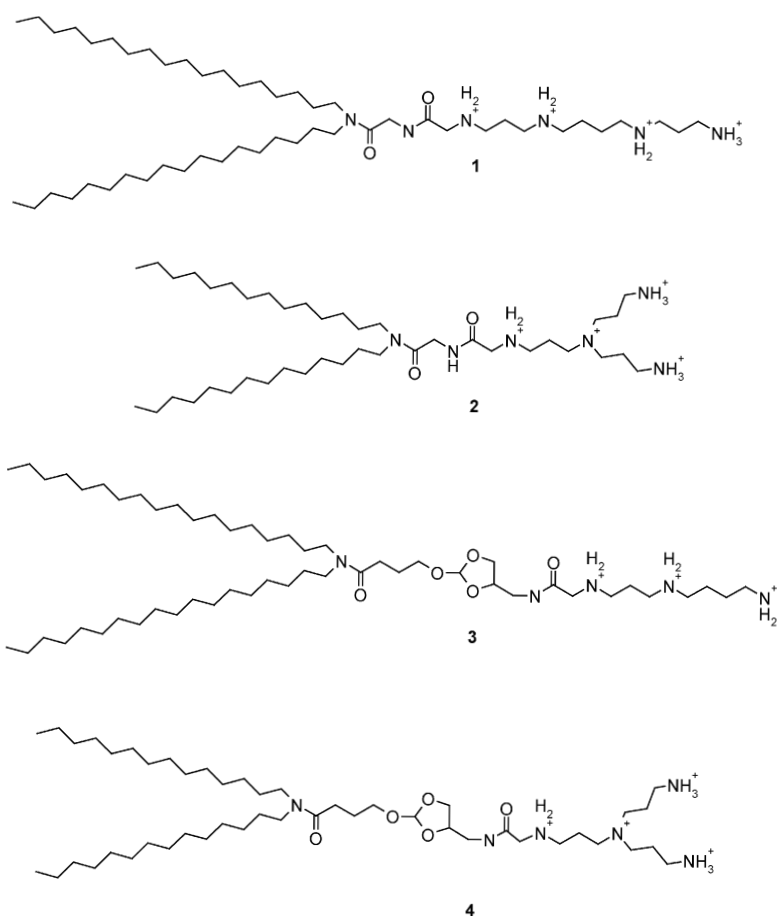
Scheme 1 pH-labile cationic lipids (*3* and *4*) and their stable analogs (*1* a[...]

elution over an ion exchange resin (quaternary ammonium type) and[...]
pH control to give the final pH-labile cationic lipids.

Physicochemistry

DNA Compaction at Neutral pH: Lipoplexes were prepare[...]
Hepes/mes/pipes buffer at pH $= 8.0$ at different charge ratios fro[...]
somes obtained with compounds *3* and *4* described above, in asso[...]
with the colipid **DOPE** (cationic lipid/DOPE 1:1), and were comp[...]
those obtained from stable cationic lipids *1* and *2*. Plasmid DNA us[...]
tained the luciferase (Luc) reporter gene under the cytomegalovirus[...]
promoter. Compaction of DNA in the liposomes was verified by add[...]
ethidium bromide (EtBr; 3 µL of a 1 g/L solution for 8 µg of DN[...]
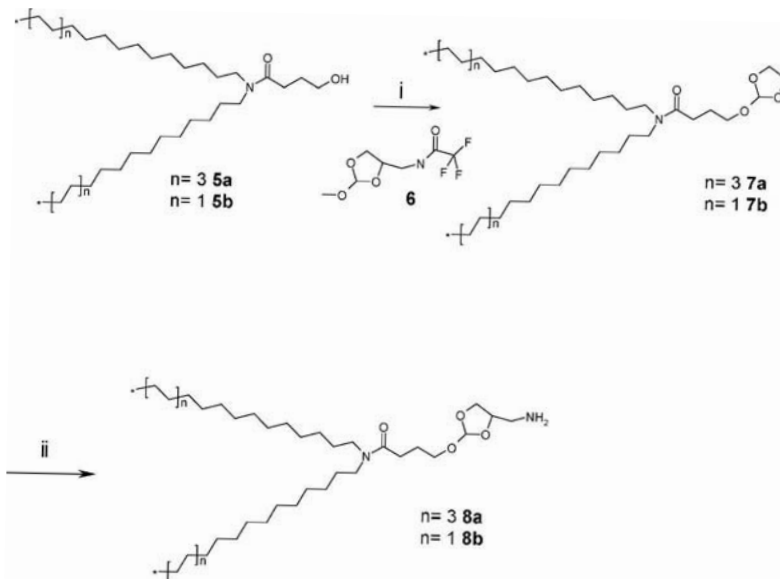
Scheme 2 (i) $6 + p$-Toluene sulfonic acid (cat), neat, 80°C; (ii) NaOH 4[...] trifluoroacetate, 50:50, 20°C, 10 hours.

measurement of the fluorescence (λ_{em} 590 nm), which decreases wh[...] DNA is compacted. The DNA compaction was also evidenced by t[...] of electrophoretical mobility of DNA on agarose gel. The size of th[...] plexes was measured as a function of the cationic lipid/DNA charg[...] by dynamic light scattering with a Coulter N4+ particle sizer at 6[...] The results, comparable to those obtained with the non–pH-labile c[...]

+ mixture of alkylated compounds
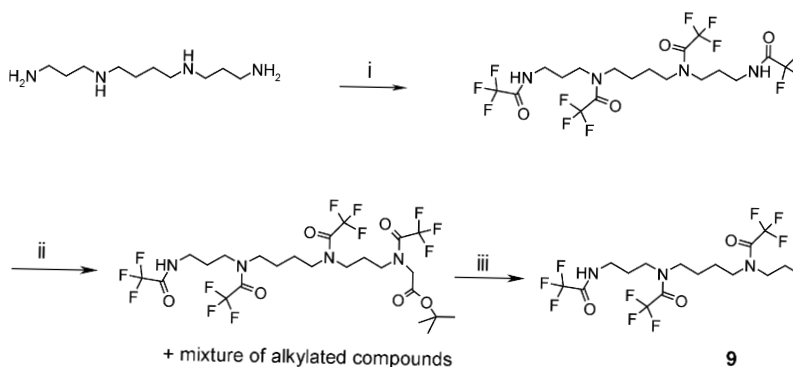
Scheme 3 (i) Trifluoroacetic anhydride, Et$_3$N, CH$_2$Cl$_2$, 0°C → 20°C, 10[...] (ii) *tert*-butyl bromoacetate, NaH, DMF, 20°C, 10 hours; (iii): trifluoroaceti[...] CH$_2$Cl$_2$, 20°C, three hours.

Scheme 4 (**i**) Ethyl trifluoroacetate, $0°C \rightarrow 20°C$, three hours; (**ii**) *tert*-butyl bromoacetate, CH_2Cl_2, $0°C \rightarrow 20°C$, five hours; (**iii**) trifluoroacetic anhydride, Et_3N, CH_2Cl_2, $0°C \rightarrow 20°C$, 10 hours; (**iv**) triphenylphosphine, carbon tetrabromide, THF, $20°C$, four hours; (**v**) K_2CO_3, CH_3CN, reflux, six hours; (**vi**): trifluoroacetic acid, CH_2Cl_2, $20°C$, three hours.

lipids, are shown on Figure 1. For cationic lipid/DNA charge ratio up to 1, small particles were obtained but DNA was not compacted, as shown by the high level of fluorescence obtained. Between 1 nmol and 4–6 nmol cationic lipid/µg DNA (which in the case of the cationic lipids described here is also equivalent to charge ratio), large aggregated particles were observed with low fluorescence, indicating compaction of DNA. Above 4 to 6 nmol catio- nic lipid/µg DNA, small particles were obtained, containing compacted DNA. The formation of complexes between DNA and pH-labile cationic lipids thus obeys similar rules as those observed with classical nonlabile cationic lipids. These lipids could then be used as gene vectors according to their stability and DNA compaction properties.

Degradation Studies at pH 5: The degradation of lipoplexes obtained with pH-labile cationic lipids *3* and *4* were evaluated by measuring the fluor- escence percentage of EtBr intercalated with DNA. Acidic degradation of pH-labile cationic lipids should result in the liberation of DNA and thus an increase in the observed fluorescence because EtBr will intercalate in
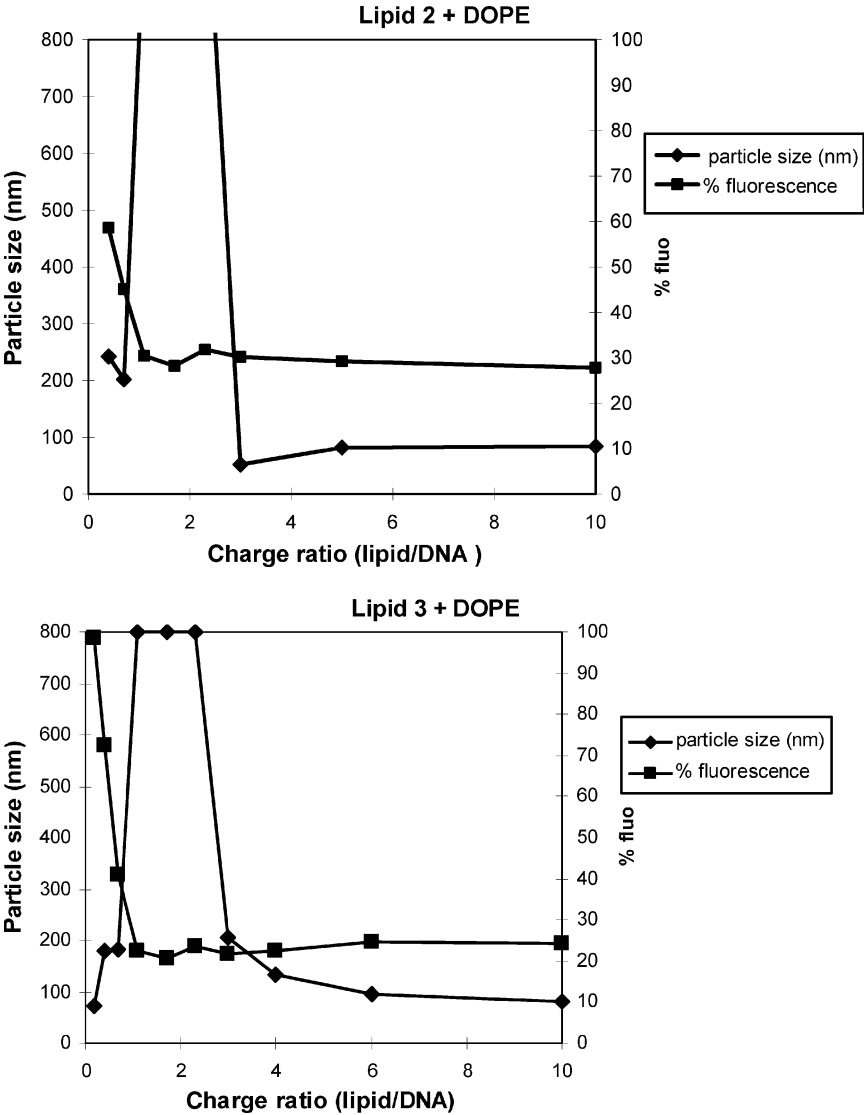
Figure 1   (*Continued on next page*) Effect of the lipid/DNA charge ratio on particle size and DNA compaction.

the uncompacted DNA. Liposomes containing either pH-labile or -stable cationic lipids were mixed with different amounts of DNA to obtain three different charge ratios: 0.4 nmol cationic lipid/μg DNA corresponding to the uncompacted zone, 1.7 nmol cationic lipid/μg DNA corresponding
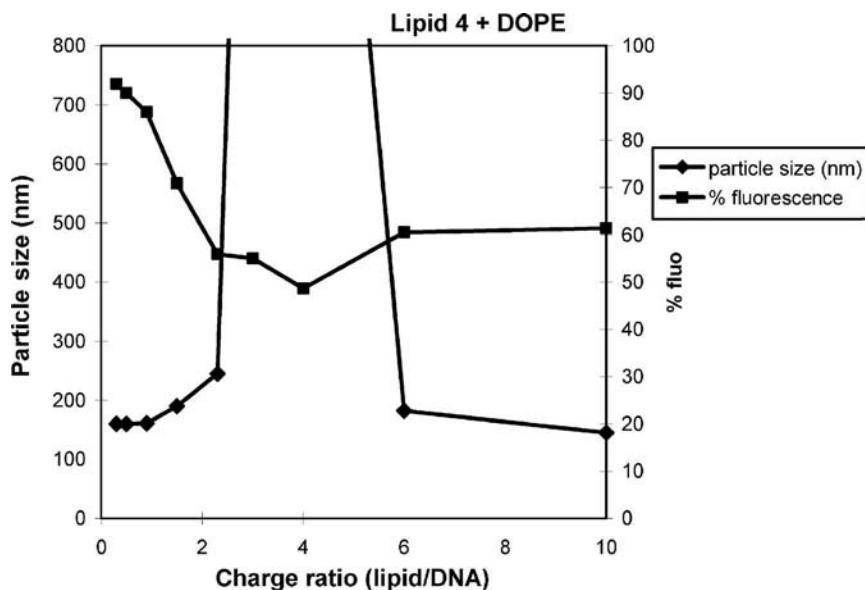
Figure 1   (*Continued from previous page*)

to the aggregated zone, and 6 nmol cationic lipid/μg DNA corresponding to small lipoplexes with compacted DNA. Preparations were incubated at 37°C in 0.1 M acetic acid/sodium acetate buffer (pH 5) and fluorescence of EtBr was measured (λ_{em} 590 nm) as a function of time. Complexes prepared at 0.4 charge ratio showed high fluorescence levels, confirming the accessibility of noncompacted DNA to EtBr (data not shown).

Fluorescence level was low and stable over time when considering lipoplexes prepared with stable cationic lipid *2* at charges ratios 1.7 and 6, whereas with lipoplexes containing pH-labile cationic lipid *4*, an increase of fluorescence was observed at pH 5, after four to six hours with a charge ratio of 1.7 and after 10 to 15 hours with a charge ratio of 6 (Fig. 2; similar results were obtained with lipids *1* and *3*). On the other hand, no fluorescence increase was observed at pH 7 for all the lipids tested (data not shown). It is noteworthy that the charge ratio influences strongly the release of DNA. In the case of an excess of cationic lipid, it is necessary to hydrolyze a larger number of molecules to destabilize the complexes, thus delaying the degradation of lipoplexes. As a matter of fact, as the cationic lipid/DNA charge ratio reaches the limit insuring colloidal stability, the kinetics of release increases. This behavior could advantageously be exploited to optimize the time needed for content release after exposition of the complexes to acidic medium, thus offering a temporal controlled delivery.

Degradation kinetics at pH 5
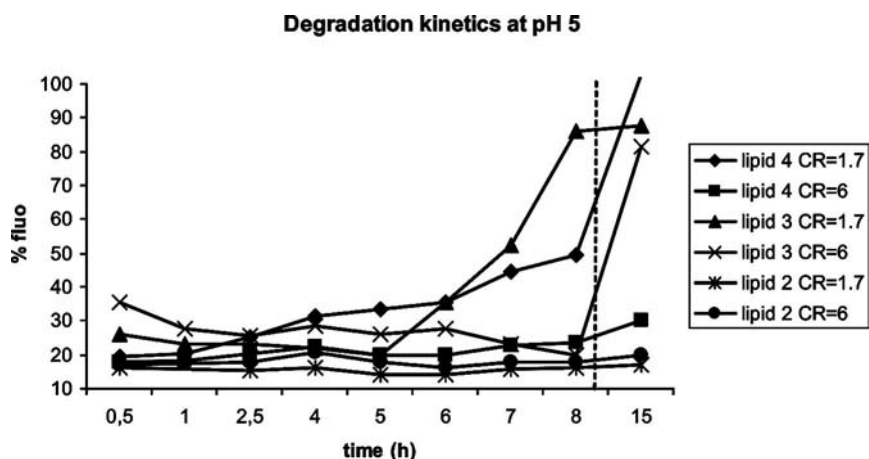
Figure 2 Degradation kinetic of lipoplexes obtained with stable lipid *2* and pH-labile lipids *3* and *4* at pH 5, and charge ratios 1.7 and 6. DNA release induced by degradation is measured by the percentage of fluorescence of intercalated ethidium bromide at 590 nm^{Em}; 260 nm^{Ex} (100% refers to naked DNA).

In Vitro Transfection Experiments with pH-Labile Lipoplexes

Formulations containing pH-labile cationic lipids *3* and *4* were evaluated in vitro in transfection experiments with Hela cells with three different charge ratios (1.5, 6.0, and 10), using plasmid DNA containing the Luc reporter gene under the CMV promoter. The results were compared to those obtained with non–pH-labile formulations. Micelle formulations were preferred to liposome because they gave better results in preliminary experiments. The complexes were prepared in 20 mM Hepes buffer at pH 7.4 and diluted to a final concentration of 1 mM, before incubation with the appropriate amount of DNA. Experiments were performed with or without addition of calf serum (10%). To evidence the influence of endosome acidification on transfection, experiments were also performed in the presence of bafilomycin A1, an inhibitor of endosome acidification (28).

The results of transfection with pH-labile lipid *4* and stable lipid *2* in the absence of serum, with or without bafilomycin A, are reported in Figure 3. Formulations containing lipids *1* and *3* gave results similar to those obtained with *2* and *4* and for the sake of clarity are not represented in the figure. Size measurements were performed for all the formulations; aggregation was observed at 1.5 charge ratio whereas small particles (85 nm) were obtained for the other ratios. For a charge ratio = 10, which is the charge ratio commonly used in systemic injection, significant enhancement (×12) of transfection was obtained with the pH-labile formulation versus stable formulation.
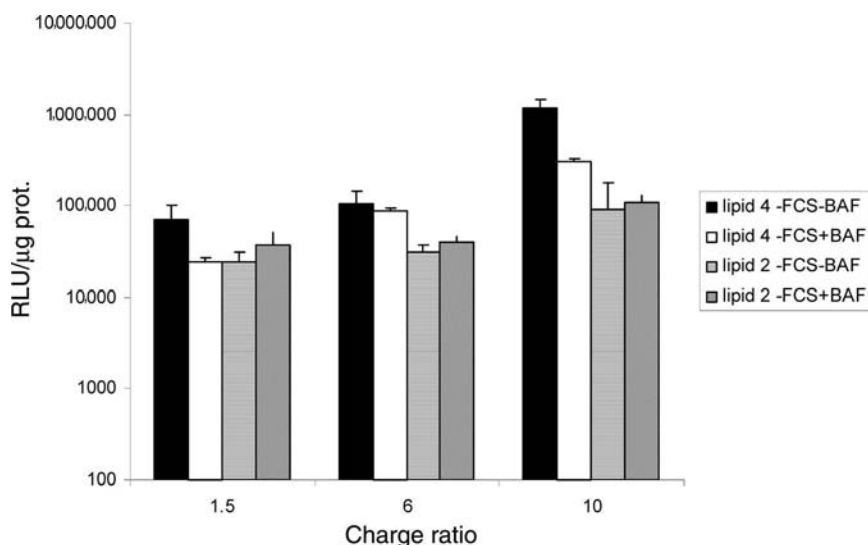
Figure 3 Transfection of Hela cells in the absence of serum with formulation including stable lipid *2* or pH-labile lipid *4*, with or without bafilomycin A.

No significant differences were observed with bafilomycin-treated cells at ratios 1.5 and 6. However, at charge ratio = 10, the transfection level was decreased to one-fourth with bafilomycin-treated cells in the case of pH-labile complexes compared to untreated cells, whereas no decrease was observed with the stable complexes in the same conditions. Serum dramatically decreased the transfection, as expected, especially at high charge ratios. Nevertheless, a better transfection was still observed with the pH-labile formulations (data not shown). In conclusion, pH-labile formulations gave a higher transfection level than their stable analogs. Results obtained in the presence of bafilomycin suggest that this effect could be attributed to a destabilization of the complexes in the endosome where acidification occurs. The dramatic loss of transfection observed in the presence of serum, especially at high charge ratios, was an expected phenomenon occurring with nonlabile cationic lipids as well.

Acid-Sensitive Lipoplexes Based on pH-Degradable Polyethylene Glycol Lipids

Generalities

As we mentioned in the introduction, cationic liposomes application in vivo has led so far to disappointing results, according to the nonspecific interactions observed between these cationic particles and circulating proteins and vessel membranes. This led invariably to undesirable effects and

rapid clearance from the blood stream. Shielding of the peripheral cationic charges has been realized by coating the particles with PEG derivatives, therefore increasing the circulation time of the particles and reducing nonspecific interactions (29). From there, it was necessary to design some triggering technology that would reinduce cell membrane interactions at the target organs or tissues. The metabolism occurring in tumors, inflammation, or ischemic sites provokes a pH decrease in the surrounding tissues (30) and this phenomenon has been exploited to help the release of encapsulated pharmaceutical drugs. However, pH variations in these tissues are small and the chemical trigger should respond efficiently to these variations, yet being stable enough to be easily handled at neutral pH and most importantly stable in the plasma. The orthoester group has been proposed as a pH-labile chemical linker to release the inserted PEG in the stabilized lipoplexes, thus recovering a cationic entity to interact with the membranes of the low pH targets (24,26).

Synthesis of pH-Labile Polyethylene Glycol Lipids

As already mentioned, the hydrolysis rate of cyclic orthoesters is tightly correlated to their structure and substituants. We thus have designed cyclic orthoester linkers that vary by the size of the cycle and substitution at the orthoester tertiary carbon.

Four pH-labile PEG lipids were prepared with different substitutions and structures (Scheme 5). Two compounds (11,13) were obtained with an octadecyl alkyl chain, and two others (12,14) with a cholesteryl group. Both types comprised an orthoester group with either a five- or six-membered cycle, respectively. The six-membered cycle in compounds *13* and *14* bore a methyl group introduced by the trimethyl orthoacetate reagent.

The detailed synthesis has been described (26). Orthoester synthons were obtained either by reaction of N-protected 1-amino-propanediol with trimethyl orthoformate or N-protected serinol with trimethyl orthoacetate, under PTSA catalysis. These orthoesters were then reacted with octadecanol, cholesterol, or (3-hydroxypropyl)-cholesteryl carbamate in the presence of a trace of PTSA in refluxing toluene, to give the corresponding orthoester-lipids. These, after deprotection, were condensed with α-carboethoxy-ω-methoxy-PEG (31) in the presence of BOP reagent to give the final products.

The stable control cholesteryl PEG was obtained by condensation of commercially available cholesteryl chloroformate and α-amino-ω-methoxy-PEG.

Degradation Studies

The rate of hydrolysis of the acid-labile PEG compounds *11*, *12*, *13*, and *14* were evaluated at pH 4.0 and 5.0 in 0.1 M acetate buffer (Fig. 4). HPLC equipped with an ELSD detector was used to determine the percentage of

11

12

13

14
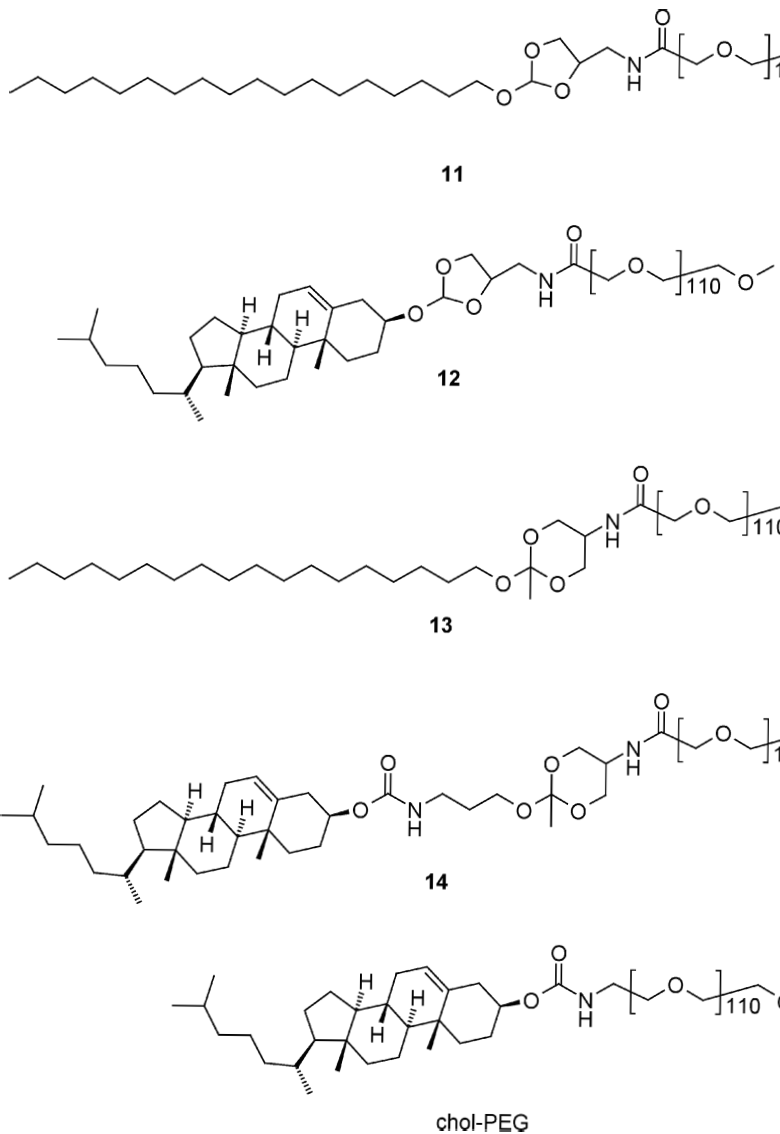
chol-PEG

Scheme 5 pH-labile PEG lipids prepared and chol PEG. *Abbreviation*: PEG ethylene glycol.

degradation, calculated as the ratio between the integration of the lyzed product and the starting material. The most sensitive six-mer orthoester derivatives *13* and *14* were half degraded at pH 5 in, respec 50 and 20 minutes, whereas at pH 4, complete degradation occurred

Degradation at pH 4

Degradation at pH 5
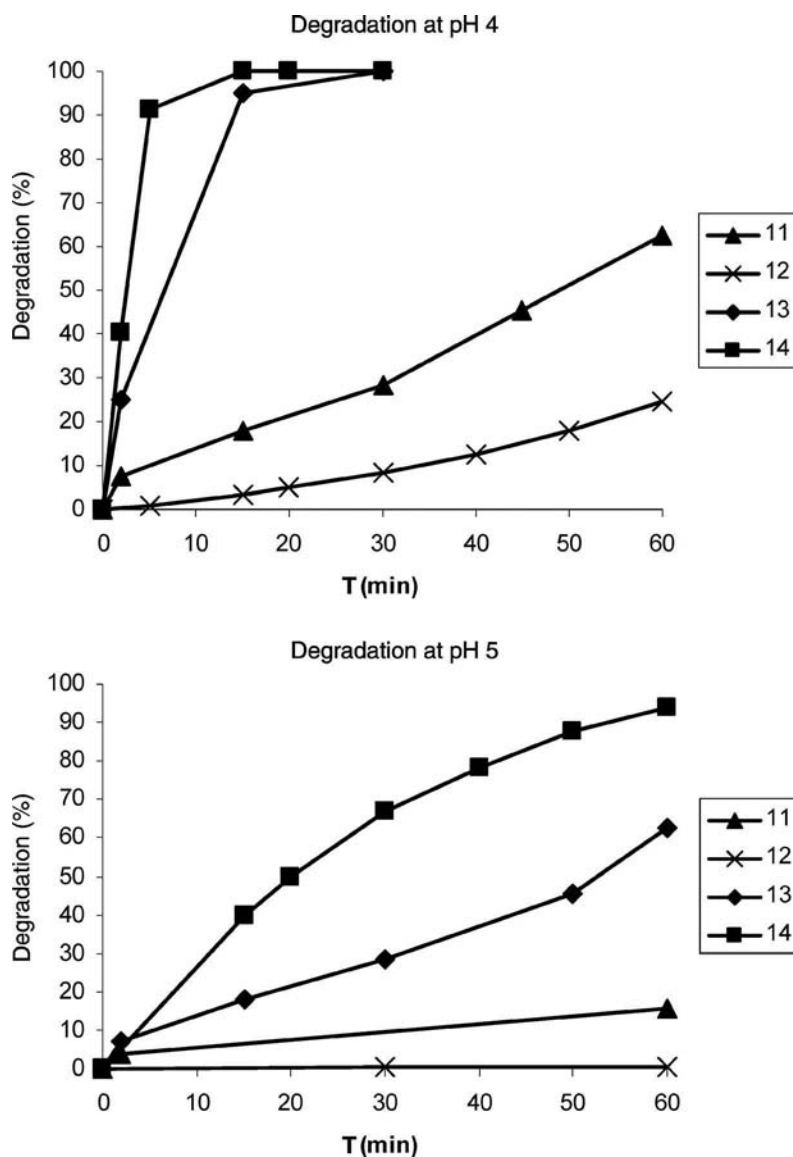
Figure 4 Hydrolysis rate of pH-labile polyethylene glycol lipids *11*, *12*, *13*, and *14* at pH 4.0 and 5.0.

10 minutes. The five-membered ring analogs were half-degraded at pH 4, only after one to few hours.

Stock solutions of the different pH-sensitive PEG lipids in pH 7.5 buffer were stable several days at room temperature and several weeks at 4°C.

Physicochemistry

The acid degradation of the PEG lipids prepared was also evidenced by aggregation studies of stabilized isoelectric lipid/DNA complexes.

The colloidal stabilization of the isoelectric lipid/DNA complexes was obtained for a PEG-lipid to total lipids ratio of 3% to 5% with compounds *11*, *13* and chol-PEG. No significant DNA release was observed.

Then, the colloidal stability of these lipoplexes at different pH (6.0 and 5.0 in sodium citrate 0.1 M buffer) was evaluated at 37°C and compared to that obtained with the non–pH-labile chol-PEG, at a ratio PEG-lipid/total lipid of 3%. This percentage was set to a minimum, ensuring stabilization of the particles, in order to enhance the sensitivity of the complexes to acidic medium. Size increase corresponding to neutral lipoplexes aggregation resulting from PEG-lipid degradation was measured (Fig. 5). The most sensitive acid-labile PEG-lipid candidate was identified as the cholesteryl six-membered ring orthoester derivative *14*, for which destabilization was obtained after only 30 minutes at pH 5.0. The observed aggregation behavior at higher pH (i.e., pH 6.0) for the monoalkyl compounds *11* and *13* might not be completely attributed to the hydrolysis of the orthoester group; the lower stability of the PEG-monoalkyl insertion in the liposome bilayer could also contribute to lipoplex destabilization.

Transfection: In Vitro

Lipoplexes were prepared in a Hepes/mes/pipes buffer at pH = 8.0 and charge ratio ($\pm$) = 10 from the liposomes described previously (cationic lipid *1*/DOPE 1:1). Plasmid DNA used contained the Luc reporter gene under the CMV promoter. Brij 700 and pH-labile alkyl PEG derivatives *11,13* were added to the preformed lipoplexes at 10% polymer/total lipids ratio and at 20% ratio for chol-PEG and pH-labile cholesteryl derivative *12*. In the absence of serum, lipoplexes without PEG-lipid gave a high transfection level, as previously shown. When lipoplexes were coated with either 10% Brij 700 or 20% Chol-PEG, the level of transfection was significantly reduced by a factor 30 and 300, respectively, as was similarly reported (32). Formulations including the least pH-labile monoalkyl compound *11* did not show significant increase in transfection efficacy. Conversely, cationic lipoplexes coated with either the most pH-labile alkyl-PEG derivative *13* or the pH-labile cholesteryl derivative *12* showed a transfection level increased by a factor of 10 and 25, respectively, compared to the formulations obtained with the stable Brij 700 or Chol-PEG (Fig. 6). It should be noted, however, that the transfection level observed with uncoated cationic lipoplexes could not be entirely recovered with lipoplexes containing pH-labile PEG-lipid. This observation might be due to incomplete hydrolysis of pH-labile PEG-lipid, thus leading to only partial release of DNA in the cytoplasm.
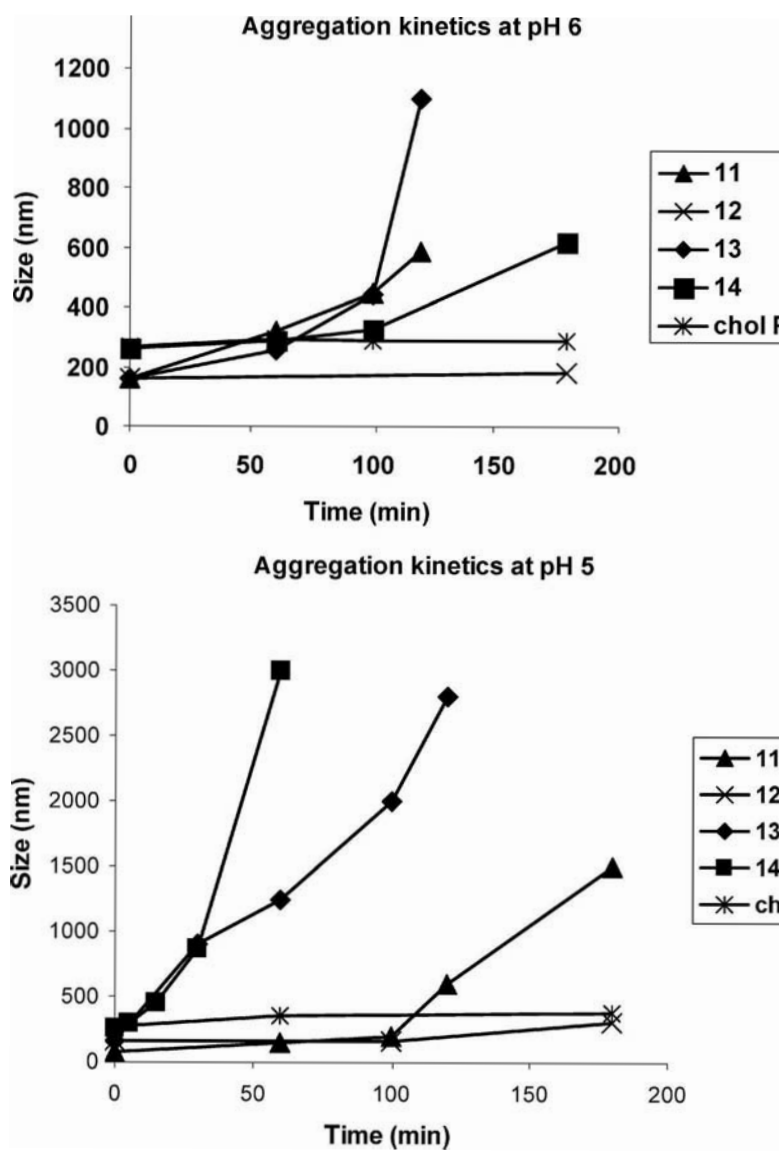
Figure 5 Aggregation kinetic of lipoplexes coated with pH-labile PEG lipic
13, and *14* at pH 5.0 and 6.0 (chol PEG as stable control). *Abbreviation*: PE
ethylene glycol.

We have shown that the presence of an acid-labile linker in PF
restored the transfection as compared to non–pH-labile PEG-lipid
lipoplexes. Because the lipoplexes were prepared at pH = 8.0 and
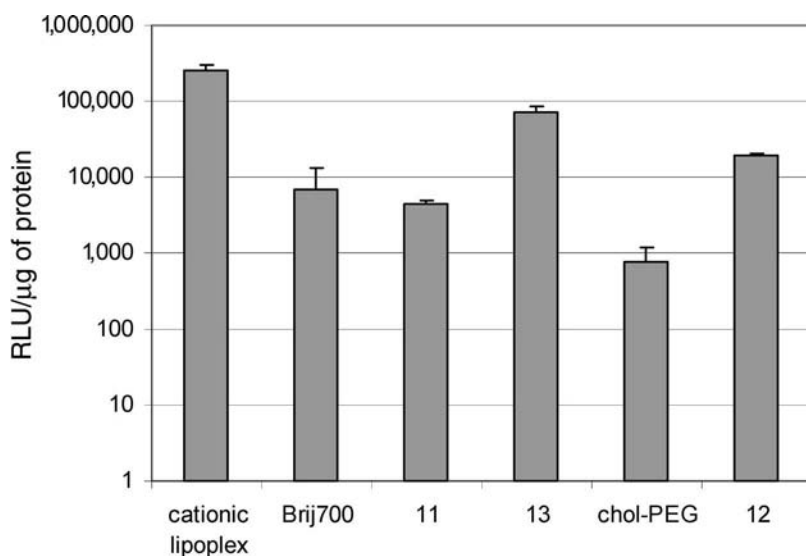
Figure 6 Transfection levels in Hela cells obtained with pH-labile PEG lipids–coated lipoplexes, compared with formulations containing stable Brij and chol PEG and uncoated cationic lipoplexes. *Abbreviation*: PEG, polyethylene glycol. *Source*: From Refs. 11–13.

pH of the cellular medium was maintained at pH 7.4, no prior degradation of the pH-labile lipid polymers could have occurred. It is well known that PEG coating of cationic lipoplexes does not completely inhibit nonspecific interactions with cell membranes, and internalization has been often observed despite the presence of PEG. Then the pH-labile complexes might have been destabilized by low pH in the endosomal compartment, thus releasing DNA.

In vivo experiments are in progress to validate the use of these pH-labile formulations in the passive targeting of tumors and/or inflammatory tissues.

DISCUSSION AND COMPARISON OF DIFFERENT SYSTEMS

pH-Labile Cationic Lipids

Among strategies promoting specific destabilization of particles to control and improve gene delivery process, pH-responsive systems seem particularly relevant as long as a pH gradient occurs during endocytosis. The endocytic pH gradient begins near the physiological pH (around 7.4), drops typically to 5.5 to 6.0 within endosomes, and reaches 4.5 to 5.0 within lysosomes. As presented in introduction, a well-documented strategy is the use of pH-sensitive liposomes for gene delivery. Recently, a new strategy was

envisioned: an acid-labile functionality was inserted in the lipids' backbones and low pH–induced hydrolysis of this linker provoked particles destabilization and leakage. Several approaches based on this methodology have been described during the last decade. In all cases, a pH-labile linkage is used to tether both the polar and hydrophobic domains. Enhancement of cationic lipid clearance through their degradation is expected to promote gene transfer and alleviate cytotoxicity.

Thomson et al. have demonstrated feasibility of such an approach using a vinyl ether linker: naturally occurring vinyl ether–linked phospholipid diplasmenylcholine (33) and synthetic analogues (34) have been described. Particularly, *O*-(2R-1,2-di-*O*-(1′Z, 9′Z-octadecadienyl)-glycerol)-3-*N*-(*bis*-2-aminoethyl)-carbamate was used as a pH-labile cationic lipid for gene transfer (35). This cationic lipid was highly efficient in terms of transfection levels; however, only a slight benefit was observed with this acid-labile system as compared with a stable analogue. According to the authors, a more acid-labile linkage would be expected to speed up cleavage reaction and thus increase the benefit of the pH-labile system.

Zhu et al. synthesized an orthoester-based pH-labile lipid (23). They developed a tricyclic linker based on the rearrangement of an oxetane to an orthoester. Degradation of this linkage is divided in two steps: ring opening followed by a rearrangement, which provokes cleavage of both parts of the molecule. This linker is by far more sensitive than the previously described vinyl ether linker (complete hydrolysis after 12 hours at 38°C at pH 4.5, whereas half-lives of vinyl ether derivatives under similar conditions were about 30 hours). According to the authors, a slight enhancement of cationic lipid–mediated gene transfer was observed with pH-labile systems. Unfortunately, no data are depicted in the article.

More recently, cationic lipids containing an acylhydrazone linker were developed by Aissaoui et al. (36); chemical stability at 25°C of four compounds was assessed at pH 4.8 versus pH 7.2 and authors measured pH-induced degradation with half-lives typically comprised between 1.2 and 2.3 days, depending on the compound. Among them, pH-labile bis-guanidinium bis(2-aminoethyl) amine hydrazine (BGBH)-cholest-4-enone and stable BGTC vectors were extensively studied and compared, both in vitro and in vivo. Unfortunately, the authors could not measure a significant enhancement of cationic lipid–mediated gene transfer with pH-labile versus stable formulations.

The orthoester linkers we developed present some significant assets with respect to other published systems. These linkers were shown to be highly sensitive, inducing particle destabilization within few minutes at low pH. Hydrolysis kinetics is a major parameter as long as endocytic pathway is a rapid phenomenon that lasts 10 to 30 minutes before ending in the lysosome-degradative pathway (37). As listed above, other envisioned systems were by far less sensitive. Another major aspect is that particle destabilization kinetics must be precisely adjusted to the internalization

kinetics. Thus, linker sensitivity must be highly adjustable. For this purpose, the linker we described is particularly interesting: slight structural modifications (for instance methyl substitution on the central carbon atom) significantly modulate sensitivity and this tool will allow us to study the influence of pH sensitivity with compounds having very similar structures. Additionally, degradation of this orthoester linker releases formic or acetic acid (respectively from orthoformate and orthoacetate hydrolysis): the degradation process is thus autocatalytic. We can expect that when degradation will begin, local release of acid will promote further degradation, improving destabilization kinetics.

It is noteworthy that in vitro transfection responses with pH-labile lipoplexes were somewhat improved with respect to classical stable particle efficacy. Nevertheless, one should stress that the whole intracellular traffic is poorly understood and that additional experiments must be performed with all these pH-labile lipoplexes to address the real benefit of these systems for DNA endosomal release.

pH-Labile Polyethylene Glycol Lipids

Different strategies have been developed to target inflammatory sites or tumors, taking advantage of the acidic environment of these damaged tissues. The one we focused on was the use of PEG-lipid containing an acid-cleavable linkage between the hydrophobic and hydrophilic parts. Indeed, the PEG moiety is necessary to prolong circulation of the complexes in the blood stream until the targeted organ is reached, but it then has to be removed to reveal the cationic charges at the surface of particles. These charges promote interactions with cell membranes, thus favoring endocytosis of lipoplexes. This strategy appears very attractive and has been investigated by different groups for several years.

The vinyl ether's function as cleavage site has been explored by Boomer and Thompson (38). They synthesized vinyl ether–linked PEG lipids, which presented good acid hydrolysis properties with good overall yields. Particularly, the compound containing a (R)-1,2-di-O-(1′Z, 9′Z-octadecadienyl)-glycerol as the hydrophobic part (39) was extensively studied. Unfortunately, physicochemical studies—including molecule degradation, calcein release, and fusion with liposomes—demonstrated a very low rate of destabilization, incompatible with in vivo applications.

A more complete study has been described, involving four acid-labile PEG-conjugated vinyl ether lipids (40). These amphiphilic molecules demonstrated a good stability in neutral medium. Release of calcein encapsulated in the formulation containing the DOPE-based vinyl ether PEG conjugates have been evaluated, as a result of disorganization of the liposome under different acidic conditions. This release was directly related to the medium pH, with low pH inducing an increased release of calcein over

time. Nevertheless, the rates of hydrolysis of the different compounds studied seemed to be too slow for a tumor-targeting strategy (only 50% of calcein was released during 3000 minutes at pH = 4.5). Comparable results were obtained on cholesteryl acid-labile derivatives (41). Such systems should allow long circulation time of the liposome in the organism before reaching the targeted organ; however, their cleavage kinetics seems too slow to target ischemia sites or tumors. Efforts are being made by the authors to enhance PEG-lipid cleavage rates to address this problem.

Szoka and coworkers investigated a PEG-diortho ester-distearoyl glycerol derivative under different pH conditions from chemical, physicochemical, and biological points of views (24).

This molecule was shown to be stable at pH = 7.4 for at least three hours at 37°C. It was very sensitive at pH = 4 and 5, being completely degraded after only one hour of incubation at 37°C. Concerning liposome formulations, the PEG moiety was excluded after 100 minutes of incubation at 37°C in a pH = 6 buffer, which is quite interesting for a systemic targeting strategy. Moreover, when incubated in serum, the acid-labile formulations demonstrated a good stability during 12 hours. After this time, the liposomes seemed to destabilize very rapidly compared to insensitive formulations.

If we refer to our study, we have seen that compounds *13* and *14* behaved in a similar manner at pH = 6: ortho-ester function hydrolysis provokes the cleavage of the PEG and consequently the aggregation of neutral lipoplexes. Although somewhat less sensitive than those from the group of Szoka and coworkers, the molecules we described in the preceding part present the advantage of being flexible in their structures, thus providing a modular sensitivity according to needs.

Szoka et al. pursued their work with preliminary in vivo studies that demonstrated that the acid-labile PEG-lipid was as stable in the blood circulation as the nonsensitive one and had a half-life of around 200 minutes, which could allow a targeting strategy. Biodistribution studies showed similar locations for acid-sensitive liposomes and insensitive formulations. Formulations including these acid-labile orthoester PEG-lipid thus revealed as good candidates to target slightly acidic tissues such as tumors or inflammatory sites.

The use of acid-sensitive delivery system is thus an interesting alternative for targeting. The deal is nevertheless challenging because the targeting molecule has to be stable in neutral conditions in order to circulate long enough in the blood to reach target sites, but then the system should destabilize quickly to allow interactions with targeted cell membranes.

Among the examples presented here, it seems that the ortho- or diortho-ester functions are the most appropriate in terms of kinetics of cleavage. Their stability in neutral medium and their high sensitivity to small variations of pH makes them promising tools for targeting lipoplexes to inflammatory sites and tumors.

CONCLUSIONS

To obtain efficient pH-triggered systems for drug and gene delive
obvious that sensitivity of the carrier to pH changes should respond
to the slight decrease of pH at potential therapeutic sites. Endosoma
in cells is known to last about 10 to 30 minutes, with pH gradien
range of 5 to 6, before ending into the lysosomal process of extensive
dation. Consequently, pH-labile lipoplexes should respond quickly
initial pH decrease and release their contents prior to the lysosoma

Around inflammatory tissues and solid tumors sites, the pH is
to 0.8 units different from that of the circulation, suggesting that pH-s
carrier systems devoted to these targets should respond to a very smal
lus. Another aspect is that the optimal kinetics of release will not only
on the carried biologically active molecule. Many other parameter
play a role, including the nature of the targeted tissue. Thus, the se
of a pH-labile system must be highly adjustable, depending on the e
therapeutic application.

Among the acid-labile linkers that have been described up to r
cyclic orthoester appears as one of the most suitable linkages. Its str
adjustable sensitivity to low acidic pH and its relative stability under
logical conditions are most of that should be expected of a pH-trigge
both acid-labile PEGylated and cationic lipids, and even coform
thereof, could improve gene transfer. Nevertheless, given that effect:
transfer requires a precise spatial and temporal DNA delivery to th
site, the benefit of such systems can only be expected if pH sensi
exactly fitted to the biological mechanism involved.
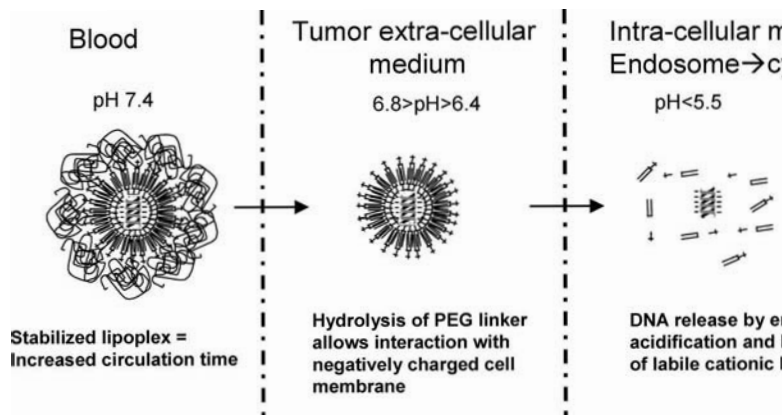
Scheme 6 Dual-step acid-labile system expected mechanism: initial rem
shielding PEG at target site allows for cell membrane interactions, then h
of acid-labile cationic lipid in the endosome provokes release of DNA in the
Abbreviation: PEG, polyethylene glycol.

The ultimate in pH-labile delivery systems would be a dual-releasing process, as presented on Scheme 6, which would allow sequential degradation of the complexes. The first step would permit interaction with the membranes by degradation of the stabilizing PEG lipids, thus unveiling the cationic charges. This should occur in the neighborhood of tumors and inflammatory tissues, where slight pH decrease has been observed. The second step is expected to proceed during the endosome acidification, where hydrolysis of the cationic lipid bilayer will induce collapsing of the liposome structure and release of the cargo. This double process would rely on differences of hydrolysis kinetics, which are precisely allowed by the use of orthoester linkers of different structures.

A lot of work still remains, especially because we are far from understanding the mechanisms of the binding and internalization of liposomes by various cells. In vivo experiments appear very important to derive conclusions regarding the efficiency of these systems, because the presence of serum highly affects the uptake of liposomes. However, preliminary results that have been presented here are very promising and encouraging for the development of pH-labile delivery systems.

REFERENCES

1. Langer R. Drug delivery and targeting. Nature 1998; 392:5.
2. Fonseca C, et al. Targeting of sterically stabilised pH-sensitive liposomes to human T-leukaemia cells. Eur J Pharm Biopharm 2005; 59:359.
3. Needham D, McIntosh TJ, Lasic DD. Repulsive interactions and mechanical stability of polymer-grafted lipid membranes. Biochim Biophys Acta 1992; 1108:40.
4. Xu L, et al. Systemic tumor-targeted gene delivery by anti-transferrin receptor scFv-immunoliposomes. Mol Cancer Ther 2002; 1:337.
5. Kim YG, et al. Ganciclovir-mediated cell killing and bystander effect is enhanced in cells with two copies of the herpes simplex virus thymidine kinase gene. Cancer Gene Ther 2000; 7:240; Robbins PD, Ghivizzani SC. Viral vectors for gene therapy. Pharmacol Therapeut 1998; 80:35; Goyenvalle A, et al. Rescue of dystrophic muscle through U7 snRNA-mediated exon skipping, Science 2004; 306:1796.
6. Preat V. Drug and gene delivery using electrotransfer. Ann Pharmaceutiques Francaises 2001; 59:239; Bloquel C, et al. Plasmid DNA electrotransfer for intracellular and secreted proteins expression: new methodological developments and applications. J Gene Med 2004; 6:S11.
7. Kichler A, et al. Intranasal gene delivery with a polyethylenimine-PEG conjugate. J Control Release 2002; 81:379; Felgner PL, et al. Lipofection: a highly efficient, lipid-mediated DNA-transfection procedure. P Natl Acad Sci USA 1987; 84:7413; Vigneron JP, et al. Guanidinium-cholesterol cationic lipids: efficient vectors for the transfection of eukaryotic cells. P Natl Acad Sci USA 1996; 93:9682.

8. Behr JP, et al. Efficient gene transfer into mammalian primary endocrine cells with lipopolyamine-coated DNA. P Natl Acad Sci USA 1989; 86:6982; Lee ER, et al. Detailed analysis of structures and formulations of cationic lipids for efficient gene transfer to the lung. Hum Gene Ther 1996; 7:1701; Bragonzi A, Conese M. Non-viral approach toward gene therapy of cystic fibrosis lung disease. Curr Gene Ther 2002; 2:295; Anderson DM, et al. Stability of mRNA/cationic lipid lipoplexes in human and rat cerebrospinal fluid: methods and evidence for nonviral mRNA gene delivery to the central nervous system. Hum Gene Ther 2003; 14:191.

9. Yang JP, Huang L. Overcoming the inhibitory effect of serum on lipofection by increasing the charge ratio of cationic liposome to DNA. Gene Ther 1997; 4:950.

10. Lechardeur D, et al. Metabolic instability of plasmid DNA in the cytosol: a potential barrier to gene transfer. Gene Ther 1999; 6:482.

11. Guo X, Szoka FC Jr. Chemical approaches to triggerable lipid vesicles for drug and gene delivery. Accounts Chem Res 2003; 36:335.

12. Drummond DC, Zignani M, Leroux J. Current status of pH-sensitive liposomes in drug delivery. Prog Lipid Res 2000; 39:409.

13. pH responsive carriers for enhancing the cytoplasmic delivery of macromolecular drugs, 7 review articles. Adv Drug Deliver Rev 2004; 56:925.

14. Yatvin MB, et al. pH sensitive liposomes: possible clinical implications. Science 1980; 210:1253.

15. Chu CJ, et al. Efficiency of cytoplasmic delivery by pH-sensitive liposomes to cells in culture. Pharm Res 1990; 7:824; Lee RJ, et al. The effects of pH and intraliposomal buffer strength on the rate of liposome content release and intracellular drug delivery. Biosci Rep 1998; 18:69; Subbarao NK, et al. pH-dependent bilayer destabilization by an amphipathic peptide. Biochemistry 1987; 26:2964.

16. Sudimack JJ, et al. A novel pH-sensitive liposome formulation containing oleyl alcohol. Biochim Biophys Acta 2002; 1564:31; Shi G, et al. Efficient intracellular drug and gene delivery using folate receptor-targeted pH-sensitive liposomes composed of cationic/anionic lipid combinations. J Control Release 2002; 80:309.

17. Singh RS, et al. On the gene delivery efficacies of pH-sensitive cationic lipids via endosomal protonation. A chemical biology investigation. Chem Biol 2004; 11:713.

18. Bell PC, et al. Transfection mediated by gemini surfactants: engineered escape from the endosomal compartment. J Am Chem Soc 2003; 125:1551; Jennings KH, et al. Aggregation properties of a novel class of cationic gemini surfactants correlate with their efficiency as gene transfection agents. Langmuir 2002; 18:2426.

19. Kakudo T, et al. Transferrin-modified liposomes equipped with a pH-sensitive fusogenic peptide: an artificial viral-like delivery system. Biochem 2004; 43:5618.

20. Cheung CI, et al. A pH-sensitive polymer that enhances cationic lipid-mediated gene transfer. Bioconjugate Chem 2001; 12:906.

21. Hanessian S, Roy R. Chemistry of spectinomycin: its total synthesis, stereocontrolled rearrangement, and analogs. Can J Chemistry 1985; 63:163.

22. Wang C, et al. Molecularly engineered poly(orthoester) microspheres for enhanced delivery of DNA vaccines. Nat Mater 2004; 3:190.
23. Zhu J, Munn RJ, Nantz MH. Self-cleaving ortho ester lipids: a new class of pH-vulnerable amphiphiles. J Am Chem Soc 2000; 122:2645.
24. Guo X, Szoka FC Jr. Steric stabilization of fusogenic liposomes by a low pH sensitive PEG diorthoester lipid conjugate. Bioconjugate Chem 2001; 12:291; Choi JS, MacKay JA, Szoka FC. Low-pH-sensitive PEG-stabilized plasmid-lipid nanoparticles: preparation and characterization. Bioconjugate Chem 2003; 14:420; Guo X Jr, MacKay JA, Szoka FC Jr. Mechanism of pH triggered collapse of phosphatidylethanolamine liposomes stabilized by an orthoester polyethyleneglycol lipid. Biophys J 2003; 84:1784.
25. Bessodes M, et al. Acid sensitive compounds for delivering drugs to the cells, US 60/239,116 October 2000. WO 02/20510. PCT Int Appl 2002:73.
26. Masson C, et al. pH sensitive PEG lipids containing orthoester linkers: new potential tools for nonviral gene delivery. J Control Release 2004; 99:423.
27. Ahmad M, et al. Ortho ester hydrolysis. The complete reaction mechanism. J Am Chem Soc 1977; 99:4827.
28. Yoshimori T, et al. Bafilomycin A1, a specific inhibitor of vacuolar-type H(+)-ATPase, inhibits acidification and protein degradation in lysosomes of cultured cells. J Biol Chem 1991; 266:17707.
29. Plank C, et al. Activation of the complement system by synthetic DNA complexes: a potential barrier for intravenous gene delivery. Hum Gene Ther 1996; 7:1437.
30. Dubos RJ. The microenvironment of inflammation of Metchnikoff revisited. Lancet 1955; 2:1; Edlow DW, Sheldon WH. The pH of inflammatory exudates. Proc Soc Exp Biol Med 1971; 137:1328; Gerweck LE. Tumor pH: implications for treatment and novel drug design. Seminars Radiat Oncol 1998; 8:176.
31. Masson C, Scherman D, Bessodes M. 2,2,6,6-tetramethyl-1-piperidinyl-oxyl/[bis(acetoxy)-iodo]benzene-mediated oxidation: a versatile and convenient route to poly(ethylene glycol) aldehyde or carboxylic acid derivatives. J Polym Sci Pol Chem 2001; 39:4022.
32. Shi F, et al. Interference of poly(ethylene glycol)-lipid analogs with cationic-lipid-mediated delivery of oligonucleotides; role of lipid exchangeability and non-lamellar transitions. Biochem J 2002; 366:333.
33. Rui Y, et al. Diplasmenylcholine-folate liposomes: an efficient vehicle for intra-cellular drug delivery. J Am Chem Soc 1998; 44:11213.
34. Boomer J, Thompson DH. Synthesis of acid-labile diplasmenyl lipids for drug and gene delivery applications. Chem Phys Lipids 1999; 99:145.
35. Boomer JA, Thompson DH, Sullivan SM. Formation of plasmid-based transfection complexes with an acid-labile cationic lipid: characterization of in vitro and in vivo gene transfer. Pharmaceut Res 2002; 19:1292.
36. Aissaoui A, et al. Novel cationic lipids incorporating an acid-sensitive acylhydrazone linker: synthesis and transfection properties J Med Chem 2004; 47:5210.
37. Schmidt SL. Toward a biochemical definition of the endosomal compartment. Sub-cell Biochem 1993; 19:1.

38. Boomer J, Thompson DH. Synthesis of acid-labile diplasmenyl lipids for drug and gene delivery applications. Chem Phys Lipids 1999; 99:145.
39. Boomer JA, et al. Acid-triggered release from sterically stabilized fusogenic liposomes via a hydrolytic dePEGylation strategy. Langmuir 2003; 19:6408.
40. Shin J, Shum P, Thompson DH. Acid-triggered release via dePEGylation of DOPE liposomes containing acid-labile vinyl ether PEG–lipids. J Control Release 2003; 91:187.
41. Bergstrand N, et al. Interactions between pH-sensitive liposomes and model membranes. Biophys Chem 2003; 104:361.

9

Bioresponsive Liposomes and Their Use for Macromolecular Delivery

Zhaohua Huang and Francis C. Szoka, Jr.

*Department of Biopharmaceutical Sciences, School of Pharmacy,
University of California, San Francisco, California, U.S.A.*

INTRODUCTION

A quarter century has passed since Yatvin et al. (1) suggested that low pH-sensitive liposomes (Scheme 1) might provide a means to preferentially localize drug release in a tumor. They made this suggestion based upon their insight that the pH in the tumor environment is 0.2 to 0.5 pH units more acidic than in the blood or in normal tissue. This novel suggestion was one of the earliest descriptions of a liposome that would change its properties in the presence of a discrete biological environment. Since then, advances in liposome technologies have solved many of the problems faced by the conventional liposomal carriers, such as the loading efficiency, contents retention, plasma stability, and circulation lifetime. These advances accelerated the transfer of liposome-encapsulated low-molecular-weight drugs from
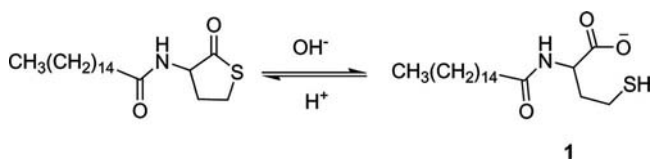
Scheme 1

the laboratory to the clinic (2). However, bioresponsive liposomes have not yet provided a clear advantage for the delivery of drugs, either low or high molecular weight, in animals. For instance, in vivo liposomal delivery of macromolecular therapeutics such as DNA, RNA, and proteins remains problematic; many groups believe success in this challenge requires more sophisticated systems, such as bioresponsive liposomes, to transfer these macromolecules across the subcellular barriers to reach their intracellular target site.

What is a bioresponsive liposome? We define a bioresponsive liposome as a liposome that will undergo a change of properties in a particular biologic environment. The trigger for this change is the presence of an enzyme, a pH difference, an ionic strength difference, a chemical substrate difference, or an ionic type difference in the target environment, as compared to the normal tissue. Upon accumulation in the target, the drug must be released at an effective level from the liposome, triggered by a specific stimulus. The most widely exploited bioresponsive approaches include pH-responsive, reduction-responsive, and enzymatic triggering. Numerous efforts have been devoted to the development of strategies to increase the liposome-mediated intracellular delivery of biologically active macromolecules (3), and in this application, it is the particular environment inside the cell that is important. For the in vivo application, an ideal liposome-encapsulated macromolecular drug should be stable in the circulation until it reaches the site of action.

Chemistry plays an important, if not critical, role in the engineering of novel bioresponsive lipids for the triggered release of macromolecular drugs. The following sections review the recent development of molecule-based bioresponsive liposome systems. There are several excellent reviews on pH-sensitive liposomes (4,5) that are triggered by a change in the physical properties on titration of the headgroup of the lipids they contain. These formulation-based pH-sensitive liposomes are not in the scope of this review.

pH-RESPONSIVE LIPOSOMES

Rationale of pH-Responsive Liposomes

The pH-responsive liposomes were initially designed to exploit the acidic environment of tumors (1,6). Unfortunately, the pH of the tumor interstitium rarely declines below pH 6.5 and the sites of the greatest acidity in the tumors are often far from the tumor microvasculature (7–9). However, the pH within endosomes is markedly lower than in the surrounding milieu, reaching 5.5 (10–12). Because most liposomes are internalized by the endocytic pathway, the concept of pH-responsive liposomes remains attractive. Theoretically, this strategy is applicable to any target that features a pH decrease. The ideal pH-responsive liposomes should be stable in the physiological pH (7.4) but undergo destabilization under acidic condition,

thus resulting in the release of their aqueous contents into the cytoplasm before degradation by the lysosomal enzymes.

Different classes of pH-triggered liposome destabilization have been reported in the literature based on different mechanisms (4,13). The novel molecule-based pH-responsive liposomes generally contain the bilayer-stabilizing pH-sensitive synthetic lipids. The acid-catalyzed hydrolysis of these lipids results in destabilizing detergents or conical lipids. The content release rate is tunable depending on the pH-sensitivity of cleavable linkages and the formulation of the liposomes. For the delivery of macromolecular therapeutics such as DNA, it is crucial to release the contents from the endosome to the cytosol before the contents traffic to the lysosomes where extensive enzymatic degradations occur.

Chemistry of pH-Responsive Lipids

The frameworks of the pH-responsive amphiphiles feature the pH-sensitive functionality in the desired location of the molecule. In general, these pH-sensitive functionalities include acetals, ketals, vinyl ethers, hydrazones, and ortho esters. Chemists can manipulate the lipid structure for the specific application by introducing different headgroups, lipid chains, linkers, and the linker configurations. However, past development of pH-responsive liposomes has focused principally on the area of formulation-based anionic liposomes. Recently, the development of molecule-based pH-responsive liposomes has gained considerable attention.

Two types of cleavable surfactants (Fig. 1) containing ketal linkage have been reported by Jaeger et al. (14,15). In the first generation of cleavable surfactants (*2–5*), the ketal linkage was placed between the major lipophilic and hydrophilic portions. The cleavage of the surfactant leads to nonsurfactant products: an ionic, water-soluble compound and a neutral, water-insoluble compound. The hydrolysis of the second-generation cleavable surfactant (*6,7*) results in another surfactant and a water-soluble neutral compound. The pH-sensitive ketal linkage was also used by Song and Hollingsworth in the design of a monoglucosyl diacylglycerol analog (*8*) (16).

In addition to the ionic ketal-linked surfactants, a series of pH-sensitive nonionic surfactants have been synthesized. Kuwamura and Takahashi first reported the acid-sensitive poly(ethylene glycol) monomethyl ether (mPEG)-based acetals (Fig. 2) (17,18). These noncyclic acetal-linked cleavable surfactants (*9*) were synthesized by condensation of aldehydes with mPEG. Other similar acetals were reported by Sokolowski and Burczyk (19–21). Later, Yue et al. synthesized a series of similar mPEG acetals with relatively longer mPEG and aliphatic chains (22). Another series of cyclic ketal–linked mPEG-lipid conjugates (*10*) have also been reported as pH-degradable non-ionic surfactants (23).

Thompson et al. have reported a number of pH-sensitive lipids using vinyl ether linkage (Fig. 3). Total syntheses have been developed for both
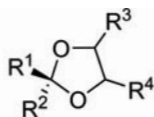
2 $R^1 = C_{17}H_{35}$, $R^2 = CH_3$, $R^3 = H$, $R^4 = CH_2N^+Me_3Br^-$
3 $R^1 = (CH_2)_3N^+Me_3Br^-$, $R^2 = CH_3$, $R^3 = R^4 = C_{16}H_{33}$
4 $R^1 = R^2 = C_{17}H_{35}$, $R^3 = H$, $R^4 = CH_2N^+Me_3Br^-$
5 $R^1 = R^2 = C_{17}H_{35}$, $R^3 = H$, $R^4 = CH_2O(CH_2)_3SO_3^-Na^+$
6 $R^1 = R^2 = CH_3$, $R^3 = (CH_2)_7CH_3$, $R^4 = (CH_2)_8N^+Me_3Br^-$
7 $R^1 = R^2 = CH_3$, $R^3 = (CH_2)_7CH_3$, $R^4 = (CH_2)_8SO_3^-Na^+$
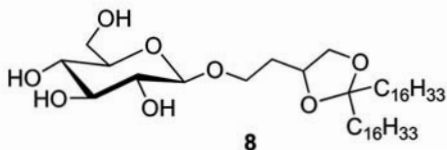
Figure 1 Ketal-based pH-sensitive surfactants.

plasmenylcholine (*11*) and diplasmenylcholine (*12*) (24,25). The pH-res
function of these lipids comes from the vinyl ether linkage at either 1-
or both 1- and 2-positions of the glycerol bridge. Replacement
phosphocholine headgroup with mPEG gave an mPEG-diplasmen
conjugate (*13*) that was used to investigate the dePEGylation tri
Four structurally related, mPEG-conjugated vinyl ether lipids (*14–*
been developed by the same group to further study the acid-t
release via a strategy of dePEGylation of 1,2-dioleoyl-*sn*-gl
phosphatidylethanolamine (DOPE) liposomes (26).

Hydrazone was frequently used as an acid-sensitive linkage
conjugate of small molecules to the polymer carriers. Recently, four
steroid derivatives (Fig. 4) were introduced by Aissaoui et al. (2
guanidinium-based headgroup was connected to the steroid tail th
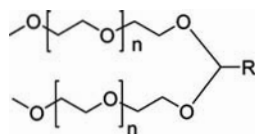
9 $n = 1 - 12$
$R = (CH_2)_mCH_3$, $m = 1 - 10$
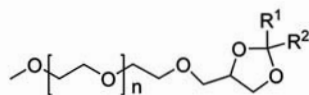
10 $R^1 = (CH_2)_{12}CH_3$, $R^2 = CH_2CH_3$, $n = 6 - 7$

Figure 2 Ketal-based pH-sensitive mPEG-lipid conjugates.
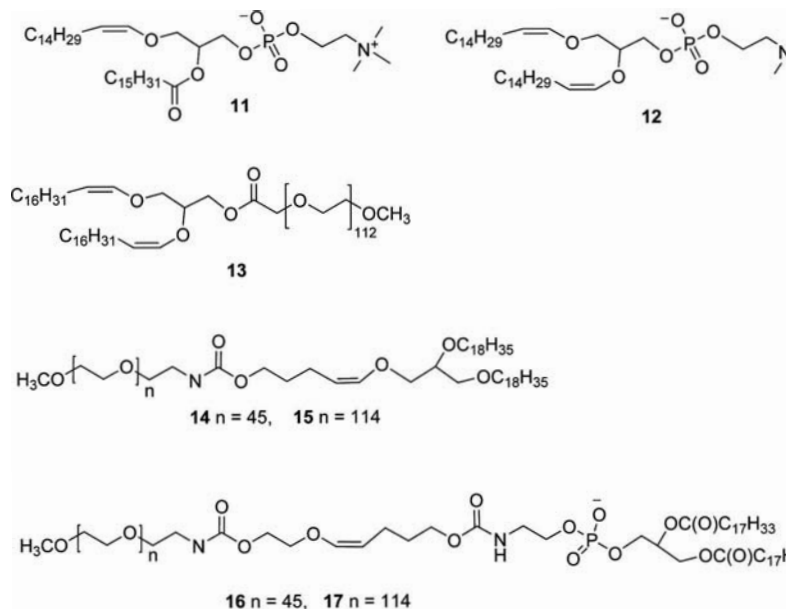
Figure 3 Vinyl ether-based pH-sensitive lipids.

pH-sensitive acylhydrazone linkage. The use of these lipids for gene [...] has also been reported.

Compared with acetal, ketal, and hydrazone, ortho esters are [...] the most acid-sensitive functional groups in the literature (28). Wh[...] pH sensitivity is desired, the incorporation of ortho ester functio[...] target molecule may greatly facilitate the acid-triggered release of t[...] tents. Poly(ortho ester)s have been extensively studied by Heller e[...] application in controlled drug delivery (29). But the use of ortho est[...] pH-responsive lipids is a recent development.

Hellberg et al. prepared a class of mixtures (Fig. 5) of ortho es[...] factant (22) by heating a mixture of short-chain ortho ester, a fatty [...] and the mPEG in certain ratios (30,31). Similarly, they prepared the [...] ortho ester surfactant (23) (32). Zhu et al. have synthesized two pH-s[...] cationic lipids (Scheme 2) based on ortho ester linkage featuring [...] trioxabicyclo(2.2.2) octane ring (33). Later, Nantz and coworkers c[...] another class of highly pH-sensitive amphiphiles: dioxazociniu[...] esters (Scheme 3) (34). Our group has developed a convenient [...] synthesis of mPEG-ortho ester-lipid conjugate (POD) (Scheme 4) (3[...] method was further optimized and applied to the synthesis of POD v[...] ferent PEG chain length or unsaturated lipid (36). Recently, Mass[...] reported a new class of mPEG-ortho ester-lipid conjugates (Scheme [...] the monocyclic ortho ester linkage (37). In addition to the single a[...]
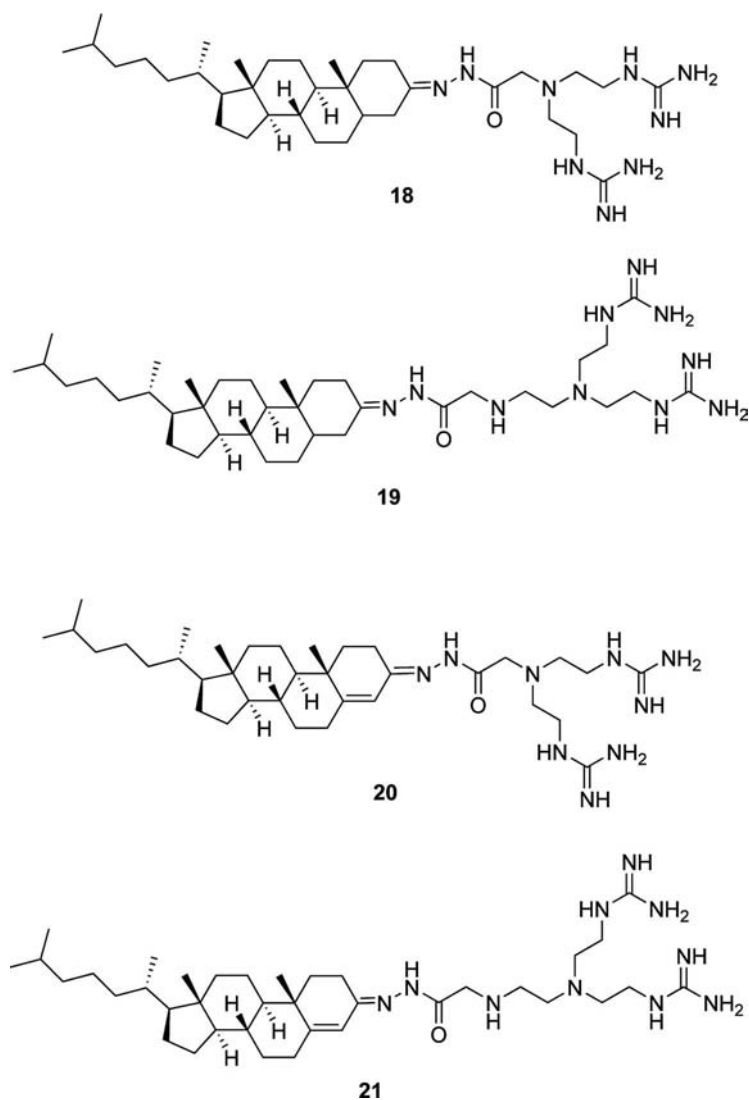
Figure 4 Acylhydrazone-based pH-sensitive cationic steroids.

chain, cholesterol was incorporated as the hydrophobic tail in the ortho ester lipids.

Hydrolysis of pH-Responsive Liposomes

The mechanism and catalysis for hydrolysis of acetals, ketals, and ortho esters are discussed in detail in an outstanding review (28). The general

$x = 0\text{-}3$, $y = 0\text{-}3$, $z = 0\text{-}3$, $x+y+z = 3$
$m = 7$ or 9, $n = 8$, 12, or 16

$x = 0\text{-}3$, $y = 0\text{-}3$, $z = 0\text{-}3$, $x+y+z = 3$
$R = $ 2-ethylhexyl, $n\text{-}C_{8\text{-}16}$
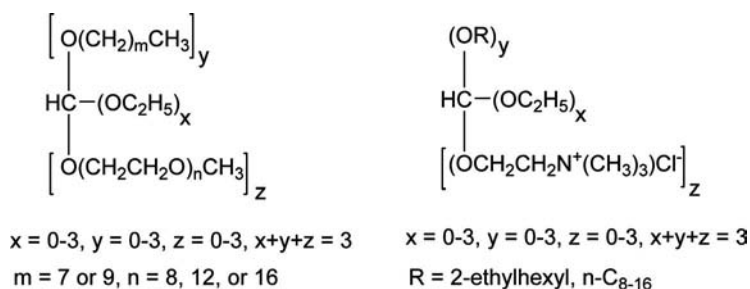
22

23

Figure 5 Mixtures of pH-sensitive orthoester surfactants.

mechanisms of hydrolysis of acetals, ketals, ortho esters, and related substrates are illustrated in Scheme 6. The hydrolysis of pH-responsive liposomes is affected by many factors such as the type of linkages, the substituent groups, pH, temperature, and the assembly of liposomes. It is difficult to point out a general rate-determining step for this complicated system. But the data of the apparent kinetics of hydrolysis of different pH-responsive liposomes will help us develop a more sophisticated system for the delivery of macromolecular drugs in future.

In the above-mentioned systems, it is generally observed that the rate of hydrolysis of acetals, ketals, vinyl ethers, and acylhydrazones is much slower than that of ortho esters. For in vivo macromolecular delivery, the pH-responsive liposomes should be carefully devised and tailored so that they are sensitive enough to the decrease of the pH in the pathological sites or endosomes. The biological active macromolecules should be able to

Scheme 2

Scheme 3 (chemical reaction scheme):

$^-OSO_3CH_3$

$\xrightarrow[\text{MeOH}]{\text{Dowex 550-OH}}$ $\xrightarrow{CH_3I}$ $\xrightarrow[\text{cat. HBF}_4]{\text{ROH}}$ OR

R= $CH_3(CH_2)_{12}CH_2$ or $\begin{matrix} CH_3(CH_2)_{12}(X)O- \\ CH_3(CH_2)_{12}(X)O- \end{matrix}$ or $\begin{matrix} CH_3(CH_2)_{12}(O)O-(CH_2 \\ CH_3(CH_2)_{12}(O)O- \end{matrix}$

26

27: X = O
28: X = H, H

29: n = 1
30: n = 4

$OC_{14}H_{29}$

$26 \xrightarrow[H_2O]{H^+}$ and / or A → $+ C_{14}H_{29}OAc$

B

C →

$+$ $C_{14}H_{29}OH$
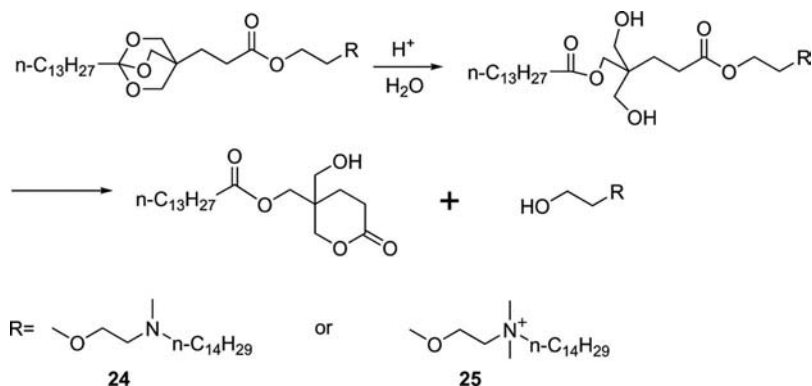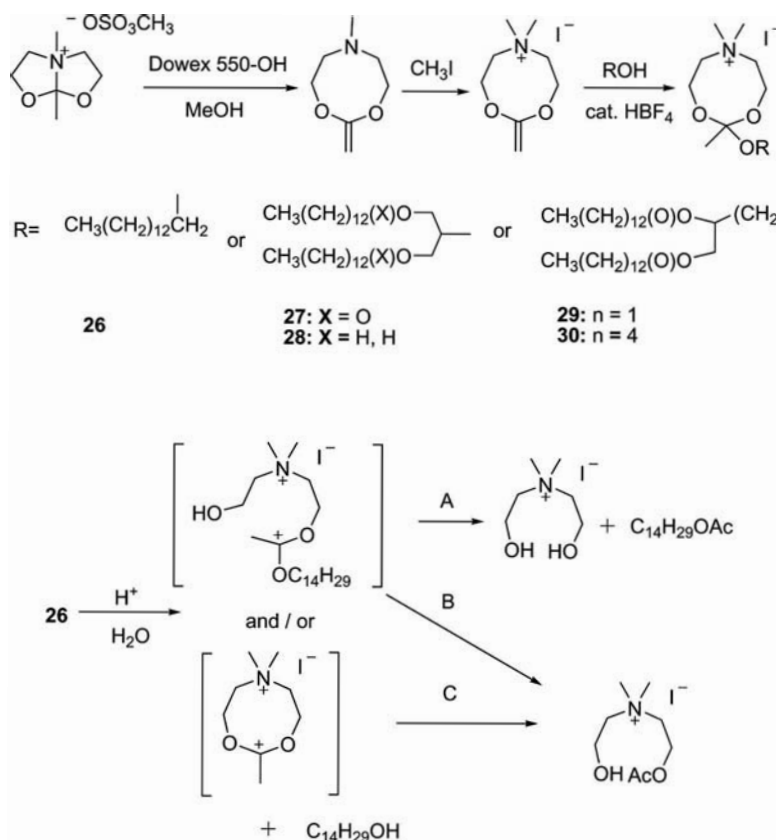
Scheme 3

escape from the endosome within 30 minutes before they get degrade
lysosome. Thus, high pH sensitivity is crucial for a successful pH-res
liposome system. Most of the acetal or ketal amphiphiles mentione
were designed for the degradable surfactants. Thus, the relati
hydrolysis of these systems may still facilitate their application. For t
ether–based systems, the hydrolysis is generally slow (hours scale) a
and requires much lower pH to achieve faster hydrolysis. The acylhyd
linked lipids showed a relatively slow rate of hydrolysis under m
conditions (days scale). The mixed ortho esters are stable at pH
degraded significantly at mild acidic pH. But these lipids have not y
purified and incorporated into the lipid vesicles.

The hydrolysis and self-cleavage of the ortho ester lipids 24
(Scheme 2) were complete within 12 hours at pH 4.5. The complete c
of the molecule was controlled by the last step, the slow hydrolysi

Scheme 4

R= $C_{17}H_{35}$, n = 45; **32** R= $C_{17}H_{35}$, n = 17;
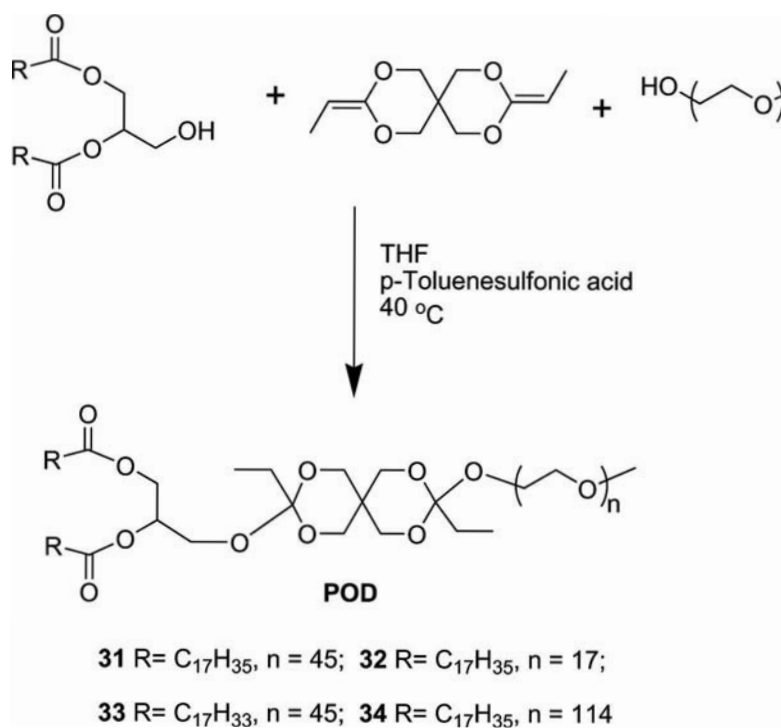
33 R= $C_{17}H_{33}$, n = 45; **34** R= $C_{17}H_{35}$, n = 114

ester bond. This cleavage pattern makes the bilayer destabilization t
for the release of macromolecular drugs from the early endoson
newly developed dioxazocinium ortho esters (Scheme 3, *26–30*) hyc
much faster than *24* and *25*. As evidenced by gas chromatography
mass spectrometry (MS), route A is the major hydrolysis pattern
results in the direct separation of the cationic headgroup with the hyc
bic tail. The rate of hydrolysis of *26* is faster than that of other
lipids. It is completely hydrolyzed at pH 5.0 within six hours ($t_{\frac{1}{2}} = 1$
utes). Substituent effect also influences the rate of hydrolysis. Lipids
and *29* were only partially hydrolyzed in a pH 5.0 buffer for si
at 38°C (approximately 10–50%). Among the double-chain lip
hydrolysis of *27* is the slowest, whereas that of *28* is the fastest. These
demonstrate that the pH sensitivity of the ortho ester lipids is
through subtle structure differences. However, the pH sensitivity
pure ortho ester liposomes is still not fast enough for a timely release
tents from early endosomes. It remains to be seen if the incorpora
these dioxazocinium lipids in a carefully formulated liposome can
rapid content release in mild acidic condition.
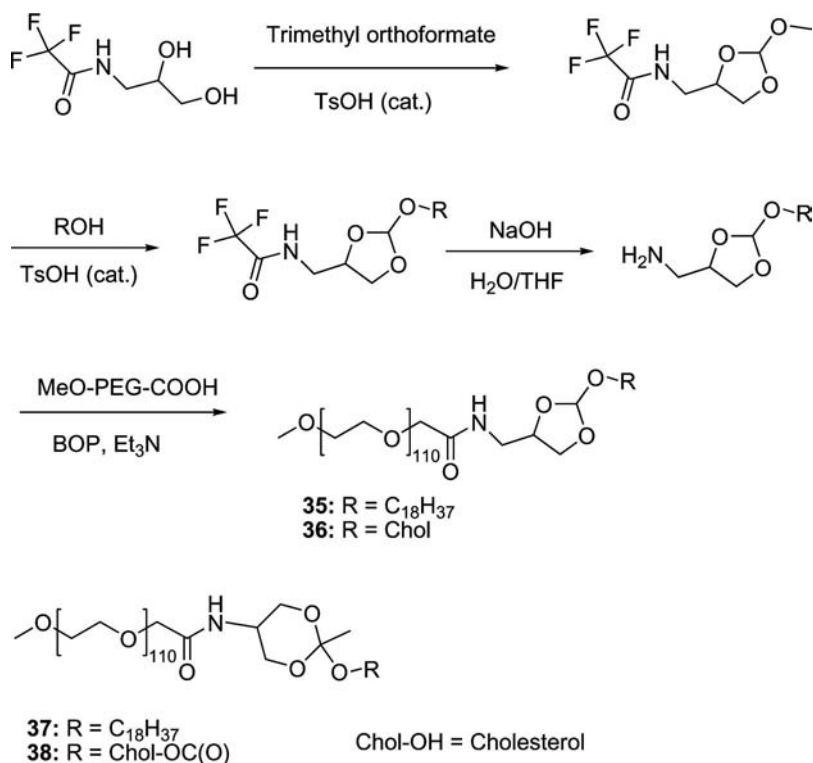
Scheme 5

The acid sensitivity of poly(ethylene glycol)-diortho ester-distearoyl glycol conjugate (POD) was first roughly estimated by thin-layer chromatography analysis and then followed by a fluorescence study. POD was stable at pH 7.4 for more than 10 hours according to the liposome aggregation study. In the acid-triggered content leakage assay, POD/DOPE (1/9) liposomes showed a lag phase of 12 hours at pH 7.4, 60 minutes at pH 6.0, and less than five minutes at pH 5.0. A minimum-surface-shielding model has been established by our group to describe the kinetics of the pH-triggered release of POD/PE liposomes (38). When acid-catalyzed hydrolysis lowers the mole percentage of POD on the liposome surface to a critical level, intervesicular lipid mixing is initiated, resulting in a burst of contents release. The burst phase occurs when the surface density of POD is 2.3 ± 0.6 mol%. These content release data are based on the POD with mPEG2000 (compound *31*). Similar pH-dependent data were observed on other PODs (Scheme 4: *32, 33*, and *34*) (39). The content leakage of POD is also dependent on the mPEG chain length of the conjugate and the initial mole percentage

Hydrolysis of acetals or ketals

Hydrolysis of ortho esters

Hydrolysis of vinyl ethers
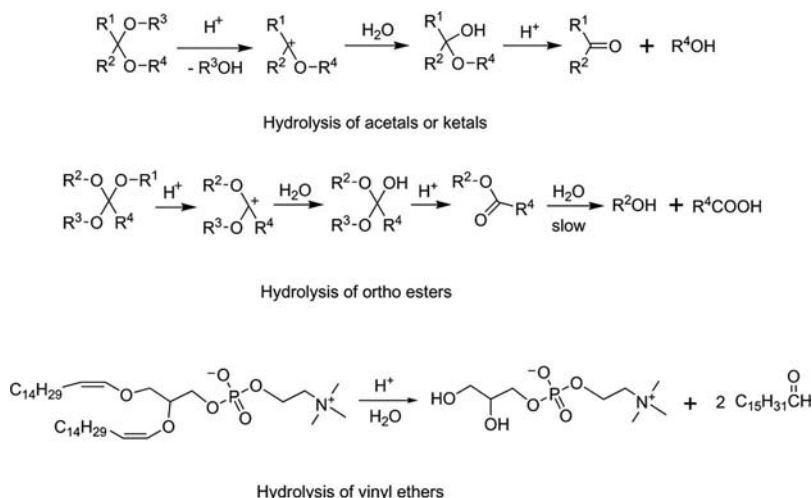
Scheme 6

of the POD in the POD/PE formulation. At pH 6.0, the POD/PE liposomes burst at this order: *34 > 32 > 31*. For compound *32* at pH 6.0, faster burst was observed with less initial percentage of *32* in the liposome. These observations and theoretical calculations provide us a versatile tool to tailor the POD liposomes for the pH-responsive release of the macromolecular drugs at a desired rate.

The recently reported compounds *35–38* (Scheme 5) are a variation of POD featuring a single cyclic ortho ester ring. Another distinct difference is that mPEG is conjugated through an amide linkage to the ring in contrast to the direct ortho ester linkage of the POD. This may have an effect on the hydrolysis behavior of *35–38* because the mPEG is cleaved from the ortho ester more easily as evidenced by electrospray ion trap mass spectrometry (ESI MS) (36). It was reported that the methyl-substituted six-membered cyclic ortho esters (*37,38*) were more acid labile than the five-membered cyclic ortho esters (*35,36*) (34). This may be explained by the fact that the intermediate carbonium was better stabilized by the electron-donating methyl group in compound *37* or *38*. Compound *38* was found to be the most pH-sensitive lipid of this class ($t_{\frac{1}{2}} < 3$ at pH 4.0, and $t_{\frac{1}{2}} = 20$ minutes at pH 5.0). The addition of this class of pH-sensitive lipids to the library of ortho ester lipids gives us more choices for the formulation of pH-responsive liposomes.

pH-Responsive Liposomes for Gene Delivery

Despite numerous pH-sensitive amphiphiles in the literature, only a few of these lipids have been formulated into the pH-responsive liposomes for

macromolecular drug delivery. Due to the low pH sensitivity, the acetal-, ketal-, or vinyl ether–based acid-labile amphiphiles have not been success-fully formulated into pH-sensitive liposomes for gene delivery. The less pH-sensitive acylhydrazone-linked guanidinium cationic lipids (Fig. 4, *18–21*) were evaluated for their transfection ability (27). Compound *20*/DOPE showed the highest activity among the four new lipids. Compared with the non-cleavable analog, *20* is less active for both the nuclear expression and the early cytoplasmic expression. In spite of these observations, the authors believed that the hydrazone vector may make use of specific mechanisms to overcome the barriers encountered. Based on the hydrolysis and transfection results, one may conclude that compound *20* transfects cells like a conventional catio-nic lipid rather than a pH-responsive liposome. If the acylhydrazone does have some contribution to the transfection ability of *20*, it could be other mechanisms.

In the transfection of national institute of health (NIH) 3T3 cells with luciferase plasmid, formulation *25*/DOPE (1/1) was claimed to be 10-fold more active than 1,2-dioleoyl-3-trimethylammonium-propane (DOTAP) and 3β-[N-(N′,N′-Dimethylaminoethane)-carbamol] (DC) Cholesterol, formula-tions. It was proposed that the detergent-like hydrolysis product of *25* may facilitate the release of DNA from the endosome to the cytoplasm. No detailed results or further experiments were reported on the transfection ability of *25* or its analogs.

Cationic lipoplexes bearing pH-responsive lipids *35, 36*, or *37* have been tested in vitro and compared with lipoplexes bearing the stable analogs (37). In the absence of serum, the lipoplexes without PEG-lipid showed high transfection activity. When coated with stable PEG-lipids (e.g., 10% Brij or 20% Chol-PEG), the level of transfection was significantly reduced by factors of 30 and 300, respectively. The incorporation of pH-responsive PEG lipids *36* or *37* increased the transfection activity by a factor of 10 and 25, respec-tively, as compared to the corresponding non–pH-sensitive formulations. Among the three pH-responsive lipoplexes, the highest level of transfection was obtained with *37*, which was one of the most pH-sensitive molecules. Unfortunately, lipoplexes containing the most pH-sensitive lipid *38* have not been tested for transfection. Additional experiments on the formula-tion and transfection of these pH-responsive lipids may help develop a pH-responsive vector for the in vivo study.

Among all those reported pH-sensitive lipids, PODs (Scheme 4, *31–34*) have been carefully characterized and extensively studied for their applica-tion in gene delivery (35,36,38–40). Compound *31* was used with a cationic lipid-phosphatidylethanolamine mixture to prepare pH-responsive stabilized plasmid-lipid nanoparticles [POD stabilized plasmid-lipid nanoparticles (SPLP)] that could mediate gene transfer in vitro by a pH-triggered escape from the endosome. DNA was encapsulated in the POD SPLP at a ratio of around 13 mol% in the presence of 20% *31* at pH 8.5 using a detergent

dialysis method. Low pH sensitivity of the POD SPLP was characterized by a lag phase followed by a rapid burst. At pH 5.3, the POD SPLP collapsed in 100 minutes. Both the POD SPLP and pH-insensitive SPLP were internalized into cultured cells within two hours of incubation at a qualitatively similar pattern. POD SPLP showed up to three orders of magnitude greater gene transfer activity than the pH-insensitive SPLP. These results suggest that the pH-responsive POD SPLP may be a useful component of synthetic vector for in vivo gene therapy.

The use of POD for gene delivery was further studied and optimized by our group. A series of POD lipids (*31–34*) were incorporated into DNA-containing nanolipoparticles (NLPs) or model liposomes as a stealth and bioresponsive component. An optimized detergent dialysis method was developed to encapsulate plasmid DNA into NLPs prepared from a mixture of various POD lipids, cationic lipid, and phosphatidylethanolamine lipid. A critical concentration (28 mM) of *n*-octyl-β-D-glucopyranoside enabled high encapsulation of DNA plasmid into 100-nm particles with a neutral surface charge. The POD NLPs are stable at pH 8.5 but rapidly collapse (10 minutes) into aggregates at pH 5.0. The transfection activity of NLPs was in the following order: *32* > *34* = *31* > pH-insensitive NLP. The particle size stability was in the reverse order. The POD NLPs showed slightly less transfection activity but considerably lower cytotoxicity than the polyethylenimine (PEI)-DNA polyplexes. In summary, the pH-responsive lipid *31* is the better choice for the preparation of pH-responsive NLPs with a small particle diameter, good stability, low cytotoxicity, and satisfactory transfection activity.

REDUCTION-RESPONSIVE LIPOSOMES

Rationale of Reduction-Responsive Liposomes

Gene transfer is revealed to be a long journey with many barriers to be overcome. One important step is the escape of DNA from the endosome. We have proposed a mechanism of DNA endosome release from cationic liposomes, which may account for the partial release of DNA into the cytoplasm (41,42). When cells were treated with double-labeled fluorescent lipoplexes, some of the oligonucleotides (ODNs) were able to escape from the endosome and enter the nucleus, but left a significant amount of ODNs that remained associated with the cationic lipids. Hence, an additional mechanism is required for unpacking DNA from the complex to enhance the gene transfer.

A disulfide bond (–S–S–) is a covalent linkage formed by the oxidation of the two sulfhydryl (–SH) groups of thiol compounds. It can also be reversibly cleaved in the presence of reducing reagents such as dithiothreitol (DTT), β-mercaptoethanol, and reduced glutathione (GSH). The reversibility and the relative stability in plasma make disulfide an appealing bioresponsive linkage. The use of a disulfide bond as the cleavable linkage for bioresponsive gene

delivery in vitro relies on the high redox potential difference between the oxidizing extracellular space and the reducing intracellular milieu (43). The rationale is that the cationic functional group would be stable in the extracellular matrix but cleaved from the lipid anchor in the reductive milieu in the cytoplasm. The cleavage of the cationic moiety from the lipid would release the charge-condensed DNA from the lipoplexes, so that the DNA could migrate toward the nucleus. Hence, the use of reduction-responsive cationic lipids may facilitate the release of the gene from the carrier into the cytoplasm.

Chemistry of Reduction-Responsive Lipids

In the synthesis of reduction-responsive lipids, there are generally three strategies being used to introduce the disulfide bond: autoxidation of thiols via air, tethering through a disulfide-containing building block, and disulfide exchange. The synthesis of well-defined asymmetrical disulfide compounds are generally achieved by the disulfide exchange method using an activating reagent such as 2,2'-pyridyl disulfide. Compared with tethering method, the disulfide exchange method introduces the disulfide bond directly between two functional moieties of the target molecule, avoiding the introduction of unnecessary atoms from the building block.

Using dithiobis(succinimidyl propionate) as the tethering molecule, Kirpotin et al. synthesized a thiolytically cleavable mPEG-1,2-distearyl-sn-glycero-3-phosphatidylethanolamine (DSPE) conjugate (Fig. 6) (44). This is the first example of cleavable PEG-lipid (*39*) used for the formulation of sterically stabilized liposomes. Later, Zalipsky et al. modified this conjugate
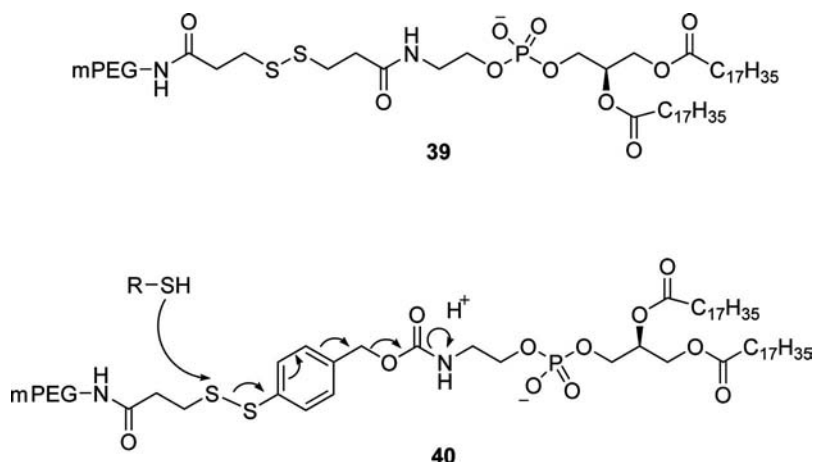
Figure 6 Thiolytically cleavable mPEG-DSPE conjugate.
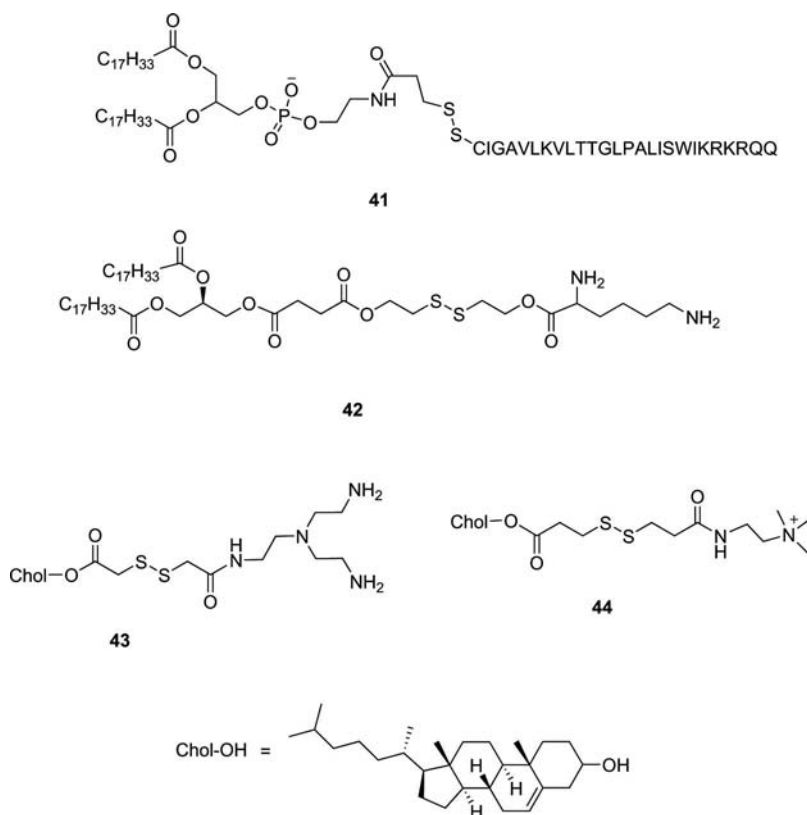
Figure 7 Reduction-sensitive lipids.

by replacing the 3,3'-dithiopropionate linkage with the dithiobenzyl urethane linkage (*40*) (45). Thiolytic decomposition of benzyl urethane–linked drugs containing aromatic disulfides in the para or ortho positions has been utilized by Senter et al. as a basis for an elegant prodrug strategy (46). With this strategy, thiolysis of conjugate *40* can regenerate the natural lipid DSPE, while the mPEG chain is removed. The disulfide linkage (Fig. 7) was first introduced into the cationic lipids by Legendre et al. (47) for the synthesis of dioleoylmelittin (*41*). Using different tethering molecules, Hughes and Tang initially synthesized one (dioleoyl glycerol)-based disulfide conjugate (*42*) (48), and then two cholesterol-based reducible cationic lipids (*43,44*) (49,50).

Our group has devised a class of base-responsive cationic detergents (51) that contain a quaternary amine group and a cleavable isothiuronium headgroup (*45*, Scheme 7). The isothiuronium group can be cleaved in a controlled manner under basic conditions, generating a thiol group that can be autoxidized later to form disulfide-linked gemini cationic lipids. In addition
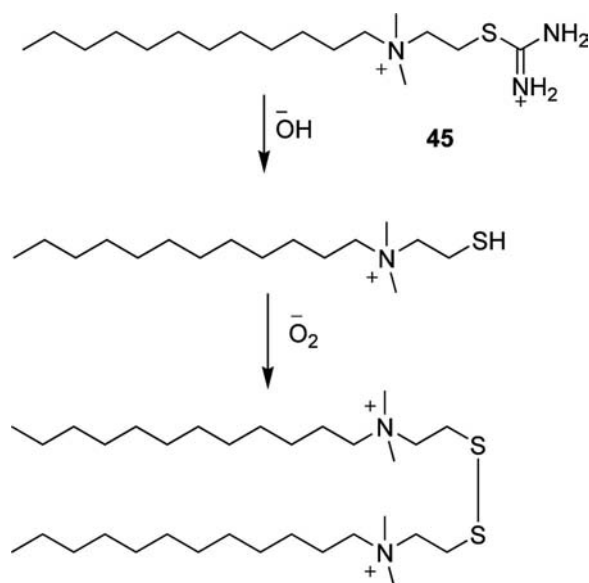
Scheme 7

to the isothiuronium-masked cationic detergent, lipoic acid–derived cationic amphiphiles (*46*, Fig. 8) were introduced by Balakirev et al. (52). The completely reduced compound *46* can be oxidized to either the intramolecular disulfide *48* or the polymer *47*. Dauty et al. have reported a series of thiol
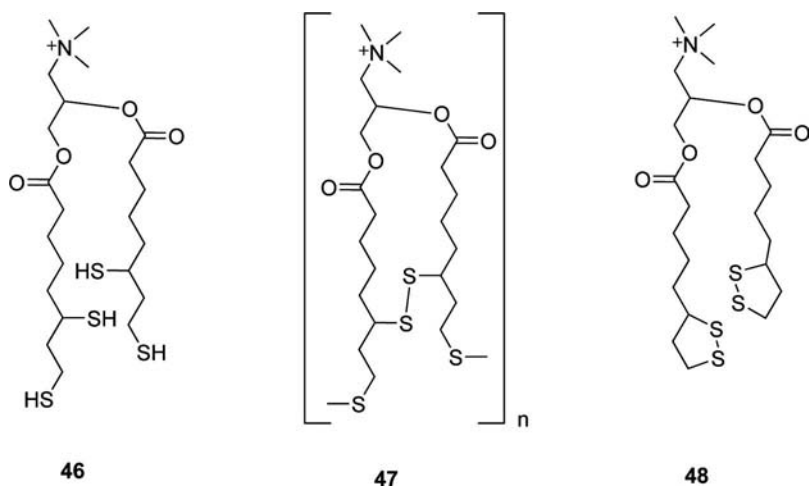
Figure 8 Lipoic acid-derived cationic amphiphiles.
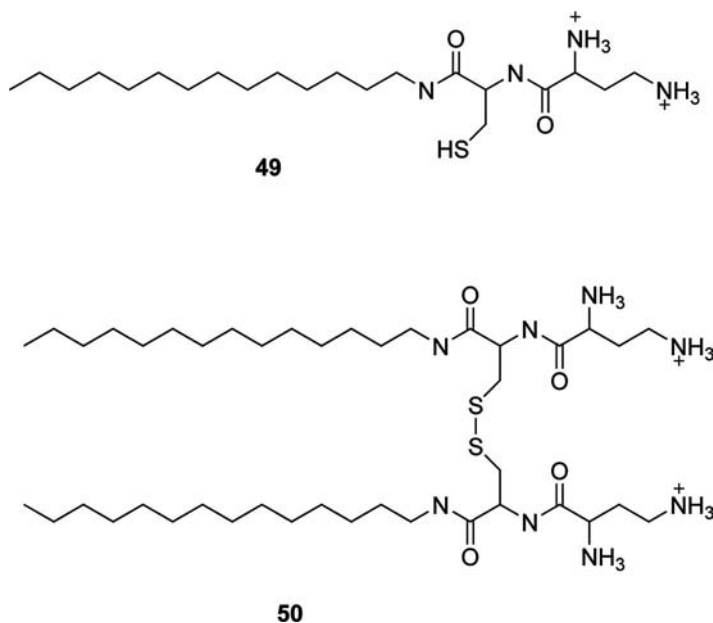
Figure 9 Thiol cationic detergents.

cationic detergents (53–55) (Fig. 9) with various chain lengths (C_{12}–C_{16}) and headgroups (ornithine or spermine). The dimer (*50*) was formed by autoxidation of the monomer (*49*). Byk and coworkers have synthesized a series of reduction-sensitive lipopolyamines (56,57) such as compound *51–54* (Fig. 10). The disulfide bond was placed at different location of the lipopolyamines by using various disulfide building blocks. The nonreducible lipopolyamines (*55–57*) were also synthesized as the control compounds.

Recently, we have devised a series of thiocholesterol-based cationic lipids (TCL) (Scheme 8) for ordered assembly of bioresponsive gene carriers (58). Thiocholesterol was first activated with 2,2'-dipyridyl disulfide. The exchange of 2-thiopyridine with *N*,*N*-dimethylaminoethyl thiol gave the key intermediate *58*. Lipids *59, 60*, and *61* were obtained by the modification of the headgroup of *58* with corresponding reagents. The synthesis is straightforward and can be easily applied to the synthesis of similar compounds with different headgroups.

Physiochemical Properties of Reduction-Responsive Lipids

Although all the reduction-responsive lipids featured a reducible disulfide bond, their structural differences showed significant influence on the physiochemical properties of these molecules. For example, the first generation of detachable mPEG-DSPE (Fig. 6, *39*) is linked through 3,3'-dithiopropionate.

Figure 10 Reduction-sensitive lipopolyamines.
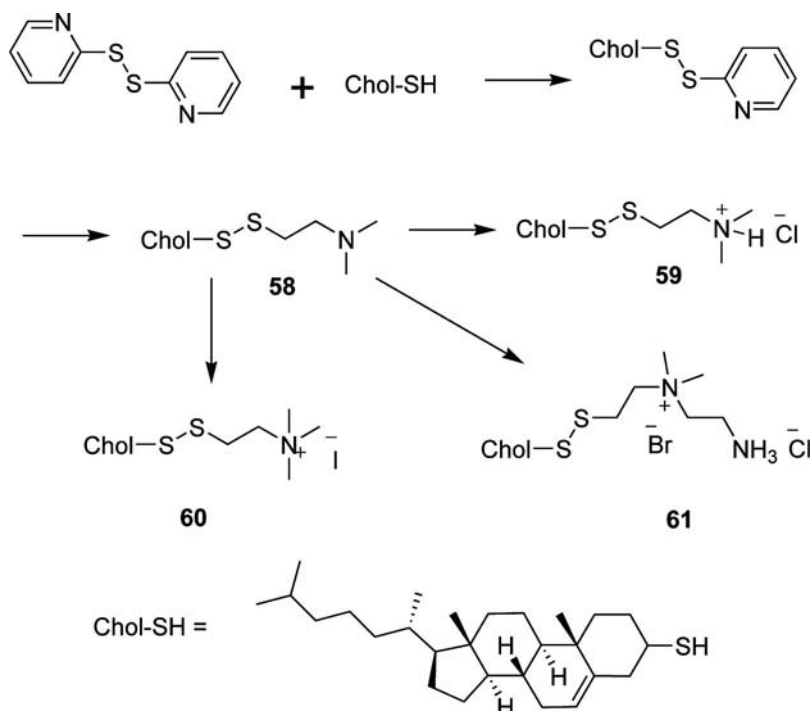
Scheme 8

Consequently, the cleavage of mPEG from the liposomes required a relatively potent thiolytic reagent, DTT, which is unacceptable for in vivo use. The introduction of the dithiobenzyl urethane linkage into the second generation of detachable mPEG-DSPE (*40*) enabled the cleavage with much mild cysteine. Similarly, compound *42* (Fig. 7) was only partially reduced by DTT and could not be reduced by GSH. On the contrary, compound *43* was successfully reduced by GSH. The disulfide bond may be weakened by the strong electron-withdrawing effect of the adjacent carbonyl groups, which makes the reduction easier.

The dimerizable thiol cationic detergents were designed for the template-assisted assembly of plasmid DNA. Ideally, this class of detergents should have a high enough critical micelle concentration (CMC) for condensing DNA at a relatively high concentration without obvious aggregation, and a very low CMC upon oxidation for the stabilization of the complex. Significant decrease of CMC upon dimerization or polymerization was generally observed in the thiol cationic detergents. For example, the CMC of *46* (1 mM) was dramatically reduced after oxidation, 0.5 µM for *47* and 1 µM for *48* (Fig. 8). The CMC for the isothiuronium detergent *45* was 10 mM, 0.21 mM for the thiol

detergent, and 0.047 mM for the disulfide. The CMC of the detergents was also affected by the aliphatic chain length and the headgroup. The CMC of isothiuronium detergents or the corresponding thiol detergents and disulfide lipids decreased as the alkyl chain length increased from 8 to 12. The same trend was observed in the CMCs of compound *49* (Fig. 9) and its analogs, and for a given hydrophobic tail, CMC increased with the headgroup polarity.

The reduction of disulfide in the lipopolyamines (Fig. 10, *51–54*) by DTT was studied by high-performance liquid chromatography. Lipids bearing disulfide bonds in the hydrophilic environment (*51,52*) were reduced within one minute of the addition of DTT. In contrast, lipids bearing disulfide bonds in the alkyl chain (*53,54*) were cleaved more slowly. These lipids were all able to condense DNA at given charge ratios. With the treatment of DTT, DNA can be released from the lipoplexes of *51* and *54*, but not from the reducible lipids *52* and *53*. This is because the reduction products of *52* and *53* still have the ability to complex DNA. However, it was not reported whether these lipids were able to be reduced by the milder reducing reagents such as cysteine and glutathione (GSH).

All the TCL (*59–61*) can be incorporated into liposomes and used to package DNA into lipoplexes, thereby protecting it from DNase digestion. The TCL lipoplexes were readily dissociated in the presence of DTT, as well as by other reducing agents such as GSH and 2-mercaptoethanol even at concentrations as low as 0.2 mM. GSH is the most abundant nonprotein thiol source in mammalian cells, and its intracellular concentration is in the millimolar range. This concentration is sufficient to rapidly reduce TCL and release DNA from the lipoplexes delivered into the cytosol. The headgroups of TCL influence the hydration of their liposome formulation. For example, *61*/DOPE was hydrated easily at room temperature. On the contrary, the complete hydration of *60*/DOPE was achieved at about 70°C.

Application of Reduction-Responsive Lipids for Gene Delivery

Most of the reduction-responsive lipids/DNA complexes were tested for their transfection ability toward a variety of cell lines. The luciferase transfection activity of dioleoylmelittin (*41*)/DNA complex was 5- to 500-fold higher than that of classical nonreducible lipoplexes, depending on the cationic lipid and cell line. But the role of the disulfide linkage was not clear. The transfection efficiency of lipid *42* and its nondisulfide analog were compared in neuronal, astroglial, and microglial cultures from newborn rat cerebral cortex. Lipid *42* was more efficient at transfecting each type of brain cell than were the nondisulfide analog and DOTAP liposomes. But the application of lipid *42* for gene transfer was limited by its low stability, relatively high toxicity, and strong reducing condition requirement. Later, Hughes and Tang introduced two cholesterol-based reduction-responsive lipids: *43* and *44*. The liposomes containing *43* had more than two orders of magnitude greater transfection

activity than the nonreducible lipid DC-Chol in Chinese Hamster Ovary (CHO) cells and seven times greater transfection activity in Human Neuroblastoma (SKnSHs) cells. Lipid *43* also demonstrated much less toxicity than the other two lipids. In the transfection experiments of *44*, DC-chol, and the nonreducible analog of *44*, it was found that 1,2-dioleoyl glycero-3-phosphatidylcholine (DOPC) proved to be a superior helper lipid than DOPE in CHO, but not in SKnSH cells. These results implied that other intracellular events, such as trafficking, might play a significant role in the enhancement of transgene expression by DOPC in CHO cells.

Using the isothiuronium detergent *45*, a 6-kg base pair plasmid DNA can be compacted into a 40-nm particle at a DNA concentration of 0.3 mg/mL. This DNA–surfactant complex was well tolerated by Normal African Green Monkey Kidney Fibrolast cells (CV-1) cells and exhibited detectable but not low transfection activity. High transfection activity was achieved when the complex was combined with a reagent that increased its association with cells.

The transfection activity of lipoic acid–derived lipids was assessed in different cell types [Hela, A549, and Baby Hamster Kidney Fibroblast Cells (BHK)] using different plasmids (pSV-lacZ, pGL3-luc, and pCMV-luc). Irrespective of the nature of either reporter gene or cell type, lipid *47* showed a 2- to 3-fold enhancement in transfection than that of DOTAP, whereas *48* was less efficient and no expression was observed for *46*. Further studies indicated that GSH- and nicotinamide adenine dinucleotide phosphate dehydrogenase-dependent reduction of lipoplexes of *47* inside cells resulted in the release of free DNA and increased the transfection activity. Because lipoic acid is a naturally occurring provitamin and relatively nontoxic, these types of lipids may be useful for nonviral gene delivery.

Lipid *50* can condense DNA very efficiently, forming a small complex (30 nm) with a tubular phase. In contrast, the C_{10} analog can only form the amorphous phase with plasmid, which may result in no transfection. These lipids were tested on 3T3 murine fibroblasts at charge ratio ($\pm$) *3–5*; the transfection activity increased in the order $C_{12} << C_{14} < C_{16}$. The in vitro luciferase expression of *50* was 2- to 10-fold less than that of PEI. Lipid *50* was later used for targeted gene delivery with folic acid as targeting ligand.

Lipoplexes formulated with the asymmetric reduction-sensitive lipids *52* and *53* showed up to a 1000-fold higher transfection activity in HeLa cells compared to complexes of the nonreducible lipids *57*. The symmetric reduction-sensitive lipid *51* showed no transfection activity when complexed alone with plasmid. However, when transfected with lipoplexes of *51*/DOPE (1/1), the gene expression level was significantly increased. Thus, additional attention should be paid to the formulation when we evaluate new lipids for gene transfer.

The recently reported TCL (*59–61*) showed encouraging transfection activity when formulated with 50 mol% DOPE. The transfection activities
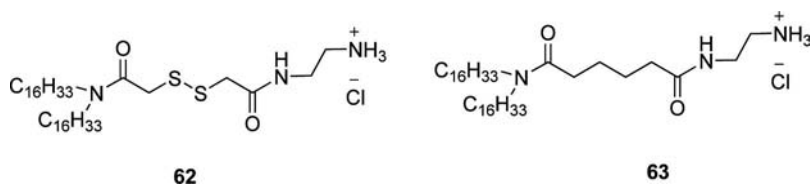
Figure 11   Reducible and nonreducible lipids.

of TCL were comparable to what can be achieved by using potent polycation PEI or typical nonreducible cationic lipid DOTAP. At the higher charge ratios, transfection activity of TCL is higher than that of the positive controls (PEI or DOTAP). Fluorescence microscopic images of cells transfected with 1,1′-dioctadecyl-3,3,3′,3′-tetramethylindocarbocyanine   perchlorate–labeled TCL/green fluorescent protein (GFP) plasmid complexes showed that most of the cells took up the lipoplex and about 15% to 20% expressed GFP at charge ratio 4/1 (±). Different headgroups did not influence the transfection activity significantly.

Although superior transfection activity was generally found for the reduction-responsive lipids compared with the corresponding nonreducible cationic lipids, there are exceptions. Kumar and Chaudhuri reported a disulfide-containing cationic lipid *62* and its highly similar nonreducible analog *63* (Fig. 11) (59). Both lipids can condense DNA at given charge ratios, and the lipoplexes of *62* were able to release DNA upon reduction. Surprisingly, the control nonreducible lipid *63* showed phenomenally superior transfection activity to its disulfide analog *62* in all the three cell lines tested [CHO, Transformed (Simian Virus 40) African Green Monkey Kidney Fibroblast Cells (COS-1), and Human Breast Cancer Cell (MCF-7)]. It was found that the lipoplexes of *62* were unable to protect the DNA from DNase digestion, which may account for the inability of transfection of *62*. This observation reminds that the disulfide linkage can only facilitate the intracellular release of DNA, which is just one of several barriers to gene delivery. Thus, in the design of an ideal reduction-responsive cationic lipid, one should consider all barriers to gene delivery: condensation and protection of DNA, cell entry, endosome escape, and intracellular release. It will be very difficult, if not impossible, to incorporate ways to overcome all barriers in just one molecule.

ENZYME-RESPONSIVE LIPOSOMES

A relatively new approach to bioresponsive liposomes is enzyme-activated release of drugs from liposomes (60). Like other bioresponsive liposomes, enzyme-responsive liposomes are stable before reaching the target site and become leaky upon activation by specific enzymes. This can be achieved through the careful design of the liposomes based on a variety of triggering mechanisms. (i) The fusogenic liposomes are stabilized by the masking lipids

such as PEG-lipids. The enzymatic cleavage of the masking lipids re
the fusion of the liposomes. (ii) The enzymatic cleavage of the lipid
ates the fusogenic lipids directly. (iii) The enzyme or functional
incorporated into the liposomes induces the leakage upon activatio
given conditions such as low pH or reducing milieu.

Elastase-responsive liposomes have been designed by Meers
workers for triggered release (61–63). Elevated extracellular activity i
under inflammatory conditions in diseases such as cystic fibrosis (64
matoid arthritis (65), and emphysema (66). Elastase has specifi
uncharged amino acid side chains, particularly small runs of alanine c
(67). The fusogenic lipid DOPE was coupled to a simple dipeptide se
N-acetylated alanyl alanine, resulting in the negatively charged nonfu
conjugate N-Ac-alanylalanine (AA)-DOPE (Scheme 9). The clea
N-Ac-AA-DOPE by elastase can generate the fusogenic DOPE, lea
liposomal fusion. A similar lipid N-methoxysuccinylanlanylalanylpro
DOPE [methoxy (MeO)-suc-AAPV-DOPE] was much more specifica
rapidly cleaved by elastase. The formulation of MeO-suc-AAPV
and the pH-dependent cationic lipid DODAP at 1:1 ratio made the
more sensitive in the low-pH endosome where the overall charge w
positive upon the elastase-activated cleavage of MeO-suc-AAPV-
The dePEGylation strategy could be also achieved through liposome
lized by the PEG-lipids linked via protease-sensitive peptides. H
more efforts are needed to carefully tune the system to be sensitive
The elastase-responsive liposomes may be formulated for trigger
delivery, although no detailed data has been reported yet.

N-Ac-AA-DOPE

enzymatic cleavage

DOPE

Scheme 9

64 R = CH$_2$CH$_2$
65 R = CH$_2$(CH$_2$)$_4$CH$_2$
66 R = CH$_2$CH$_2$OCH$_2$CH$_2$
67 R = CH$_2$CH$_2$OCH$_2$CH$_2$OCH$_2$CH$_2$

Figure 12 Cholesterol derivatives sensitive to alkaline phosphatase.

Our group has designed and synthesized a series of cholester phate derivatives (68) (Fig. 12) that are sensitive to alkaline phos which is known to be elevated in many diseases such as cancer (cholesterol C2 phosphate (64)/DOPE liposome was the most sens among all the cholesterol derivatives. This liposome was also sen the acid-phosphatase and collapsed in the presence of calcium. L plasmid DNA was encapsulated into the negatively charged liposom a modified Reverse Phase Evaporation Vesicle (REV) methodolo transfection was mediated by calcium for certain formulations, b transfection mechanisms played a role in the less calcium-sensitive terol triethylene phosphate 67/DOPE formulations. The role of pho in the transfection has not been resolved yet.

The aforementioned disulfide-containing lipids can also be t by the corresponding cytosol enzymes. For example, the 47/DNA can be rapidly reduced by the mammalian thioredoxin reductase (52 ing in the DNA release. Other reduction-sensitive lipids may also be by certain reductases in the cell. Saito et al. (70) reported the use of lysin O (LLO), an SH-activated pore-forming protein, for pr plasmid DNA delivery into the cytosol of cells in culture. LLO wa gated to polycationic peptide protamine (PN) at a 1:1 molar ratio disulfide bond at the site of cysteine 484. Condensed PN/pDNA co incorporating LLO-s-s-PN were tested for their gene delivery capa HEK293, RAW264.7, and P388D1 cell lines and bone marrow macrophages in the presence of serum. Dramatic enhancement was for all tested complexes with varying weight ratios. This is a good of the use of functional enzyme or protein for the triggered release although it is based on the PN.

The use of enzyme-responsive systems for drug and gene has also been demonstrated with other enzymes such as sphingon (71), phospholipase C (72), phospholipase A$_2$ (73,74), and α-hemoly Although the development of enzyme-responsive liposomes is st early stage, this strategy has shown some advantages such as high sp and has potential for future application. A practical bioresponsive l

drug delivery system may be achieved with an appropriate enzyme and liposome formulation.

MULTIFUNCTIONAL BIORESPONSIVE LIPOSOMES (ARTIFICIAL VIRUSES)

Towards Artificial Virus

The challenge of nonviral gene delivery was proven to be much higher than it was initially expected. There are too many barriers to be overcome by a simple monofunctional synthetic vector for the efficient transfer and stable expression of gene in the target tissues. Viral vectors, as another approach, are able to accomplish the efficient transfection by exploiting the invasive properties of viruses. However, over millions of years of evolution, viruses developed the invasion ability for their propagation, not for the safe transfection of the host tissues. On the other hand, the human immune system has evolved to prevent the viral invasion. Thus, the use of viral vectors may result in unpredictable toxicities to the patients. In contrast, the synthetic vectors are generally less toxic and less expensive, yet less efficient. In many instances, the stunning results are often achieved by mimicking the art of nature. Efficient gene transfer could be achieved by the so-called "artificial virus," the multifunctional bioresponsive synthetic vector mimicking virus.

The ideal artificial virus should be able to overcome all those barriers faced by gene transfer: DNA condensation, membrane crossing, endosome escape, and nucleus entry. For the systematic administration, the vector should also be able to circulate long enough in the blood without degradation to reach the target. Despite the huge challenges, the development of pH-responsive liposomes and reduction-responsive liposomes is bringing us continually closer to constructing an artificial virus capable of delivering macromolecular drugs to defined cells in vivo. A better artificial virus may be obtained by the combination of these functionalities and the incorporation of the targeting ligand, cytosol motor protein, and nuclear location sequence in the vector through an appropriate assembling method. There are some good reviews on the artificial viruses (76,77). Here, we only discuss recent examples of multifunctional bioresponsive liposomes.

Sequential Assembly of Artificial Virus

Synthetic vectors formed by mixing cationic lipids with plasmid directly generally have relatively large diameters and are not suitable for in vivo application. To emulate virus, the particle of the complex should be formulated small enough (<120 nm) and should be stable under physiologic conditions. The formation of artificial virus requires more complicated formulation procedure than the preparation of lipoplexes, such as the use of dimerizable

cationic detergents for template-assisted assembly or the detergent
method to encapsulate DNA within liposomes. The incorporation
lipid in the formulation can greatly stabilize the vector formed an
longer circulation time in the blood. However, the presence of the P
on the vector significantly reduces their binding to target cells and the
fection activity. The use of pH-sensitive PEG-lipid such as POD (38
partially restore the transfection activity of the vector. A straight
approach to enhance the specific cell-binding ability of the vector is th
ment of the targeting ligand directly on the vector surface. A wide v.
targeting ligands could be used for enhanced gene delivery, such a
clonal antibody, oligosaccharide, peptide, and folate.

Zuber et al. reported a stepwise assembly of nanometric DN.
cles using the dimerizable cationic detergent 49 (Fig. 9) as an
component (78). DNA was first condensed with an equimolar
amount of cationic detergent 49, which was autoxidized to the d
upon exposure to air overnight. The template-assisted formation
gemini lipid 50 significantly stabilized the complex. The particle
was further coated with a folate-PEG envelope through a strong
minor-groove-binding reagent prepared from distamycin and I
33258. This multifunctional vector showed cell recognition proper
could be efficiently internalized by the target cells. However, in c
to the classical cationic lipids, the folate-PEG–coated vectors only
poor transfection activity. If the PEG envelope is not removed in end
it may prevent DNA release. The DNA-minor-groove-binding reage
to attach the folate-PEG envelope may also impair the expression of t
This model has demonstrated the possibility of stepwise assemb
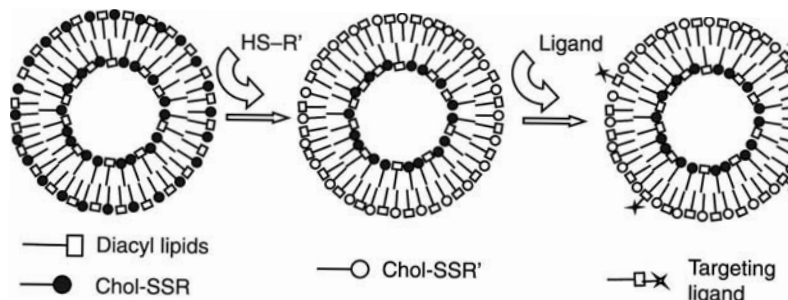
Figure 13 Sequential assembly of the artificial virus. First, DNA was encap
into the nanosized cationic liposome by the dialysis method. Then the parti
face was modified by disulfide exchange with the reducing agent HS–R'.
the targeting ligand was incorporated onto the surface of the particle either
micelle transfer method or through disulfide exchange. *Abbreviations*: SSR, c
linked R group; HS, trinol group.

multifunctional DNA-containing nanoparticle. Further work is needed to tune the system for efficient gene transfer.

Based on the detergent dialysis (79,80) and micelle transfer methods (81), we have developed a unique method for the sequential assembly of DNA-containing multifunctional bioresponsive liposomes with tunable surface attribute (58). The idea is to first make a nanosized cationic particle stabilized by a PEG lipid and then to alter the surface charge of the particle using a disulfide exchange reaction (Fig. 13). The targeting ligand can be introduced either by disulfide exchange or through micelle transfer. Using this tactic, one can create a particle with a neutral, zwitterionic, or nonionic surface. It is not surprising that the transfection activities of NLPs made by this method were much less than those of corresponding lipoplexes because the incorporation of stable PEG-lipid significantly reduced the cell-binding of NLP. The introduction of a cell-binding ligand *trans*-activating transcriptional activator protien-PEG-lipid on the NLP substantially enhanced the transfection at very low DNA concentration. The gene transfer efficiency may be further improved by replacing the stable PEG-lipid with the pH-sensitive PEG-lipid POD in the NLP. Based on this model, an efficient artificial virus could be made by careful integration of multiple functionalities into the NLP.

CONCLUSION

Bioresponsive liposomes were originally designed to enhance local delivery of drugs to tumors but, in the past decade, they have been proposed as components to solve problems faced in the delivery of DNA and other nucleic acid drugs such as siRNA. Enhanced gene delivery remains a potential for such systems and has not yet been achieved using most of the bioresponsive liposomes. Undoubtedly, future advances in the bioresponsive liposomes will bring us closer to the ideal artificial virus. Whether or not such systems ever are more than a laboratory curiosity remains to be seen. The systems could be too complicated to assemble and store if all of the strategies used by virus are incorporated into the artificial virus. Moreover, as the complexity of the components increases, a successfully assembled artificial virus may become immunogenic. The breakthrough of such technology will depend on the development and interaction of several scientific areas such as material chemistry, nanotechnology, and bioengineering. A better understanding of the function of the viral proteins involved in the process of viral gene transfer should also help improve the current bioresponsive liposomes. After all, liposomes have only been around for 40 years (82); with a few more years of development, perhaps the components and assembly methodologies will be suitable for preparing a modestly efficient gene delivery vector.

ACKNOWLEDGMENTS

REFERENCES

1. Yatvin MB, Kreutz W, Horwitz BA, Shinitzky M. pH-Sensitive liposomes—possible clinical implications. Science 1980; 210(4475):1253–1254.
2. Drummond DC, Meyer O, Hong KL, Kirpotin DB, Papahadjopoulos D. Optimizing liposomes for delivery of chemotherapeutic agents to solid tumors. Pharmacol Rev 1999; 51(4):691–743.
3. Guo X, Szoka FC. Chemical approaches to triggerable lipid vesicles for drug and gene delivery. Accounts Chem Res 2003; 36(5):335–341.
4. Drummond DC, Zignani M, Leroux J. Current status of pH-sensitive liposomes in drug delivery. Prog Lipid Res 2000; 39(5):409–460.
5. Simoes S, Moreira JN, Fonseca C, Duzgunes N, de Lima MC. On the formulation of pH-sensitive liposomes with long circulation times. Adv Drug Deliv Rev 2004; 56(7):947–965.
6. Andresen TL, Jensen SS, Jorgensen K. Advanced strategies in liposomal cancer therapy: problems and prospects of active and tumor specific drug release. Prog Lipid Res 2005; 44(1):68–97.
7. Helmlinger G, Yuan F, Dellian M, Jain RK. Interstitial pH and pO_2 gradients in solid tumors in vivo: high-resolution measurements reveal a lack of correlation. Nat Med 1997; 3(2):177–182.
8. Dellian M, Helmlinger G, Yuan F, Jain RK. Fluorescence ratio imaging of interstitial pH in solid tumours: effect of glucose on spatial and temporal gradients. Br J Cancer 1996; 74(8):1206–1215.
9. Huang SK, Lee KD, Hong K, Friend DS, Papahadjopoulos D. Microscopic localization of sterically stabilized liposomes in colon carcinoma-bearing mice. Cancer Res 1992; 52(19):5135–5143.
10. Ohkuma S, Poole B. Fluorescence probe measurement of the intralysosomal pH in living cells and the perturbation of pH by various agents. Proc Natl Acad Sci USA 1978; 75(7):3327–3331.
11. Tycko B, Maxfield FR. Rapid acidification of endocytic vesicles containing alpha 2-macroglobulin. Cell 1982; 28(3):643–651.
12. Daleke DL, Hong K, Papahadjopoulos D. Endocytosis of liposomes by macrophages: binding, acidification and leakage of liposomes monitored by a new fluorescence assay. Biochim Biophys Acta 1990; 1024(2):352–366.
13. Gerasimov OV, Boomer JA, Qualls MM, Thompson DH. Cytosolic drug delivery using pH- and light-sensitive liposomes. Adv Drug Deliv Rev 1999; 38(3):317–338.
14. Jaeger DA, Li B, Clark T. Cleavable double-chain surfactants with one cationic and one anionic head group that form vesicles. Langmuir 1996; 12(18):4314–4316.

15. Jaeger DA. Cleavable surfactants. Supramol Chem 1995; 5(1):27–30.
16. Song J, Hollingsworth RI. Synthesis, conformational analysis, and phase characterization of a versatile self-assembling monoglucosyl diacylglycerol analog. J Am Chem Soc 1999; 121(9):1851–1861.
17. Kuwamura T, Takahash H. Structural effects on properties of nonionic surfactants. 1. Synthesis and some surface-activities of acetal type homogeneous nonionics. Bull Chem Soc Japan 1972; 45(2):617–622.
18. Takahash H, Kuwamura T. Structural effects on properties of nonionic surfactants. 2. Acetal type homogeneous nonionics having polyoxyethylene chains terminated with methoxyl group. Bull Chem Soc Japan 1973; 46(2):623–626.
19. Sokolowski A, Burczyk B. Acetals and ethers. 5. Kinetics of hydrolysis of acetals formed from aliphatic-aldehydes and mono-alkyl ethers of ethylene glycols. Polish J Chem 1979; 53(10):1995–2002.
20. Sokolowski A, Burczyk B. Acetals and ethers. 4. Synthesis of acetals from aliphatic-aldehydes and mono-alkyl ethers of ethylene glycols. Polish J Chem 1979; 53(4):905–912.
21. Burczyk B, Sokolowski A. Cleavable surfactants derived from poly(ethylene glycol) monomethyl ether. J Am Oil Chem Soc 1997; 74(7):895–895.
22. Yue CY, Harris JM, Hellberg PE, Bergstrom K. Synthesis and characterization of cleavable surfactants derived from poly(ethylene glycol) monomethyl ether. J Am Oil Chem Soc 1996; 73(7):841–845.
23. Iyer M, Hayes DG, Harris JM. Synthesis of pH-degradable nonionic surfactants and their applications in microemulsions. Langmuir 2001; 17(22):6816–6821.
24. Thompson DH, Gerasimov OV, Wheeler JJ, Rui YJ, Anderson VC. Triggerable plasmalogen liposomes: improvement of system efficiency. Biochim Biophys Acta-Biomembr 1996; 1279(1):25–34.
25. Kim JM, Shin J, Shum P, Thompson DH. Acid- and oxidatively-labile vinyl ether surfactants: synthesis and drug delivery applications. J Disper Sci Tech 2001; 22(5):399–407.
26. Shin J, Shum P, Thompson DH. Acid-triggered release via dePEGylation of DOPE liposomes containing acid-labile vinyl ether PEG-lipids. J Control Release 2003; 91(1–2):187–200.
27. Aissaoui A, Martin B, Kan E, et al. Novel cationic lipids incorporating an acid-sensitive acylhydrazone linker: synthesis and transfection properties. J Med Chem 2004; 47(21):5210–5223.
28. Cordes EH, Bull HG. Mechanism and catalysis for hydrolysis of acetals, ketals, and ortho-esters. Chem Rev 1974; 74(5):581–603.
29. Heller J, Barr J, Ng SY, Abdellauoi KS, Gurny R. Poly(ortho esters): synthesis, characterization, properties and uses. Adv Drug Deliv Rev 2002; 54(7):1015–1039.
30. Hellberg PE, Bergstrom K, Holmberg K. Cleavable surfactants. J Surf Deterg 2000; 3(1):81–91.
31. Hellberg PE, Bergstrom K, Juberg M. Nonionic cleavable ortho ester surfactants. J Surf Deterg 2000; 3(3):369–379.
32. Hellberg PE. Ortho ester-based cleavable cationic surfactants. J Surf Deterg 2002; 5(3):217–227.
33. Zhu J, Munn RJ, Nantz MH. Self-cleaving ortho ester lipids: a new class of pH-vulnerable amphiphiles. J Am Chem Soc 2000; 122(11):2645–2646.

34. By K, Nantz MH. Dioxazocinium ortho esters: a class of highly pH-vulnerable amphiphiles. Angewandte Chem 2004; 43(9):1117–1120.
35. Guo X, Szoka FC. Steric stabilization of fusogenic liposomes by a low-pH sensitive PEG-diortho ester-lipid conjugate. Bioconjug Chem 2001; 12(2): 291–300.
36. Guo X, Huang Z, Szoka FC. Improved preparation of PEG-diortho ester-diacyl glycerol conjugates. Methods Enzymol 2004; 387:147–152.
37. Masson C, Garinot M, Mignet N, et al. pH-sensitive PEG lipids containing orthoester linkers: new potential tools for nonviral gene delivery. J Control Release 2004; 99(3):423–434.
38. Guo X, MacKay JA, Szoka FC. Mechanism of pH-triggered collapse of phosphatidylethanolamine liposomes stabilized by an ortho ester polyethyleneglycol lipid. Biophys J 2003; 84(3):1784–1795.
39. Li W, Huang Z, MacKay JA, Grube S, Szoka FC Jr. Low-pH-sensitive poly(ethylene glycol) (PEG)-stabilized plasmid nanolipoparticles: effects of PEG chain length, lipid composition and assembly conditions on gene delivery. J Gene Med 2005; 7(1):67–79.
40. Choi JS, MacKay JA, Szoka FC. Low-pH-sensitive PEG-stabilized plasmid-lipid nanoparticles: preparation and characterization. Bioconjug. Chem 2003; 14(2):420–429.
41. Xu Y, Szoka FC Jr. Mechanism of DNA release from cationic liposome/DNA complexes used in cell transfection. Biochemistry 1996; 35(18):5616–5623.
42. Zelphati O, Szoka FC Jr. Mechanism of oligonucleotide release from cationic liposomes. Proc Natl Acad Sci USA 1996; 93(21):11493–11498.
43. Saito G, Swanson JA, Lee KD. Drug delivery strategy utilizing conjugation via reversible disulfide linkages: role and site of cellular reducing activities. Adv Drug Deliver Rev 2003; 55(2):199–215.
44. Kirpotin D, Hong KL, Mullah N, Papahadjopoulos D, Zalipsky S. Liposomes with detachable polymer coating: destabilization and fusion of dioleoylphosphatidylethanolamine vesicles triggered by cleavage of surface-grafted poly (ethylene glycol). FEBS Lett 1996; 388(2–3):115–118.
45. Zalipsky S, Qazen M, Walker JA, Mullah N, Quinn YP, Huang SK. New detachable poly(ethylene glycol) conjugates: cysteine-cleavable lipopolymers regenerating natural phospholipid, diacyl phosphatidylethanolamine. Bioconjug Chem 1999; 10(5):703–707.
46. Senter PD, Pearce WE, Greenfield RS. Development of a drug-release strategy based on the reductive fragmentation of benzyl carbamate disulfides. J Org Chem 1990; 55(9):2975–2978.
47. Legendre JY, Trzeciak A, Bohrmann B, Deuschle U, Kitas E, Supersaxo A. Dioleoylmelittin as a novel serum-insensitive reagent for efficient transfection of mammalian cells. Bioconjug Chem 1997; 8(1):57–63.
48. Tang FX, Hughes JA. Introduction of a disulfide bond into a cationic lipid enhances transgene expression of plasmid DNA. Biochem Bioph Res Commun 1998; 242(1):141–145.
49. Tang FX, Hughes JA. Use of dithiodiglycolic acid as a tether for cationic lipids decreases the cytotoxicity and increases transgene expression of plasmid DNA in vitro. Bioconjug Chem 1999; 10(5):791–796.

50. Tang F, Hughes JA. Synthesis and evaluation of a quaternary amino disulfide cationic lipid in plasmid DNA delivery. Stp Pharma Sci 2001; 11(1):83–90.
51. Ouyang M, Remy JS, Szoka FC. Controlled template-assisted assembly of plasmid DNA into nanometric particles with high DNA concentration. Bioconjug Chem 2000; 11(1):104–112.
52. Balakirev M, Schoehn G, Chroboczek J. Lipoic acid-derived amphiphiles for redox-controlled DNA delivery. Chem Biol 2000; 7(10):813–819.
53. Dauty E, Remy JS, Blessing T, Behr JP. Dimerizable cationic detergents with a low cmc condense plasmid DNA into nanometric particles and transfect cells in culture. J Am Chem Soc 2001; 123(38):9227–9234.
54. Dauty E, Behr JP, Remy JS. Development of plasmid and oligonucleotide nanometric particles. Gene Ther 2002; 9(11):743–748.
55. Dauty E, Behr JP. Monomolecular condensation of DNA by cationic detergents. Polym Int 2003; 52(4):459–464.
56. Wetzer B, Byk G, Frederic M, et al. Reducible cationic lipids for gene transfer. Biochem J 2001; 356(Pt 3):747–756.
57. Byk G, Wetzer B, Frederic M, et al. Reduction-sensitive lipopolyamines as a novel nonviral gene delivery system for modulated release of DNA with improved transgene expression. J Med Chem 2000; 43(23):4377–4387.
58. Huang Z, Li W, Mackay JA, Szoka FC Jr. Thiocholesterol-based lipids for ordered assembly of bioresponsive gene carriers. Mol Ther 2005; 11(3): 409–417.
59. Kumar VV, Chaudhuri A. On the disulfide-linker strategy for designing efficacious cationic transfection lipids: an unexpected transfection profile. Febs Letters 2004; 571(1–3):205–211.
60. Meers P. Enzyme-activated targeting of liposomes. Adv Drug Deliv Rev 2001; 53(3):265–272.
61. Pak CC, Erukulla RK, Ahl PL, Janoff AS, Meers P. Elastase activated liposomal delivery to nucleated cells. Biochim Biophys Acta-Biomembr 1999; 1419(2): 111–126.
62. Pak CC, Ali S, Janoff AS, Meers P. Triggerable liposomal fusion by enzyme cleavage of a novel peptide-lipid conjugate. Biochimi Biophys Acta-Biomembr 1998; 1372(1):13–27.
63. Ahl PL, Bhatia SK, Meers P, et al. Enhancement of the in vivo circulation lifetime of L-alpha-distearoylphosphatidylcholine liposomes: importance of liposomal aggregation versus complement opsonization. Biochim Biophys Acta-Biomembr 1997; 1329(2):370–382.
64. Berger M, Sorensen RU, Tosi MF, Dearborn DG, Doring G. Complement receptor expression on neutrophils at an inflammatory site, the pseudomonas-infected lung in cystic fibrosis. J Clin Invest 1989; 84(4):1302–1313.
65. Al-Haik N, Lewis DA, Struthers G. Neutral protease, collagenase and elastase activities in synovial fluids from arthritic patients. Agents Actions 1984; 15(3–4): 436–442.
66. Damiano VV, Tsang A, Kucich U, et al. Immunolocalization of elastase in human emphysematous lungs. J Clin Invest 1986; 78(2):482–493.
67. Powers JC, Gupton BF, Harley AD, Nishino, N, Whitley RJ. Specificity of porcine pancreatic elastase, human leukocyte elastase and cathepsi G

inhibition with peptide chloromethyl ketones. Biochim Biophys Acta 1977; 485(1):156–166.

68. Davis SC, Szoka FC Jr. Cholesterol phosphate derivatives: synthesis and incorporation into a phosphatase and calcium-sensitive triggered release liposome. Bioconjug Chem 1998; 9(6):783–792.

69. Millan JL, Fishman WH. Biology of human alkaline phosphatases with special reference to cancer. Crit Rev Clin Lab Sci 1995; 32(1):1–39.

70. Saito G, Amidon GL, Lee KD. Enhanced cytosolic delivery of plasmid DNA by a sulfhydryl-activatable listeriolysin O/protamine conjugate utilizing cellular reducing potential. Gene Ther 2003; 10(1):72–83.

71. Ruiz-Arguello MB, Basanez G, Goni FM, Alonso A. Different effects of enzyme-generated ceramides and diacylglycerols in phospholipid membrane fusion and leakage. J Biol Chem 1996; 271(43):26616–26621.

72. Basanez G, Fidelio GD, Goni FM, Maggio B, Alonso A. Dual inhibitory effect of gangliosides on phospholipase C-promoted fusion of lipidic vesicles. Biochemistry 1996; 35(23):7506–7513.

73. Cohen S, Alonso MJ, Langer R. Novel approaches to controlled-release antigen delivery. Int J Technol Assess Health Care 1994; 10(1):121–130.

74. Davidsen J, Jorgensen K, Andresen TL, Mouritsen OG. Secreted phospholipase A(2) as a new enzymatic trigger mechanism for localised liposomal drug release and absorption in diseased tissue. Biochim Biophys Acta 2003; 1609(1):95–101.

75. Panchal RG, Cusack E, Cheley S, Bayley H. Tumor protease-activated, pore-forming toxins from a combinatorial library. Nat Biotechnol 1996; 14(7):852–856.

76. Demeneix B, Hassani Z, Behr JP. Towards multifunctional synthetic vectors. Curr Gene Ther 2004; 4(4):445–455.

77. Zuber G, Dauty E, Nothisen M, Belguise P, Behr JP. Towards synthetic viruses. Adv Drug Deliv Rev 2001; 52(3):245–253.

78. Zuber G, Zammut-Italiano L, Dauty E, Behr JP. Targeted gene delivery to cancer cells: directed assembly of nanometric DNA particles coated with folic acid. Angew Chem Int Ed Engl 2003; 42(23):2666–2669.

79. Zhang YP, Sekirov L, Saravolac EG, et al. Stabilized plasmid-lipid particles for regional gene therapy: formulation and transfection properties. Gene Ther 1999; 6(8):1438–1447.

80. Harvie P, Wong FMP, Bally MB. Use of poly(ethylene glycol)-lipid conjugates to regulate the surface attributes and transfection activity of lipid-DNA particles. J Pharm Sci 2000; 89(5):652–663.

81. Uster PS, Allen TM, Daniel BE, Mendez CJ, Newman MS, Zhu GZ. Insertion of poly(ethylene glycol) derivatized phospholipid into pre-formed liposomes results in prolonged in vivo circulation time. FEBS Lett 1996; 386(2–3):243–246.

82. Bangham AD, Standish MM, Watkins JC. Diffusion of univalent ions across the lamellae of swollen phospholipids. J Mol Biol 1965; 13(1):238–252.

Polymeric Vesicles Based on Hydrophilic Polymers Bearing Hydrophobic Pendant Groups

Ijeoma Florence Uchegbu, Shona Anderson, Anthony Brownlie, and Xiaozhong Qu

Department of Pharmaceutical Sciences, University of Strathclyde, Glasgow, Scotland, U.K.

INTRODUCTION

Polymeric vesicles are a form of vesicular self-assembly (Fig. 1). As has been emphasized elsewhere in this volume, vesicular systems arise when amphiphilic molecules self-assemble in aqueous media in an effort to reduce the high-energy interaction between the hydrophobic portion of the amphiphile and the aqueous disperse phase and maximize the low-energy interaction between the hydrophilic head group and the disperse phase (Fig. 1). Vesicular self-assemblies reside in the nanometer to micrometer-size domain. Excellent reviews exist on the self-assembly of amphiphiles (1,2), and hence this topic will not be dealt with in great detail here. The most well-known vesicular assemblies, the liposomes (3), have formed the basis of licensed medicines (4), and although the anticancer doxorubicin formulation (Doxil® or Caelyx®) does contain an amphiphilic poly(oxyethylene) derivative, such vesicles, with bilayers comprising relatively small proportions of amphiphilic polymers, be they nonionic surfactant vesicles (niosomes) (5) or liposomes (6), are not to be dealt with in this chapter, especially as the
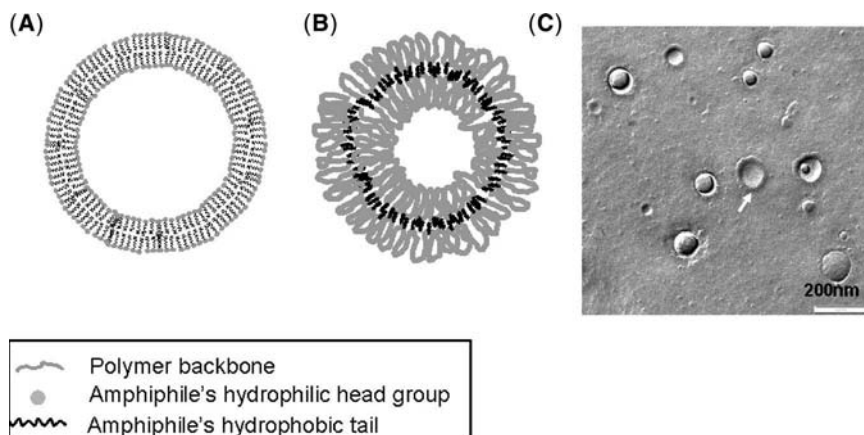
Figure 1 The self-assembly of (**A**) low-molecular-weight amphiphiles to form liposomes or niosomes or (**B** and **C**) polymers bearing hydrophobic grafts to form polymeric vesicles. Polymer 1 (Fig. 2) was used to prepare the vesicles imaged in (**C**).

latter are well explored in other parts of the volume. Rather this chapter will focus on polymeric vesicle self-assemblies arising from polymers bearing lipid pendant groups (Fig. 2) (8–10). Such vesicles are formed from the self-assembly of linear soluble polymers bearing hydrophobic pendant groups. An early form of these vesicles, in which amphiphilic groups were attached to a polymer chain via a hydrophilic spacer (Fig. 2), were first investigated as a means of stabilizing the metastable vesicles formed from low-molecular-weight amphiphiles, with the polymer providing a kinetic trap for the self-assembled system (9,11).

Vesicular self-assembly is not a spontaneous process and normally requires an input of energy in the form of probe sonication, for example (12). It is known that vesicle formation from low-molecular-weight amphiphiles in aqueous media is controlled by two opposing forces, namely the steric or ionic repulsion between hydrophilic head groups, which maximizes the interfacial area per molecule, and the attractive forces between hydrophobic groups, which serve to reduce the interfacial area per molecule (2). Attaining a minimal interfacial energy is thus served by the formation of a closed spherical bilayer. In general terms the less hydrophobic amphiphiles form micelles, whereas amphiphiles of intermediate hydrophobicity form vesicles (2). The self-assembly of polymers into vesicles is governed by similar constraints and as such the hydrophobic–lipophilic balance of polymers determines whether a polymer will self-assemble into vesicles (7,12) in a similar manner as is found in liposomes and niosomes. Also there are some polymer-specific factors that impact on vesicle-forming ability. For example, the degree of polymerization is critical to vesicle-forming ability (12).
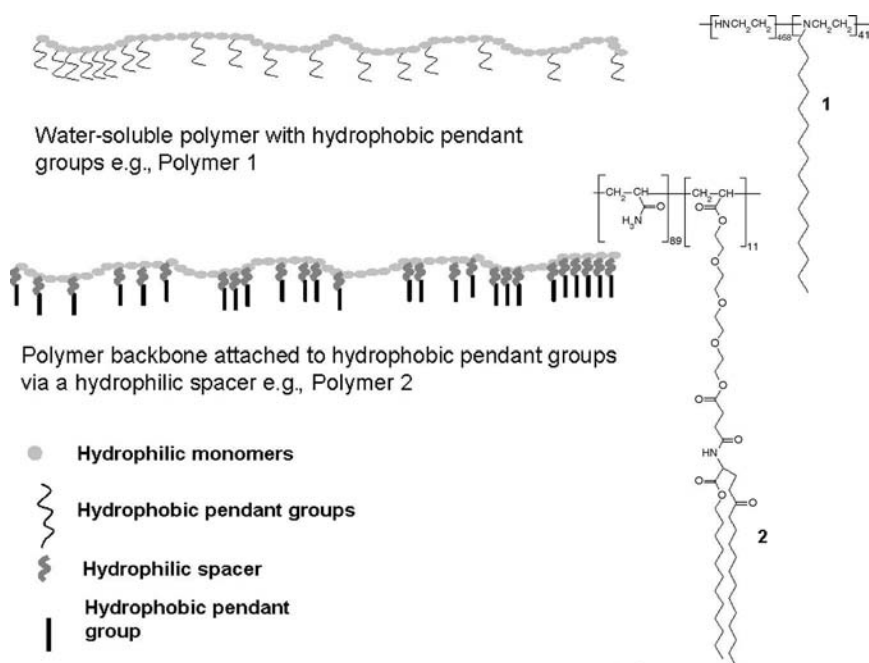
Figure 2 Self-assembling vesicle-forming polymers. Vesicles prepared from Polymer 1 are shown in Figure 1C. *Source*: From Refs. 1 and 7.

Polymeric vesicles appear to be largely unilamellar (8,12,13), and unilamellarity is specifically favored when the molecular weight of the amphiphile increases (7).

Polymeric vesicles often possess superior stability characteristics. For example, there is reduced intermixing of bilayer contents with polymeric vesicles (14) when compared with niosomes or liposomes. Additionally, polymeric vesicles are less permeable to low-molecular-weight solutes when compared to vesicles prepared from low-molecular-weight amphiphiles (8,9,15). The exploitation of these fascinating nanocarriers in the development of responsive and biomimetic nanomedicines with superior stability characteristics is what awaits the science.

FACTORS GOVERNING SELF-ASSEMBLY

The first report on the use of preformed polymers to prepare polymeric bilayer vesicles was presented in 1981 by Kunitake et al. (1). In this report, bilayer vesicles were prepared from Polymer 2 shown in Figure 2. Polymer 2 comprises a hydrophilic polyacrylamide backbone and dialkyl hydrophobic pendant groups separated from the polymer backbone by hydrophilic oligooxyethylene spacers as shown schematically in Figure 2.

The hydrophilic spacer group between the dialkyl moieties was shown by Ringsdorf and others to be essential for vesicle formation for these polyacrylamide type polymers (9) because the hydrophilic spacer allows the decoupling of the polymer motion from the ordering of the bilayer (15).

The introduction of essentially water-soluble carbohydrate [e.g., Polymer 3 (8,13)—Fig. 3], polyelectrolyte [e.g., Polymer 1 (7)—Fig. 2], and polyamino acid [e.g., Polymer 6 (12)—Fig. 3] polymer backbones bearing hydrophobic pendant groups is a fairly recent development. For these bilayers, there is no requirement for a hydrophilic spacer between the soluble main chain and the hydrophobic pendant groups. The bilayer arrangement is as depicted in Figure 4 and the thick polymer coat is clearly visible on micrographs (Fig. 1). For drug delivery applications, it is important to appreciate that the conversion of the poly(L-lysine) into vesicles reduces its cytotoxicity (17), thus potentially allowing the molecules to be exploited as a pharmaceutical excipient (18).
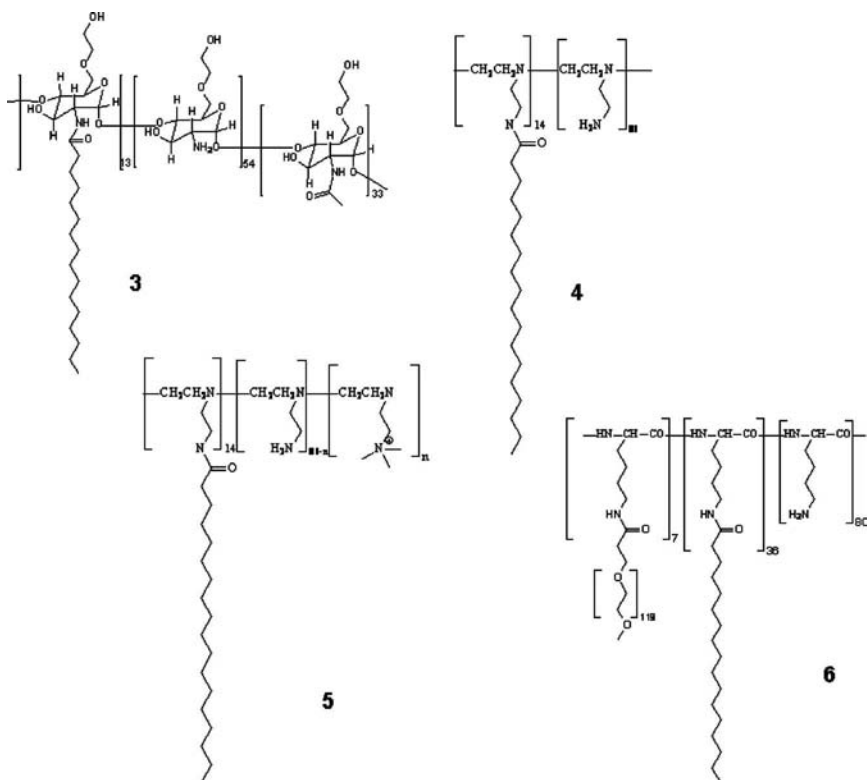
Figure 3 Representative vesicle-forming polymers from the chitosan (Polymer **3**) and polyamine (Polymers **4** and **5**), and polyamino acid (Polymer **6**) classes of polymers. *Source*: From Refs. 7, 8, 12, 13 and 16.
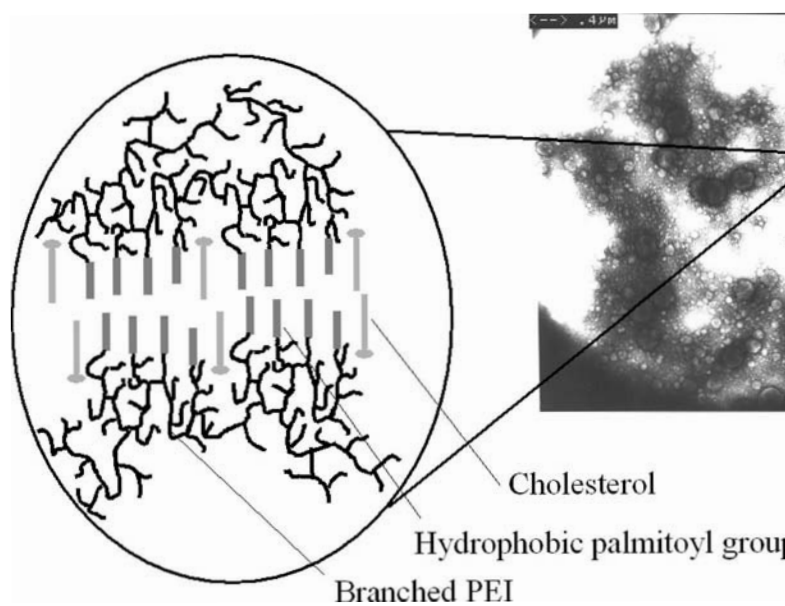
Figure 4 The polyethylenimine polymers (e.g., Polymer 4—Fig. 3) are arr[...] the bilayer as shown. *Abbreviation*: PEI, polyethylenimine.

Poly(ethylenimine) [Polymer 1, Fig. 2 (7)] and poly(L-lysine) [Po[...] Fig. 3 (12,19)]-based amphiphiles have been studied in some det[...] the formation of vesicles from these amphiphiles is dependant on the [...] lipid pendant groups. Hydrophobically modified poly(ethylenimine), fo[...] ple, forms dense nanoparticles, bilayer vesicles, or micellar self-ass[...] depending on its hydrophobic content (7). Hence poly(ethylenimine)[...] philes with a hydrophobic content of 58% and above favor[...] nanoparticle self-assemblies, whereas a hydrophobic content of [...] 58% favors bilayer vesicle assemblies and a hydrophobic content of l[...] 43% favors the formation of micellar assemblies (7). Hydrophobic co[...] measured by weight and is expressed as the proportion of the molec[...] clear hydrophobic character (parts of the molecule whose protons [...] upfield chemical shift less than 1.8 ppm in a nuclear magnetic resonan[...] trum, when the reference standard, tetramethylsilane, has a chemical [...] 0 ppm). The hydrophobic part of the polymer thus comprises the ter[...] carbons on the cetyl pendant group.

A remarkably similar trend has been reported for the p[...] ethylene)-*block*-poly(lactic acid) system, in that a poly(lactic acid) [...] of equal to or more than 80% favors dense nanoparticles, wh[...] poly(lactic acid) fraction of 58% to 80% favors bilayer vesicle ass[...]

and a poly(lactic acid) fraction of less than 50% favors the production of micellar self-assemblies (20).

Cholesterol improves the tendency for vesicle formation by improving hydrophobic interactions in the bilayer (7) and is required for the formation of stable vesicle formulations (12,13).

Vesicles produced by the polymers, depicted in Figure 2, are in the 100–600 nm size range, and vesicles are rarely formed with a mean size of less than 100 nm. The hydrodynamic diameter of the vesicle is determined by two intrinsic properties of the polymers, i.e., the level of hydrophobic modification as shown in (7) and the molecular weight of the polymer as shown in the below equations (13).

$$d_v = 1.95Ct + 139$$

Above equation has been derived for cetyl poly(ethylenimine) amphiphiles, where d_v = z-average mean vesicle hydrodynamic diameter and Ct = mol% cetylation.

$$\sqrt{M_w} = 0.782d_v + 107$$

Above equation has been derived for palmitoyl glycol chitosan amphiphiles, where M_w = polymer weight average molecular weight and d_v = vesicle z-average mean hydrodynamic diameter.

The molecular weight of the polymer is also an important factor to be considered when choosing vesicle-forming polymers. The importance of this parameter has been demonstrated with the poly(L-lysine) vesicle system (12) (e.g., Polymer 6, Fig. 3). With these amphiphiles, a vesicle formation index F′ was computed:

$$F' = \frac{H}{L\sqrt{DP}}$$

where H = mol% unreacted L-lysine units, L = mol% L-lysine units substituted with palmitic acid, and DP = the degree of polymerization of the polymer. An F′ value in excess of 0.168 was found to be necessary for vesicle formation (12).

It is clear from the foregoing that the more hydrophobic and larger molecules are constrained in their attempts at self-assembly into bilayer vesicles. Hydrophobic polymers are unable to reduce their free energy by exposing sufficient levels of hydrophilic areas to the aqueous disperse phase, and high-molecular-weight materials are also constrained possibly by the curvature requirements needed to enable a sufficient level of closed bilayer-type hydrophobic associations.

VESICLE PREPARATION

Polymeric vesicles are relatively simple to prepare and are prepared by the probe sonication of the amphiphilic polymer in the disperse phase (12,13).

However, clearly the energy barrier required for the attainment of vesicle structures is not trivial because polymeric vesicles are not easily formed by hand shaking unlike low-molecular-weight surfactant formulations (5). Vesicles, once formed, are morphologically stable for months (13) and may be loaded with hydrophilic (21–23) and hydrophobic (Fig. 5B) solutes by probe sonicating in the presence of such solutes. Commercially, it is envisaged that polymeric vesicles may be fabricated by microfluidization and high-pressure homogenization techniques.

DRUG DELIVERY APPLICATIONS

Polymeric vesicles, in which the polymeric backbone comprises an integral part of the vesicle bilayer, are yet to be commercially exploited to enhance the properties of medicines. The latter groups of polymeric vesicles have not been studied to the same extent as the more established liposomes; however, these technologies are suitable candidates for the development of robust, controllable, and responsive nanomedicine drug carriers.

Gene Delivery

Cationic polyelectrolytes, by virtue of their electrostatic binding to DNA, are capable of serving as DNA carriers (24). As such, both poly(ethylenimine) (25) and poly(L-lysine) (26) have been used as gene delivery systems. Gene delivery is a crucial element of gene therapy as without the aid of gene carriers, the administered exogenous gene is unable to reach the nucleus in sufficient quantity to produce clinical levels of expressed therapeutic protein (24). Poly(L-lysine)-based vesicles, prepared from Polymer 6 (Fig. 3), have been used for gene delivery (17,18) because these vesicles are less toxic than unmodified poly(L-lysine) and produce higher levels of in vitro gene transfer (Table 1) (17), due to the fact that more of the cells survive the gene transfer procedure and express the desired protein. The production of polymeric vesicles and resultant reduction in cytotoxicity enable poly(L-lysine) to be used as an in vivo gene carrier (18). The unmodified polymer is too toxic to be used as an in vivo gene transfer system.

These materials may also be used for the targeting of particular cell types in vitro. When the targeting ligand-galactose was bound to the distal ends of the poly(oxyethylene) chains, gene expression was increased in HepG2 cells in vitro with poly (L-lysine) based vesicles (18). However, disappointingly, in vivo targeting to the liver hepatocytes was not achieved with these systems (18).

In a similar manner to that described above, poly(ethylenimine) amphiphiles synthesized from branched poly(ethylenimine) (Polymers 4 and 5, Fig. 3) have been used to fabricate polymeric vesicles (Fig. 4). Polymeric vesicles prepared from Polymer 5, while being less cytotoxic and more avid binders of DNA than the parent polymer (Table 1), were however inferior gene transfer systems when compared to the parent polymer (16).

(A)
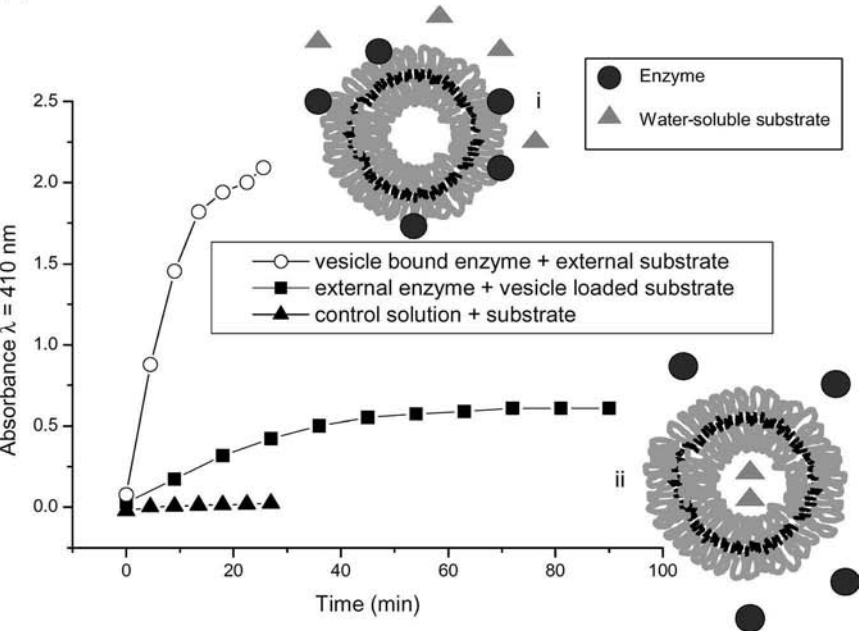
(B)
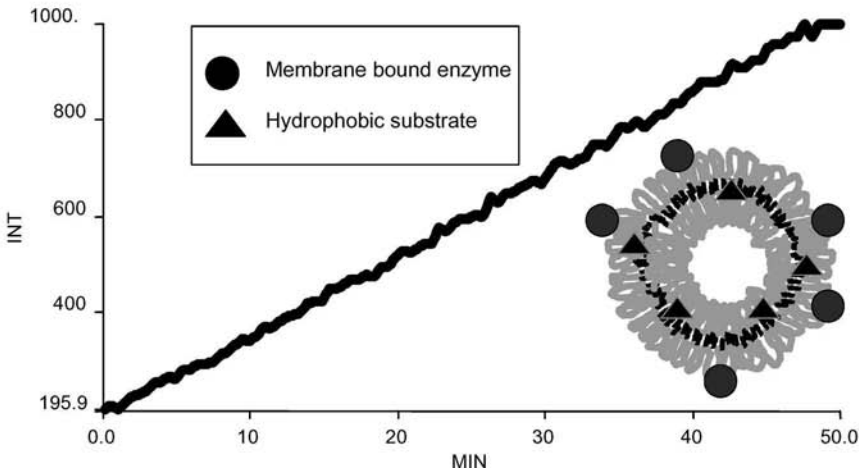
Figure 5 (*Caption on facing page*)

Table 1 Biological Activity of Poly(ethylenimine) and Poly(L-lysine) Vesicles

Polymer	Nitrogen-to-phosphate ratio for complete DNA binding	A431 cells		A549	
		IC50 (µg/mL)	Gene transfer relative to parent polymer	IC50 (µg/mL)	Gene transfer relative to parent polymer
Poly(ethylenimine)	8:1	1.9	1	5.2	1
Polymer 5 (Fig. 3)	6:1	16.9	0.2	12.6	0.08
Polymer 5, cholesterol vesicles 2:1 (g/g)	6:1	15.9	0.2	11	0.08
Poly(L-lysine)	–	7	1	7	1
Polymer 6 (Fig. 3)	–	74	7.8	63	2.3

Source: From Refs. 16 and 17.

Drug Delivery

Carbohydrate polymeric vesicles may also be used as drug-targeting agents. Vesicles prepared from glycol chitosan vesicles improve the intracellular delivery of hydrophilic macromolecules (22) and anticancer drugs (23);

Figure 5 (*Figure on facing page*) (**A**) Enzyme-activated polymeric vesicles. Vesicles bearing membrane-bound enzyme (i) were formed by probe-sonicating Polymer 3 (Fig. 3), cholesterol, and *N*-biotinylated dipalmitoyl phosphatidyl ethanolamine (8:4:1 g/g) in neutral phosphate buffer (2 mL); isolation of the vesicles by ultracentrifugation (150,000 g); redispersion in a similar volume of neutral phosphate buffer and incubation of the vesicles with β-galactosidase streptavidin (3 U). Membrane-bound enzyme (0.2 mL) was then incubated with *O*-nitrophenyl-β-D-galactoside (2.1 mM, 2 mL-substrate) and the absorbance monitored ($\lambda = 410$ nm). The control solution contained similar levels of substrate but no enzyme. Vesicles encapsulating *O*-nitrophenyl-β-D-galactoside (ii) were prepared by probe-sonicating Polymer 3, cholesterol (8:4 g/g) in the presence of *O*-nitrophenyl-β-D-galactoside solution (34 mM, 2 mL), and isolation of the vesicles by ultracentrifugation and redispersion in neutral phosphate buffer. These latter vesicles (0.4 mL) were then incubated with β-D-galactosidase (2 U/mL, 0.1 mL) and the absorbance once again monitored. (**B**) Enzyme-activated polymeric vesicles. Vesicles bearing membrane-bound enzyme and containing the hydrophobic substrate fluorescein di-β-D-galactospyranoside were formed by probe-sonicating Polymer 3 (Fig. 3), cholesterol, *N*-biotinylated dipalmitoyl phosphatidyl ethanolamine, and fluorescein di-β-D-galactospyranoside (8:4:1:0.0005 g/g) in neutral phosphate buffer (2 mL), and incubation of the resulting vesicles with β-galactosidase streptavidin (0.3 U). The fluorescence of the enzyme-hydrolyzed substrate was monitored (excitation wavelength = 490 nm, emission wavelength = 514 nm).

the latter is achieved with the help of a transferrin ligand attached to the surface of the vesicle. These carbohydrate vesicles improve the in vivo tolerability of the cytotoxic agent, doxorubicin; however, they are not as active as the plain drug against subcutaneously implanted A431 tumors.

The ultimate goal of all drug delivery efforts is the simple fabrication of responsive systems that are capable of delivering precise quantities of their payload in response to physiological or more commonly pathological stimuli. Preprogrammable and intelligently responsive pills, implants, and injectables are so far merely the unobtainable ideal; however, polymeric systems have been fabricated with responsive capability and it is possible that, in the future, these may be fine tuned to produce truly intelligent and dynamic drug delivery devices or systems.

We have experimented with enzymatically triggered systems. Vesicles that release their contents in the presence of an enzyme may be formed by loading polymeric vesicles with an enzyme-activated prodrug (Fig. 5). The particulate nature of the drug delivery system should allow the drug to accumulate in tumors, for example, where they may be activated by an externally applied enzyme (Fig. 5A) in a similar manner to the antibody-directed enzyme prodrug therapeutic strategy. The antibody-directed enzyme prodrug therapeutic strategy enables an enzyme to be homed to tumors, using antibodies followed by the application of an enzyme-activated prodrug (27). Alternatively, a membrane-bound enzyme may be used to control and ultimately prolong the activity of either an entrapped hydrophilic drug (entrapped in the vesicle aqueous core) or an entrapped hydrophobic drug (entrapped in the vesicle membrane) as illustrated in Figure 5. It is possible that the enzyme may be chosen such that it is activated in the presence of pathology-specific molecules, thus achieving pathology-responsive and localized drug activity.

CONCLUSIONS

Over the past few years, a new type of vesicle has emerged, fabricated from hydrophobized carbohydrates and polyamino acids. These vesicles enjoy good stability and are suitable for the carriage of drugs. A further point not often appreciated is that the concepts outlined above may be extended to yield vesicles formed from bioactive entities (peptides, oligosaccharides, or carbohydrates), thus forming drug particles with intrinsic tumor-targeting properties, for example. For such systems to be of any value, the site of activity will have to be preserved and left free of chemical or destructive conformational modification. The polymeric amphiphiles outlined above are constrained in the architectures that yield vesicular self-assemblies, and a low-molecular-weight and specific level of hydrophobic pendant groups must be adhered to in constructing such vesicle-forming drug carriers or indeed the futuristic vesicle-forming bioactives.

REFERENCES

1. Kunitake T, Nakashima K, Takarabe M, Nagai A, Tsuge A, Yanagi H. Vesicles of polymeric bilayer and monolayer membranes. J Am Chem Soc 1981; 103:5945–5947.
2. Israelachvili J. Intermolecular and Surface Forces. 2nd ed. London: Academic Press, 1991.
3. Bangham AD, Standish MM, Watkins JC. Diffusion of univalent ions across the lamellae of swollen phospholipids. J Mol Biol 1965; 13:238–252.
4. Gabizon AA. Pegylated liposomal doxorubicin: metamorphosis of an old drug into a new form of chemotherapy. Cancer Invest 2001; 19:424–436.
5. Uchegbu IF, Florence AT. Nonionic surfactant vesicles (niosomes)—physical and pharmaceutical chemistry. Adv Colloid Interface Sci 1995; 58:1–55.
6. Blume G, Cevc G. Liposomes for the sustained drug release in vivo. Biochim Biophys Acta 1990; 1029:91–97.
7. Wang W, Qu X, Gray AI, Tetley L, Uchegbu IF. Self assembly of cetyl linear polyethylenimine to give micelles, vesicles and nanoparticles is controlled by the hydrophobicity of the polymer. Macromolecules 2004; 37:9114–9122.
8. Uchegbu IF, Schatzlein AG, Tetley L, et al. Polymeric chitosan-based vesicles for drug delivery. J Pharm Pharmacol 1998; 50:453–458.
9. Ringsdorf H, Schlarb B, Venzmer J. Molecular architecture and function of polymeric oriented systems: models for the study of organisation, surface recognition, and dynamics of biomembranes. Angewandte Chemie (International Edition in English) 1988; 27:113–158.
10. Wakita M, Hashimoto M. Bilayer vesicle formation of *N*-octadecylchitosan. Kobunshi Ronbunshu 1995; 52:589–593.
11. Hub HH, Hupfer B, Koch H, Ringsdorf H. Polymerizable phospholipid analogues—new stable biomembrane cell models. Angew Chem Int Ed Engl 1980; 19:938–940.
12. Wang W, Tetley L, Uchegbu IF. The level of hydrophobic substitution and the molecular weight of amphiphilic poly-L-lysine-based polymers strongly affects their assembly into polymeric bilayer vesicles. J Colloid Interface Sci 2001; 237:200–207.
13. Wang W, McConaghy AM, Tetley L, Uchegbu IF. Controls on polymer molecular weight may be used to control the size of palmitoyl glycol chitosan polymeric vesicles. Langmuir 2001; 17:631–636.
14. McPhail D, Tetley L, Dufes C, Uchegbu IF. Liposomes encapsulating polymeric chitosan based vesicles—a vesicle in vesicle system for drug delivery. Int J Pharm 2000; 200:73–86.
15. Elbert R, Lashewsky A, Ringsdorf H. Hydrophilic spacer groups in polymerizable lipids: formation of biomembrane models from bulk polymerised lipids. J Am Chem Soc 1985; 107:4134–4141.
16. Brownlie A, Uchegbu IF, Schatzlein AG. PEI based vesicle-polymer hybrid gene delivery system with improved biocompatibility. Int J Pharm 2004; 274:41–52.
17. Brown MD, Schatzlein A, Brownlie A, et al. Preliminary characterization of novel amino acid based polymeric vesicles as gene and drug delivery agents. Bioconjugate Chem 2000; 11:880–891.

18. Brown MD, Gray AI, Tetley L, et al. In vitro and in vivo gene transfer with poly-amino acid vesicles. J Control Rel 2003; 93:193–211.
19. Uchegbu IF, Tetley L, Wang W. Nanoparticles and polymeric vesicles from new poly-L-lysine based amphiphiles. In: Mallapragada S, et al., eds. Biomaterials for Drug Delivery and Tissue Engineering. Pennsylvania: Materials Research Society, 2001:NN6.8.1–NN6.8.6.
20. Ahmed F, Discher DE. Self-porating polymersomes of PEG-PLA and PEG-PCL: hydrolysis-triggered controlled release vesicles. J Control Rel 2004; 96:37–53.
21. Sludden J, Uchegbu IF, Schatzlein AG. The encapsulation of bleomycin within chitosan based polymeric vesicles does not alter its biodistribution. J Pharm Pharmacol 2000; 52:377–382.
22. Dufes C, Schatzlein AG, Tetley L, et al. Niosomes and polymeric chitosan based vesicles bearing transferrin and glucose ligands for drug targeting. Pharm Res 2000; 17:1250–1258.
23. Dufes C, Muller J-M, Couet W, Olivier JC, Uchegbu IF, Schatzlein A. Anti-cancer drug delivery with transferrin targeted polymeric chitosan vesicles. Pharm Res 2004; 21:101–107.
24. Brown MD, Schatzlein AG, Uchegbu IF. Gene delivery with synthetic (non viral) carriers. Int J Pharm 2001; 229:1–21.
25. Boussif O, Lezoualc'h F, Zanta MA, et al. A versatile vector for gene and oligonucleotide transfer into cells in culture and in vivo: polyethylenimine. Proc Natl Acad Sci USA 1995; 92:7297–7301.
26. Wu GY, Wu CH. Receptor-mediated in vitro gene transformation by a soluble DNA carrier system. J Biol Chem 1987; 262:4429–4432.
27. Bagshawe KD, Sharma SK, Springer CJ, et al. Antibody directed enzyme prodrug therapy (ADEPT): clinical report. Dis Markers 1991; 9:233–238.

11

Mixed Vesicles and Mixed Micelles: Formation, Thermodynamic Stability, and Pharmaceutical Aspects

Patrick Garidel and Jürgen Lasch

Institute of Physical Chemistry, Martin Luther University Halle/Wittenberg, Halle/Saale, Germany

INTRODUCTION

The addition of detergents to artificial lipid bilayers and liposomes induces the formation of a number of intermediates [mixed vesicles (MVs) and various types of mixed micelles (MMs)], which, besides their interesting physicochemical properties, attract more and more attention as potential nanocarrier systems for the delivery and/or solubility of drugs (1,2). In dermatological research, for example, such nanocarriers were used to increase skin penetration and thus transdermal drug delivery (3). Technical terms associated with these endeavors are surfactant-based elastic vesicles and Transfersomes® (4–6). Depending on the lipid to detergent ratio, various intermediate structures can be found: MVs, bilayered phospholipids fragments (BPFs), cylindrical mixed micelles (CMMs), lipid-rich spherical or ellipsoidal mixed micelles (SMMs or EMMs) and at low lipid to detergent ratios lipid-poor MMs are formed (7). The existence of these structures was confirmed and made visible by using techniques like freeze-fracture electron microscopy (FFEM) and cryo transmission electron microscopy (cryo-TEM). The stability and formation of the different structures is governed by their thermodynamic properties (8,9). In the presented paper, isothermal titration

calorimetry (ITC) is used to study the stoichiometry as well as the thermodynamic properties of the detergent to lipid interactions and stability of the formed mixed systems. The latter is the main focus of this discussion. Different ITC experiments are presented for studying phospholipids–detergent interactions, accompanying the partitioning of detergent molecules in to the lipidic phase of vesicles and the formation of MVs (10). From these results, a complete thermodynamic picture of the mixed system formation is derived. The obtained information allows a deeper insight and understanding with respect to the formation of mixed systems and their thermodynamic stability. Additionally, various selected biophysical methods for the characterization of mixed lipid-detergent systems are briefly discussed. The chapter ends with considering the pharmaceutical aspects of these nano carriers for future drug delivery systems.

DETERGENTS, LIPIDS, AND WATER

Mechanism of Micelle Formation

Micelle Formation and the Hydrophobic Effect

Lipids and detergents are amphiphilic molecules, consisting of a hydrophobic group [e.g., hydrocarbon chain(s)] and a hydrophilic polar group. The polar group can be ionic or nonionic. In water, the polar group is capable of preventing phase separation of the amphiphilic molecules, thus able to keep the hydrocarbon residues in the aqueous medium. However, the system tries to minimize the unfavorable water–hydrocarbon interface. As a consequence, supramolecular structures are formed. The state of aggregation of a pure amphiphile in an aqueous solution is a complex function of its structure and charge. The type of supramolecular structure formed by amphiphilic molecules can be predicted on the basis of geometric considerations (8). The driving force for this self-assembly is not cohesion between the hydrocarbon chains, but is the so-called hydrophobic effect (11,12). The hydrophobic effect responsible for the self-assembly is in principle an entropically driven effect arising from the hydrogen-bonded structure of water. In the pure water phase, strong hydrogen bonds between water molecules are formed. When a hydrocarbon molecule is brought into the water phase, the water–water bonds have to be disrupted. Around the hydrocarbon molecule dissolved in water, a clathrate-like structure ("iceberg" model) is formed, causing a rearrangement of water molecules and as a consequence losing configurational entropy [for more details see Tanford (11), Moroi (1), and Widom et al. (12)]. Recent findings by Finney (13) showed that there is a small but significant change in the solvent water network beyond the first neighbor shell of the hydrocarbon in water.

The formation of micelles (8) usually occurs only when the amphiphile molecule concentration is higher than a critical specific concentration, denoted as the critical aggregation concentration [for micelles: critical micelle

concentration (CMC)]. This is the case under the assumption that the micelle formation represents a true phase separation (1). Under this condition, the Gibbs phase rule predicts that, at a fixed temperature and pressure, monomers and micelles can be in equilibrium only at a fixed detergent concentration. Below this concentration, the detergent molecules behave as normally dissolved solutes with no detectable association/aggregation between the single molecules. As a consequence, the concentration of detergent monomers (c_{mono}) is equal to the total detergent concentration (c_{t}). When $c_{\mathrm{t}} > cmc$, c_{mono} increases only slightly upon increasing c_{t}, and the excess monomers form aggregates (micelles), whose concentration (c_{mic}) increases linearly with c_{t} (14).

Determination of the Critical Aggregation Concentration

A number of various biophysical methods can be used for the determination of the *cmc*, e.g., surface tension, electrical conductivity, fluorescence depolarization, hyper-Rayleigh scattering, gel filtration chromatography, density measurements, viscosity measurements, spectrophotometry, cyclic voltametry, nuclear magnetic resonance, capillary electrophoresis, light scattering, turbidity, methods measuring colligative solution properties like depression of vapor pressure, depression of freezing point and osmotic pressure. For more details, the reader is referred to (15) and references cited therein. This paper focuses on the use of ITC for the investigation of the critical aggregation concentration of MMs and micelles.

Thermodynamics of Micelle Formation as Investigated by ITC

A powerful method for the investigation of the *cmc* and, e.g., the aggregation number of association colloids is ITC (16–18). In addition to these data, the thermodynamic parameters revealing the stability of the micellar colloids [pure micelles and MMs (18)] can be determined in one and the same ITC experiment. A so-called demicellization/deaggregation protocol is briefly described (Fig. 1) for the determination of the *cmc*. The experiment is performed with an ITC instrument at constant temperature (isotherm), which allows the detection of extremely small heat flows (in the range of 10^{-6} cal). The titration device, e.g., a syringe, is filled with a colloidal solution (e.g., micelles) of a detergent with a concentration much higher than the expected *cmc* ($c_{\mathrm{syr}} \gg cmc$). The cell of the ITC instrument is filled with the corresponding buffer solution. The titration experiment is initiated by injecting step-by-step small aliquots (e.g., 2–10 μL) of the colloidal/ micellar solution into the cell (Fig. 1) and the heat flow observed during this process is measured as a function of time. The first injection represents the dilution of the colloidal/micellar solution (Fig. 1A) and as a consequence, deaggregation of the colloids/micelles is induced. Thus, at the beginning of the experiment, the detergent molecules in the cell are only presents as monomers. During the titration experiment, step by step the detergent
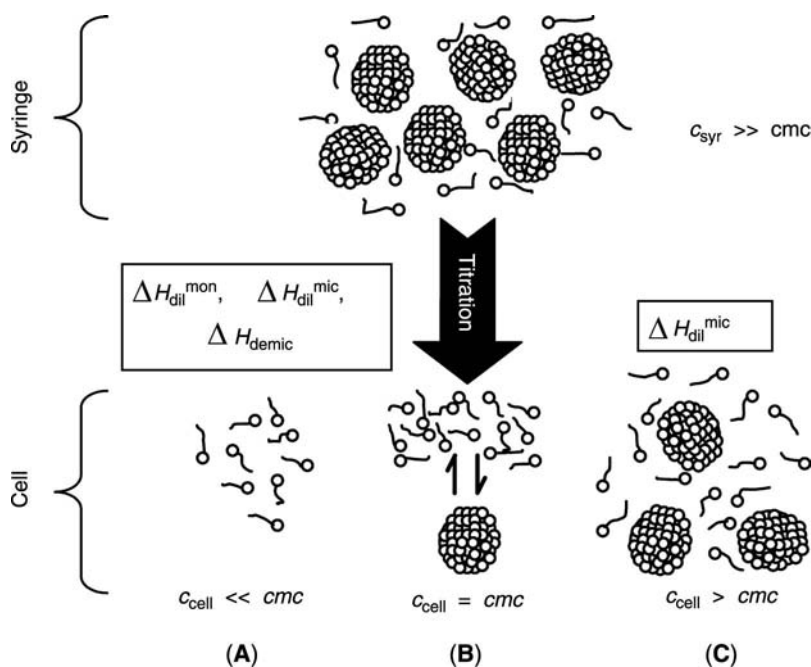
Figure 1 Schematic representation of the demicellization experiment for the determination of the deaggregation/demicellization process with c_{syr}:detergent concentration in the syringe and c_{cell}:detergent concentration in the reaction cell. (**A**) The beginning of the titration experiment with $c_{cell} \ll cmc$ showing the dilution of the colloidal/micellar solution, (**B**) first colloidal aggregates/micelles are formed with $c_{cell} = cmc$, (**C**) end of the titration experiment with $c_{cell} > cmc$ and concentration of formed micelles/aggregates increase, whereas c_{mono} remains cmc. *Abbreviation*: cmc, critical micellization concentration.

concentration in the cell is increased, and consequently the monomer concentration in the cell increases and a concentration is reached, where the first colloidal aggregates/micelles are formed (Fig. 1B). At this point, the detergent concentration in the cell c_{cell} equals the *cmc*. With further titration steps, the detergent concentration in colloidal/micellar form increases continuously, whereas $c_{mono} = cmc$.

Figure 2 shows a typical ITC detergent dilution experiment (SDS: sodium dodecylsulphate, 100 mM NaCl, *pH* 7, T = 38°C). The titration consists of 100 injections of 2.5 µL aliquots of a highly concentrated SDS solution (17 mM). Each injection induces a heat flow as a function of time (Fig. 2A). The reaction heat of each injection is obtained by integration (Fig. 2B). In the presented example, endothermic heat flows are measured with increasing concentration in the sample cell, and the heat flow decreases
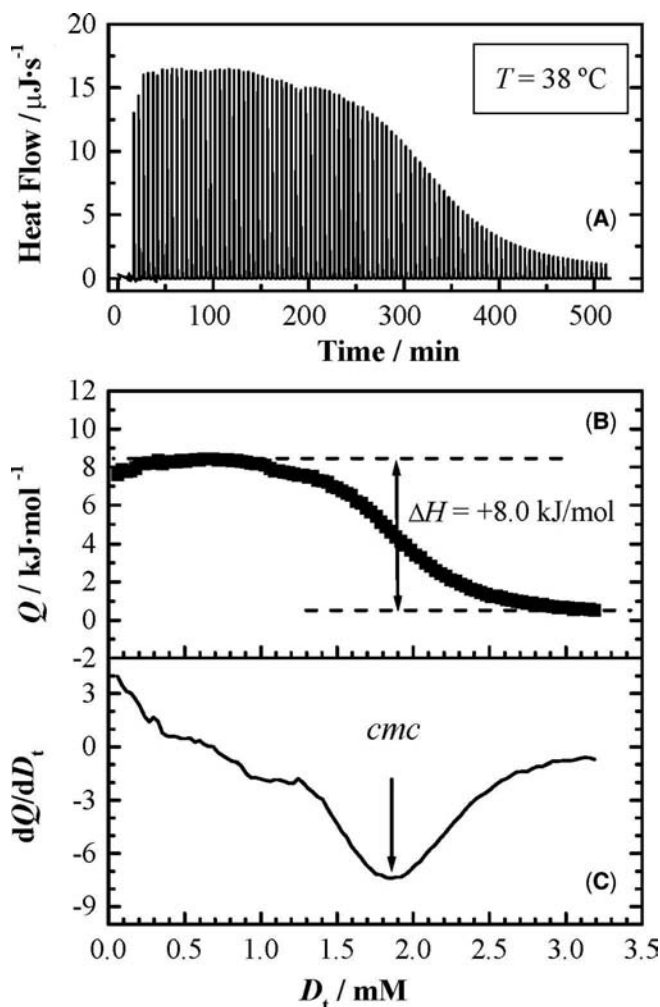
Figure 2 Titration of 100 mM sodium dodecylsulphate in 100 mM NaCl at pH 7 into 1.34 mL 100 mM NaCl at pH 7 at 38°C using an ITC Omega titration calorimeter from MicroCal. (**A**) Calorimetric traces (100 injections a 2.5-μL aliquots), (**B**) reaction enthalpy (*Q*) versus the total detergent concentration D_t in the reaction cell, (**C**) first derivative (dQ/dD_t) of curve B calculated numerically from interpolated values. *Abbreviations*: *cmc*, critical micellization concentration; ITC, isothermal titration calorimetry.

and becomes constant, i.e., almost zero at the end of the titration experiment. Whether this process is exothermic or endothermic depends on the investigated temperature and environmental conditions (17). As can be seen from Figure 2B, the heat effects as a function of total detergent in the

measuring cell has a sigmoid shape, which can be subdivided in regions due to three different processes. At the beginning titration experiment, the reaction heat (ΔH) is composed of changes for (i). the dilution of monomers ($\Delta H_{\text{mon, dil}}$), (ii). dilution o loidal system (e.g., micelles or MMs) ($\Delta H_{\text{colloid, dil}}$) and (iii), deaggreg the colloidal system (ΔH_{deag}). The relation between the aggregation zation and deaggregation/demicellization enthalpy is $\Delta H_{\text{ag}} = -\Delta$ separate experiments, it has to be shown that $\Delta H_{\text{deag}} \gg \Delta H_{\text{colloi}}$ $\Delta H_{\text{mon, dil}}$. (15–17). For the first injections, the major enthalpy cont to ΔH is dominated by ΔH_{deag}. During the titration, the process of gation/demicellization decreases continuously and as a consequenc and thus ΔH. This is shown in Figure 2B.

The critical aggregation/micelle concentration is easily determin ITC experiment by calculating the first derivative of the reaction h respect to the total detergent concentration D_t in the cell (Fig. 2C) (1

The temperature dependence of the cmc of detergents shows a minimum at room temperature (10). Figure 3 represents t tion of the cmc of different detergents (OG: 1-O-octyl-β-D-glucopy NaC: sodium cholate, DM: 1-O-dodecyl-β-D-maltosid) in water (p a function of temperature (19). For OG the cmc-minimum is sh
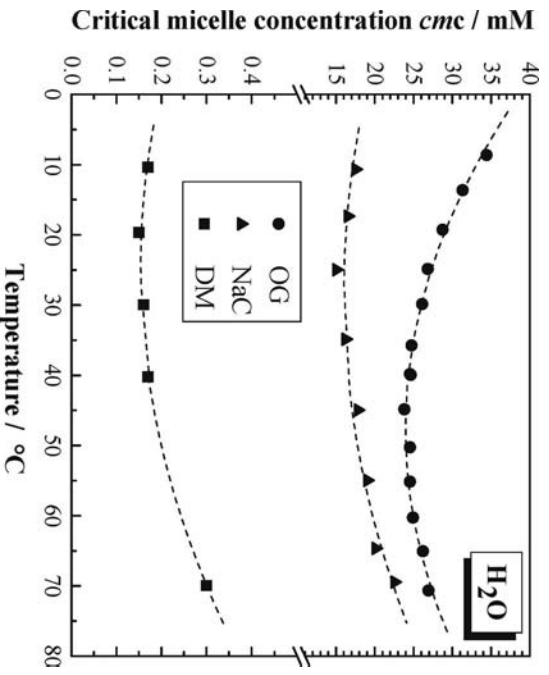
Figure 3 Temperature dependence of the critical micellization concent different detergents (OG: 1-O-octyl-β-D-glucopyranosid, NaC: sodium chol 1-O-dodecyl-β-D-maltosid) in water (pH 7) as a function of temperature. are obtained using a second-order polynomial fit. *Source:* Adapted from F

higher temperatures (for more details, see Ref. 19). Other detergents like sodium oleate show even two different *cmc*s (18).

From the presented experiment, the complete thermodynamic para-meter set describing the thermodynamic stability of the formed colloidal system can be determined.

ΔH_{demic} data for dodecylmaltoside (water, *pH* 7) are shown in Figure 4 as a function of temperature. The Gibbs free energy ΔG_{demic} for the demi-cellization process is obtained from the following equation:

$$\Delta G_{\text{demic}} = -RT \cdot \ln cmc'$$

with R being the gas constant, T the temperature, *cmc'* the *cmc* expressed in mole fraction units. Using the Gibbs–Helmholtz relation, the entropic term $T \cdot \Delta S_{\text{demic}}$ is calculated:

$$T \cdot \Delta S_{\text{demic}} = \Delta H_{\text{demic}} - \Delta G_{\text{demic}}$$

The corresponding data are summarized in Figure 4.

Below room temperature ΔH_{demic} is negative and becomes positive above 25°C to 30°C. In the temperature range where $\Delta H_{\text{demic}} = 0$, the formation of the colloidal system is completely entropy driven. In this tem-perature range, a minimum is observed for *cmc* (Fig. 3). With increasing temperature, the driving force for the deaggregation becomes more and more enthalpic in nature. The entropic contribution $T \cdot \Delta S_{\text{demic}}$ vanishes
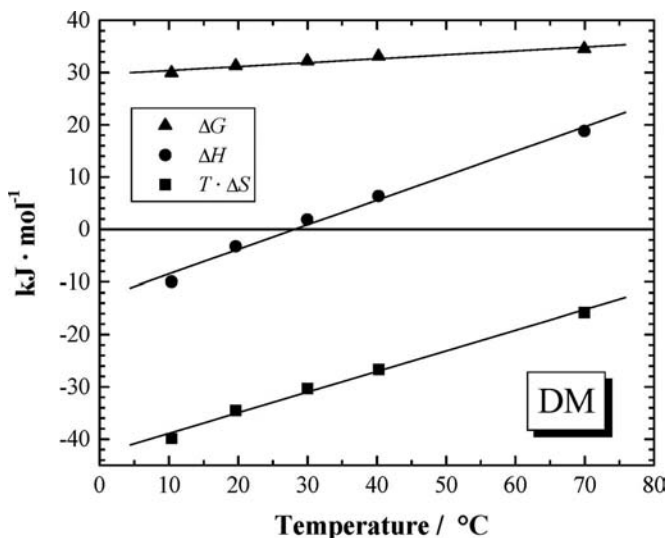
Figure 4 Thermodynamic parameters of the demicellization of 1-*O*-dodecyl-β-D-maltosid (DM) in water (pH 7) as a function of temperature. *Source*: Adapted from Ref. 19.

around 110°C, and become then positive with increasing temperature. The observed behavior for the different thermodynamic functions is caused by the hydrophobic effect, which describes an enthalpy–entropy compensation during the formation of colloids like micelles (18).

Due to the fact that the temperature dependence of the transfer enthalpy and transfer entropy from the colloidal system (e.g., micelle) to water is caused by the hydrophobic effect, the slope of the transfer enthalpy is related to the change in heat capacity $\Delta C_p = (\partial \Delta H / \partial T)_p$ and gives information concerning the change in hydrophobic surface area exposed to water (15,17–20).

The number of molecules forming a micelle, the aggregation number, can be derived from ITC data by simulating the titration curves using a mass action model (for more details, see Ref. 15.) For example., the bile salt sodium cholate (NaC), it was found that the aggregation number is about four to six (25°C) and rather independent of the ionic strength (0 to 100 mM NaCl, pH 7.5) and temperature (10–60°C). However, for sodium deoxycholate (NaDC), the micelles in water (pH 7.5) at 25°C are formed of seven monomers, and with increasing ionic strength up to 100 mM NaCl, the aggregation number increases to 12. For NaDC, increasing the temperature induces a decrease of the aggregation number (17). Much higher aggregation numbers of 40 to 60 (water, 25°C) are observed for SDS.

Mechanism of Vesicle Formation

Techniques for the Preparation of Lipid Vesicles

There are seven techniques by which amphiphiles, including bilayer-forming lipids, can be induced to form vesicles of various morphologies: (i) hand-shaken multilamellar vesicles, (ii) ethanol injection vesicles, (iii) sonicated small (unilamellar) vesicles [S(U) Vs], (iv) freeze-dried rehydration vesicles, (v) reverse-phase evaporation vesicles, (vi) high pressure homogenization vesicles, and (vii) detergent depletion producing unilamellar and oligolamellar vesicles (LUVs, OLVs). Protocols of all these techniques can be found in Ref.(21).

Detergent Depletion Method

In the context of this chapter, only the detergent depletion method for the formation of well-defined vesicles will be discussed. In contrast to all other methods where vesiculation occurs almost instantly, the intermediate structures of detergent and lipid formed during detergent removal have a longer stability. The type of formed structure depends on the geometrical shape of the dispersed amphiphile in water and the detergent to lipid ratio (7,8,22).

The mechanism of vesicle formation as obtained from the detergent depletion method can be described by considering the principle of minimization of total excess energy to MVs, by assuming that the basic relation of this

energy is the sum of boundary (b) and curvature (c) energy, $E_e = E_b + E_c$ (23–25). E_b is Y_{eff} (effective edge tension) times the sum over the perimeter (r_i) of all disk-like micelles, $2\pi\Sigma r_i$, and the curvature energy, E_c, is composed of an inelastic and an elastic contribution. The edge tension of "naked" phospholipid bilayers is 7×10^{-20} J/nm. The effective edge tension, however, is lower and depends on shielding effects by the hydrophilic parts of a detergent in the mixed system. As a consequence, E_b decreases. If MMs (see below) are subjected to a very slow detergent removal (quasi thermodynamic equilibria), there will not be enough detergent molecules in the end caps to shield the exposed hydrocarbon core from the polar environment (Y_{eff} increases progressively). As a consequence, the micelles start to bend, therewith reducing the exposed perimeter (the other factor in the boundary energy) until they eliminate this unfavorable exposure completely by closing upon themselves. The MMs overcome the energy barrier in the profile of the total excess energy by their thermal energy and close upon themselves to form vesicles. Of course, the system has to compensate for this decrease of boundary interactions by increasing the curvature energy. Vesicles are formed when the boundary energy E_b becomes zero, i.e., E_e becomes equal to E_c. In other words, the self-closing occurs at a critical point of the balance of bending (curvature) and boundary (edge) energy. With this concept of lipid vesicle formation, disk-like micelles, which are denoted as open vesicles are essential intermediates. Nozaki et al. (26) called them bilayered (BPF) Phospholipid fragments. The direct visualization of BPFs or large disk-like micelles is still a challenge, because of possible artefacts during sample preparation and mechanical instability of the BPFs. However, Vinson et al. (27) were able to visualize CMMs (27) using cryo-TEM and thus gave a direct proof of the existence of these interesting intermediates.

When the BPFs close, MVs are formed. The mechanism of self-closing bilayered fragments was analyzed by FFEM. Freeze fracture electron micrographs taken during the removal of detergent by dialysis are shown in Figure 5. These MVs were prepared from DPPC and the neutral detergent octylglucoside (28) at an effective molar detergent to lipid ration of 2.0. "Open vesicles" or BPFs are seen in Figure 5A. Cross-fractures show up in Figure 5B, indicating MVs, i.e., vesicles which have incorporated detergent below R_{sat} (below solubilization, Fig. 6). When all detergent is removed by e.g. dialysis, correctly fractured vesicles are obtained (Fig. 5C).

THE FORMATION OF MIXED LIPID-DETERGENT SYSTEMS

Detergent Partitioning into Vesicles as Investigated by ITC

From an ITC experiment, the partition coefficient P as well as the heat of transfer ΔH^T of detergent molecules from the buffer phase to lipid vesicles
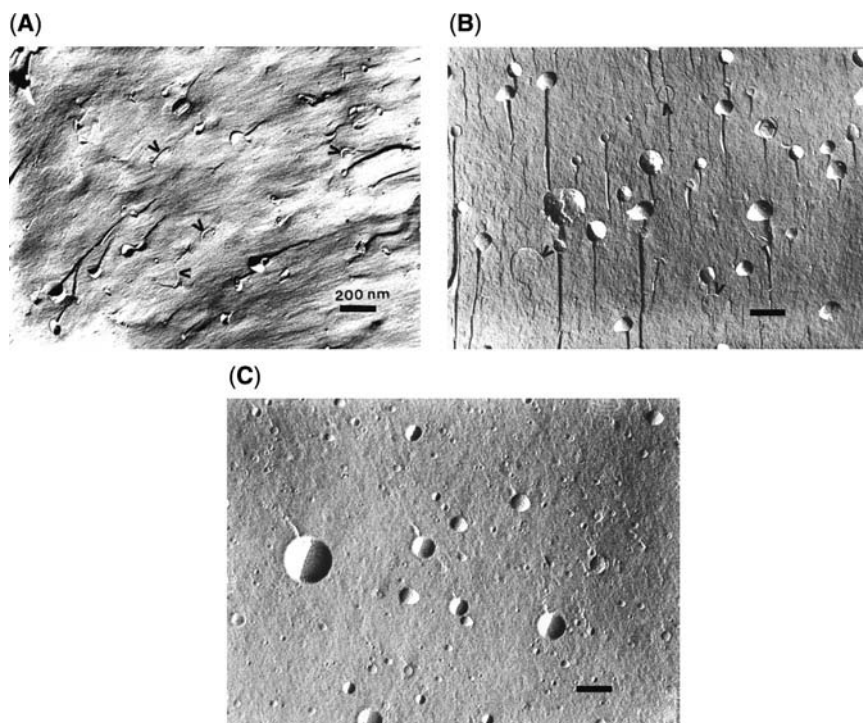
Figure 5 Freeze-fractured micrographs of egg-yolk octylglucoside mixtures after 2 hours (**A**), 6 hours (**B**), and 12 hours (**C**) dialysis in a homemade microdialysis chamber. Starting concentrations: lipid 30 mM, octyl glucoside 40 mM. Freeze-fracturing was done after jet-freezing with the BAF 400 D (Balzers, Liechtenstein) and PtC replicas were examined in a JEM 100 microscope (Jeol, Tokyo), bar = 200 nm. *Source*: From Ref. 28.

can be determined (formation of MVs). This is done by titrating detergent to vesicles. The used partitioning model for the determination of these parameters is briefly described. The incorporation of negatively charged detergent molecules (e.g., bile acids) into lipid membranes induces an increase of the negative surface charge density of the vesicles. As a consequence, the incorporation of additional detergent molecules is reduced. Therefore, the electrostatic repulsion between negatively charged detergent molecules and vesicles loaded with negatively charged detergent molecules have to be considered for the correct calculation of the partition coefficient. The partition coefficient P is defined as the ratio of the mole fractions of bound detergent in the MVs x_b and free detergent in the aqueous solution x_w:

$$P = \frac{x_b}{x_w}$$

(A)

(B)
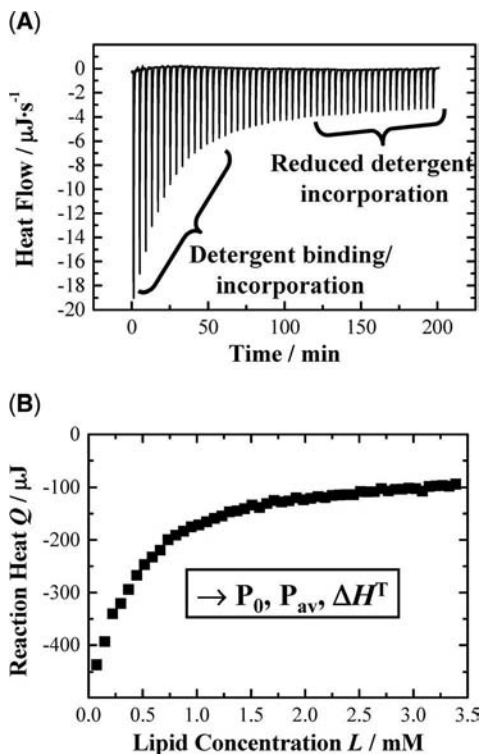
Figure 6 Partition titration experiment of a vesicle dispersion into a detergent solution with $c_{det} <$ cmc. **(A)** Calorimetric traces, **(B)** change of reaction heat ΔQ of each injection versus lipid concentration L in the cell.

Using the approach proposed by Kuchinka and Seelig (29), the correction of the electrostatic effects is introduced by calculating the surface charge density σ according to:

$$\sigma = z \cdot e_0 \cdot \frac{\dfrac{D_b}{L \cdot A_L}}{1 + \dfrac{D_b \cdot A_D}{L \cdot A_L}}$$

with e_0 being the elementary electric charge, z the electric charge of the detergent, D_b the concentration of bound detergent, L the lipid concentration in the sample cell, A_L the average surface area of a lipid molecule and A_D the average surface area of a the detergent molecule (30). Using the Graham equation the surface potential ψ_0 can be calculated. For 1:1 electrolytes one obtains:

$$\psi_0 = -k_B \cdot \frac{T}{e_0} \cdot a \cosh\left(\frac{\sigma^2}{4\varepsilon_0\varepsilon_r RT \cdot 1000 \cdot c_{el}} + 1\right)$$

with k_B being the Boltzmann constant, T the absolute temperature, e_0 the elementary electric charge, ε_0 the permittivity of free space, ε_r the dielectric constant of water, R the gas constant, and c_{el} the electrolyte concentration. The relation between the surface potential ψ_0 and the partition coefficient P is:

$$P = P_0 \cdot \exp\left(-\frac{z \cdot e_0 \cdot \psi_0}{k_B \cdot T}\right) \cdot \exp\left(-\rho \frac{(1 - x_b)^2}{R \cdot T}\right)$$

where ρ (nonideality parameter) takes into account the nonideal mixing of the two components and P_0 represents the intrinsic partition coefficient.

The concentration of bound detergent D_b is expressed as a function of the total detergent concentration in the sample cell, D_t, taking the molar water concentration W ($55.5\,\mathrm{mol}^{-1}$) into account (for more details, see Ref. 10):

$$D_b = \frac{1}{2}(D_t - L) - \frac{W}{2P} + \sqrt{\frac{1}{4}(D_t + L)^2 - \frac{1}{2}(D_t - L) \cdot \frac{W}{P} + \frac{1}{4}\left(\frac{W}{P}\right)^2}$$

The detergent concentration at the membrane surface D_w varies due to electrostatic effects. Based on the Gouy–Chapman theory, D_w can be calculated using the approximation for the bulk concentration of the detergent $D_{wbulk} = D_t - D_b$.

$$D_w = D_{wbulk} \cdot \exp\left(-\frac{z \cdot e_0 \cdot \psi_0}{k_B \cdot T}\right)$$

Due to the fact that during the titration experiment, the amount of detergent in the vesicles changes, the exact concentrations of the components has to be calculated. The following equation considers the change of the bound detergent concentration in the aggregates as a function of the injected lipid dispersion:

$$\frac{\Delta D_b}{\Delta L} = \frac{D_{b(n+1)} - D_{b(n)}}{L_{(n+1)} - L_{(n)}}$$

where the concentration differences of the $(n + 1)$th injection (index 1) and the nth injection are included.

With the equation for D_b (7), the experimentally observed reaction heat change ΔQ is given by

$$\Delta Q = \left(\frac{\Delta D_b}{\Delta L} \cdot \Delta H^T + \Delta H_{dil}\right) \cdot L_{t,syr} \cdot v_{inj}$$

where v_{inj} denotes the injection volume and $L_{t,syr}$ the total lipid concentration in the syringe. ΔH^T represents the transfer enthalpy of the incorporation of detergent monomers into the lipid bilayers and ΔH_{dil} the dilution heat of the phospholipid dispersion. ΔH_{dil} can be obtained from a separate experiment by titrating the phospholipid dispersion into the buffer and subtracting the dilution term from the reaction heat change ΔQ.

For the calculation of the partition coefficients $P_\#$ ($P_\#$-index $\#$ means "0" or "av," P_0 intrinsic coefficient partition, P_{av} average partition coefficient describing the partition of the "middle" injection number of the partitioning experiment) and the transfer enthalpy ΔH^T, a two-parameter nonlinear least square fit is used. Based on the relation $\Delta G^T_\# = -RT \ln P_\#$, the changes in Gibbs free energy $\Delta G^T_\#$ are obtained and using the Gibbs–Helmholtz equation ($T\Delta S^T_\# = \Delta H^T - \Delta G^T_\#$) the entropy term $T\Delta S^T_\#$ is calculated. Thus all relevant thermodynamic parameters are obtained for the intrinsic partition coefficient P_0 and the average partition coefficient P_{av}.

The ITC protocol is as follows (31–34). The titration syringe is filled with a monomeric detergent solution and titrated to a unilamellar vesicular lipid dispersion. At the beginning of the partitioning experiment, large peaks are detected (Fig. 7A) indicating binding and incorporation of the detergent in the vesicle. During the partitioning experiment, more and more detergent is distributed into the lipidic phase and incorporation is reduced. As a consequence, the enthalpic effects decrease continuously (Fig. 6). From the simulation of the curve, shown in Figure 6B, the partitioning coefficients and transfer enthalpy are obtained. Table 1 summarizes the two partition coefficient P_0 and P_{av} (water, pH 7.4) for three different phospholipid systems (DPPC: dipalmitoyl phosphatidylcholine, POPC: palmitoyl oleoyl phospatidylcholine, SBPC: soy bean phosphatidylcholine) in the liquid crystalline phase ($T = 60°C$) for the three-hydroxy (NaC, sodium cholate)
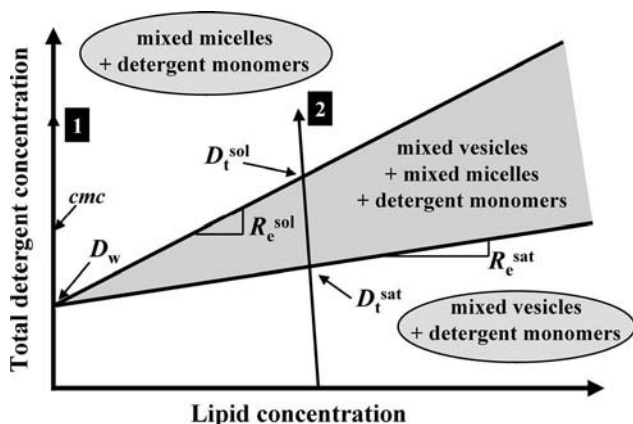
Figure 7 Schematic phase diagram of phospholipid/detergent mixtures (total detergent concentration D_t vs. lipid concentration L) for the vesicle-to-micelle phase transition, indicating the phase boundaries D_t^{sat} and D_t^{sol}, the detergent/lipid ratios R_e^{sat} and R_e^{sol}, and the hypothetical detergent concentration in presence of lipid D_w^{sat} and D_w^{sol} for the saturation and solubilization process. *Abbreviaton*: cmc, critical micellization concentration.

Table 1 Partitioning Coefficients P_0 and P_{av} for Dipalmitoyl Phosphatidylcholine, Palmitoyl Oleoyl Phosphatidylcholine, Soy Bean Phosphatidylcholine at $T = 60°C$ for Sodium Cholate and Sodium Deoxycholate in Water (pH 7)

System ($T = 60°C$)		Water, pH 7	
		P_0	P_{av}
DPPC	NaC	6.4×10^6	7.8×10^3
	NaDC	4.4×10^7	3.1×10^5
POPC	NaC	1.0×10^7	1.1×10^4
	NaDC	6.6×10^7	4.0×10^4
SBPC	NaC	6.9×10^6	8.1×10^3
	NaDC	4.3×10^7	3.2×10^5

Abbreviations: DPPC, dipalmitoyl phosphatidylcholine; POPC, palmitoyl oleoyl phospatidylcholine; SBPC, soy bean phosphatidylcholine; NaC, sodium cholate; NaDC, sodium deoxycholate.

and two-hydroxy bile acid (NaDC, sodium deoxycholate). As can be seen from Table 1, $P_0 > P_{av}$ and comparing the partitioning coefficient of the two bile salt, it is found that for the more hydrophobic bile salt P (NaDC) > P (NaC). ΔH^T represents the transfer enthalpy of the incorporation of detergent monomers of the aqueous phase into the lipid vesicles is all negative, and thus favored under the chosen experimental conditions. For bilayer systems with unsaturated hydrocarbon chains, ΔH^T is more negative than for corresponding liposomes with saturated acyl chains (Table 2). The influence of the ionic strength is also clear from Table 2: ΔH^T (water) > ΔH^T (NaCl). This behavior can be explained by taking into account electrostatic shielding effect of the detergent in the aqueous phase (for more details see Refs. 31,34,35).

Table 2 Transfer Enthalpy ΔH^T for Sodium Cholate and Sodium Deoxycholate into Dipalmitoyl Phosphatidylcholine, Palmitoyl Oleoyl Phosphatidylcholine, and Soy Bean Phosphatidylcholine Vesicles at $T = 60°C$ in Water and at an Ionic Strength of 100 mM NaCl (pH 7)

System ($T = 60°C$)		$\Delta H^T / kJ \cdot mol^{-1}$	
		Water	0.1 M NaCl
DPPC	NaC	−1.2	−1.9
	NaDC	−0.7	−6.7
POPC	NaC	−1.6	−2.2
	NaDC	−0.4	−7.3
SBPC	NaC	−3.6	−5.3
	NaDC	−5.8	−15.8

Abbreviations: DPPC, dipalmitoyl phosphatidylcholine; POPC, palmitoyl oleoyl phosphatidylcholine; SBPC, soy bean phosphatidylcholine; NaC, sodium cholate; NaDC, sodium deoxycholate.

The ΔH^T values for the monomer transfer into a micelle are much more negative than for a bile salt monomer from water to a lipid bilayer phase. The comparison of the Gibbs free energy changes shows that ΔG^T for the micellization process (transfer of a detergent monomer to its micelle) is in the range of -20 to $-26\,kJ\,mol^{-1}$ and thus less negative than ΔG^T for the transfer to bilayers.

From the temperature dependence of the transfer enthalpy ΔH^T for the partitioning process, the change in heat capacity $\Delta C_p = \left(\partial \Delta H^T / \partial T\right)_p$ can be calculated. The temperature dependence of ΔH^T is caused by a negative ΔC_p when the hydrophobic surface exposed to water is decreased when transferring the molecule into an apolar environment (36). The ΔC_p data are more negative for NaDC compared to NaC. Furthermore, an increase of the ionic strength makes ΔC_p considerably more negative (17).

Analyzing the temperature dependency of the transfer enthalpy, it can be concluded that the change in exposed hydrophobic surface area is smaller for the transfer of bile salt molecules into a lipid phase compared to a micellar phase. As described previously (17), it is possible that a partial compensation of this effect occurs due to the exposition of hydrophobic surfaces in the lipid molecules when the detergents are incorporated and perturb the bilayer by forming a mixed vesicular system.

Physicochemical Characterization of Mixed Vesicles and Mixed Micelles

The most prominent biophysical methods used for the physicochemical characterization of MVs and MMs, respectively, for analyzing the transition from one aggregation state to another are fluorescence spectroscopy, photon-correlation spectroscopy (PCS), small-angle X-ray scattering (SAXS), and small-angle neutron scattering (SANS). Additionally, methods enabling the direct visualization of the analyzed mixed systems as FFEM (Fig. 5) or cryo-transmission electron microscopy (cryo-TEM) are effective techniques (37–39). The introduction of cryo-TEM allows direct observation of lipid vesicles in their hydrated form (Fig. 8) and allows conclusions with respect to the lamellarity of the formed vesicular systems without latent ambiguity.

Fluorescence Spectroscopy

Fluorescence depolarization measurements (41,42) in lipid membranes labelled with the rod-like apolar probe 1,6-diphenyl-1,3,5-hexatriene (DPH) can be used to follow the transition from MVs to MMs. The quantity $r_S = (I_{VV} - I_{VH})/(I_{VV} + 2 \cdot I_{VH})$, the steady state fluorescence anisotropy, describes the depolarization of the exciting light. I_{VV} and I_{VH} are the fluorescence intensities measured parallel and perpendicular to the vertically polarized exciting beam. The extent of depolarization of the emitted
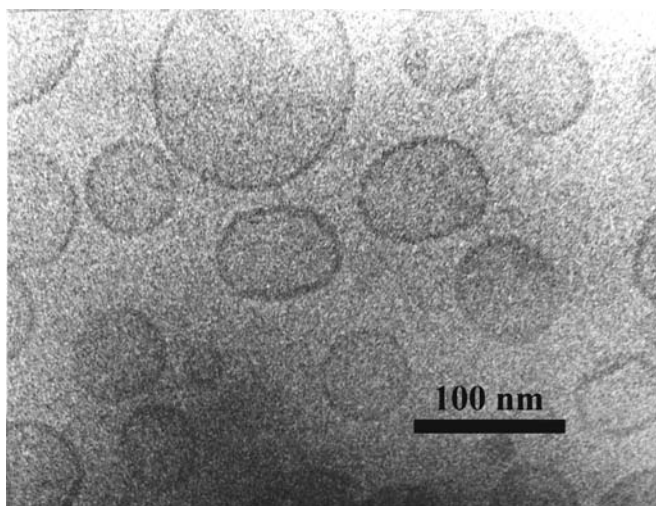
Figure 8 Lipid vesicles made from human stratum corneum lipids by octylglucoside depletion (dialysis). Monolamellarity is clearly seen. Specimen were shock-frozen by plunging them into liquid ethane and transferred to a Zeiss CEM 902, equipped with cryo-stage (90 K, accelerating voltage 80 kV and a beam current of 12 µA). *Source*: From Ref. 40.

fluorescence of a "reporter fluorophore" (like DPH) reflects the degree to which a subpopulation of photo selected excited fluorophores loses its selected orientation and becomes randomized (photoselection is the selective excitation of absorption dipoles parallel to the electric vector). This process is dependent on molecular order and the dynamics of lipid chains. The steady state anisotropy is the sum of two components, $r_S = r_f + r$, a fast-decaying component, r_f, which can be measured only by the time resolved nanosecond technique (43), and an infinitely slow-decay component, r. The slow-decay component is proportional to the square of the lipid order parameter. Van Blitterswijk et al. (44) derived an empirical relation between r_S and r based on the extended Perrin equation describing the restricted rotational dynamics of fluorophores. One can identify the probe order parameter with the lipid order parameter S_{middle} due to the fact that DPH is deeply located in the bilayer in a mean position along the lipid chain. Thus, the lipid order parameter in membranes titrated with detergents can be obtained in a good approximation from steady state fluorescence anisotropy measurements using DPH (28). In pure Egg Phosphatidyl cholinle (EPC) vesicles, r_S is rather low ($r_S = 0.14$, Fig. 9) and drops if detergent is incorporated into the bilayer. Whether or not detergents like octylglucoside induce a titration curve with decreasing r_S values for the transition from MVs to MMs (Fig. 9) depends on the structure of the formed MMs. Other
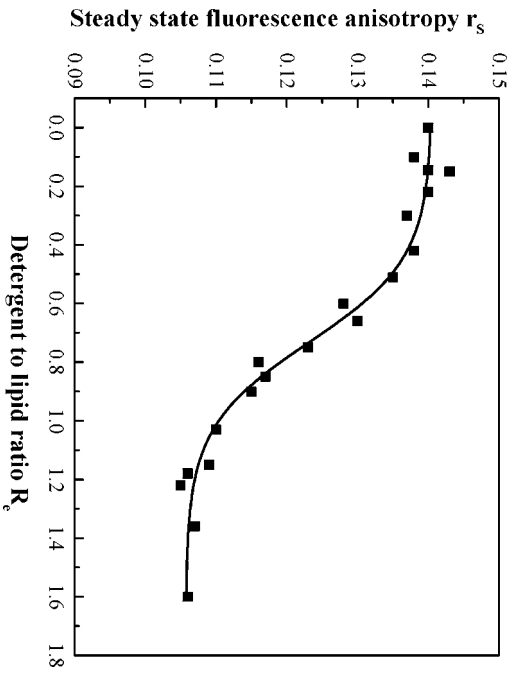
Figure 9 Stead-state fluorescence anisotropy of DPH incorporated into s... EPC vesicles and titrated with octylglucoside. Probe/lipid ratio = 3... concentration = 0.64 mM, Aminco SPF-500 spectrofluorimeter (E_x = 360 n... 430 nm). *Source:* From Ref. 28.

detergents, like Triton™ X-100, and bile salts increase the lipid ord... meter at onset of "micellar solubilization" (28,38,38,43). This sug... improvement of the packing behavior of phospholipids molecules ... with certain detergents.

Photon Correlation Spectroscopy

Dynamic light scattering, also known as photon correlation spect... PCS (45,46) is an easy-to-perform technique to measure with high se... particle sizes. The basic principles are described in an excellent pa... The intensity of light scattered in a particular direction by parti... solution tends to periodically change with time. These fluctuation... intensity versus time profile are due to Brownian motion. From the... of intensity fluctuations a correlation function is derived. This expo... decay function is analyzed for characteristic decay times. The hydro... particle radii (R_i) are related to the diffusion coefficients (D_i) ac... to the Stokes–Einstein relationship for spheres, $R_i = k \cdot T/6$... Boltzmann constant; T, temperature; η, viscosity coefficient). Co... the fact that the transition from micelles to vesicles occurs via a nu... mixed intermediates adopting different particle sizes and shapes (1... one must be well aware of the strengths and weaknesses of this te... Three situations have to be considered: (i) uniform parti...
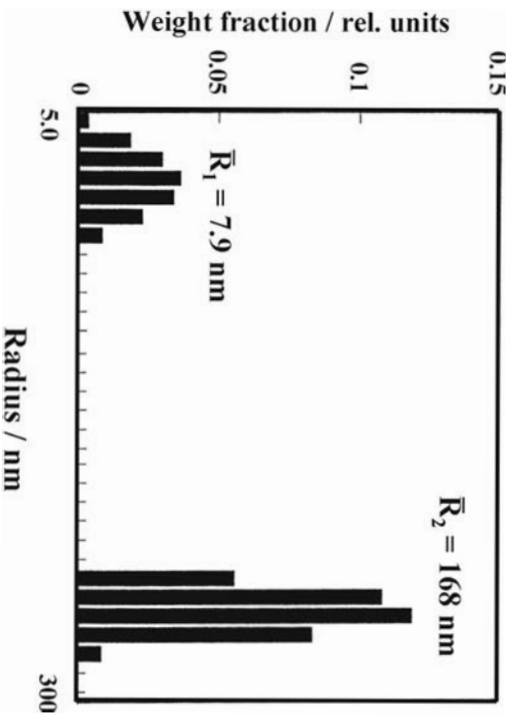
Figure 10 Bimodal distribution of mixed aggregates of octyl glucoside lecithin in the coexistence region of mixed vesicles and mixed micelles. R corresponds to mixed micelles and R2 (mean) to mixed vesicles. Measurer a homemade particle sizer at 20°C, wavelength 632.8 nm, scattering angle autocorrelation functions were calculated by a multibit multiple-τ correla were analyzed online by the CONTIN program of Provencher. *Source:* Fron

(trivial analysis); (ii) broad unimodal distribution (Gaussian analy (iii) multimodal distribution (distribution analysis). As mentione in PCS photons of scattered light are always counted normalized a digital autocorrelation function recorded.

Uniform Particle Size: the correlation function is $C(t) = A$ ex $+ B$, where t' is the delay or sampling time, τ the half-time of c the correlation function, A and B are constants calculated fr intensities of scattered light. Because $1/\tau = 2DK^2$ follows $D = (1/2K$ where $K = (4\pi n/\lambda) \sin \Phi/2$ is the scattering wave vector, relating the tion function to the index of refraction of the solvent (n), the wavele and the scattering angle (Φ). According to this, $\ln(C(t) - B) = \ln A -$ The slope yields the diffusion coefficient D_i and via the Einstei relationship, the hydrodynamic radius R_h is obtained.

Broad Unimodal Particle Size Distribution: This simple size tion needs an analysis taking into account a nonexponential beh $C(t') - B$. This is the method of cumulants. In the case of an unimo metric distribution (Gaussian) light intensity-weighted diffusivities a sured. From this analysis two parameters of the Gaussian dist D_{mean} and the standard deviation, ΔD are obtained. In terms of cu

up to the second order we have $1/2\ln(C(t') - B) = a_0 + a_1(t') + a_2(t'2)$ ΔD is related to the coefficient a_2, which describes the extent of the curvature in the data. The best quadratic fit to the logarithm of the data yields $a_1 = -D_{mean}K^2$ or $D_{mean} = -a_1/K^2$ and $\Delta D/D_{mean} = 2a_2/(-a_1)$, which is the coefficient of variation describing the width of the distribution and which is identical with the poly dispersity index PI.

Multimodal Particle Size Distribution: It yields typically three to four independent parameters (bimodal). $C(t')$ is replaced by a weighted sum of individual exponentially decaying functions (one for each particle size distribution): $C(t') = A\left[\sum f_i \exp(-D_iK^2t')\right]^2 + B$. This equation is a discrete representation of an integral equation known as Laplace transform. The inverse Laplace transform yields the weighting coefficients f_i. Such a method has been developed by Provencher and is known as CONTIN program (47).

Light scattering is weighted by the intensity of scattered light that varies as the sixth power of the diameter. A few large particles can dominate the scattered light signal obscuring the presence of small particles. The amount of particles is often given as either their number or volume (mass). Although it is a simple matter to write the equations for converting one type of weighting to another, the results calculated this way are often in error and the percentage of each particle population changes dramatically.

In addition, calibration with mono- and polydisperse latex standards of known nominal size is mandatory. A favorable situation was found to be the titration of unilamellar vesicles, which were produced by the extrusion technique from egg lecithin, with Triton X-100. At a R_e of 2.0, the coexistence region of MVs and MMs, a bimodal distribution with well-separated peaks could be observed by dynamic light scattering (Fig. 11).

Small-Angle Scattering Techniques

Small-angle scattering techniques (48–53) using X ray (SAXS) or neutrons (SANS) are powerful analytical methods for the examination of colloidal systems in solution, due to the fact that these methods offer the possibility to analyze colloidal systems without disturbing their natural environment. From the obtained scattering data, different interesting information can be derived like the internal morphology of colloidal systems, aggregation properties, supra molecular architecture of micelles, size and shape of the colloidal particles, interaction between different particles, etc. For colloidal systems with typical dimensions between 1 and 300 nm, the interesting region of scattering falls between 0.001° and 1°. Therefore, the method is termed small-angle scattering. During the scattering experiment, a scattering length density is obtained. In the case of X-rays, this is simply the electron density. Important is not the absolute density, but the difference between the colloidal system and the surrounding medium, the contrast (increased by using deuterated media). Data as obtained from SAXS or SANS are

Increase of detergent concentration

(A) (B) (C) (D) (E) (F) (G)

● ⊂ Lipid
○ ~ Detergent
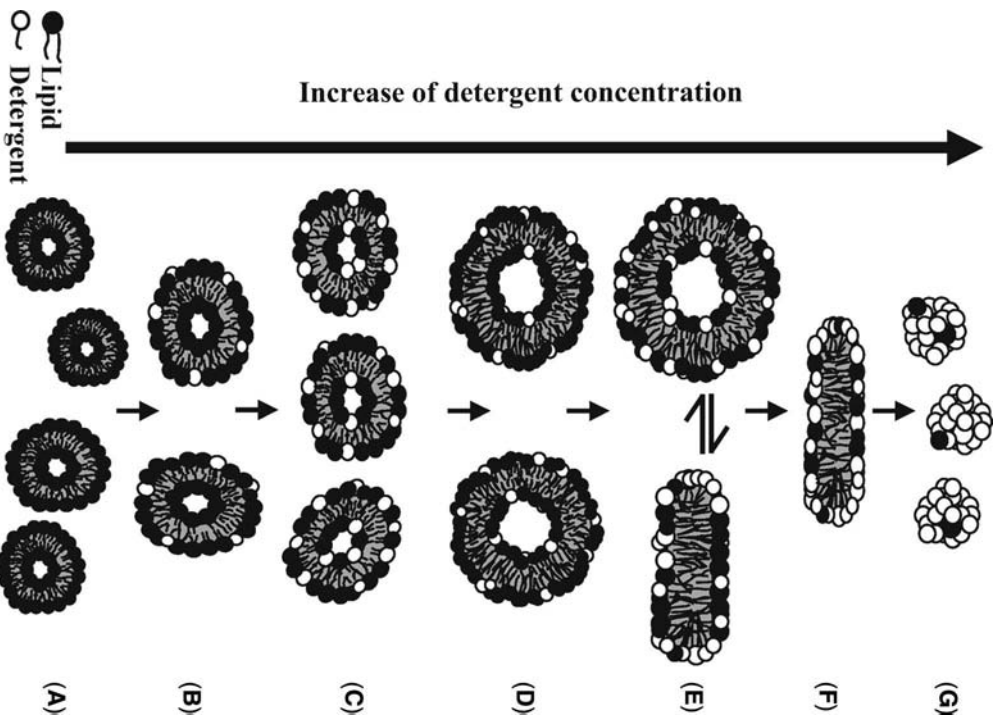
Figure 11 Schematic representation of the different structures occurring d transition from vesicles to mixed micelles (for more details, see text).

analyzed through the modelling of the colloidal form factor and int function, as well as by means of the distance distribution function [details see Winter and Noll (45)].

Long et al. (52), used SANS and dynamic light scattering for t acterization of the aggregates formed upon dilution of mixed leci salt micelles. They found that the micelles adopt cylindrical or and elongated structures upon dilution. Using these methods, th able to show that the transition from micelles to vesicles is a

transformation involving a region (Fig. 7) where micelles and vesicles coexist (52). The used SANS measurements are more sensitive to the presence of, e.g., two aggregate populations than the dynamic light scattering method.

The study of binary lipid-detergent phase diagrams at constant lipid concentration but with varying detergent-to-lipid ratio or temperature has shown that several intermediate pseudophases could be encountered before the biphasic vesicle to micelle equilibrium wasreached (50).

Thermodynamic Stability Considerations and Phase Diagrams

The incorporation of low amounts of detergent in lipid vesicles leads to the formation of MVs as illustrated in Figure 11A–D. Increasing the detergent concentration induces a saturation of the lipid membrane with detergent (saturation process). At a certain detergent concentration, the MVs become unstable and structural changes are observed, inducing the solubilization of the vesicles (solubilization process). MVs are transformed into MMs (Fig. 11E–G). Depending on the amount of detergent available, different micellar phases and structures are formed (54–56).

Using ITC, a so-called detergent-versus-lipid phase diagram can be constructed (Fig. 7). The arrow #2 in Figure 7 describes the solubilization protocol used for analyzing the stability of the mixed systems. The detergent concentration where vesicle solubilization occurs is dependent on the total concentration of lipid vesicles, as the scheme in Figure 7 shows. At higher lipid concentrations, a surfactant concentration higher than the *cmc* is needed.

The effective molar (e) detergent to lipid ratio R_e: $R_e = D_b/L$ describes the composition of the mixed aggregates (L is the lipid concentration and D_b the detergent concentration in the mixed aggregates).

The total detergent concentration is expressed as $D_t = D_w + D_b$, with D_w is the detergent concentration in the aqueous and D_b in the bilayer phase. The relation between D_t and R_e is given as:

$$D_t^{\#} = R_e^{\#} \cdot L + D_w^{\#}$$

where "#" means "sat" and "sol," respectively. The effective detergent/lipid ratios R_e for the saturation and the solubilization of the vesicles can be determined from the slopes of the straight lines indicating the phase boundaries that are obtained from linear least square fits of the experimental data for D_t^{sat} and D_t^{sol}. The intercepts, D_w^{sat} and D_w^{sol}, established by extrapolation of the phase boundaries to a lipid concentration $L = 0\,mM$, correspond to the hypothetical detergent concentration of aggregation in the presence of phospholipid vesicles and are the minimal detergent concentration required for the solubilization of lipid membranes.

The heat flow of an ITC experiment showing the titration of a micellar detergent solution above the *cmc* into a vesicle dispersion is represented in

Figure 12A. Three different regions are observed. The first region is characterized, in the presented case, by continuous endothermic heat flow versus time. In this range, the detergent concentration in the cell remains lower than the critical concentration for membrane solubilization. Thus, in this concentration range, the peaks are caused by the demicellization process of the pure micelles followed by the incorporation of the monomers into the lipid membrane. The observed reaction enthalpy in Figure 12A is the sum of the demicellisation enthalpy and the partitioning enthalpy of the detergent monomers from water to the lipid membrane, the latter multiplied by the fraction of bile salts partitioning into the bilayers.
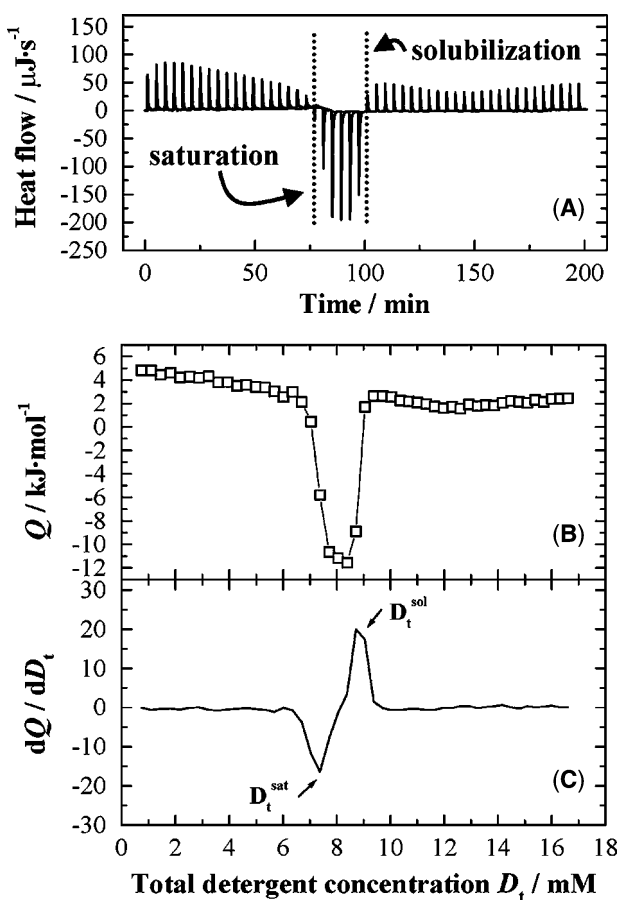
Figure 12 Typical solubilization experiment representing the titration of a micellar solution into a vesicle dispersion at a constant temperature. (**A**) Calorimetric traces, (**B**) normalized titration heat Q versus total detergent concentration in the cell D_t, (**C**) first derivative of curve (**B**).

As more and more detergent is titrated to the vesicular dispersion, a sudden change of the enthalpic effects is observed. Large exothermic reaction heats are observed (Fig. 12A). At the beginning of this range, the free concentration of detergent in the cell reaches a critical concentration at which the bilayer membrane becomes saturated with detergent molecules and is unable to incorporate more detergent in the bilayer. At this concentration D_t^{sat}, the detergent saturated MVs of the composition R_e^{sat} start to disintegrate and form mixed lipid detergent micelles of the composition R_e^{sol}. With increasing amount of detergent concentration, this equilibrium is shifted toward the mixed micellar structures (Fig. 11). As can be seen from Figure 12B, the observed reaction enthalpies are constant in this range. This is in accordance with the phase rule approximation, which predicts that the reaction enthalpies are constant over the whole coexistence range.

Further addition of detergent induces a second drastic change and smaller endothermic peaks are observed at the end of the titration (region three). During the titration experiment the second phase boundary detected corresponds to the complete disintegration and transformation of MVs to MMs. Above this concentration, only MMs occur in the sample in coexistence with detergent monomers (Fig. 7). The reaction enthalpy observed in this range is therefore the heat measured for the equilibration of injected pure micelles with MMs in the sample cell.

The solubilization of DPPC vesicles induced by NaC (100 mM NaCl, pH 7.5, $T = 60°C$) is exemplarily shown in Figure 12. Integration of the peaks yields the molar titration heat Q as a function of the total detergent concentration D_t in the sample cell (Fig. 12B). The two breakpoints in the titration curve correspond to points on the phase boundaries of the coexistence range. The specific values for saturation (D_t^{sat}) and solubilization (D_t^{sol}) i.e., points on the phase boundaries, are usually determined from the extreme values of the first derivative curve (Fig. 12C).

Resulting phase diagrams for the solubilization of SBPC, POPC, and DPPC dispersed in 100 mM NaCl (pH 7.5) at $T = 60°C$ (liquid crystalline phase) by NaC are summarized in Figure 13.

It can be clearly seen that the detergent amount required for the solubilization of saturated phospholipids is much lower compared to the amount needed for the formation of MMs composed of unsaturated phospholipids. The lowest NaC detergent amount necessary for the induction of DPPC solubilization and thus formation of MMs is ∼6 mM. Below the saturation curve only MVs are present, whereas above the solubilization only MMs are found, in addition to monomers (Fig. 7).

The breakdown of a lipid vesicles and the formation of MMs depend on the nature and length of the hydrocarbon chains. Thus it appears as if saturated PC are more susceptible to transformation into MMs than PCs with unsaturated chains, which prefer surfaces with negative spontaneous curvature.
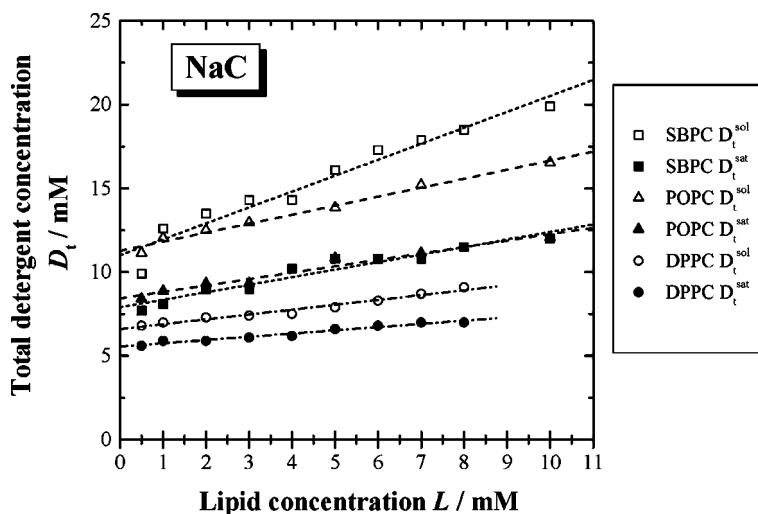
Figure 13 Phase diagrams for the vesicle-to-micelle transition for sodium cholate (NaC) and various phospholipid systems (DPPC: dipalmitoyl phosphatidylcholine, POPC: palmitoyl oleoyl phosphatidylcholine, SBPC: soy bean phosphatidylcholine) in 100 mM NaCl at $T=60°$ C; D_t^{sat} and D_t^{sol} open symbols, dashed lines: R_e^{sat} and R_e^{sol} values obtained from linear last square fits of the experimental data (see text). D_w^{sat} and D_w^{sol} values are obtained from the extrapolation to $L=0$ mM

There is a clear difference between the trihydroxy bile salt NaC and NaDC with only two hydroxyl groups per molecule with respect to the detergent concentration, which is necessary for the onset of the phase transition. A considerably smaller detergent concentration is necessary for the solubilization of DPPC membranes with the more hydrophobic NaDC than with NaC (data not shown).

The value describing the ratio between detergent and lipid in the mixed system R_e at the phase boundary can be quite different. The comparison of R_e-values of nonionic detergents with ionic detergents shows large differences (Table 3). For both bile salts, R_e-values are much smaller and the difference between R_e^{sat} and R_e^{sol} is also very small, compared to nonionic detergents. For OG/DMPC systems studied by Keller (19), the following values were found: $R_e^{sat}=1.66$ and $R_e^{sol}=2.03$ at 70° C and for $C_{12}EO_6$/ POPC systems investigated by Heerklotz et al. (32,33) $R_e^{sat}=1.45$ and $R_e^{sol}=5.0$ at 25°C. For NaC and NaDC, however, the R_e values are in the range from 0.03 to 0.2. That means that the saturation limit is reached at a very low effective bile salt concentration in the bilayer, a much lower concentration than needed with alkyl glucosides, for instance.

It is also found that the required detergent concentration for the solubilization is significantly lower for lipids with shorter hydrocarbon chains

Table 3 Different Detergent to Lipid Ratio R_e for the Saturation and Solubilization Process

System (water, pH 7)	R_e^{sat}	R_e^{sol}
OG/DMPC (70°C)	1.66	2.03
OG/DPPC (70°C)	1.49	1.90
OG/DSPC (70°C)	1.30	2.51
OG/DAPC (70°C)	1.2	2.4
$C_{12}EO_6$/POPC (25°C)	1.45	5.0
DM/DMPC (70°C)	0.8	1.2
DM/DPPC (70°C)	0.8	1.3
DM/DSPC (70°C)	0.9	1.7
DM/DAPC (70°C)	0.9	1.9
NaC/DPPC (60°C)	0.15	0.25
NaDC/DPPC (60°C)	0.2	0.3

Abbreviations: DMPC, dimyristoyl phosphatidylcholine; DPPC, dipalmitoyl phosphatidylcholine; DSPC, distearoyl phosphatidylcholine; DAPC, diarachidoyl phosphatidylcholine; OG, 1-*O*-octyl-β-ᴅ-glycopyranoside; DM, 1-*O*-dodecyl-β-ᴅ-maltoside; NaC, sodium cholate; NaDC, sodium deoxycholate.

[e.g., dimyristoyl phosphatidylcholine (DMPC)] compared to a lipid analogue with a longer acyl chain length, although with identical head group (e.g., DPPC) (31).

Comparing the R_e data of the DMPC/NaDC system, it is found that the slopes of the phase boundaries are smaller and almost identical ($R_e \sim 0.065$). This implies that the amount of detergent in the MVs and micelles is even lower for the PC with the C_{14} chains compared to C_{16} analogue on. As already mentioned above, PCs with saturated chains are more susceptible to solubilization than their counterparts with unsaturated chains and, in addition, bilayers with the shorter chain PCs are even more unstable. Thus MMs are formed more easily. This can be explained by the fact that it is easier to form positively curved surfaces as they occur in micelles with saturated phospholipids, particularly when their chain length is short. Unsaturated lipids have in general the tendency for negative spontaneous curvature. Therefore, unsaturated PCs are more stable toward transformation into micelles with their positively curved interface.

PHARMACEUTICAL ASPECTS OF MIXED VESICLES AND MIXED MICELLES

Since about 100 years, ago, it has been known that the presence of bile acids enhances the lipid absorption (57). Dietary lipids like triglycerides are hydrolyzed by pancreatic lipase to fatty acid and 2-monoglycerides. These

molecules are rather insoluble under physiological *pH* conditions. It was found, that the ability of bile acids to solubilize these lipolysis products is related to the formation of mixed micellar structures (56,58). This concept was further investigated and studied in the last few years to develop colloidal drug delivery systems, especially for the solubilization of hydrophobic drugs.

Various toxicological, safety, and in vivo studies have shown that bile salts, especially formulated with phosphatidylcholine, can be used for the development of drug delivery systems, especially for the solubilization of hydrophobic drugs (57,59–62). The bile salt micelles solubilization effect of various drugs has been reviewed recently by Wiedmann and Kamel (63). In particular, the availability of the used excipients produced under GMP conditions and thus available at pharmaceutical grade make it possible to use these excipients for human applications.

Berry et al. (64) have described the anticoagulant properties of a mixed micellar formulation composed of an equimolar amount of sodium glycocholate and egg lecithin, administered subcutaneously to rats, rabbits, dogs and primates. They found that such a formulation has beneficial effects (e.g., enhanced solubility of argatroban) and that it can be used for subcutaneous administration. Rotunda et al. (65) have used the detergent effect of NaDC in phosphatidylcholine injections for the localised dissolution of fat. MMs are also used for the development of contrast agents (66).

Efforts were undertaken to design emulsion vehicles based on bile salt and lecithin for the formulation of paclitaxel (67).So-called bilosomes (bile salt stabilized vesicles) were developed as a drug delivery system for oral applied vaccines (68,69).Mixed systems containing phospholipids and a bile salt have also been used for the preparation of amphotericin B formulation for oral use or intravenous injections (70–72). Even MMs containing depot formulations loaded with diclofenac diethyl ammonium were investigated with respect to their release characteristics (73–75).As described in the introduction, mixed micellar and mixed vesicular systems are still evaluated as drug delivery systems for topical applications (3–5,40,76).

Various marketed products containing a bile acid and a phospholipid are nowadays available. Konakion® MM is a liquid dosage form (ampoule) containing as active ingredient phytomenadione (synthetic vitamin K_1) formulated with glychocholic acid, lecithin, sodium hydroxide, hydrochloric acid and water for injection (77). A similar formulation (glychocholic acid, lecithin) is found in the product Valium® MM. Cernevit® MM is available as a lyophilisate for parenteral use containing per vial 140 mg glycocholic acid and 140 mg soybean phosphatides in addition to 250 mg glycine and sodium hydroxide and hydrochloric acid (78). The pharmacological properties of Cernevit MM are based on the balanced association of all water soluble and fat soluble vitamins essential for the metabolism of the adult and child aged over 11 years (with the exception of vitamin K). These are just a few examples of the use of

mixed system for pharmaceutical applications. One major challenge for the development of these galenic forms is the preparation of stable mixed systems.

CONCLUSIONS

Different concepts are used for the development of colloidal systems with the focus to generate smart drug delivery systems for pharmaceutical applications. The presented chapter describes the formation and stability of MVs and MMs, composed of various amounts of lipid and detergent. The ''pure'' systems, vesicles and micelles, are only briefly described (it is referred to other chapters of this book) for a better understanding of the formation of the mixed systems. Using mixed aggregates as a drug delivery system imposes a comprehensive physicochemical characterization of the relevant nanocarrier.

Various biophysical techniques (electron microscopy, fluorescence spectroscopy, PCS, SAXS or SANS) for the characterization of MVs and MMs are presented. The focus of the biophysical methods lies on ITC, because described much information with respect to thermodynamic stability can be derived from ITC data. From the presented calorimetric ITC experiments, e.g., the critical aggregation concentration, partition coefficients, changes in transfer enthalpy, thermodynamic parameters like the change in Gibbs free energy, and the change in enthalpy or entropy are obtained. Additionally, a so-called lipid-versus-detergent phase diagram is derived indicating the coexistence lines of the different phases in equilibrium during the solubilization of vesicles. At the end of this contribution, the relevance of mixed systems (especially formulated with bile salts) for pharmaceutical applications is briefly considered, and a few marketed products are presented.

ACKNOWLEDGMENTS

REFERENCES

1. Moroi Y. Micelles. Theoretical and Applied Aspects. New York and London: Plenum Press, 1992.
2. Larsson K. Lipids - Molecular Organization, Physical Functions and Technical Applications. Vol. 5.Dundee The Oily Press Ltd, 1994.
3. Cevc G. Lipid vesicles and other colloids as drug carriers on the skin. Adv Drug Del Rev 2004; 56:675.

4. Bouwstra JA, de Graaff A, Groenink W. Honeywell L. Elastic vesicles: interaction with human skin and drug transport. Cell Mol Biol Lett 2002; 2:222.

5. Cevcs G. Transdermal drug delivery of insulin with ultradeformable carriers. Clinical Pharmacokinetics 2003; 42:461.

6. Honeywell-Nguyen PL, Gooris GS, Bouwstra JA. Quantitative assessment of the transport of elastic and rigid vesicle components and a model drug from these vesicle formulations into human skin in vivo. J Invest Dermatol 2004; 123(5):902.

7. Almgreen M. Mixed micelles and other structures in the solubilisation of bilayer lipid membranes by surfactants. Biochim Biophys Acta 2000; 1508:146.

8. Israelachvili J. Intermolecular and Surface Forces. 2nd ed. London Academic Press, 1992.

9. Gladyshev GP. Thermodynamic trend in biological evolution. Biol Bulletin 1995; 22:1.

10. Blume A, Garidel P. Lipid model membranes and biomembranes. In: Gallagher PK, Kemp RB, series, eds. The Handbook of Thermal Analysis and Calorimetry. From Macromolecules to Man. Vol. 4. 1st ed. Amsterdam: Elsevier, 1999:109–173.

11. Tanford C. The Hydrophobic Effect: Formation of Micelles and Biological Membranes. 2nd ed. New York: Wiley, 1980.

12. Widom B, Bhimalapuran P, Koga K. The hydrophobic effect. Phys Chem Chem Phys 2003; 5:3085.

13. Finney JL. The Structural Basis of the Hydrophobic Interaction. Hydration Processes in Biology. Bellissent-Funel: IOS Press, 1999:115–124.

14. Garidel P, Hildebrand A, Blume A. Understanding the self-organisation of association colloids. MicroCal application note, 2004.

15. Garidel P, Hildebrand A. Thermodynamic properties of association colloids. J Therm Anal Calorimetry 2005; 82:483.

16. Keller M, Kerth A, Blume A. Thermodynamics of interaction of octyl glucoside with phosphatidylcholine vesicles: partitioning and solubilisation as studied by high sensitivity titration calorimetry. Biochim Biophys Acta 1997; 1326:178.

17. Garidel P, Hildebrand A, Neubert R, Blume A. Thermodynamic characterization of bile salt aggregation as a function of temperature and ionic strength using isothermal titration calorimetry. Langmuir 2000; 16:5267.

18. Hildebrand A, Garidel P, Neubert R, Blume A. Thermodynamic of demicellisation of mixed micelles composed of sodium oleate and bile salts. Langmuir 2004; 20:320.

19. Keller M. Thermodynamik der Demizellisierung und Solubilisierung von Alkylglucosiden mit ausgewählten Phospholipiden sowie das rheologische Verhalten der Solubilisierung am Beispiel Octylglucosid/Dimyristoylphosphatidylglyzerol. Ph.D. thesis. Universität Kaiserslautern, Germany, 2001.

20. Hildebrand A. Physikochemische Charakterisierung von Gallensalz-Mischmizellen als Grundlage für innovative Arzneistoffträgersystemen. PhD. Thesis, Martin Luther Universität Halle/Wittenberg, 2002.

21. Lasch J, Weissig V, Brandl M. Preparation of liposomes. In: Torchilin, Weissig, eds. Liposomes. 2d ed. New York: Oxford University Press, 2003:3–29.

22. Schubert R. Relationship between the structure of bile salts and their interaction with membrane lipids. Proc MoBBEL 1989; 4:1.

23. Lasic DD. The mechanism of vesicle formation. Biochem J 1988; 256:1.

24. Lasic DD, Liposomes: From Physics to Application. In: Lasic ed. Amsterdam: Elsevier, 1993.
25. Andelman D, Koszlov MM, Helfrich W. Phase transition between vesicles and micelles driven by competing curvatures. Europhys Lett 1994; 25:231.
26. Nozaki Y, Lasic DD, Tanford JA. Size analysis of phospholipid vesicle preparations. Science 1982; 217:366.
27. Vinson PK, Talmon Y, Walter A. Vesicle-micelle transition of phosphatidylcholine and octylglucoside elucidated by cryo-transmission electron microscopy. Biophys J 1989; 56:669.
28. Lasch J. Interaction of detergents with lipid vesicles. Biochim Biophys Acta 1995; 1241:269.
29. Kuchinka E, Seelig J. Interaction of melitin with phosphatidylcholine membrane. Binding isotherm and lipid head-group conformation. Biochemistry 1989; 28:4216.
30. Gouin S, Zhu XX. Fluorescence and NMR studies of the effect of a bile acid dimmer on the micellisation of bile salts. Langmuir 1998; 14:4025.
31. Hildebrand A, Neubert R, Garidel P, Blume A. Bile salt induced solubilization of synthetic phosphatidylcholine vesicles studied by isothermal titration calorimetry. Langmuir 2002; 18:2836.
32. Heerklotz HH, Lantsch G, Binder H, Klose G, Blume A. Application of isothermal titration calorimetry for detecting lipid membrane solubilisation. Chem Phys Lett 1995; 235:517.
33. Heerklotz HH, Binder H, Lantsch G, Klose G, Blume A. Lipid/detergent interaction thermodynamics as a function of molecular shape. J Phys Chem 1997; 101:639.
34. Hildebrand A, Beyer K, Neubert R, Garidel P, Blume A. Temperature dependence of the interaction of cholate and deoxycholate with fluid model membranes and their solubilisation into mixed micelles. Colloids Surf B 2003; 32:335.
35. Hildebrand A, Beyer K, Neubert R, Garidel P, Blume A. Solubilization of negatively charged DPPC/DPPG liposomes by bile salts. J Colloid Interface Sci 2004; 279:559.
36. Garidel P, Blume A. The interaction of alkaline earth cations with the negatively charged phospholipid 1,2-dimyristoyl-sn-glycero-3-phosphoglycerol: a differential scanning and isothermal titration calorimetric study. Langmuir 1999; 15:5526.
37. Schubert R, Schmidt KH. Structural changes in vesicle membranes and mixed micelles of various lipid compositions after binding of different bile salts. Biochemistry 1988; 27:8787.
38. Schubert R. Gallensäure-Membran-Wechselwirkung. Proc MoBBEL 1987; 2:29.
39. Schubert R, Beyer K, Wolburg H, Schmidt KH. Structural changes in membranes of large unilamellar vesicles after binding of sodium cholate. Biochemistry 1986; 25:5263.
40. Schmidtgen MC, Drechsler M, Lasch J, Schubert R. Energy-filtered cryotransmission electron microscopy of liposomes prepared from human stratum corneum lipids. J Microscopy 1998; 191:177.
41. Valeur B. Molecular Fluorescence. Principles and Applications. Wiley-VCH, 2003.
42. Lakowicz JR. Principles of Fluorescence Spectroscopy. 2nd ed. New York: Kluwer Academic Plenum Publisher, 1999.

43. Lasch J, Schubert R. The interaction of detergents with liposomal membranes. In: Gregoriadis G. ed. Liposome Technology. Vol. II. 2nd ed. CRC Press, 1993:233–260 (Chapter 14).

44. Van Blitterswijk WJ, Van Hoeven RP, Van der Meer BW. Lipid structural order parameters (reciprocal fluidity) in biomembranes derived from steady-state fluorescence polarization measurements. Biochim Biophys Acta 1981; 644(2):323.

45. Winter R, Noll F. Methoden der Biophysikalischen Chemie, Teubner Studienbücher Chemie, Stuttgart, 1998.

46. NICOMP, Model 370, Submicron Particle Sizer, Version 5.0, Instruction Manual, 1989.

47. Provencher SW. CONTIN: A general purpose constrained regularization program for inverting noisy linear algebraic and integral equations. Comput Phys Commun 1982; 27:229.

48. Galantini L, Giglio E, Pavel NV, Punzo F. QELS and X-ray of two dihydroxy bile salt aqueous solutions. Colloids Surf A 2004; 248:79.

49. Dingenouts N, Ballauff M. Structural investigation of latexes by small angle X-ray scattering: measurements and evaluation of data. Acta Polymerica 1998; 49:178.

50. Ollivon M, Lesieur S, Grabielle-Mandelmont C, Paternoster M. Vesicle reconstitution from lipid-detergent mixed micelles. Biochim Biophys Acta 2000; 1508:34.

51. Alami E, Abrahmsén-Alami S, Eastoe J, Grillo I, Heeman RK. Interactions between a non-ionic Gemini surfactant and cyclodextrins investigated by small-angle neutron scattering. J Colloid Interface Sci 2002; 255:403.

52. Long MA, Kaler EW, Lee SP. Structural characterisation of the micelle-vesicle transition in lecithine-bile salt solutions. Biophys J 1994; 67:1733.

53. Yue B, Huang CY, Nieh MP, Glinka CJ, Katsara J. Highly stable phospholipid unilamellar vesicle from spontaneous vesiculation: a DLS and SANS study. J Phys Chem B 2005; 109:609.

54. Lichtenberg D. Characterisation of the solubilisation of lipid bilayers by surfactants. Biochim Biophys Acta 1985; 821:470.

55. López O, Cócera M, Wehrli E, Parra JL, de la Maza A. Solubilisation of liposomes by sodium dodecyl sulfate: New mechanism based on the direct formation of mixed micelles. Arch Biochem Biophys 1999; 367:154.

56. Hjelm RP, Schteingart CD, Hofmann AF, Silvia DS. Form and structure of self-assembling particles in mono-olein-bile salt mixtures. J Phys Chem 1995; 99:16395.

57. Hofmann AL. Bile acids: the good, the bad, and the ugly. News Physiol Sci 1999; 14:24.

58. Hofmann AF, Mysels KJ. Bile salts as biological surfactants. Colloids Surfaces 1988; 10:145.

59. Martine GP, Marriott C. Membrane damage by bile salts: the protective function of phospholipids. J Pharmacy & Pharmacol 1981; 31:754.

60. Wiedmann TS, Liang W, Herrington H. Interaction of bile salts with gastrointestinal mucins. Lipids 2004; 39:51.

61. Kuntsche J, Westesen K, Drechsler M, Koch MH, Bunjes H. Supercooled smectic nanoparticles: a potential novel carrier system for poorly water soluble drugs. Pharm Res 2004; 21:1834.

62. Li CY, Zimmermann CL, Wiedmann TS. Solubilisation of retinoids by bile salt phospholipids aggregates. Pharm Res 1996; 13:907.
63. Wiedmann TS, Kamel L. Examination of the solubilisation of drugs by bile salt micelles. J Pharm Sci 2002; 91:1743.
64. Berry CN, Lunven C, Lecoffre C, et al. Anticoagulant activity and pharmacokinetic properties of a sub-cutaneously administred mixed micellar formulation of argatroban in experimental animals. Thrombosis & Haemostasis, 2000; 84:278.
65. Rotunda AM, Susuki H, Moy RL, Kolodney MS. Detergent effects of sodium deoxycholate are a major feature of an injectable phosphatidylcholine formulation used for localised fat dissolution. Dermatol Surg 2004; 30:1001.
66. Tournier H, Hyacinthe R, Schneider M. Gadolinium-containing mixed micelle formulations: a new class of blood pool MRI? MRA contrast agents. Acad Radiology 2002; 9:S20.
67. Han J, Davis SS. Papandreou,m C, Melia CD, Washington C. Design and evaluation of an emulsion vehicle for paclitaxel. I. Physicochemical properties and plasma stability. Pharm Res 2004; 21:1573.
68. Conacher M, Alexander J, Brewer JM. Oral immunisation with peptide and protein antigens by formulations in lipid vesicles incorporating bile salts (bilosomes). Vaccine 2001; 19:2965.
69. Singh P, Prabakaran D, Jain S, Mishra V, Jaganathan KS, Vyas SP. Cholera toxin B subunit conjugated bile salt stabilised vesicles (biolosomes) for oral immunisation. Int J Pharm 2004; 278:379.
70. Echevarria I, Barturen C, Renedo MJ, Troconiz IF, Dios-Vieitez MC. Comparative pharmacokinetics, tissue distributions, and effects on renal function of novel polymeric formulations of amphotericin B and amphotericin B-deoxycholate in rats. Antimic Agents & Chemother, 44, 898, 2000.
71. Risovic, V, Boyd, M, Choo, E, Wasan, KM. Effects of lipid based oral formulations on plasma and tissue amphotericin B concentrations and renal toxicity in male rats. Antimic Agents & Chemother 2003; 47:3339.
72. Sarbolouki MN, Parsaee S, Kosary P. Mixed micelle proliposomes for preparation of liposomes containing amphotericin B, in-vitro and ex-vivo studies. Pda J Pharm Sci Tech 2000; 54:240.
73. Parsaee S, Sarbolouki MN, Parniannpour M. In-vitro release of diclofenac diethylammonium from lipid based formulations. Int J Pharm 2002; 241:185.
74. Forrest P, Galletly DC. A double-blind comparative study of three formulations of diazepam in volunteers. Anaesth Intensive Care 1988; 16:158.
75. Hendradi E, Obata Y, Isowa K, Nagai T, Takayama K. Effect of mixed micelle formulations including terpenes on the transdermal delivery of diclofenac. Biol & Pharm Bulletin 2003; 26:1739.
76. Simões SI, Marques CM, Cruz MEM, Cevc G, Martins MBF. The effect of cholate on solubilisation and permeability of simple and protein-loaded phosphatidylcholine/sodium cholate mixed aggregates designed to mediate transdermal delivery of macromolecules. Eur J Pharm Biopharm 2004; 58:509.
77. Konakion® data sheet, available online, www.medsafe.govt.nz
78. Cernevit® MM data sheet, online, www.medsafe.govt.nz

12

Vesicular Phospholipid Gels

Martin Brandl

*Department of Pharmaceutics and Biopharmaceutics, Institute of Pharmacy,
University of Tromsø, Breivika, Tromsø, Norway*

Ulrich Massing

*Clinical Research Unit, Tumor Biology Center at Albert Ludwigs University
Freiburg, Freiburg, Germany*

INTRODUCTION

Definitions

Vesicular phospholipid gels (VPGs) were first described in References 1–3.
In the decade since their discovery, they have emerged both as storage-stable
intermediates for small unilamellar vesicles (SUV dispersions) yielding
extraordinarily high encapsulation efficiencies as well as semisolid depot
formulations for sustained release of drugs.

What are VPGs? They are gels formed by phospholipid vesicles. Gels
in the common rheological understanding are systems that do not show
macroscopic flow until an applied mechanical stress reaches a defined criti-
cal value, the yield point. More practically, such systems do not flow under
their own weight, i.e., when turned upside down and entrapped air bubbles
do not float. The specific characteristic of VPGs as compared to other
hydrogels is that the three-dimensional structure (network) responsible for
the gel-like rheological behavior is made up by phospholipid vesicles, rather
than polymeric thickeners. This means in VPGs the vesicles are so tightly
packed that a steric interaction between them occurs. VPGs are, thus, also

different from hydrogel liposome-systems, often called "liposome-gels" (4,5), where a hydrophilic polymer like polyacrylate forms a three-dimensional matrix and liposomes are embedded in this hydrogel-matrix. We also want to point out that VPG is not to be confused with the term "gel phase," which in the context of phospholipid bilayer systems often is employed for phases, where the alkyl chains of the phospholipid are in the crystalline state, i.e., below their phase-transition (melting point) rather than in the fluid state, i.e., above the melting point. VPGs may be formed by phospholipids both in the gel and the fluid state.

HYDRATION AND SWELLING OF PHOSPHOLIPIDS

Lamellar Phases

Phospholipid crystals hydrate and swell instantaneously upon contact with aqueous medium forming lamellar structures, the so-called neat phase, which consists of stacks of swollen planar bilayer sheets. For phosphatidylcholine (PC), hydration of the lipid crystals is completed at a lipid/water–mixing ratio of approximately 55:45 (6). Up to this ratio the water is completely absorbed by hydration of the crystalline phospholipid forming monophasic systems. Above this water/lipid–blending ratio, with increasing water contents, a transition from monophasic to biphasic systems was identified in terms of occurrence of single water droplets and vesicular structures within the lamellar phase (7).

Vesicles

On the other hand, it has long been known that liposome dispersions (vesicles dispersed in a continuous water phase) are formed if phospholipid is dispersed in excess aqueous medium, i.e., at lipid concentrations typically at 1 to 100 mg/g ($\sim$ 1–150 mM). The size of the liposome and lamellarity depend on the level of mechanical stress (stirring, shaking etc.) during the dispersion process. High levels of mechanical stress, e.g., high-pressure homogenization, lead to small and unilamellar vesicles (8).

Vesicular Phospholipid Gels

We could demonstrate that vesicular rather than lamellar structures are formed as well if the hydration of phospholipid crystals with minimal amounts of water is performed under high levels of mechanical stress: upon high-pressure homogenization of phospholipid dispersions, at PC contents as high as 400 mg/g ($\sim$ 500 mM) and above, systems of true vesicular morphology were obtained (9,10). The term "vesicular phospholipid gels" was introduced because such preparations behave like gels (11).

PREPARATION OF VPGs

High-Pressure Homogenization and High-Pressure Filter Extrusion

For preparing VPGs of small and uniform vesicle sizes, high-pressure homogenization is preferred. A detailed protocol for preparing VPGs, which consist of a single phospholipid, is given in Ref. (12). This approach is based on the one-step liposome preparation technique originally described in Refs. (8) and (13). In brief, a crude mixture of dry crystalline phospholipid in buffer or, if applicable, drug solution is processed using a high-pressure homogenizer. Homogenization leads to an ultrafine dispersion of the crystalline lipid in the aqueous phase and instantaneous swelling and formation of vesicles occur (14). Among the lab-scale homogenizers, the APV MicronLab 40 is well suited to prepare VPGs. Our groups reported positive experience with a microfluidizer M110 (not published), but problems have been reported elsewhere (15). For preparing VPGs consisting of two or more lipids, a different approach (12) is recommended, which first transfers the lipids into a solid solution (molecular dispersion) by freeze-drying from an organic solution. This ensures homogeneous distribution of the lipids over the bilayer, which otherwise can only be achieved by extended recirculation through the homogenizer (8). The common thin-film hydration technique is not suited for VPGs due to the relatively high concentrations of lipids present. The homogeneous lipid dispersions are subsequently homogenized as described above to ensure small, uniform vesicular morphology.

By using specially designed high-pressure filter extruders (16), filter extrusion may be carried out on highly concentrated phospholipid dispersions as well. Pressures of up to 10 MPa (100 bar) are used to force the lipid through the filter pores. Results on contrast agent–carrying liposome dispersions of lipid concentrations up to 160 mg/g have been published (16,17) and the authors claim that this approach may be extended up to 400 mg/g lipid dispersions.

Loading of VPGs with Drugs

VPGs, as conventional liposomes, contain both aqueous compartments and bilayer-membrane-compartments suited to accommodate water-soluble and lipid-soluble drugs, respectively. Different approaches have been described to load VPGs with drugs (9,18,19). For hydrophilic drugs, one may choose between *direct entrapment* during the formation of the VPG and so-called *passive loading* into preformed VPGs. For amphiphilic or lipophilic drugs an *incorporation/association* approach is to be used.

Direct Entrapment

Direct entrapment is achieved if the formation of VPGs is carried out in the presence of drug-containing aqueous medium as described in Refs. 3, 9, 12,

and 18. Together with a distinct proportion of the aqueous medium, a distinct fraction of the drug ends up encapsulated within the aqueous core of the vesicles; another fraction is trapped in the aqueous space between the vesicles. The percentage of drug entrapped in the aqueous core and the space between the vesicles is close or even equal to the total amount of drug present (almost 100% entrapment). Upon dilution, the intravesicularly entrapped portion is retained within the vesicles (see below) while the intervesicular portion is set free.

Passive Loading

The process of passive loading was originally described by Massing and coworkers (19). In principle, it comprises the blending of "empty" VPG with concentrated drug solution and subsequent incubation until the drug is equally distributed all over the preparation by diffusion. The method takes advantage of the fact that vesicle bilayers are sufficiently permeable for drugs to allow diffusion into the liposomes within reasonable time spans. When added to preformed "empty" (i.e., drug-free) VPGs, the drug permeates through the bilayers into the vesicles following the concentration gradient until equilibrium between the interior of the vesicles and the surrounding medium is achieved. Gentle warming can further facilitate the equilibration process. For a detailed description of such passive loading processes, see Ref. 12.

Passive loading has certain advantages. Because the active ingredient is not yet present during the preparation of the liposomes, safety precautions that have to be taken when toxic drugs are handled may be minimized. Furthermore, the composition of the aqueous medium used for VPG-preparation on one hand and for the drug solution on the other may be chosen independently with respect to optimum shelf life, e.g., pH 6.5 for VPGs and pH 4 for doxorubicin (20). Drug-induced hydrolytic degradation of liposomal phospholipid as observed, e.g., for Gemcitabine, Camptothecin, and certain nucleotides can be avoided (21,22). This approach is suited for loading VPGs in a bedside preparation as well.

Incorporation/Association

Drugs that are poorly soluble in water but soluble in nonpolar solvents (hydrocarbons) are likely to be incorporated in the liposome membrane. For loading into VPGs, the ideal approach is to treat such lipophilic compounds such as lipids, i.e., to transfer them into a molecular mixture with the lipid components before hydration, e.g., by dissolving drug and lipid(s) in organic solvent and removing the latter by freeze-drying to form a solid solution as described in Refs. 12 and 23. Solvent and process conditions during solvent removal have to be chosen individually for each drug/lipid-combination in order to avoid recrystallization of one of the components and inhomogeneous distribution within the lipid cake and, upon hydration, the bilayer. The amount of hydrophobic drug that can be incorporated in a

VPG preparation is, as with conventional liposome dispersions, dependent on packing restrictions within the bilayer, only that the amount of lipid available for accommodation of the drug is substantially bigger with VPGs. Amphiphilic compounds are usually also treated like lipid compounds. For preparing a VPG containing a lipophilic drug, the binary lipid blends protocol (see above) can be used.

Sterilization of VPGs

Terminal steam sterilization is the method of choice to ensure sterility of aqueous parenteral drug products because it provides the highest sterility assurance levels. Unfortunately, chemical degradation, i.e., hydrolysis of the phospholipid and/or structural rearrangements, vesicle fusion or aggregation, as well as leakage of the drug out of the liposomes do rule out the use of this sterilization technique for conventional liposome dispersions. To limit the hydrolytic degradation of phospholipids to lyso-phospholipids, appropriate choice of buffer composition and pH have been described (24). The leakage of drug substances out of conventional liposomes during autoclaving, however, could not be overcome so far. With VPGs, in contrast, there is no gradient in drug concentration between the core and the water phase surrounding the vesicles and no leakage occurs during autoclaving (25). Structural rearrangements such as fusion to bigger vesicles have been seen with VPGs to a certain degree. This in turn influences their viscoelastic behavior, sustained-release behavior, and encapsulation efficiency and requires stringent monitoring (25). Nevertheless, the results gained so far seem to support the potential use of steam sterilization as an appropriate approach to gain sterile VPGs in many cases.

CHARACTERISTICS OF VPGs

Morphology: Freeze-Fracture Electron Microscopy-Analysis

The morphology of VPGs was investigated systematically by freeze-fracture transmission electron microscopy as described in Refs. 9 and 10. Primarily, the influence of PC-content and mechanical stress on the morphology of highly concentrated phospholipid dispersions was studied. When 40:60 PC/buffer-blends of natural egg or soy PC were prepared by magnetic stirring, i.e., at low mechanical stress conditions, vesicles in tight packing were seen, which were heterogeneous in terms of size and lamellarity. Sizes ranging from 0.1 μm to several microns and concentric lamellae, typical for multilamellar vesicles (MLVs), were observed. When dispersions of identical PC/buffer-ratio (9), prepared by high-pressure homogenization, were visualized, the morphology was quite different: SUVs were seen throughout (with a minute proportion of large multivesicular vesicles only) (10). Furthermore, all homogenized PC dispersions investigated so far showed predominantly
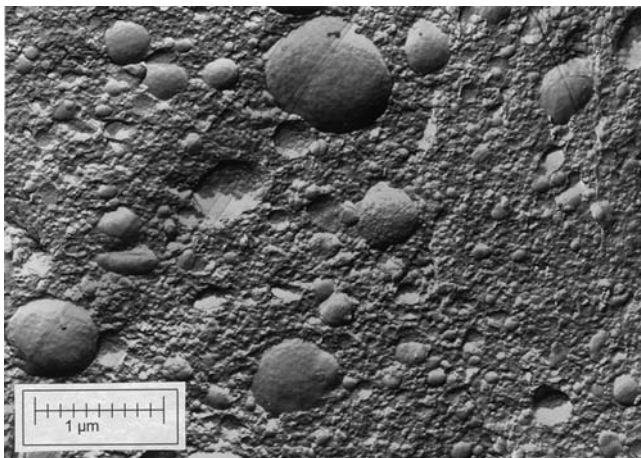
Figure 1 Freeze-fracture electron micrograph of vesicular phospholipid gel containing 450 mg/g soy phosphatidylcholine, prepared by high-pressure homogenization [10 cycles at 70 megapascal (MPa)]. Tightly packed vesicles, predominantly small unilamellar vesicles (SUVs) in the size range well below 100 nm, with some larger vesicles in the several hundred nanometer range. Larger vesicles partly exhibiting golf-ball-like surface textures, most probably due to filling with SUVs, i.e., representing multivesicular vesicles.

vesicular morphologies up to lipid contents of 600 mg/g PC. With gradually increasing phospholipid concentrations from 450 to 600 mg/g, however, a change in prevailing morphology from SUVs toward large multivesicular vesicles and, finally, MLVs occurred (10). Representative freeze-fracture images are given in Figures 1 and 2 displaying high-pressure homogenized soy PC dispersions of 450 and 500 mg/g PC-content, respectively.

Rheometric Analysis

The rheological behavior of VPGs was studied by a rotational viscometer (plate/plate set-up ø 20-mm) in the rotational or, preferably, in the oscillating mode as described in Refs. 26 and 27. VPGs represent viscoelastic bodies with defined yield points. The yield point depends on lipid-concentration, lipid-composition, and vesicle-size distribution (26). Yield points in the range from 4 to 40 Pa were measured (26–28).

Sustained Drug Release Behavior In Vitro

Because such VPGs appeared to retain drugs when coming into contact with excess aqueous medium (1), the idea arose to investigate their potential as depot formulations for sustained release of drugs.
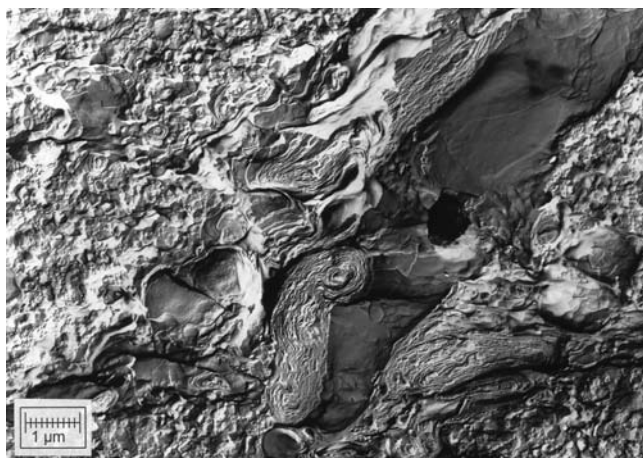
Figure 2 Freeze-fracture electron micrograph of vesicular phospholipid gel containing 500 mg/g soy PC, prepared by high-pressure homogenization (10 cycles at 70 MPa). Tightly packed vesicles, partly small unilamellar vesicles in the size range well below 100 nm, as well as larger vesicles in the micrometer-range. Larger vesicles partly with concentric packing of lamellae, i.e., representing multilamellar vesicles.

Release Test Method

For assessment of the in vitro release of drug from VPG formulations, a test method based on a custom-made flow-through cell, as displayed in Figure 3, has been established (29,30). An acceptor medium (buffer) is run through
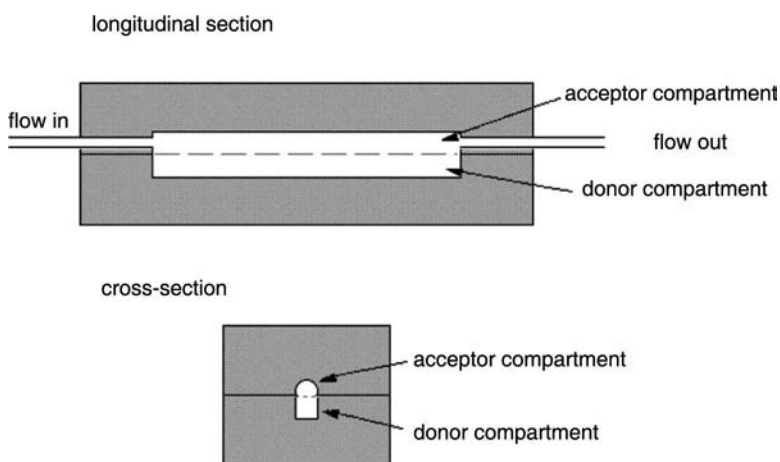
Figure 3 Custom-made release-cell. Schematic drawing of longitudinal and cross-section.

the cell at a rate of 10 mL/hr, to mimic the flow of tissue fluid at the site of injection or implantation. Because in this model the donor and acceptor compartments are *not* separated by a (semipermeable) membrane, not only drug-release via diffusion through the matrix but also erosion of the lipid matrix can be followed. Fractions collected over distinct time intervals are analyzed for both their drug and phospholipid content. Differentiation between drug released in free and liposomal form was done by fractionation of the eluate using size-exclusion chromatography (SEC) on Sephadex G-50 gel. The amount of lipid released over time was quantified gravimetrically upon freeze-drying as described in Ref. (30) or a modified enzymatic PC-assay as described in Ref. (31).

In Vitro Disintegration and Release of a Hydrophilic Marker

By means of the hydrophilic low-molecular-mass model-compound calcein, the sustained-release properties of VPGs were studied systematically. Slow release of the compound over periods of hours up to several days took place via two separate mechanisms: (i) disintegration (erosion) of the vesicular network with release of marker-filled vesicles and calcein, which had been trapped between the vesicles and (ii) diffusion of calcein through the bilayer-membranes. For lipid concentrations up to 300 mg/g, almost spontaneous disintegration occurred. Somewhat more concentrated pastes (350–400 mg/g), in contrast, showed zero-order erosion kinetics over time periods ranging from four to six hours (Fig. 4). Erosion was rate limiting for the release. For even more concentrated VPGs (450 and 500 mg/g), the release of nonliposomal calcein followed square root of time kinetics over 13 or 21 hours (Fig. 4), respectively, which is typical for matrix-controlled diffusion. In parallel to this diffusion process, there was a slow zero-order erosion of the matrix.

In Vitro Release of Drug Compounds

The sustained release from VPGs has been studied for a number of drug compounds, such as Gemcitabine (28), Vincristine (32), Carboplatin (32), and the peptide hormone antagonist Cetrorelix® (33,34).

SUV DISPERSIONS PREPARED FROM VPGs

Preparation Technique

By dilution and gentle mechanical agitation, VPGs can easily be transferred into dispersions of SUVs. Both, manual shaking and use of a ball mill have proven appropriate. A detailed description of the dilution process is given in Ref. (12). The dilution technique determined the homogeneity of the liposome dispersions. Handshaking yielded heterogeneous dispersions, which according to cryo-electron microscopy contained large multivesicular vesicles
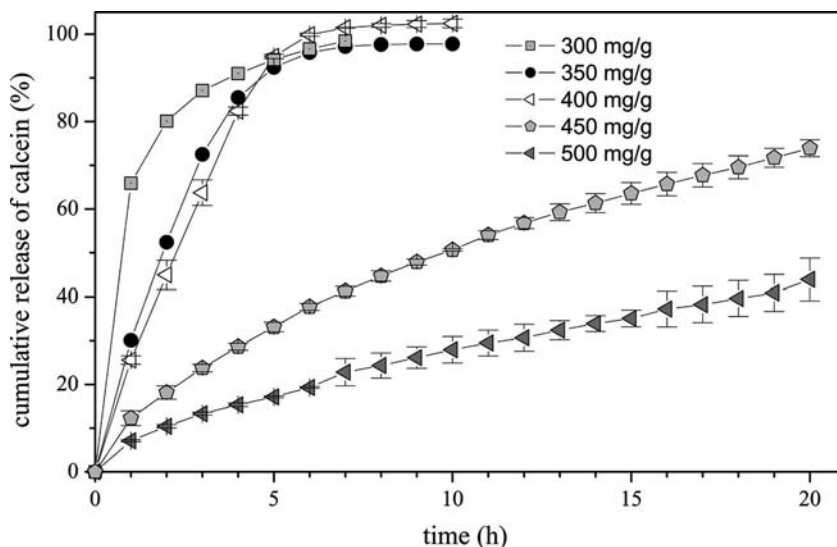
Figure 4 Cumulative release of the fluorescent marker calcein from vesicular phospholipid gels (VPGs) with increasing egg PC-content (300–500 mg/g) versus time (mean ± SD, $n = 3$). VPGs prepared by high-pressure homogenization (10 cycles of 70 MPa).

(MVVs) as well as SUVs (18). In contrast, when diluting the VPGs step by step using a ball mill, the occurrence of larger particles (in the micrometer range) could be widely suppressed, as indicated by photon correlation spectroscopy (PCS) and filtration experiments. Diluted VPGs were characterized in terms of size distribution and encapsulation efficiency.

Characteristics of SUV Dispersions Prepared from VPGs

Vesicle Size and Morphology

The vesicle size of dispersed VPGs were assessed by two standard techniques, PCS and electron microscopy as well as a novel approach based on size-exclusion chromatographic fractionation with subsequent PCS analysis and PC-quantification within the subfractions. When using PCS, one should be aware that a minute "contamination" of the SUV-dispersions with bigger particles such as bigger liposomes or aggregates renders the PCS results difficult to interpret and unreliable. In model studies employing blends of latex beads of defined sizes, we could demonstrate that a routine PCS instrument can resolve bimodal distributions only within very limited blending ratios of the two size-species (35). Outside these blending ratios, PCS neglects either one of the two species. The bigger the difference in size between the

species, the narrower is the blending range at which proper results are obtained. For a blend of 20- and 270-nm particles, for example, the ratio of bigger particles in the dispersion should not exceed 0.005% (by number). Otherwise the PCS instrument will not be able to detect the 20-nm particles at all.

In order to avoid such problems, an alternative approach was developed, where liposome dispersions first are fractionated according to their particle sizes by SEC and the subfractions subsequently analyzed by PCS as well as enzymatic PC assay for their mean particle sizes and liposome contents, respectively (31,36). When plotting the measured relative lipid contents of all fractions versus the obtained mean diameters, a complete quantitative overview of the liposome size distribution can be obtained. Liposomes obtained by dilution of 400 mg/g egg PC-VPGs had mean particle sizes over a range from 15 to 50 nm, with a peak of the size distribution at 20 to 30 nm (Fig. 5). Liposomes obtained by dilution of 400 mg/g VPGs composed of hydrogenated egg PC and cholesterol (2:1, mole/mole) showed upon fractionation mean particle sizes in the range from 40 to 120 nm with a
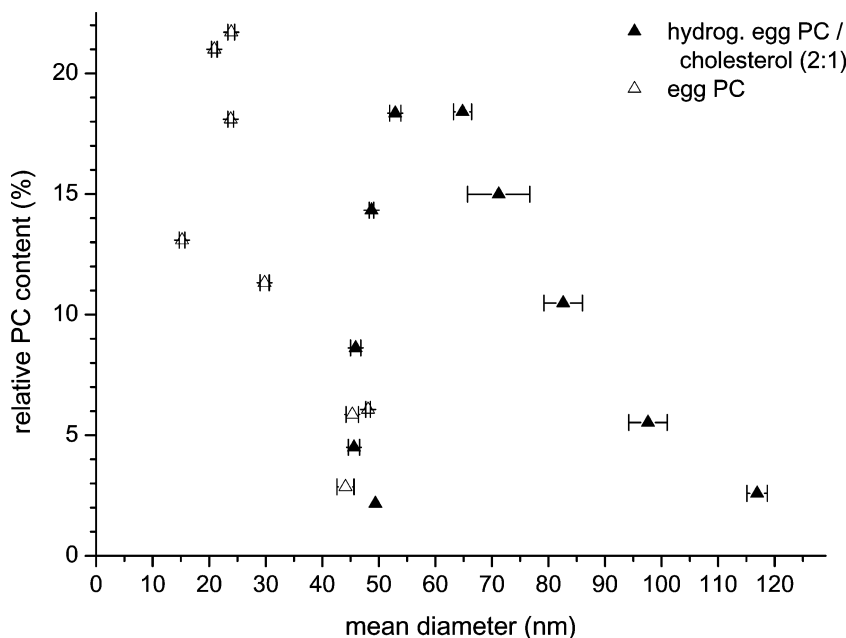
Figure 5 Particle size distribution of egg PC- and hydrogenated egg-PC/cholesterol vesicular phospholipid gels upon dilution obtained by size-exclusion fractionation (Sephacryl S 1000) and subsequent particle size measurement (PCS Nicomp 380) and PC-content analysis. Relative lipid content versus mean particle size (mean ± SD, $n = 3$).

peak at 60 to 70 nm (Fig. 5). Obviously, by the described ball-mill dispersion VPGs can be transferred into quite small liposomes of rather narrow size distribution.

The observed size ranges were nicely confirmed by various electron-microscopic techniques, such as negative staining (18,25) and cryo-electron microscopy (Cryo-TEM) (18). Furthermore, Cryo-TEM has proven useful not only to determine vesicle sizes but also to observe vesicle morphologies (18,26). The particles observed upon dilution were vesicles. The vesicles were mostly very small and unilamellar. Besides these SUVs, some large vesicles in the several hundred nanometer to 1μm range were seen. For some of these larger vesicles, clearly a different morphology could be discerned: they were surrounded by one bilayer membrane and filled with SUVs. These vesicle-filled vesicles resemble the MVVs as already seen in the freeze-fracture micrographs of some of the VPGs before dilution. Lipid composition and concentration as well as the extent of mechanical energy applied during preparation and dispersion of VPGs have an influence on size and morphology of the vesicles (18,26,28).

Encapsulation Efficiency

Upon dilution of VPGs with excess aqueous medium under appropriate conditions, e.g., by using a ball mill, a liquid SUV-dispersion is obtained. Ideally, the fraction of drug, which had been encapsulated in the aqueous core of the vesicles remains entrapped while the fraction of drug which had been trapped in the aqueous space between the vesicles is set free. This means if the vesicles are not ruptured during the dispersion process, the encapsulation efficiency for hydrophilic compounds is determined by the ratio of vesicle core volume as compared to overall aqueous volume in the VPG at the time of VPG formation. Depending on the lipid content and the vesicle size, this ratio is quite favorable as compared to conventional SUV dispersions. When the phospholipid concentration and the vesicle diameter are known, the encapsulation efficiency can be predicted using the following formula:

$$ee = \frac{v_{in} \cdot n_{ves}}{v_{tot} - v_{bil} \cdot n_{ves}} \bullet 100 \ \%$$

where ee is the encapsulation efficiency; v_{in} is the aqueous core volume of one vesicle; n_{ves} is the number of vesicles per unit volume; v_{tot} is the total unit volume; v_{bil} is the bilayer volume of one vesicle. We made the following assumptions: small unilamellar liposomes with 21-nm external diameter and a bilayer thickness of 3.7 nm containing 2377 PC molecules per vesicle with a lipid volume of 1.223 nm^3 per PC molecule.

When doing this calculation for increasing phospholipid contents, one can see that the encapsulation efficiency with this type of vesicles will reach its maximum at a phospholipid concentration of about 550 mg/g. At this

lipid concentration, density sphere packing is reached with 74% of the total volume of the preparation taken by the vesicles and the aqueous core of these vesicles representing 51% of the overall aqueous volume. For hydrophilic model compounds calcein and carboxyfluorescein, encapsulation efficiencies in the magnitude 30% to 70% were found experimentally (18). Increasing encapsulation efficiencies were obtained with increasing lipid concentrations of the VPGs (prior to dilution) (Fig. 6). Experimental values may deviate from theory because the above assumptions may be not fully fulfilled. Tighter packing may be achieved due to elastic deformation of the vesicles. In practice, however, it is hard to achieve experimentally the theoretically predicted maximum encapsulation efficiency and true SUVs. Preparations which have a lipid content at or close to the maximum density packing tend to be inhomogeneous in terms of vesicle size and lamellarity.

Some examples of encapsulation efficiencies of various drugs in VPGs and subsequent dilution are given in Table 1. Encapsulation efficiencies vary with the type of drug and lipid used.
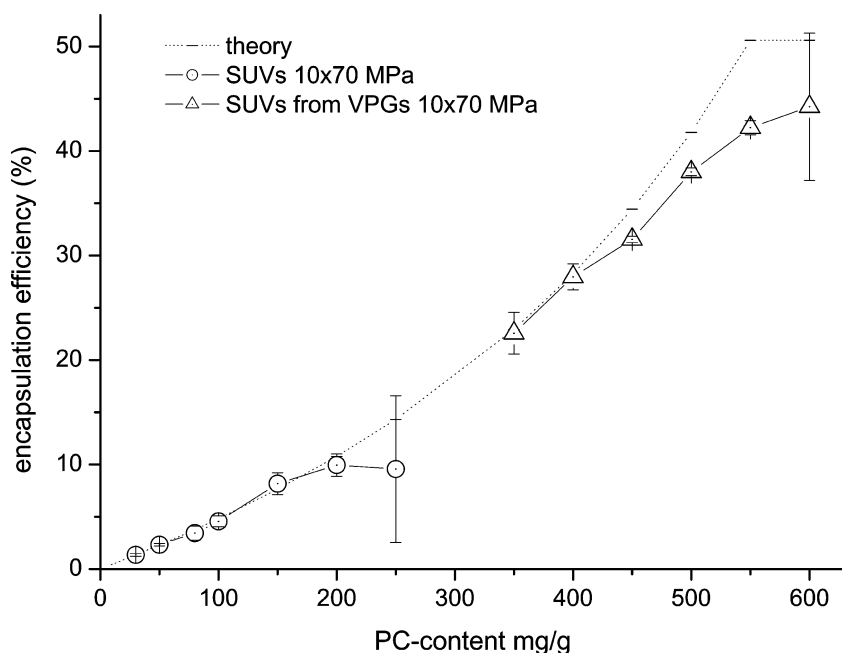
Figure 6 Encapsulation efficiency of the hydrophilic marker carboxyfluorescein within conventional liposome dispersions as well as vesicular phospholipid gels of different lipid content (400–600 mg/g) upon dilution to 100 mg/g and size exclusion separation of entrapped from nonentrapped marker (mean ± SD, $n = 3$) as compared to theory. *Abbreviations*: SUV, small unilamellar vesicles; VPG, vesicular phospholipid gels.

Table 1 Characteristics of Drug-Containing VPGs

Drug compound	Lipid(s)	Lipid content in vesicular phospholipid gel (mg/g)	Loading technique	Encapsulation efficiency	References
Gemcitabine	Hydrogenated egg PC/cholesterol 1:1 (molar)	400	Passive loading	33.2 ± 4.2	Moog et al. (37)
Vincristine	Hydrogenated egg PC/cholesterol 1:1 (molar)	400	Passive loading	54.0 ± 3.3	Guethlein et al. (38)
Cisplatin	Hydrogenated egg PC/cholesterol 1:1 (molar)	400	Direct loading, passive loading	58.6 ± 1.2 (whereof $60.1 \pm 0.6\%$ intact) 9.8 ± 1.3 (whereof $95.7 \pm 2.1\%$ intact)	Guethlein (32)
Cetrorelix	Egg PC	480	Direct loading	68.8 ± 1.0	Grohganz et al. (34)
5-fluorouracil	Hydrogenated soy PC/cholesterol 7.5:2.5 (molar)	300	Direct loading	33.3 ± 0.3 (pH 8.0) 39.6 ± 0.9 (pH 8.6)	Kaiser et al. (39)

In any case, these values are significantly higher than those of other SUVs preparations, i.e., SUVs prepared by common techniques (11,40). To our knowledge, there are only two exceptions found in the literature where encapsulation efficiencies (of hydrophilic compounds) have been achieved in the same magnitude as with VPGs or even higher: (i) with certain radio-labeled, e.g., iodine-labeled compounds, which induces considerable association of the drug with the bilayer and leads to falsely too high values (41); (ii) with SUVs, which are actively loaded by a pH- or ammonium sulphate-gradient. The active loading approach, however, is restricted to a small range of drugs that behave as weak amphipathic bases or acids and can permeate bilayers in the uncharged but not in the charged state (see respective sections in this book for references). The use of VPG technology appears especially attractive for entrapping such water soluble drugs, which cannot easily be entrapped with high trapping efficiency by using

other liposomal formulations and other techniques such as active loading (pH- or electrolyte gradient). Furthermore, for those of the water-soluble drugs, which rapidly diffuse through phospholipid bilayers, entrapping within VPG seems to be the only way to produce a liposomal formulation with a long shelf life. This long shelf life results from the equal distribution of the drug inside and outside the vesicles, which results—even when the drug is able to diffuse through bilayers—in a constant absolute drug amount inside the vesicles (no concentration gradient).

EXAMPLES OF PHARMACEUTICAL APPLICATIONS

As an example for such a water-soluble drug to prepare a liposomal VPG formulation and to investigate the resulting change in antitumoral activity and pharmacokinetics (PK), we chose the nucleoside analogue Gemcitabine (dFdC). dFdC is an approved anticancer agent, with good efficacy in solid cancers with poor prognosis, such as pancreatic carcinoma. dFdC is a fluorinated cytidine analogue with a molecular weight of 299 (hydrochloride), which cannot be stably entrapped within conventional liposomes. Preliminary investigations showed that dFdC is leaking rapidly from the liposomes. DSPC/Chol-liposomes (6/4 molar ratio), for example, showed leakage half-lives of $t_{1/2} = 6.8$ hours. (28)

   Furthermore, from a biological view, we presumed that PK and antitumoral activity of dFdC would improve by its liposomal entrapment because the compound has a very short half-life in systemic circulation (8–17 minutes in human plasma) only. This is due to the metabolic conversion of dFdC into its inactive uridine analogue dFdU by desoxycytidin deaminases in blood, liver, and kidneys (dFdU is approximately 1000 times less active). As a consequence, for the clinical use of dFdC to reach therapeutic concentrations in tumors, it has to be administered in quite high doses (e.g., $1\,g/m^2$ in a weekly schedule). Thus, entrapment within liposomes is expected to prolong dFdC's half-life because liposomes are known for a long time to provide protection from rapid metabolic inactivation of drugs (42).

   The intended goal of the liposomal entrapment of dFdC was to prolong its plasma half-life significantly and, as a consequence of this, to improve its antitumoral activity. Furthermore, when using very small liposomes, typical for VPGs, passive tumor-accumulation of the liposomes by the EPR effect (see above) can be expected, which not only further improves the antitumoral activity, but also might result in an improvement of the therapeutic index.

Preparation and In Vitro Characterization of Gemcitabine-Containing VPG

VPG was prepared using high-pressure homogenization and a total of 400 mg/g lipid (hydrogenated egg PC and Chol in equimolar ratio). For the

entrapment of dFdC, passive loading was used (see above) because dFdC induced phospholipid hydrolysis, especially at harsh conditions such as high-pressure homogenization and steam sterilization (21). After 10 cycles of high-pressure homogenization, a considerable fraction of the phospholipids was found hydrolyzed. Upon passive loading of the VPG with dFdC, in contrast, only minor hydrolytic degradation was seen. Gemcitabine-containing VPG is stable for at least eight months at 4°C. VPGs are cream-like formulations and suitable for subcutaneous (SC) or intramuscular injection but not for intravenous (IV) injection unless diluted. For IV injection, the dFdC-containing VPG was diluted prior to application by blending with sodium chloride solution (0.9%), resulting in a dual drug formulation consisting of 33% liposomally entrapped and 67% nonentrapped (free) Gemcitabine and the liposome dispersion has a mean liposome diameter of 40 to 60 nm. The diluted formulation, called GemLip, is stable for a limited period of time only because the concentration of Gemcitabine inside and outside the liposomes is no longer the same and, as a consequence, the entrapped drug molecules start to diffuse out of the liposomes. To avoid any loss of liposomally entrapped Gemcitabine, Gemcitabine containing VPG was diluted to an intravenously injectable liposomal dispersion (GemLip) directly prior application.

Antitumor activity of GemLip, both after intratumoral (IT) and IV application as well as PK and biodistribution of the redispersed Gemcitabine containing VPG (GemLip), was evaluated in human tumor xenografts grown subcutaneously or orthotopically in nude mice. As a control, conventional Gemcitabine was used (GemConv).

Intratumoral Application of Gemcitabine Containing VPG

Using the subcutaneously growing soft-tissue sarcoma SXF 1301, upon IT application of 4 and 6 mg/kg GemLip, a transient tumor regression was seen (28). No effect could be demonstrated by using the same concentration of GemConv. However, some necrotic changes of the tumor-surrounding tissue were observed. Astonishingly, control tumors SC growing on the opposite flank of the mice significantly reduced as well, which was interpreted as redistribution of the liposomal Gemcitabine; thus, in subsequent studies, systemic administration (IV injection) of GemLip was favored.

Intravenous Application of Gemcitabine Containing VPG

In vivo efficacy of GemLip against GemConv was tested using the subcutaneously growing human soft-tissue sarcoma SXF 1301 and the orthotopically growing human bladder cancer BXF 1299T. PK and biodistribution were evaluated using radiolabeled drug and lipid in SXF 1301 tumor-bearing nude mice. GemLip and GemConv were injected into the tail vein of the mice. This study has been described in detail elsewhere (43). In brief, following

the theoretical considerations discussed above, GemLip turned out to be much more toxic than GemConv. Maximum tolerated dose (MTD) for the GemLip was 6 to 9 mg/kg, which was more than 40 to 60 times lower than the MTD found for GemConv (360 mg) (both given at days 1, 8, and 15). Taken into account that one-third of the drug is entrapped, liposomal entrapment increases the toxicity of Gemcitabine by the impressing factor of 120 to 180. Not only was the toxicity of Gemcitabine increased by its liposomal entrapment, but the antitumoral activity was also dramatically higher. GemLip was already highly active in the SXF 1301–bearing mice at a Gemcitabine dose of 6 to 9 mg/kg (MTD). In the 6 mg/kg groups, complete tumor remissions were observed in seven out of eight mice. Equimolar doses of GemConv resulted only in a moderate tumor growth inhibition. Even at equi-toxic doses (360 mg/kg given on days 1, 8 , 15, or 120 mg/kg on days 1, 5, and 8) GemConv was less active than GemLip. Furthermore, GemLip was active in the orthotopically growing BXF 1299T human bladder cancer model at 6 mg/kg and prevented completely distant organ metastasis.

The PK-study revealed that GemLip achieved 35-fold higher plasma area under the curve (AUC) (1680 mg hr/mL) than GemConv (47.6 mg hr/mL); $t_{1/2}$ were 0.15 hour for free and 13.3 hour for liposomal Gemcitabine (IV 6 mg/kg each). Moreover, Gemcitabine levels in tumors were fourfold higher when injected as GemLip in comparison to GemConv. GemLip and GemConv were administered intravenously on days 1, 8, and 15 at a dFdC-dose of 6 mg/kg into BXF 130–bearing nude mice. GemLip was highly active at 6 mg/kg, a dose around MTD: complete tumor remission was observed in four out of five mice after three weeks. The same dose of the free drug (GemConv) resulted only in a moderate tumor growth inhibition. This was explained by improved PK and biodistribution: upon application of GemConv, dFdC was eliminated from serum with a terminal half-life of 0.15 hour. In contrast, GemLip, which contained 35% liposomally entrapped and 65% free dFdC, resulted in a biphasic elimination kinetics with the following half-lives: $t_{1/2\alpha} = 0.15$ hour (attributed to free dFdC) and $t_{1/2\beta} = 13.3$ hour (attributed to the liposomally entrapped dFdC). Reduced elimination resulted in an increased AUC for GemLip (1680 mg hr/mL for GemLip versus 47.6 mg hr/mL for GemConv). Due to this prolonged half-life and passive targeting due to the enhanced permeability and retention effect, an improved dFdC accumulation in the tumor tissues was observed: using the same dose of 6 mg dFdC/kg mice, a fourfold AUC of dFdC in the tumors could be achieved.

Taken together, our data demonstrate that VPG formulations of the low-molecular-weight, water-soluble, and metabolic unstable dFdC are promising drug delivery systems, which may help to overcome common problems of entrapping drug molecules with similar limitations (as the most anticancer agents) in conventional small liposomes in terms of trapping efficiency and stable entrapment. As shown in the pilot study with dFdC,

the anticancer efficiency of a drug was improved when administered in the form of VPGs—a result that can be explained (i) by the prolonged tumor exposure time of dFdC due to its entrapment into liposomes and (ii) by the passive tumor targeting due to the EPR effect as explained above. In further studies, it has been shown that the described VPG technology is also suitable to entrap a broad range of other water soluble and nonsoluble drug molecules (32,33,39). As an important example, even promising technological and preclinical results as for Gemcitabine containing VPG were found for VPG containing the anticancer drug Vincristine (VCRlip) (38).

SUMMARY OF THE VPG CONCEPT

In summary, VPGs:

- contain aqueous compartments both within the core of the vesicles as well as in-between the vesicles,
- can be loaded with hydrophilic, amphiphilic, and lipophilic drugs in different ways,
- retain a constant drug load within the core of the vesicles during long-term storage because there is no concentration gradient between the vesicles' core and surrounding water phase,
- release drugs in a controlled manner over extended periods of time, and
- can be transferred into "conventional" small-sized liposome (SUV) dispersions adding excess aqueous medium and gentle mechanical agitation shortly before use. Under appropriate conditions, the preformed vesicles remain intact during this dilution process and retain their drug load.

    1. Thus, drugs can be entrapped into SUVs with an unusually high efficiency.
    2. A high ratio of entrapped to unentrapped drug may render removal of free drug unnecessary. In this case, diluted VPGs represent dual-drug formulations. They contain free and liposomally entrapped drug at a defined ratio.

REFERENCES

1. Brandl M, Reszka R. Preparation and characterization of phospholipid membrane gels as depot formulations for potential use as implants. Proc Int Symp Control Rel Bioactive Mater 1995; 22:472–473.
2. Brandl M, Bachmann D, Reszka R, Drechsler M. Application: DE, DE 94–4430592 4430592, 1996. Liposomal carrier for active agents. 19940820.

3. Brandl M, Bachmann D, Reszka R, Drechsler M. Application: US, US 97–803435 6399094, 2002. Unilamellar vesicular lipids for liposomal preparations with high active substance content. 19970220.

4. Ciceri S, Hamann HJ, Huerner I, Kurka P, Maasz J. Application: EP, EP 95–115899, 707847, 1996, Ketoprofen liposome gel. 19951009.

5. Pavelic Z, Skalko-Basnet N, Schubert R. Liposomal gels for vaginal drug delivery. Int J Pharm 2001; 219(1–2):139–149.

6. Small DM. Phase equilibria and structure of dry and hydrated egg lecithin. J Lipid Res 1967; 8(6):551–557.

7. Klose G, Koenig B, Meyer HW, Schulze G, Degovics G. Small-angle x-ray scattering and electron microscopy of crude dispersions of swelling lipids and the influence of the morphology on the repeat distance. Chem Phys Lipids 1988; 47(3):225–234.

8. Brandl MM, Bachmann D, Drechsler M, Bauer KH. Liposome preparation using high-pressure homogenizers. Liposome Technol (2d ed.) 1993; 1:49–65.

9. Brandl M, Drechsler M, Bachmann D, Bauer KH. Three-dimensional networks of liposomes: preparation and electron microscopical characterization. Proc Int Symp Control Rel Bioactive Mater 1996; 23:25–26.

10. Brandl M, Drechsler M, Bachmann D, Bauer K-H. Morphology of semisolid aqueous phosphatidylcholine dispersions, a freeze fracture electron microscopy study. Chem Phys Lipids 1997; 87(1):65–72.

11. Brandl M. Liposomes as drug carriers: a technological approach. Biotechnol Ann Rev 2001; 7:59–85.

12. Brandl M, Massing U. Vesicular phospholipid gels. In: Torchilin VP, Weisssig V, eds. Liposomes. 2d ed. Oxford: Oxford Press, 2003:353–372.

13. Brandl M, Bachmann D, Drechsler M, Bauer KH. Liposome preparation by a new high-pressure homogenizer Gaulin Micron LAB 40. Drug Dev Indust Pharm 1990; 16(14):2167–2191.

14. Brandl M. High-pressure homogenization techniques for the production of liposome dispersions: potential and limitations, emulsions and nanosuspensions for the formulation of poorly soluble drugs, based on the invited lectures and communications presented at the Colloidal Drug Carriers Expert Meeting, 3rd, Berlin, May 29–31, 1997. 1998; 267–294.

15. Sorgi FL, Huang L. Large scale production of DC-Chol cationic liposomes by microfluidization. Int J Pharm 1996; 144(2):131–139.

16. Schneider T, Sachse A, Roessling G, Brandl M. Large-scale production of liposomes of defined size by a new continuous high pressure extrusion device. Drug Dev Indust Pharm 1994; 20(18):2787–2807.

17. Schneider T, Sachse A, Roessling G, Brandl M. Generation of contrast-carrying liposomes of defined size with a new continuous high pressure extrusion method. Int J Pharm 1995; 117(1):1–12.

18. Brandl M, Drechsler M, Bachmann D, Tardi C, Schmidtgen M, Bauer K-H. Preparation and characterization of semi-solid phospholipid dispersions and dilutions thereof. Int J Pharm 1998; 170(2):187–199.

19. Unger C, Massing U, Moog R. Application: DE, DE 98–19813773, 19813773, 1999. Method for the production of liposomal substance formulations. 19980327.

20. Beijnen JH, Van der Houwen OAGJ, Underberg WJM. Aspects of the degradation kinetics of doxorubicin in aqueous solution. Int J Pharm 1986; 32(2–3):123–131.
21. Moog R, Brandl M, Schubert R, Unger C, Massing U. Effect of nucleoside analogs and oligonucleotides on hydrolysis of liposomal phospholipids. Int J Pharm 2000; 206(1–2):43–53.
22. Saetern AM, Skar M, Braaten A, Brandl M. Camptothecin-catalyzed phospholipid hydrolysis in liposomes. Int J Pharm 2005; 288(1):73–80.
23. Sætern AM. Parenteral Liposome- and Cyclodextrin Formulations of Camptothecin. Dr. Scient.-thesis, University of Tromsoe, 2004.
24. Grit M, Underberg WJM, Crommelin DJA. Hydrolysis of saturated soybean phosphatidylcholine in aqueous liposome dispersions. J Pharm Sci 1993; 82(4):362–366.
25. Tardi C, Drechsler M, Schubert R, Brandl M. Three-dimensional networks of liposomes: change of properties upon autoclaving. Proc Int Symp Control Rel Bioactive Mater 1996; 23:27–28.
26. Bender J. Vesikuläre Phospholipidgele: Herstellungsmethoden, Dispergierverhalten, Lagerstabilität und physikalische Charakterisierung, Diss. rer. nat. Albert-Ludwigs-Universität, 2000.
27. Bender J, Michaelis W, Schubert R. Morphological and thermal properties of vesicular phospholipid gels studied by DSC, rheometry, and electron microscopy. J Thermal Anal Calor 2002; 68(2):603–612.
28. Moog R. Einschluss von Gemcitabin (dFdC) in vesikuläre Phospholipidgele, Diss. rer. nat. Albert-Ludwigs-Universität, 1998.
29. Tardi C, Brandl M, Schubert R. Erosion and controlled release properties of semisolid vesicular phospholipid dispersions. J Control Release 1998; 55(2,3):261–270.
30. Tardi C. Vesikuläre Phospholipidgele: in-vitro Charakterisierung, Autoklavierbarkeit, Anwendung als Depotarzneiform, Diss. rer. nat. Albert-Ludwigs-Universität, 1999.
31. Grohganz H, Ziroli V, Massing U, Brandl M. Quantification of various phosphatidylcholines in liposomes by enzymatic assay. AAPS Pharm Sci Tech 2003; 4(4).
32. Guethlein F. Darstellung und Pruefung von vesikulaeren Phospholipidgelen (VPG) zur Therapie solider Tumoren, Diss. rer. nat. Albert-Ludwigs-Universitaet, 2001.
33. Grohganz H. Vesicular Phospholipid Gels as a Potential Implant System for Cetrorelix. Dr. Scient.-thesis, University of Tromsoe, 2004.
34. Grohganz H, Tho I, Brandl M. Development and in vitro evaluation of a liposome based implant formulation for the decapeptide cetrorelix. Eur J Pharm Biopharm 2005; 59(3):439–448.
35. Frantzen CB, Ingebrigtsen L, Skar M, Brandl M. Assessing the accuracy of routine photon correlation spectroscopy analysis of heterogeneous size distributions. AAPS Pharm Sci Tech 2003; 4(3):295–303.
36. Ingebrigtsen L, Brandl M. Determination of the size distribution of liposomes by SEC fractionation, and PCS analysis and enzymatic assay of lipid content. AAPS Pharm Sci Tech 2002; 3(2).

37. Moog R, Burger AM, Brandl M, et al. Change in pharmacokinetic and pharma-codynamic behavior of gemcitabine in human tumor xenografts upon entrapment in vesicular phospholipid gels. Cancer Chemother Pharmacol 2002; 49(5): 356–366.

38. Guethlein F, Burger AM, Brandl M, et al. Pharmacokinetics and antitumor activity of vincristine entrapped in vesicular phospholipid gels. Anti-Cancer Drugs 2002; 13(8):797–805.

39. Kaiser N, Kimpfler A, Massing U, et al. 5-Fluorouracil in vesicular phospholipid gels for anticancer treatment: entrapment and release properties. Int J Pharm 2003; 256(1–2):123–131.

40. Bachmann D, Brandl M, Gregoriadis G. Preparation of liposomes using a Mini-Lab 8.30 H high-pressure homogenizer. Int J Pharm 1993; 91(1):69–74.

41. Brandl M, Gregoriadis G. Entrapment of Hb into liposomes by the dehydration-rehydration method: vesicle characterization and in vivo behavior. Biochim Biophys Acta 1994; 1196(1):65–75.

42. van Borssum Waalkes M, van Galen M, Morselt H, Sternberg B, Scherphof GL. In-vitro stability and cytostatic activity of liposomal formulations of 5-fluoro-2′-deoxyuridine and its diacylated derivatives. Biochim Biophys Acta 1993; 1148(1):161–172.

43. Moog R, Haring AB, Burger AM, et al. Enhanced in vivo anticancer efficacy of gemcitabine after encapsulation into vesicular phospholipid gels. Proc Int Symp Control Rel Bioactive Mater 1999; 26:48–49.

13

Stabilization of Liposomes by Freeze-Drying: Lessons from Nature

John H. Crowe, Nelly M. Tsvetkova, Ann E. Oliver, Chad Leidy, Josette Ricker, and Lois M. Crowe

Section of Molecular and Cellular Biology, University of California, Davis, California, U.S.A.

INTRODUCTION

Stabilization of liposomes by freeze-drying has been intensively investigated over the past two decades, since the initial reports appeared (1–6), which led to rapid adoption in the commercial arena. In fact, Ambisome, a liposome-based product for treatment of systemic fungal infections, has been delivered as a freeze-dried product since its first approval for use in the United Kingdom in 1991. Since those early reports, freeze-dried liposomes have been nebulized for use as an aerosol (7–10), sterilized by gamma radiation (11); the technology has been applied to cross-linked (12) and polyethyleneglycoxylated complexes (13,14); and stability of freeze-dried liposomes has been studied in several contexts (15–17). Investigations on freeze-drying have established the fundamental principles underlying the process, although, as we will discuss in this review, much is still to be learned about the mechanism.

Our studies on freeze-dried liposomes had their origin in a biological phenomenon: many organisms, from prokaryotes to animals and plants, are able to survive extreme dehydration, a phenomenon known as "anhydro-biosis." A theme among such organisms is that they accumulate large quantities of disaccharides, the most common of which are sucrose (in the case of higher plants) and trehalose (in the case of fungi, lower plants, and

261

animals). Survival in the dry state is strongly correlated with the presence of one of these sugars. In the initial studies, trehalose appeared to be particularly effective at stabilizing liposomes, and reports continue to appear in the literature that this is the case. However, under carefully controlled conditions, other sugars and even polymers can work as well as trehalose. The physical basis for this effect is fairly well understood now, and we will present data describing it in this review.

We summarized the state of knowledge about freeze-dried liposomes in the preceding edition of this series, so we do not intend to review earlier material here, but instead will provide a brief summary of findings up to that time, followed by a discussion of more recent work.

TREHALOSE AND BIOSTABILITY

More than 20 years have passed since we first reported that biomolecules and molecular assemblages such as membranes and proteins could be stabilized in the dry state in the presence of trehalose (18). We also reported that when comparisons were made with other sugars, trehalose was clearly superior (19). The superiority of trehalose seemed so clear it quickly led to widespread, and often uncritical, use of the sugar for preservation and other purposes. In fact, an astonishing array of applications for trehalose have been reported, ranging from stabilization of vaccines and liposomes to hypothermic storage of human organs (20). Other studies suggested that it might even be efficacious in the treatment of dry-eye syndrome (21) or dry skin (22) in humans. Trehalose is prominently listed as an ingredient in cosmetics (23). Apparently, the only basis for its use in cosmetics is that trehalose is reputed to inhibit oxidation of certain fatty acids in vitro that might be related to body odor (23). Trehalose has been shown by several groups to suppress free-radical damage (24), protect against damage from anoxia (25,26), inhibit dental caries (27), enhance ethanol production during fermentation (28), stabilize the flavor in foods (29), and protect plants against abiotic stress (30). More recently, Tanaka et al. (31) reported that trehalose could be used to inhibit the protein aggregation associated with Huntington's disease in vivo in a rat model for this disease. This report has already led to an unorthodox clinical trial in humans (32).

The point we want to make is that a myth has grown up about trehalose and its properties, as a result of which it is being applied, sometimes rather uncritically, to a myriad of biological and clinical problems. Thus, we are making special efforts in the literature to clarify the properties of trehalose that make it useful for stabilization of biomaterials and to dispel the most misleading aspects of this myth.

ORIGINS OF THE TREHALOSE MYTH

We recently reviewed the history of this field (9) and provide only a brief summary here. The key observations were as follows. (i) The first model

membrane investigated was sarcoplasmic reticulum, isolated from lobster muscle (33). When we compared the ability of a variety of sugars to preserve the SR during drying, we found that trehalose was without question superior to all other sugars tested. Some years later, however, we obtained evidence that these sarcoplasmic reticulum (SR) membranes have a mechanism for translocating trehalose across the bilayer. We suggest that other sugars such as sucrose might preserve the membranes at concentrations similar to those seen with trehalose if they had access to the aqueous interior. (ii) Initial studies with liposomes from the mid-1980s (34) were done with a phosphoplipid with low T_m. When the liposomes were freeze-dried with trehalose and rehydrated, the vesicles were seen to be intact and nearly 100% of the trapped solute was retained. It quickly emerged that stabilization of these liposomes, and other vesicles prepared from low melting point lipids, had two requirements: (a) inhibition of fusion between the dry vesicles; and (b) depression of T_m in the dry state. In the hydrated state, T_m for egg PC is about $-1°C$ and rises to about $+70°C$ when it is dried without trehalose. In the presence of trehalose, T_m is depressed in the dry state to $-20°C$. Thus, the lipid is maintained in liquid-crystalline phase in the dry state and phase transitions are not seen during rehydration. The significance of this phase transition during rehydration is that, when phospholipids pass through such transitions, the bilayer becomes transiently leaky. [The physical basis for this leakiness has recently been investigated in some detail by Hays et al. (35).] These effects were reported first for trehalose (23). When we compared the effects of other sugars and polymers on the preservation, we found that, with vesicles made from lipids with low T_m, trehalose appeared to be significantly superior to the best of the additives tested. Oligosaccharides larger than trisaccharides did not work at all (36). Other sugars, particularly disaccharides, did provide good stabilization of egg phosphatidylcholine (PC) vesicles in the dry state, but much higher concentrations than trehalose were required, at least according to initial reports. However, because freeze-drying technology improved, the differences between disaccharides tended to disappear, and the myth eventually got modified to encompass disaccharides in general. Nevertheless, the observation that trehalose was significantly more effective at low concentrations under suboptimal conditions for freeze-drying requires explanation, which we provide later. (iii) At first it appeared that the ability to preserve liposomes in the dry state is restricted to disaccharides. Subsequently, we found this is not the case. For example, dipalmitoylphosphatidylcholine (DPPC) is a lipid with saturated acyl chains and thus an elevated T_m (41°C); this lipid is in gel phase at all stages of the freeze-drying and rehydration process, and one would expect that inhibition of fusion might be sufficient for the stabilization (37). In other words, any inert solute that would separate the vesicles in the dry state and thus prevent aggregation and fusion should stabilize the dry vesicles. That appears to be the case; a high molecular weight (450,000) hydroxyethyl starch (HES) has no effect on T_m in dry DPPC, but nevertheless preserves the vesicles (38).

EFFECT OF LIPID TYPE AND THERMAL HISTORY ON T_M IN THE DRY STATE

Low-temperature–melting lipids such as palmioyloleyoylphosphatidylcholine (POPC) all seem to behave as described previously; T_m is depressed to a minimal value immediately in the presence of trehalose after drying, independent of the thermal history (Fig. 1). Saturated lipids with high T_m, such as DPPC, behave quite differently, and effects of trehalose on T_m depend strongly on the thermal history (Fig. 1). When T_m in DPPC dried without trehalose is measured, it is seen to rise from 41°C in the hydrated
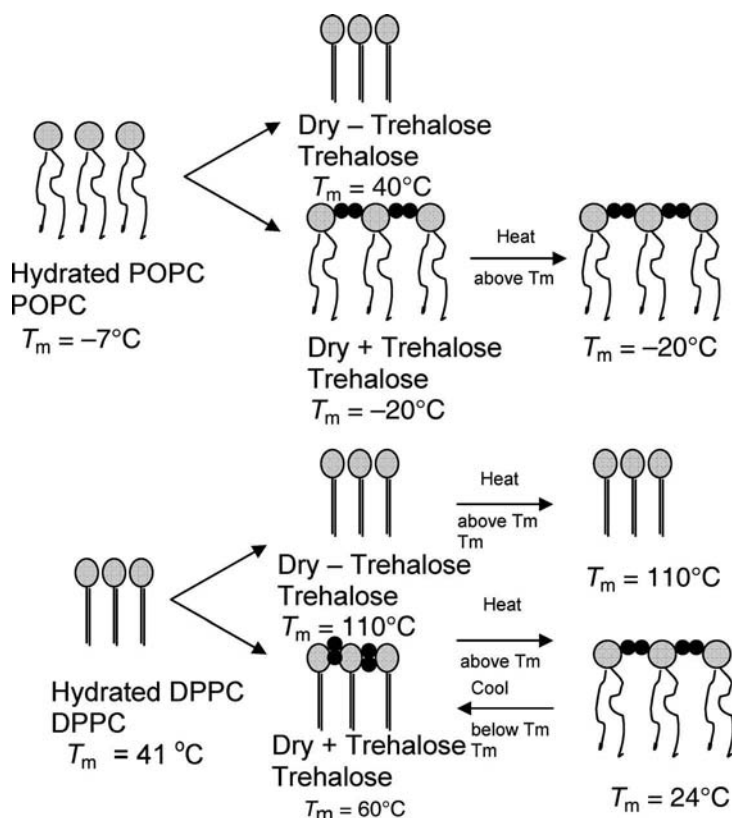
Figure 1 Effects of addition of trehalose and thermal history on phase behavior of two lipids during drying. POPC achieves a minimal, stable T_m immediately after drying with trehalose, regardless of the thermal history. DPPC, by contrast, shows a reduced, stable T_m immediately after drying, but if the acyl chains are melted T_m falls to 24°C. If DPPC is then chilled below that value T_m reverts to the stable value at 60°C. We interpret these effects as resulting from accessibility of the polar headgroup to the trehalose, as suggested in this figure. *Source*: From Refs. 36–38.

lipid to 110°C when it is dried. In the presence of trehalose, T_m is about 60°C until the acyl chains are melted once, after which T_m is depressed to 24°C (38,39). If the lipid is then incubated at temperatures less than 24°C, T_m rapidly reverts to about 60°C. Thus, the stable T_m renders DPPC in gel phase at physiological temperatures, regardless of whether it is hydrated or dry. This effect may have special relevance for biological membranes because microdomains contain lipids with elevated T_m.

The mechanism by which trehalose depresses T_m in dry phospholipids has been a matter of some debate, with at least three alternative, but not necessarily mutually exclusive, hypotheses in the literature (36,40,41). Discussion of this mechanism is beyond the scope of the present review.

THERE IS MORE THAN ONE WAY TO ACHIEVE THE SAME END

Although the occurrence of trehalose at high concentrations is common in anhydrobiotic animals, some such animals have vanishingly small amounts of trehalose (42,43) or none at all (44–46). It is tempting to construe these findings as evidence against a role for sugars in anhydrobiosis (46). We suggest that it is not the sugars per se that are of interest in this regard, but rather the physical principles of the requirements for stabilization, as described above, and we can learn a great deal in this regard that is useful for stabilizing liposomes in the dry state. There are multiple ways to achieve such stabilization. (i) HES alone will not stabilize dry membrane vesicles composed of lipids with low T_m, but a combination of a low molecular weight sugar such as glucose and HES can be effective (47). Here is the apparent mechanism: glucose depresses T_m in the dry lipid, but has little effect on inhibiting fusion, for reasons we will make clear below, except at extremely high concentrations. On the other hand, the polymer has no effect on the phase transition, but inhibits fusion. Thus, the combination of the two meets both requirements, while neither alone does so (Fig. 2). A glycan isolated from the desiccation-tolerant alga *Nostoc* apparently works in conjunction with oligosaccharides to stabilize liposomes in the dry state (48). Similarly, certain proteins have been shown to affect the phase state of the sugars and either enhance or be required for stabilization (49). Combinations of such molecules could be useful more generally for stabilizing liposomes. (ii) Hincha et al. (50) have shown that fructans from desiccation-tolerant higher plants will by themselves both inhibit fusion and reduce T_m in dry phospholipids such as egg PC. The mechanism behind this effect is still unclear. Vereyken et al. (51) provided evidence that the interaction is similar to that shown by sugars, but that it is also specific to fructans and is not shown by other polymers. In a related study, Hincha et al. (52) reported that a series of raffinose family oligosaccharides are all capable of stabilizing dry liposomes. (iii) Hincha and Hagemann (53) recently studied effects of other compatible solutes on stabilization of liposomes by sugars.
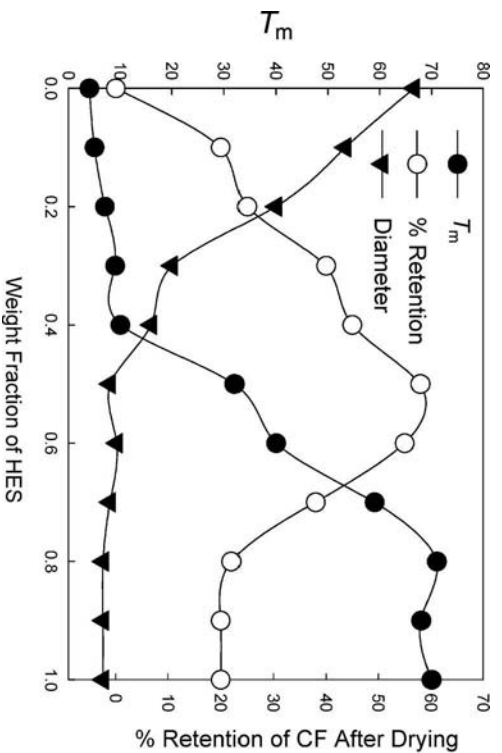
Figure 2 Combined effects of weight fraction of hydroxyethyl starch in v... PC liposomes were dried on retention of trapped carboxyfluorescein follow... dration, transition temperature in the dry state, and average diameter... rehydration. *Source*: Modified from Ref. 47.

This approach is in its earliest stages, but those authors found th... compatible solutes improve the stabilization in the presence of sug... gesting that the solutes might decrease the amount of sugar requir... (iv) Popova and Hincha (54) have shown that this is the case for... amphiphiles, tryptophan, and that the interaction depends on the li... position. This latter finding, along with other evidence (55,56), sug... the protective molecules themselves may vary depending on lipid... sition. (v) Goodrich et al. (57) reported that disaccharides tethere... bilayer surface by a flexible linker esterified to cholesterol has an... membrane stability similar to that seen in the free sugar.

Lipid composition of the liposome alters the requirements for s... tion dramatically. For instance, we showed that in lipids with high T... never pass through the lipid phase transition during drying and reh... inhibition of fusion is sufficient for the stabilization (37,38). At t... end of the spectrum, liposomes composed of dioleoylphosphatidy... (DOPC) ($T_m = -22°C$), the disaccharide maltose provided little or no... tion from dehydration damage, possibly due to reduced interactions... polar headgroup (58). Oliver et al. (56) reported that arbutin, a gly... hydroquinone found in combination with sucrose in a desert res... plant that survives dehydration, damages egg PC liposomes durin... However, when liposomes were prepared with 20% monogalac... cylglycerol (a lipid commonly found in plants), arbutin was seen t... remarkable stabilizing effect during drying.

The point is there are many ways to achieve stability in dry liposomes, both by variations on the solute used as the protectant and by altering the lipid composition. Once an understanding of the physical requirements for preservation was achieved, it became apparent that many routes could lead to the same end. Similar observations on the stability of dry proteins have been made by Carpenter and coworkers (59–61).

TREHALOSE HAS USEFUL PROPERTIES, NEVERTHELESS

We implied above that trehalose works well for freeze-drying liposomes under less than optimal conditions. The same applies for storage under conditions that would normally degrade the biomaterial. Leslie et al. (62) reported that bacteria freeze-dried in the presence of trehalose showed remarkably high survival immediately after freeze-drying. Furthermore, they found that the bacteria freeze-dried with trehalose retained high viability even after long exposure to moist air. By contrast, when the bacteria were freeze-dried with sucrose, they showed lower initial survival, and when they were exposed to moist air, viability decreased rapidly. More recently, Esteves et al. (63) reported that when immunoconjugates were freeze-dried with trehalose or other disaccharides all the sugars provided reasonable levels of preservation. However, when the dry samples were stored at high relative humilities and temperatures, those dried with trehalose were stable for much longer than those dried with other sugars. This finding is of some considerable significance because there is a need for shipping immunoconjugates, vaccines, antisera, and the like to locales where they would be exposed to high temperatures and humidities as soon as they are exposed to air.

GLASS TRANSITIONS AND STABILITY

Using liposomes as a model, we attempted to find a mechanism for long-term stability in the presence of trehalose. As with the bacteria and immunoconjugates, the dry liposomes exposed to increased relative humidity rapidly leaked their contents when they were dried with sucrose, but not when they were dried with trehalose-6 (39,64,65). The liposomes underwent extensive fusion in the moist air when dried with sucrose, but not with trehalose.

Trehalose, along with many other sugars, forms a glass when it is dried. This glass undergoes a transition from a highly viscous fluid to a highly mobile system when it is heated above a characteristic temperature, T_g, which increases sharply as dehydration progresses, resulting in what is known as a state diagram (Fig. 3). The importance of the state diagram is as follows. It has become widely accepted that stability of dry materials in which close approach of surfaces must be prevented requires that the material
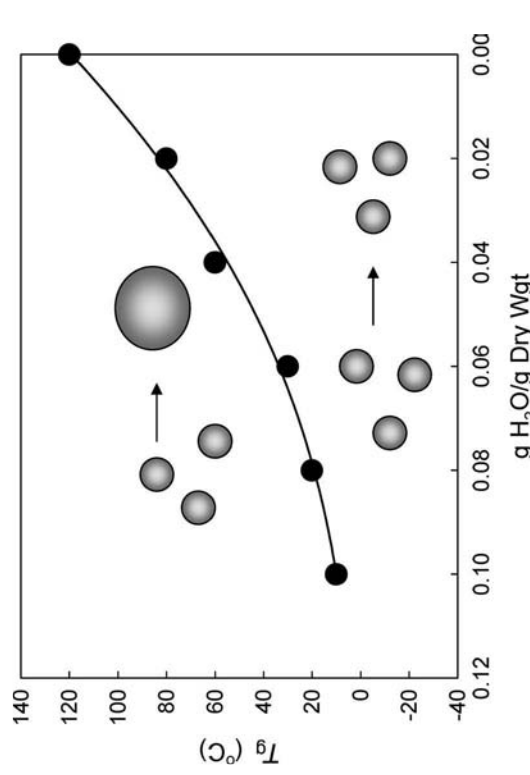
Figure 3 Effects of the glass transition temperature on inhibition of ag and fusion of liposomes at the indicated water contents. *Source:* Data for Ref. 66 and observations on liposomes from Ref. 65.

remain below the curve for the state diagram, i.e., it must be maint the glassy state. Above the curve, the mobility of the system i whereas below it, the materials are held in a relatively rigid matrix For instance, heating a sample containing liposomes above T_g r increased mobility to the point where fusion occurs in the co ted solution. (Brief excursions above the curve are not necessarily d because the surface-to-surface interaction has a kinetic component. of this kinetic component, there is a lot of confusion in the literat cerning whether the glassy state is even required for stabilization.)

T_g for trehalose is much higher than that for sucrose (Fig. 4), first reported by Green and Angell (65) and later refined by Crowe e As a result, one would expect that addition of small amounts of sucrose by adsorption in moist air would decrease T_g to below the temperature, while at the same water content T_g for trehalose w above the storage temperature. Indeed, at water contents around 5% trehalose is about 40°C, whereas that for sucrose is about 15°C. T_g cose at a similar water content is about −10°C (Fig. 4). One would that at such water contents trehalose would be the only one of the sugars that would stabilize the sample, and this appears to be the c would seem to provide an explanation for the superior stability of, fe ple, the immunoconjugates stored in sucrose or trehalose describe We stress, however, that the elevated T_g seen in trehalose is not an
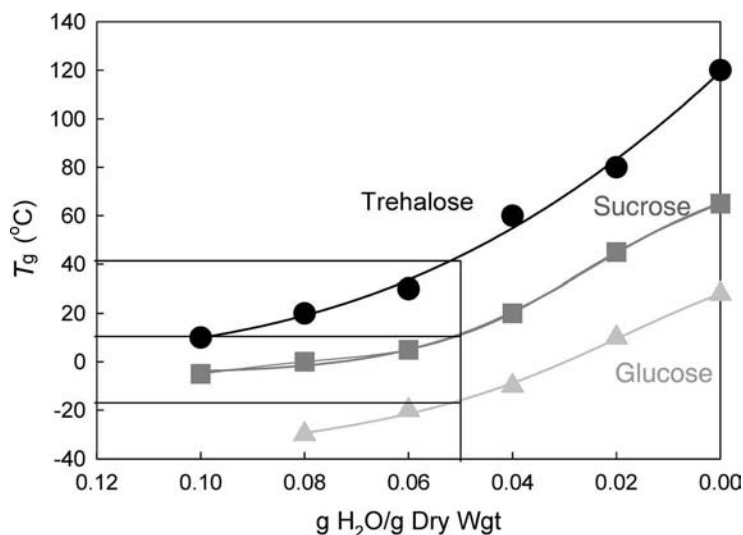
Figure 4 Comparison between glass transition temperatures in trehalose, sucrose, and glucose at the indicated water contents. The reference lines show values for T_g at about 5% water content.

Indeed, trehalose lies at the end of a continuum of sugars that show increasing T_g (67), although the basis for this effect is not understood.

Allison et al. (66) have presented an alternative, but not mutually exclusive, hypothesis concerning the mechanism of inhibition of aggregation of cationic lipid-DNA complexes following freezing or freeze-drying. They observed that polymers such as HES are less effective than disaccharides at inhibiting aggregation, unlike the case with liposomes. Disaccharides, on the other hand, did inhibit the aggregation, despite the fact that T_g for the disaccharides was lower than that for HES. They ascribed this difference to the lower surface tension of the sugars.

NONENZYMATIC BROWNING AND STABILITY OF THE GLYCOSIDIC BOND

The Maillard (browning) reaction between reducing sugars and proteins in the dry state has often been invoked as a major source of damage (68), and the fact that both sucrose and trehalose are nonreducing sugars may explain at least partly why they are the natural products accumulated by anhydrobiotic organisms. However, the glycosidic bonds linking the monomers in sucrose and trehalose have very different susceptibilities to hydrolysis (69,70). For instance, the activation energy for acid hydrolysis in aqueous solution is nearly twice that for other disaccharides (71) (Fig. 5). When
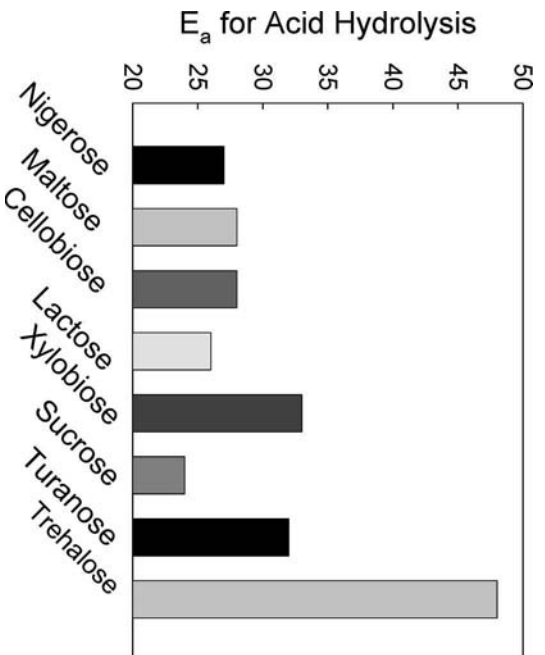
Figure 5 Activation energy for acid hydrolysis of a variety of sugars. From Ref. 72.

O'Brien (69) and subsequently Schebor et al. (70) incubated a freeze-dried model system (albumin, with the addition of lysine) with sucrose, trehalose, and glucose at relative humidities in excess of 20%, the rate of browning with sucrose approached that of glucose—as much as 2000 times faster than that with trehalose, although they observed a distinct lag in the onset of browning (Fig. 6). Schebor et al. (70) found that a peak in the appearance of monosaccharides occurs prior to the onset of browning, after which free monosaccharides decline, coincidentally with the onset of browning (Fig. 6). These observations strongly suggest that the browning seen with sucrose—but not with trehalose—is due to hydrolysis of the glycosidic bond during storage.

The glassy state is undoubtedly related to these effects; if the liposomes are stored at very low humidities, only minimal amounts of hydrolysis and subsequent browning were seen in the sucrose preparations (69,70).

ENZYMATIC DESTABILIZATION OF LIPOSOMES IN THE DRY STATE

We realize that it will probably be a rare event that liposomes will be freeze-dried with an enzyme that could utilize either the lipid or the protective molecule as a substrate, but here is a case illustrating the consequences. Oliver et al. (72) found that when dielaidoylphosphatidylcholine liposomes were freeze-dried with phospholipases and stored at r

(A)

Browning Index

Trehalose ——
Sucrose ——

Days

(B)

Monosaccharides Produced

Trehalose ——
Sucrose ——

Days
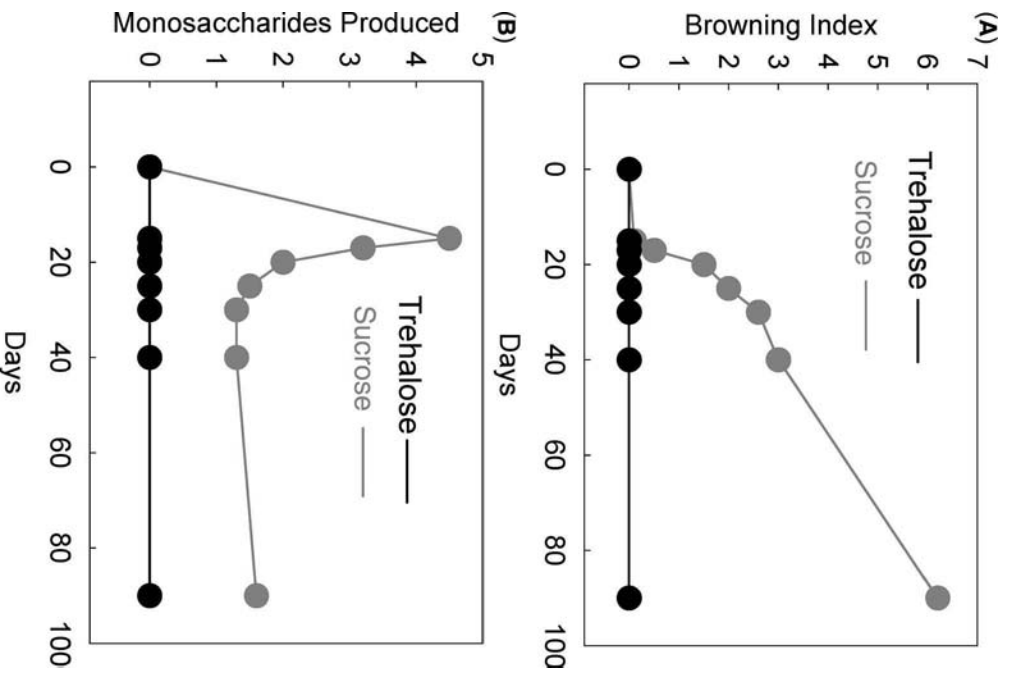
Figure 6 Browning of dry proteins **(A)** and release of monosaccharide[s] trehalose and sucrose during storage. *Source:* Adapted from Ref. 71.

relative humidities, the phospholipase A$_2$ (PLA$_2$) showed a su[...] amount of activity—enough to destabilize the bilayer to the poin[...] the vast majority of trapped solute leaked out (Fig. 7). The enzymat[...] ity proceeded when the water content was as little as two H$_2$O mo[...] headgroup. A similar pattern was seen for accumulation of diacyl[...] when the liposomes were dried with phospholipaseC (PLC) (72). The [...] then arose concerning how anhydrobiotic organisms escape such en[...] activity. It emerged that arbutin, a molecule found at high concentra[...]
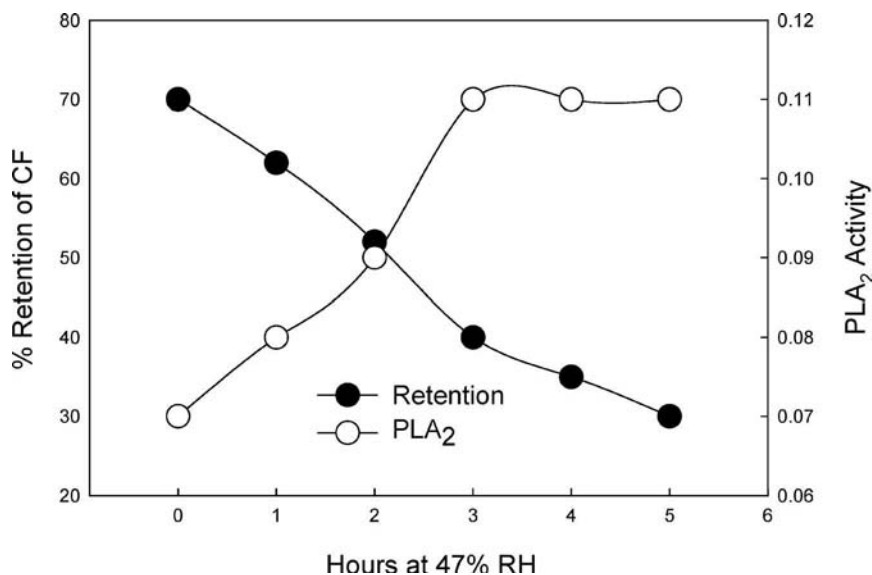
Figure 7 Retention of trapped carboxyfluorescein and enzymatic activity in lipo-somes freeze-dried with trehalose and PLA_2 and stored at the indicated relative humidity. *Abbreviation*: PLA_2, Phospholipase A_2. *Source*: Adapted from Ref. 73.

resurrection plants and which we have mentioned previously, almost comple-tely inhibits PLA_2 activity in the dry liposomal preparations (Fig. 8). Thus, consideration of enzymatic activity and ways to inhibit such activity may be required in the formulation steps for dry liposomes.

PHASE SEPARATION AS A SOURCE OF DAMAGE

Binary or higher mixtures of lipids present special problems; even if the lipids mix ideally in the hydrated state, they may undergo lateral phase separation during the drying process that can lead to irreversible damage. Several binary lipid mixtures have been analyzed using a variety of techniques, including differential scanning calorimetry (DSC) (74–76), Fourier-transformed infrared spectroscopy (FTIR) (77–79), nuclear magnetic resonance spectro-scopy (80,81), and computer simulations (82–86). Phase diagrams for a large variety of mixtures have thus been generated. In general, in a binary mixture in which the lipid species have similar phase transition temperatures, there is a high degree of mixing, and the phase transitions merge. In the case of lipid mixtures that have lipids with phase transitions that differ by more than $10°C$, the system behaves as a nonideal mixture, in which case the phase transitions of the lipid species do not merge completely. This is observed
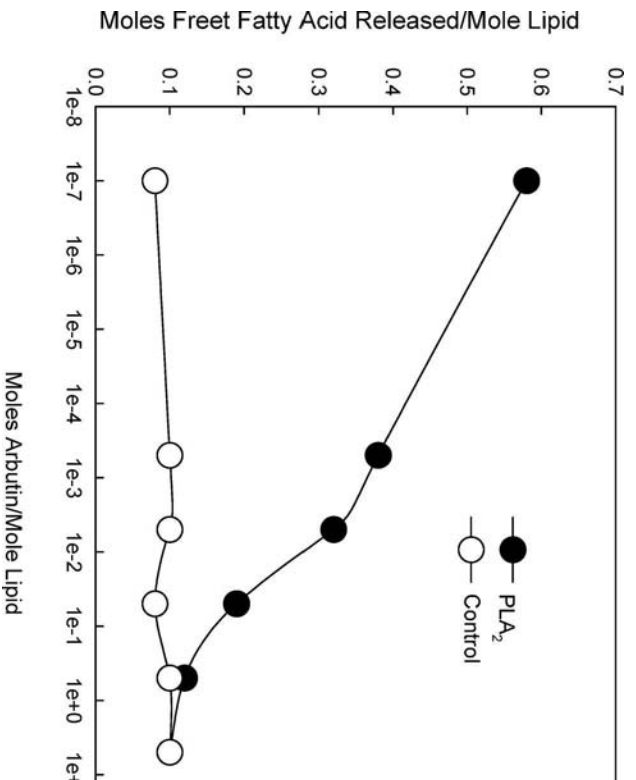
Figure 8 Inhibition of PLA$_2$ activity by arbutin in liposomes freeze-d... trehalose and PLA$_2$. *Source:* From Ref. 74.

Moles Freet Fatty Acid Released/Mole Lipid

Moles Arbutin/Mole Lipid

PLA$_2$
Control

by DSC as two cooperative events representing a fraction enriche... lower melting lipid and a fraction enriched in the higher melti... respectively (74). The lower the miscibility between the lipid spe... farther the phase transitions are from each other, and the closer th... transitions are to the individual lipid components' transition tempe... This implies that a multicomponent bilayer with a degree of imm... between lipid species can show multiple cooperative phase transiti...

Phase separation is segregation of membrane components in th... of the bilayer. Although several forces are involved, one of the m... ving forces for phase separation is the hydrophobic mismatch, whi... from a difference in membrane thickness between two species v... bilayer, such as a protein and a lipid or a lipid and a lipid (87,8... differences in thickness lead to exposure of hydrophobic residues... (Fig. 9) and, consequently, to a decrease in entropy of the system r... from ordering of the water. Thus, the assembly of components of... thickness into relatively homogeneous domains is entropically dri... net increase in entropy driving the process is contributed by water.

Now consider the consequences of such an event for a binary m... lipids that is almost ideally mixed at room temperature. When a bin... ture of POPC and phosphatidylserine (PS) (9:1) prepared as multi...
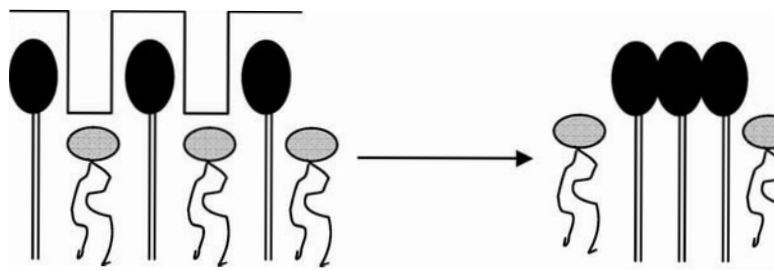
Figure 9 A membrane bilayer formed by a binary mixture of lipids, [with] one component in the gel phase and one component in the liquid-crystalline ph[ase. The] mismatch in chain lengths and exposure of acyl chains to water in the interfac[ial region] is thought to lead to aggregation of the gel phase lipids. *Source*: Redrawn from [ ].

vesicles (MLVs) was dried without sugar additive, the data shown in F[ ] were obtained (4). The three melting endotherms were assigned to: (a [com]pletely phase separated PS; (b) incompletely phase-separated PO[ ] (c) completely phase separated POPC. When the same mixture wa[s] dried with trehalose, the *Transition c* disappeared at low concentra[tion of] trehalose. With the addition of more trehalose, the enthalpy of the *T[ransition]* *a* increased, at the expense of the *Transition b* (Fig. 11). The interp[retation] placed on these findings is that the PS is so fluid that its T_m is little [affected] by dehydration, while T_m for POPC rises during dehydration, leading [to phase] separation. Addition of trehalose drives down T_m for POPC during d[ehydra]tion, thus maintaining the pair in a single mixed phase.

More recently, Ricker et al. (90) have done a similar analysi[s on a] binary mixture of DPPC and distearoylphosphatidylcholine (DSPC[ ), using] FTIR to measure the transitions. One of the pair has deuterated acy[l chains,] thus permitting simultaneous measurement of the two transitio[ns. The] results show that in the hydrated state the two are completely mixe[d, with] a transition intermediate between those for the two pure lipids. In [the dry] state without trehalose, the lipids showed some signs of slight de[mixing,] but the vast majority remained mixed, with or without the presenc[e of tre]halose. Because these two lipids are in gel phase at every step of pro[cessing,] this is the expected result. That is not to say that trehalose has no e[ffect; it] certainly will inhibit fusion between liposomes composed of these lip[ids, and] it does depress T_m in the dry mixture, but not below room tempera[ture.]

MAINTENANCE OF DOMAINS IN THE DRY STATE

Phase separated domains in lipid bilayers are becoming increasin[gly well] understood (89). Although such domains seem not to have been ut[ilized in] the liposome field, one can imagine that this organized structure mi[ght]
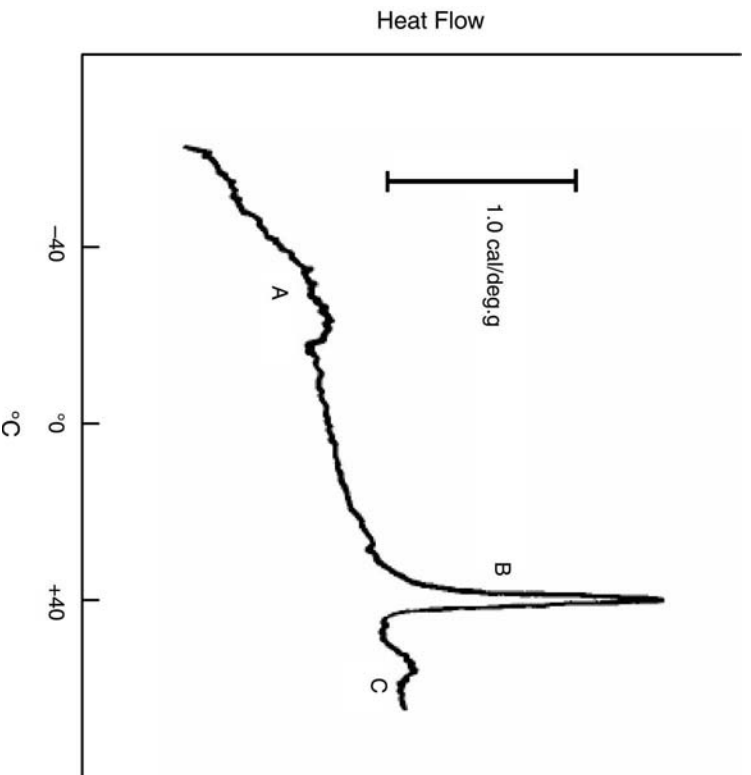
Figure 10 Differential scanning calorimetry data for a freeze-dried m[...] POPC and PS (9:1). (A) mixed phase PS and POPC, dominated by PS; ([...] phase POPC and PS, dominated by POPC; (C) completely phase separate[...]
Source: Adapted from Ref. 14.

have utility in, for instance, targeting. Thus, we have investigated the domains can be maintained in freeze-dried liposomes dilauroylp[...] tidylcholine (DLPC) ($T_m = 0°C$) and DSPC ($T_m = 50°C$) are well k[...] undergo complete phase separation in the fully hydrated state (74[...] shown in Figure 12. When these liposomes were dried, the tw[...] remained in two phases, but they are mixed phases rather than pur[...] and DSPC; the lower one (Fig. 12) is apparently a mixture of mostly[...] while the upper one (Fig. 12) is mostly DSPC. In samples dri[...] trehalose, by contrast, the DLPC transition is depressed to abou[...] (Fig. 12B, *inset*), and the DSPC transition increases by about 10[...] becomes more cooperative, suggesting that it is more like pure DSP[...] the phase separation—and the domain structure—are maintained by [...] halose in the dry state. Other pairs of lipids that phase separate wh[...] hydrated give similar results.
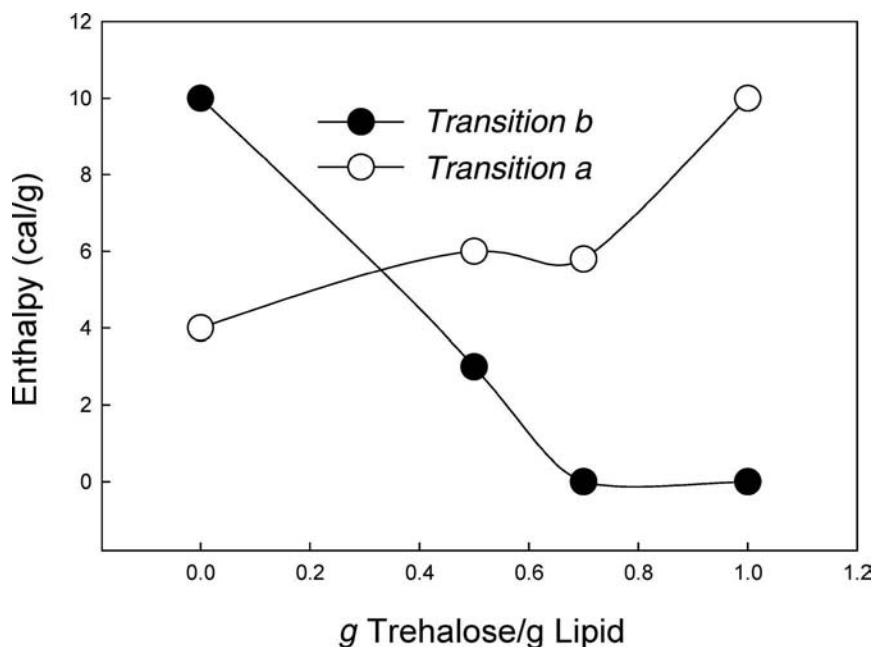
Figure 11   Effects of freeze-drying the lipid mixture from Figure 10 in the presence of trehalose. With increasing trehalose, *Transition a* grows at the expense of *Transition b*. *Source*: From Ref. 14.

We propose that trehalose maintains phase separation in this mixture of lipids in the dry state by the following mechanism. The DLPC fraction, with its low T_m in the hydrated state, might be expected to behave like unsaturated lipids described earlier, in that T_m in the dry state is reduced to a minimal and stable value immediately after drying with trehalose, regardless of the thermal history. That appears to be the case. The DSPC fraction, by contrast, would be expected to behave like DPPC, as described earlier. DSPC is in gel phase in the hydrated state at room temperature, and it remains in gel phase when it is dried with trehalose. In other words, we are proposing that by maintaining one of the lipids in liquid-crystalline phase during drying, while the other remains in gel phase, trehalose maintains the phase separation (Fig. 13). We suggest that this is the fundamental mechanism by which trehalose maintains phase separated domains in liposomes drying. Furthermore, although there are lingering doubts about whether or not phase separated domains in native membranes are real (91–96) or artifacts (97–99), there is abundant evidence that these domains, known as "rafts," are involved in such processes (among others) as signaling (100–102), endocytosis (103), and viral assembly (104,105). Furthermore, evidence is accumulating rapidly that
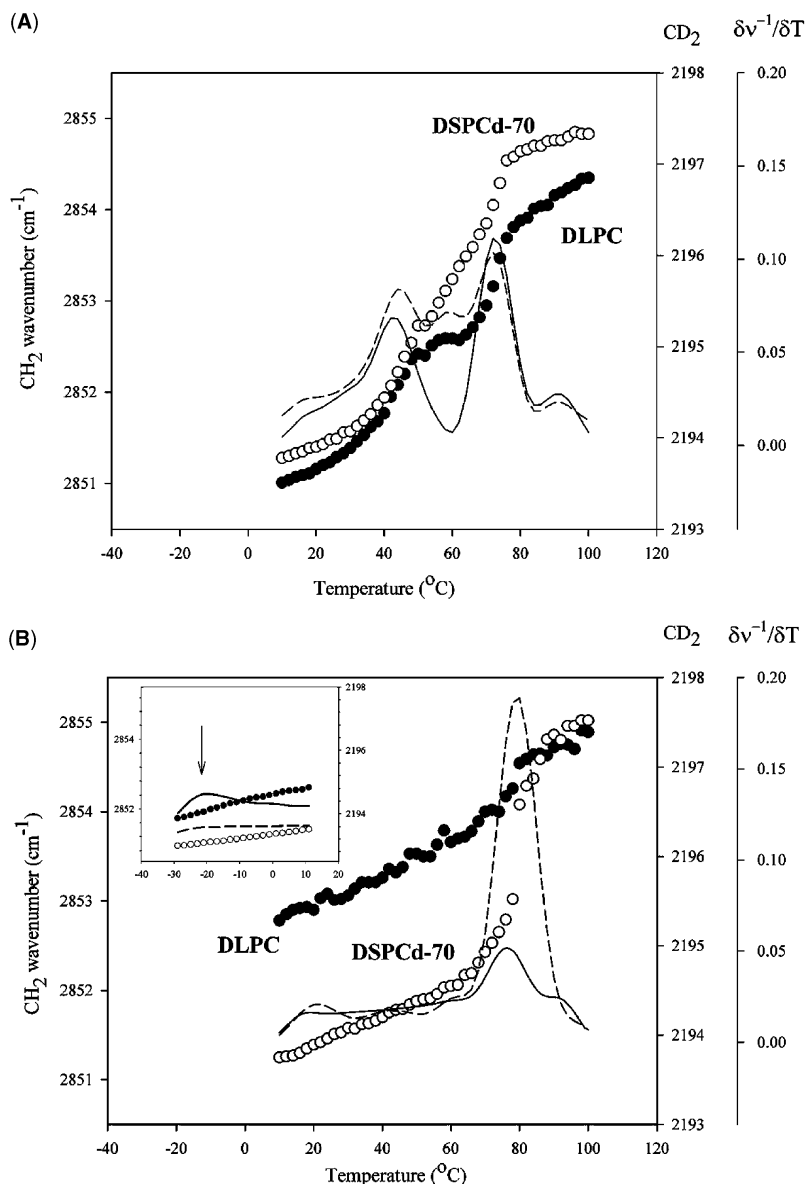
Figure 12 Changes in the wave number of the CH_2 symmetric stretch and CD_2 asymmetric stretch as a function of temperature during heating of DLPC:DSPCd-70 1:1 mixtures, air-dried in the absence (**A**) and presence (**B**) of trehalose (5:1 sugar:lipid); first derivative CH_2 (*solid lines*); and first derivative CD_2 (*dashed lines*). Low temperature wave number versus temperature plot of air-dried DLPC/DSPCd-70 in the presence of trehalose (**B**, *inset*). *Source*: Adapted from Ref. 90.
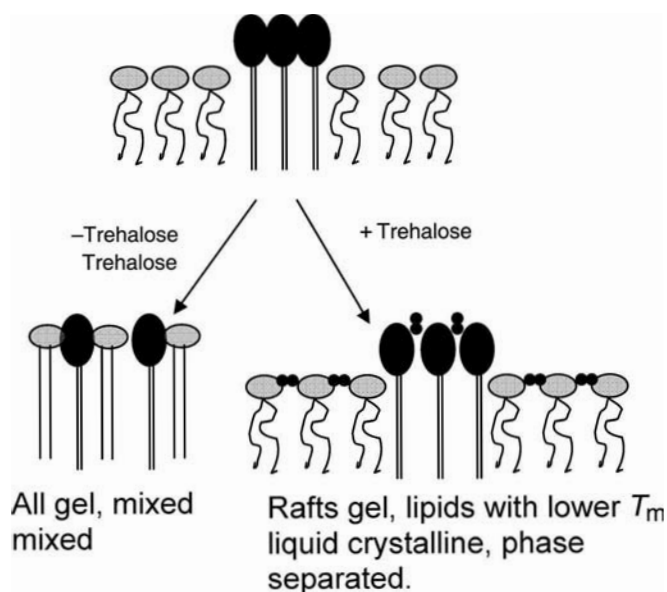
Figure 13 A hypothesis for the mechanism by which trehalose stabilize[s] domains in dry liposomes. Phase separation in the hydrated state is d[ue to] hydrophobic mismatch (Fig. 9). If the liposomes are dried without trehal[ose, all] lipids in the pair enter gel phase and mix. In liposomes dried with treha[lose, the] more fluid lipid has a depressed T_m in the dry state, while T_m for the gel ph[ase lipid] is affected to a less extent (Fig. 1). As a result, the lipid pair is maintained [in] states similar to those seen in the presence of water. In addition, formation [of glass] by dry trehalose almost certainly affects lateral mobility and thus inhibit[s ...]
Source: From Refs. 36–38, 90.

the processes leading to assembly of rafts in vivo can be modeled ad[equately] in vitro (106–110), a viewpoint entirely consistent with the suggest[ion that] studies models such as liposomes are applicable to native membra[nes. We] have previously shown that rafts are critical to blood platelet [function] (110) and that the rafts are maintained intact when the platelets a[re dried] with trehalose (89). We propose that the mechanism of stabiliz[ation is] similar to that proposed here for pure lipid systems.

ACKNOWLEDGMENTS

REFERENCES

1. Crowe LM, Crowe JH, Rudolph A, Womersley C, Appel A. Preservation of freeze-dried liposomes by trehalose. Arch Biochem Biophys 1985; 242:240.

2. Madden TD, Bally MB, Hope MJ, Cullis PR, Schieren HP, Janoff AS. Protection of large unilamellar vesicles by trehalose during lyophilization: retention of vesicle contents. Biochim Biophys Acta 1985; 817:67.

3. Womersley C, Uster PS, Rudolph AS, Crowe JH. Inhibition of dehydration-induced fusion between liposomal membranes by carbohydrates as measured by fluorescence energy transfer. Cryobiology 1986; 23:245.

4. Crowe LM, Womersley C, Crowe JH, Reid D, Appel L, Rudolph A. Prevention of fusion and leakage in freeze-dried liposomes by carbohydrates. Biochim Biophys Acta 1986; 861:131.

5. Crowe JH, Spargo BJ, Crowe LM. Preservation of dry liposomes does not require retention of residual water. Proc Natl Acad Sci USA 1987; 84:1537.

6. Harrigan PR, Madden TD, Cullis PR. Protection of liposomes during dehydration or freezing. Chem Phys Lipids 1990; 52:139.

7. Bridges PA, Taylor KMG. The effects of freeze-drying on the stability of liposomes to jet nebulization. J Pharm Pharmacol 2002; 53:393.

8. Desai TR, Wong JP, Hancock REW, Finlay JH. A novel approach to the pulmonary delivery of liposomes in dry powder form to eliminate the deleterious effects of milling. J Pharm Sci 2002; 91:482.

9. Abu-Dahab R, Schafer UF, Lehr C-F. Lectin-functionalized liposomes for pulmonary drug delivery: effect of nebulization on stability and bioadhesion. Eur J Pharm Sci 2001; 14:37.

10. Darwis Y, Kellaway IW. Nebulisation of rehydrated freeze-dried beclomethasone dipropionate liposomes. Int J Pharm 2001; 215:113.

11. Zuidam NJ, Lee SS, Crommelin DJ. Gamma-irradiation of non-frozen, frozen, and freeze-dried liposomes. Pharm Res 1995; 12:1761.

12. Liu S, O'Brien DF. Stable polymeric nanoballoons: lyophilization and rehydration of cross-linked liposomes. J Am Chem Soc 2002; 124:6037.

13. Armstrong TKC, Girouard LG, Anchordoquy TJ. Effects of PEGylation on the preservation of cationic lipid/DNA complexes during freeze-thawing and lyophilization. J Pharm Sci 2002; 91:2549.

14. Hinrichs WLJ, Sanders NN, De Smedt SC, Demeester J, Frijlink HW. Inulin is a promising cryo- and lyoprotectant for PEGylated lipoplexes. J Control Rel 2005; 103:465.

15. van Winden ECA, Crommelin DJA. Short term stability of freeze-dried, lyoprotected liposomes. J Control Rel 1999; 58:69.

16. van Winden ECA, Zhang W, Crommelin DJA. Effect of freezing rate on the stability of liposomes during freeze-drying and rehydration. Pharm Res 1997; 14:1151.

17. Zhang W, van Winden ECA, Bouwstra JA, Crommelin DJA. Enhanced permeability of freeze-dried liposomal bilayers upon rehydration. Cryobiology 1997; 35:277.

18. Crowe JH, Crowe LM, Jackson SA. Preservation and functional activity in lyophilized sarcoplasmic reticulum. Arch Biochem Biophys 1983; 220:477.

19. Crowe LM, Mouradian R, Crowe JH, Jackson SA, Womersley C. Effects of carbohydrates on membrane stability at low water activities. Biochim Biophys Acta 1984; 769:141.

20. Crowe JH, Crowe LM, Oliver AE, Tsvetkova NM, Wolkers WF, Tablin F. The trehalose myth revisited: introduction to a symposium on stabilization of cells in the dry state. Cryobiology 2001; 43:89.

21. Matsuo T. Trehalose protects corneal epithelial cells from death by drying. Br J Ophthalmol 2001; 85:610.

22. Norcia MA. Compositions and methods for wound management. Official Gazette of the U.S. Patent and Trademark Office 1232, 424 2000.

23. Higashiyama T. Novel functions and applications of trehalose. Pure Appl Chem 2002; 74:1263.

24. Benaroudj N, Lee DH, Goldberg AL. Trehalose accumulation during cellular stress protects cells and cellular proteins from damage by oxygen radicals. J Biol Chem 2001; 276:24261.

25. Chen Q, Haddad GG. Role of trehalose phosphate synthase and trehalose during hypoxia: from flies to mammals. J Exp Biol 2004; 207:3125.

26. Chen Q, Enbo N, Behar KL, Xu T, Haddad GG. Role of trehalose phosphate synthase in anoxia tolerance and development in Drosophila melanogaster. J Biol Chem 2002; 277:3274.

27. Neta T, Takada K, Hirasawa M. Low-cariogenicity of trehalose as a substrate. Dent 2000; 2:571.

28. Gimeno-Alcañiz JV, Pèrez-Ortìn JE, Matallana E. Differential pattern of trehalose accumulation in wine yeast strains during the microvinification process. Biotechnol Lett 1999; 21:271.

29. Komes D, Lovri T, Kovaevi Gani K, Gracin L. Study of trehalose addition on aroma retention in dehydrated strawberry puree. Food Technol Biotechnol 2003; 41:111.

30. Garg AK, Kim J-K, Owens TG, et al. Trehalose accumulation in rice plants confers high tolerance levels to different abiotic stresses. Proc Natl Acad Sci USA 2002; 99:15898.

31. Tanaka M, Machida Y, Niu S, et al. Trehalose alleviates polyglutamine-mediated pathology in a mouse model of Huntington disease. Nat Med 2004; 10:148.

32. Couzin J. Huntington's disease. Unorthodox clinical trials meld science and care. Science 2004; 304:816.

33. Crowe JH, Crowe LM, Carpenter JF, Aurell Wistrom C. Stabilization of dry phospholipid bilayers and proteins by sugars. Biochem J 1987; 242:1.

34. Crowe JH, Crowe LM. Preservation of liposomes by freeze drying. In: Gregoriadis G, ed. Liposome Technology. 2d ed. CRC Press, Inc., 1993.

35. Hays LM, Crowe JH, Wolkers W, Rudenko S. Factors affecting leakage of trapped solutes from phospholipid vesicles during thermotropic phase transitions. Cryobiology 2001; 42:88.

36. Crowe JH, Carpenter JF, Crowe LM. The role of vitrification in anhydrobiosis. Annu Rev Physiol 1998; 6:73.

37. Crowe JH, Crowe LM. Factors affecting the stability of dry liposomes. Biochim Biophys Acta 1988; 939:327.

38. Crowe LM, Crowe JH. Trehalose and dry dipalmitoylphosphatidylcholine revisited. Biochim Biophys Acta 1988; 946:193.
39. Crowe JH, Hoekstra FA, Nguyen KHN, Crowe LM. Is vitrification involved in depression of the phase transition temperature in dry phospholipids? Biochim Biophys Acta 1996; 1280:187.
40. Koster KL, Lei YP, Anderson M, Martin S, Bryant G. Effects of vitrified and nonvitrified sugars on phosphatidylcholine fluid-to-gel phase transitions. Biophys J 2000; 78:1932.
41. Sussich F, Skopec K, Brady J, Cesaro A. Reversible dehydration of trehalose and anhydrobiosis: from solution state to an exotic crystal? Carbohydrate Res 2001; 334:165.
42. Womersley C. Dehydration survival and anhydrobiotic potential of entomopathogenic nematodes. In: Gaugler R, Kaya HK, eds. Entomopathogenic Nematodes in Biological Control. Boca Raton, FL: CRC Press, 1990:117–130.
43. Westh P, Ramlbv H. Trehalose accumulation in the tardigrade adorybiotus coronifer during anhydrobiosis. J Exp Zool 1991; 258:303.
44. Lapinski J, Tunnacliffe A. Anhydrobiosis without trehalose in bdelloid rotifers. FEBS Lett 2003; 553:387.
45. Caprioli M, Katholm AK, Melone G, Ramløv H, Ricci C, Santo N. Trehalose in desiccated rotifers: a comparison between a bdelloid and a monogonont species. Comp Biochem Physiol A 2004; 139:527.
46. Tunnacliffe A, Lapinski J. Resurrecting Van Leeuwenhoek's rotifers: a reappraisal of the role of disaccharides in anhydrobiosis. Philos Trans R Soc Lond B 2003; 358:1755.
47. Crowe JH, Oliver AE, Hoekstra FA, Crowe LM. Stabilization of dry membranes by mixtures of hydroxyethyl starch and glucose: the role of vitrification. Cryobiology 1997; 3:20.
48. Hill DR, Keenan TW, Helm RF, Potts M, Crowe LM, Crowe JH. Extracellular polysaccharide of Nostoc commune (Cyanobacteria) inhibits fusion of membrane vesicles during desiccation. J Appl Physcol 1997; 9:237.
49. Buitink J, Leprince O. Glass formation in plant anhydrobiotes: survival in the dry state. Cryobiology 2004; 48:215.
50. Hincha DK, Hellwege EM, Meyer AG, Crowe JH. Plant fructans stabilize phosphatidylcholine liposomes during freeze-drying. Eur J Biochem 2000; 267:535.
51. Vereyken IJ, Chupin V, Hoekstra FA, Smeekens SCM, de Kruijff B. The effect of fructan on membrane lipid organization and dynamics in the dry state. Biophys J 2003; 84:3759.
52. Hincha DK, Zuther E, Heyer AG. The preservation of liposomes by raffinose family oligosaccharides during drying is mediated by effects on fusion and lipid phase transitions. Biochim Biophys Acta 2003; 1612:172.
53. Hincha DK, Hagemann M. Stabilization of model membranes during drying by compatible solutes involved in the stress tolerance of plants and microorganisms. Biochem J 2004; 383:277.
54. Popova AV, Hincha DK. Specific interactions of tryptophan with phosphatidylcholine and digalactosyldiacylglycerol in pure and mixed bilayers in the dry and hydrated state. Chem Phys Lipids 2004; 132:171.

55. Hincha DK, Oliver AE, Crowe JH. Lipid composition determines the effects of arbutin on the stability of membranes. Biophys J 1999; 77:2024.

56. Oliver AE, Hincha DK, Tsvetkova NM, Vigh L, Crowe JH. The effect of arbutin on membrane integrity during drying is mediated by stabilization of the lamellar phase in the presence of nonbilayer-forming lipids. Chem Phys Lipids 2001; 111:37.

57. Goodrich RP, Crowe JH, Crowe LM, Baldeschwieler JD. Alteration in membrane surfaces induced by attachment of carbohydrates. Biochemistry 1991; 30:2313.

58. Komatsu H, Saito H, Okada S, Tanaka M, Egashira M, Handa T. Effects of the acyl chain composition of phosphatidylcholines on the stability of freeze-dried small liposomes in the presence of maltose. Chem Phys Lipids 2001; 113:29.

59. Allison SD, Manning MC, Randolph TW, Middleton K, Davis A, Carpenter JF. Optimization of storage stability of lyophilized actin using combinations of disaccharides and dextran. J Pharm Sci 2000; 89:199.

60. Anchordoquy TJ, Izutsu K-I, Randolph TW, Carpenter JF. Maintenance of quaternary structure in the frozen state stabilizes lactate dehydrogenase during freeze-drying. Arch Biochem Biophys 2001; 390:35.

61. Heller MC, Carpenter JF, Randolph TW. Protein formulation and lyophilization cycle design: prevention of damage due to freeze-concentration induced phase separation. Biotechnol Bioeng 1999; 63:166.

62. Leslie SB, Israeli E, Lighthart B, Crowe JH, Crowe LM. Trehalose and sucrose protect both membranes and proteins in intact bacteria during drying. Econ Environ Microbiol 1995; 61:3592.

63. Esteves MI, Quintilio W, Sato RA, Raw I, De Araujo PS, Da Costa MHB. Stabilisation of immunoconjugates by trehalose. Biotechnol Lett 2000; 22:417.

64. Sun WQ, Leopold AC, Crowe LM, Crowe JH. Stability of dry liposomes in sugar glasses. Biophys J 1996; 70:1769.

65. Green JL, Angell CA. Phase relations and vitrification in saccharide–water solutions and the trehalose anomaly. J Phys Chem 1989; 93:2880.

66. Allison SD, Molina MDC, Anchordoquy TJ. Stabilization of lipid/DNA complexes during the freezing step of the lyophilization process: the particle isolation hypothesis. Biochim Biophys Acta 2000; 1468:127.

67. Crowe LM, Reid DS, Crowe JH. Is trehalose special for preserving dry biomaterials? Biophys J 1996; 71:2087.

68. Li S, Patapoff TW, Overcashier D, Hsu C, Nguyen TH, Borchardt RT. Effects of reducing sugars on the chemical stability of human relaxin in the lyophilized state. J Pharm Sci 1996; 85:873.

69. O'Brien J. Stability of trehalose, sucrose and glucose to nonenzymatic browning in model systems. J Food Sci 1996; 61:679.

70. Schebor C, Burin L, del Pilar Bueras M, Chirife J. Stability to hydrolysis and browning of trehalose, sucrose, and raffinose in low-moisturesystems in relation to their use as protectants of dry biomaterials. Lebensm-Wiss U-Technol 1999; 32:481.

71. BeMiller JN. Acid-catalyzed hydrolysis of glycosides. Adv Car Chem 1967; 22:25.

72. Oliver AE, Fisk E, Crowe LM, de Araujo PS, Crowe JH. Phospholipase A 2 activity in dehydrated systems: effect of the physical state of the substrate. Biochim Biophys Acta 1995; 1267:92.

73. Oliver AE, Crowe LM, de Araujo PS, Fisk E, Crowe JH. Arbutin inhibits PLA$_2$ in partially hydrated model systems. Biochim Biophys Acta 1996; 1302:69.

74. Mabrey S, Sturtevant JM. Investigation of phase transitions of lipids and lipid mixtures by sensitivity differential scanning calorimetry. Proc Natl Acad Sci USA 1976; 73:3862.

75. Mabrey S, Mateo PL, Sturtevant JM. High-sensitivity scanning calorimetric study of mixtures of cholesterol with dimyristoyl- and dipalmitoylphosphatidyl-cholines. Biochemistry 1978; 17:2464–2468.

76. McMullen TP, Lewis RN, McElhaney RN. Differential scanning calorimetric and Fourier transform infrared spectroscopic studies of the effects of choles-terol on the thermotropic phase behavior and organization of a homologous series of linear saturated phosphatidylserine bilayer membranes. Biophys J 2000; 79:2056.

77. Silvius JR, del Giudice D, Lafleur M. Cholesterol at different bilayer concentra-tions can promote or antagonize lateral segregation of phospholipids of differing acyl chain length. Biochemistry 1996; 35:15198.

78. Mendelsohn R, Moore DJ. Vibrational spectroscopic studies of lipid domains in biomembranes and model systems. Chem Phys Lipids 1998; 96:141.

79. Chen H, Mendelsohn R, Rerek ME, Moore DJ. Effect of cholesterol on misci-bility and phase behavior in binary mixtures with synthetic ceramide 2 and octadecanoic acid. Infrared studies. Biochim Biophys Acta 2001; 1512:345.

80. Thewalt JL, Bloom M. Phosphatidylcholine:cholesterol phase diagrams. Bio-phys J 1992; 63:1176–1181.

81. Sankaram MB, Thompson TE. Cholesterol-induced fluid-phase immiscibility in membranes. Proc Natl Acad Sci USA 1991; 8:8686.

82. Mouritsen OG, Jorgensen K. Dynamical order and disorder in lipid bilayers. Chem Phys Lipids 1994; 73:3–25.

83. Sugar IP, Michonova-Alexova E, Chong PL. Geometrical properties of gel and fluid clusters in DMPC/DSPC bilayers: Monte Carlo simulation approach using a two-state model. Biophys J 2001; 8:2425–2441.

84. Saxton MJ. Single-particle tracking: effect of corrals. Biophys J 1995; 69: 389–398.

85. Saxton MJ. Anomalous diffusion due to binding: a Monte Carlo study. Bio-phys J 1996; 70:1250.

86. Saxton MJ. Single-particle tracking: the distribution of diffusion coefficients. Biophys J 1997; 72:1744–1753.

87. Gil T, Ipsen JH, Mouritsen OG, Sabra MC, Sperotto MM, Zuckermann MJ. Theoretical analysis of protein organization in lipid membranes. Biochim Biophys Acta 1998; 1376:245.

88. Killian JA. Hydrophobic mismatch between proteins and lipids in membranes. Biochim Biophys Acta 1998; 137:401–416.

89. Leidy C, Gousset K, Ricker JV, et al. Lipid phase behavior and stabilization of domains in membranes of platelets cell. Biochem Biophys 2004; 40:123.

90. Ricker JV, Tsvetkova NM, Wolkers WF, et al. Trehalose maintains phase separation in an air-dried binary lipid mixture. Biophys J 2003; 84:3045.
91. Brown DA. Seeing is believing: visualization of rafts in model membranes. Proc Natl Acad Sci USA 2001; 98:10517.
92. Brown DA, London E. Structure and origin of ordered lipid domains in biological membranes. J Mem Biol 1998; 164:103–114.
93. Brown DA, London E. Structure and function of sphingolipid- and cholesterol-rich membrane rafts. J Biol Chem 2000; 275:17221.
94. Galbiati F, Razani B, Lisanti MP. Emerging themes in lipid rafts and caveolae. Cell 2001; 106:403.
95. London E. Insights into lipid raft structure and formation from experiments in model membranes. Curr Opin Struct Biol 2002; 12:480.
96. Simons K, Ikonen, E. How cells handle cholesterol. Science 2000; 290:1721.
97. Horejsi V. Membrane rafts in immunoreceptor signaling: new doubts, new proofs? Trends Immunol 2002; 23:562.
98. Heerklotz H. Triton promotes domain formation in lipid raft mixtures. Biophys J 2002; 83:2693.
99. Shogomori H, Brown DA. Use of detergents to study membrane rafts: the good, the bad, and the ugly. Biol Chem 2003; 384:1259.
100. Draber P, Draberova L. Lipid rafts in mast cell signaling. Mol Immunol 2002; 38:1247.
101. Horejsi V. The roles of membrane microdomains (rafts) in T cell activation. Immunol Rev 2003; 191:148.
102. Cheng PC, Dykstra ML, Mitchell RN, Pierce SK. A role for lipid rafts in b cell antigen receptor signaling and antigen targeting. J Exp Med 1999; 190:1549.
103. Fukl IV, Meyer ME, Williams KJ. Transmembrane and cytoplasmic domains of syndecan mediate a multi-step endocytic pathway involving detergent-insoluble membrane rafts. Biochem J 2001; 351:607.
104. Ono A, Freed EO. Plasma membrane rafts play a critical role in HIV-1 assembly and release. Proc Natl Acad Sci USA 2001; 98:13925.
105. Vincent S, Gerlier D, Manié SN. Measles virus assembly within membrane rafts J Virol 2000; 74:9911.
106. Kuzmin PI, Akimov SA, Chizmadzhev YA, Zimmerberg J, Cohen FS. Line tension and interaction energies of membrane rafts calculated from lipid splay and tilt. Biophys J 2005; 88:1120.
107. Bacia K, Scherfeld D, Kahya N, Schwille P. Fluorescence correlation spectroscopy relates rafts in model and native membranes. Biophys J 2004; 87:1034.
108. de Almeida RFM, Fedorov A, Prieto M. Sphingomyelin/phosphatidylcholine/cholesterol phase diagram: boundaries and composition of lipid rafts. Biophys J 2003; 85:2406.
109. Lawrence JC, Saslowsky DE, Edwardson JM, Henderson RM. Real-time analysis of the effects of cholesterol on lipid raft behavior using atomic force microscopy. Biophys J 2003; 84:1827.
110. Gousset K, Tsvetkova NM, Crowe JH, Tablin F. Important role of raft aggregation in the signaling events of cold-induced platelet activation. Biochim Biophys Acta 2004; 1660:7.

14

Hydrolysis of Phospholipids in Liposomes and Stability-Indicating Analytical Techniques

Daan J. A. Crommelin

Department of Pharmaceutics, Utrecht Institute for Pharmaceutical Sciences, Utrecht University, Utrecht, and Octoplus, Leiden, The Netherlands

Nicolaas J. Zuidam

Foods Research Centre, Unilever Research and Development, Vlaardingen, The Netherlands

INTRODUCTION

Drug-loaded liposomes are now being used in the clinic for different indications. This implies that these liposome formulations are stable for prolonged periods of time when properly stored. Besides the retention of the encapsulated agent, there are two stability aspects when considering therapeutic systems containing liposomes: (i) the liposome components may degrade by hydrolysis and oxidation, and (ii) the physical structure of the liposomes may be affected, by changes within the bilayer, aggregation, or fusion. Chemical changes in the bilayer-forming molecules may affect physical stability; e.g., if the phospholipids lose one of their acyl chains (turn into their lysoforms), the bilayer structure is affected.

In this chapter, the chemical stability of major bilayer constituents of liposomes currently being used in the pharmaceutical context is discussed. The focus will be on hydrolytic reactions occurring with phosphatidylcholine, phosphatidylglycerol, and phosphatidylethanolamine. Progress in

stability-indicating analytical techniques is reviewed as well. This chapter builds on earlier publications on these subjects, and the reader is referred to those for basic information (1,2).

ANALYTICAL APPROACHES: PROGRESS OVER THE LAST 10 YEARS

The existing arsenal of analytical techniques, as described in 1993 (3,4), has been supplemented and evolved. High-performance liquid chromatography (HPLC) column material with superior separation properties was introduced. On the detector side, several technologies entered the field providing quantification approaches as alternative to ultraviolet (UV) and refractive index–based detectors [evaporative light scattering detectors evaporative light scattering detector (ELSD)] and structural information as well (mass spectrometry). Alternatively, commercial enzyme-based assays for phospholipids were found to be useful in monitoring phospholipid concentrations in pharmaceutical formulations.

Column Material

Silica, diol-silica, and amino-silica columns are used for HPLC separation of phospholipids with different head groups. With amino (NH_2) phase columns, the separation is based both on differences in head groups and on large differences in acyl groups. Because of the separation between lysoforms and their parent lipids, these columns are regularly used in pharmaceutical test laboratories. Other column materials have been described as well. De Miguel et al. (5) discussed the use of a perfluorinated stationary bond in combination with a hydrophilic mobile (ethanol–water) phase and an ELSD.

Evaporative Light Scattering Detectors

ELSD is becoming the detector of choice to quantitate UV-insensitive material such as most phospholipids. Moreover, the response of a UV detector is sensitive toward oxidative changes in phospholipids. The mobile phase should readily evaporate without leaving a trace of solid material except for the separated lipids. After proper calibration, ELSDs can be used to monitor phospholipid stability during liposome formulation studies (6).

Mass Spectrometry

Mass spectrometric analysis in combination with HPLC not only enables quantification of the different phospholipids in the sample, but also has another use. In a reverse-phase high-performance liquid chromatography–electrospray ionization–mass spectrometer setup, Vernooij et al. (7) not only quantified the lipids, but were also able to assign acyl chain positions (position 1 or 2 on the glycerol backbone) on the phospholipid molecule.

Matrix-assisted laser desorption and ionization–time of flight (MALDI–TOF) mass spectrometry is a highly sensitive method to detect lipids and to obtain structural information of these lipids. However, efforts to use MALDI–TOF to quantify lipids have not been highly successful (yet) (8). It is expected that mass spectroscopy will gain importance in the coming years because this technology will become more readily accessible and dedicated systems will become available.

Enzymatic Assays

A review on the proper use of commercially available enzyme-based assays for quantifying phospholipids in liposome dispersions was published by Shmeeda et al. (9). Enzymatic assays for the determination of phosphatidylcholine are based on cleaving off the head group. In one protocol, phospholipase D cleaves off the choline group. Subsequently, the choline group is oxidized by choline oxidase, and a stoichiometric amount of hydrogen peroxide is formed. Via peroxidase, this hydrogen peroxide contributes to the coupling of 4-aminoantipyrine to phenol and a colored product can be quantified. Grohganz et al. (10) describe an evaluation of an assay for the measurements of phospholipids and conclude that proper solubilization of the liposome structure by detergents is essential for a robust assay.

POLYETHYLENEGLYCOL DETERMINATION

Polyethyleneglycol (PEG)-coated liposomes are extensively used in drug-loaded liposomes. The presence of PEG can be monitored by a classical Stewart color reaction upon separating the phospholipid part from the PEG (11). We developed a 1H-nuclear magnetic resonance method to determine the relative amounts of poly(ethylene glycol)- 1,2-distearoyl-*sn*-glycero-3-phosphoethanolamine [PEG-DSPE] in mixtures of phosphatidylcholine, phosphatidylglycerol, and cholesterol (12).

The hydrolysis of PEG from phosphatidylethanolamine is difficult to follow. Fourier transform infrared spectroscopy can be used to monitor this reaction. The C=O stretching bands of the various components of partially hydrolyzed PEG–phospholipids are deconvoluted, and the stability of (among others) the carbamate bond is established (13).

CHEMICAL DEGRADATION

Hydrolysis

Grit and, later, Zuidam worked on the stability issues related to (drug-loaded) liposomes. The insights gained by Grit were discussed in our 1993 chapter. Basically, dispersions containing neutral liposomes as used by Grit (egg lipid–based phosphatidylcholine) showed the lowest hydrolysis rate

(k_{obs}) at pH 6.5. Phospholipid concentration, buffer type, and acyl chain length hardly affected the k_{obs} under the chosen circumstances. Table 1 lists the k_{obs} at pH 4 and 30°C.

　　　When moving away from pH 6.5, in both the acidic and basic direction, a log-linear increase in hydrolysis rate constant versus pH was observed.

Table 1 k_{obs} of PC in Neutral Liposomes or Micelles in 50 mM Acetate (pH 4.0) and 0.12 M NaCl at 30°C[a]

Parameter of investigation	Composition liposomes	Remark	k_{obs} (10^{-7}/sec)
	DPPC, 20 mM	diC$_{16}$-PC	1.2 ± 0.3
Effect of concentration	DPPC, 4 mM		1.2 ± 0.1
	DPPC, 100 mM		1.2 ± 0.1
	DPPC, 200 mM		1.1 ± 0.1
Length of fatty acid chain	DCPC	diC$_6$-PC	0.8 ± 0.1
	DLPC	diC$_{12}$-PC	0.9 ± 0.1
	DMPC	diC$_{14}$-PC	1.2 ± 0.3
	DSPC	diC$_{18}$-PC	1.3 ± 0.2
	EPC	diC$_{14-22}$-PC	1.0 ± 0.1
Effect of α-tocopherol	DPPC/α-tocopherol 10/2		1.3 ± 0.1
	DPPC/α-tocopherol 10/4		1.2 ± 0.2
Effect of hydrolysis products	DPPC/LPC 1/1		1.1 ± 0.1
	DPPC/PA 10/1		1.0 ± 0.1
	DPPC/PA 2/1		1.0 ± 0.1
	DPPC/PA 1/1		0.7 ± 0.1
Effect of sodium chloride	DPPC without sodium chloride		1.3 ± 0.2
Effect of cryoprotectant	DPPC + 10% glucose[b]		1.1 ± 0.1
	DPPC + 10% trehalose[b]		1.2 ± 0.1
	DPPC + 10% sucrose[b]		1.2 ± 0.1
	DPPC + 10% propylene glycol[b]		1.1 ± 0.1
Effect of Triton X-100	DPPC/Triton X-100 1/1		1.1 ± 0.1[c]
	DPPC/Triton X-100 1/8		0.08 ± 0.07[d]

[a]Experimental data represent mean ± S.D. for at least three determinations. The concentration of PC was 20 mM, unless stated otherwise.
[b]The 10% cryoprotectants are shown as weight/volume measurements.
[c]After 45% hydrolysis, the hydrolysis rate decreased suddenly. The hydrolysis rate shown in this table has been derived from the values present before this deviation.
[d]Hardly any decrease was found in the experimental time period. Therefore, the S.D. is relatively large here.
Abbreviations: DPPC, 1,2-dipalmitoyl-*sn*-glycero-3-phosphocholine; DLPC, 1,2-dilauroyl-*sn*-glycero-3-phosphocholine; LPC, lysophosphatidylcholine; PA, phosphatidic acid; EPC, egg phosphatidylcholine.
Source: From Ref. 14.

When charged lipids are present in the bilayer, the bilayer surface pH is different from the bulk pH. This pH difference depends on the surface charge density (related to the molar fraction of the charged lipid in the bilayer) and the ionic strength and can be estimated by using the Gouy–Chapman–Stern nonlinear approximation model to estimate the surface potential and the Boltzmann equation to assess the pH shift. In our experiments, it turned out that the surface pH for the minimum hydrolysis rate remained around 6.5, but this surface pH corresponds with a different, shifted bulk pH (Table 2) (14,15).

The effects of hydrolysis on bilayer permeability and the bilayer stability upon heating were studied by Grit and Zuidam, respectively (14,16,17). In a later study, more restricted in terms of variables, Zhang and Pawelchak found similar results (18).

Interestingly, in the case of liposomes consisting of partially hydrogenated phosphatidylcholine and phosphatidylglycerol, the permeability for the hydrophilic marker molecule calcein decreased until about 10% of the phosphatidylcholine was hydrolyzed. At higher levels of hydrolysis, the permeability increased. Apparently, initially the lysophosphatidylcholine that was formed and the ''released'' fatty acid improve the barrier function of the bilayer (16). Zuidam continued this line of experiments and observed a conversion of liposomal structures to micellar structures upon heating if the liposomes passed through a gel-to-liquid phase transition and if a certain threshold level of hydrolysis was reached (19). This threshold level depended on the type of phospholipids used: $\pm 6\%$ for 1,2-dimyristoyl-sn-glycero-3-phosphocholine (DMPC), $\pm 9\%$ for 1,2-dipalmitoyl-*sn*-glycero-3-phosphocholine (DPPC), and $\pm 20\%$ for 1,2-distearoyl-*sn*-glycero-3-phosphocholine (DSPC).

Bilayer components can also affect the hydrolysis kinetics of each other via other mechanisms than surface pH changes. Under basic conditions, the hydrolysis-pH profile of 1,2-dioleoyl-*sn*-glucero-3-phosphoethanolamine (DOPE) in DOPE/DPPC vesicles was clearly different from the DOPE hydrolysis in 1,2-dioleoyltrimethylammoniumpropane (DOTAP)/DOPE (Fig. 1). In particular, under acidic conditions both DOPE and DOTAP showed no pH dependency for their hydrolysis kinetics. The hydrolysis rate constant was almost pH independent between pH 4 and 6.5. The authors suggest that this unusual phenomenon should be ascribed to ''amine-influenced'' hydrolysis, as earlier reported for amoxicillin (20). Another example of a liposome component influencing the hydrolysis kinetics was described by Saetern et al. (21). The cytostatic camptothecin was liposome associated and tended to catalyze the hydrolysis of egg phosphatidylcholine.

An interesting approach where hydrolysis can play a beneficial role in carrier-mediated drug transport is presented by Shin et al. (22). Here, liposomes consisting of DOPE and cleavable PEG–lipid conjugates are prepared. The PEG–lipid bond is acid labile. Upon acidification, e.g., in the endosome upon liposome uptake into the cell, the PEG is clipped off

Table 2 k_{obs} of Phospholipids in Charged Liposomes in 50 mM Acetate Buffer (pH 4.0) and 0.12 M NaCl at 30°C

Liposome composition and phospholipid concentration	k_{obs} of DPPC (10^{-7}/sec)	k_{obs} of DPPG or DPPE (10^{-7}/sec)	σ_{el} (C/m²)	σ_{eff}^d (C/m²)	Ψ^d (V)	pH at bilayer surface[e]
20 mM DPPC	1.2±0.3	–	0	0	0	4.0
22 mM DPPC/DPPG 10/1	2.4±0.1	3.0±0.1	−0.028	−0.023	−0.027	3.6
22 mM DPPC/DPPG 10/1 (sized)[a]	2.6±0.1	3.3±0.4	−0.028	−0.023	−0.027	3.6
30 mM DPPC/DPPG/ CHOL 10/1/4	2.0±0.1	2.6±0.1	−0.023	−0.019	−0.023	3.6
30 mM DPPC/DPPG 10/5[b]	9.7±0.8	10±1	−0.105	−0.058	−0.059	3.0
40 mM DPPC/DPPG 10/10[b]	9.7±0.1	11.4±0.6	−0.160	−0.073	−0.069	2.9
20 mM DPPG[b]	–	19±3	−0.334	−0.271	−0.134	1.8
22 mM DPPC/DCP 10/1[c]	3.5±0.2	–	−0.029	−0.029	−0.033	3.5
22 mM DPPC/DPPE 10/1	1.1±0.1	0.8±0.1	0	0	0	4.0
22 mM DPPC/SA 10/1[c]	0.40±0.04	–	0.029	0.029	0.034	4.6

Notes: Experimental data represent mean±S.D. for three determinations. σ is the surface charge density and ψ is the surface potential.

[a]Size of these liposomes was 0.18 μm with a polydispersity index of ±0.1 (indicating narrow particle-size distribution).

[b]The k_{obs} of these liposomes with a relatively high DPPG content has been derived from the values above 50% hydrolysis.

[c]DCP and SA were analyzed by an high-performance liquid chromatography method and did not degrade in the experimental time period. An apparent pK$_a$ was reported for DCP in egg phosphatidylcholine of 4.7 and 4.5. In the present study, we did not find any indication for protonation of DCP.

[d]The buffer used to maintain the pH at 4.0 at 30°C consisted of 39 mM acetic acid, 11 mM sodium acetate, and 0.12 M sodium chloride. Therefore, the values used in the calculations of Ψ and σ_{eff} were 0.131 for ionic strength, 0.131 M for [Na$^+$], and 8.3×10^{-10} m for the Debye screening length, λ.

[e]The surface pH can be calculated by using the Boltzmann equation for a given potential: $4.0 + \mathrm{pH} = 4.0 + (e\Psi)/(2.303 \times kT)$, where e is the electron charge.

Abbreviations: DCP, dicetylphosphate; DPPC, 1,2-dipalmitoyl-*sn*-glycero-3-phosphocholine; DPPG, 1,2-dipalmitoyl-*sn*-glycero-3-phosphoglycerol (sodium salt); DPPE, 1,2-dipalmoyl-*sn*-glycero-3-phosphoethanolamine; SA, stearylamine.
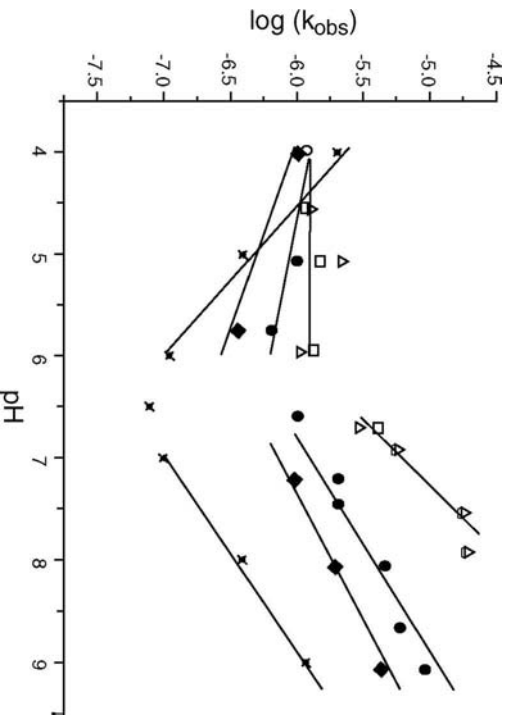
Figure 1 Effect of pH on k_{obs} of DOPE in DPPC DOPE 3:1 liposomes (●). DPPC DOPE (3:1) liposomes (♦), DOPE in DOTAP DOPE (1:1) liposomes... DOTAP in DOTAP DOPE 1:1 liposomes (△). The temperature was 70°C... k_{obs} pH$_{bulk}$ profile of saturated soybean phosphatidyl choline (SSPC) in SSPC liposomes at 70°C and buffer concentration 50 mM [20] "×" is sho... reference. For clarity, only a part of the available data points is shown. I... determinations of k_{obs} values typically differed by less than 10%. *Source:* Fro...

and the remaining DOPE/lipid combination is unstable and exer... brane-fusing characteristics.

STERILIZATION

Most liposomes for clinical use are administered via the parentera... This implies that the end product should be sterile. The first choice a... ilization approach is heat sterilization of the end product by autocla... 15 to 20 minutes at 121°C. Sterilization of liposomes by autocla... been studied by Zuidam et al. (3). Subsequently, the options to steri... somes by gamma radiation were explored.

Sterilization by Autoclaving

Liposomal dispersions composed of combinations of DPPC, 1,2-... toyl-*sn*-glycero-3-phosphoglycerol (sodium salt) (DPPG), egg PC,... and/or cholesterol were treated for 20 minutes at 121°C. Buffered s... at pH 4 and pH 7.4 were chosen and model compounds (rangi... highly hydrophilic to highly lipophilic) were built into the liposo...

the three processes—hydrolysis, oxidation, and model compound release—were monitored.

The results show that at pH 7.4, hydrolysis and oxidation hardly occurred. At pH 4.0, no change was detected in the extent of oxidation after autoclaving; however, 4% to 10% of the phospholipids was hydrolyzed. Before autoclaving, between 1% and 2.5% of the lipids were present in the hydrolyzed lysoform. Lipophilic model compounds stayed liposome associated, but the hydrophilic compound calcein was released to a high extent. In conclusion, if proper pH conditions are chosen and lipophilic (heat stable) drugs are dealt with, autoclaving of liposome end products may be considered. Later, the group around Brandl published on the effects of steam sterilization of vesicular phospholipid gels (23). They reported that upon autoclaving, these gels retained much of their main characteristics but changes were observed in morphology and functional properties of the gel.

Sterilization by Gamma Irradiation

The question can be raised whether gamma irradiation may offer an alternative sterilization technique to autoclaving of liposomes. In the mid-1990s, this question was still unresolved. Zuidam et al. set up a systematic series of studies in which liposomes were gamma irradiated at dose levels up to 58 kGy (in the United States Pharmacopeia (USP), dose levels of 25 kGy are mentioned for sterilization purposes) (24,25). This group worked with aqueous liposome dispersions. The liposomes were composed of DPPC and DPPG, and the analytical assays comprised gas-liquid chromatography, thin-layer chromatography, HPLC, mass spectroscopy [differential scanning calorimetry (DSC), dynamic light scattering (DLS)] and fluorescence anisotropy. DPPG tended to hydrolyze faster than DPPC. Interestingly, the smaller the particles, the more sensitive were they to irradiation damage (Fig. 2). Up to 60% of the DPPG in the DPPC/DPPG vesicles was degraded after exposure to 25 kGy. The chemical nature of a number of identified degradation products was assessed by mass spectroscopy. In general, no changes in particle size were found, and bilayer rigidity was not affected either upon irradiation. In contrast, the bilayer-melting behavior, as monitored by DSC, was changed upon irradiation because peak broadening occurred.

Then, the group analyzed liposome dispersions irradiated in a frozen or freeze-dried state. Here, both liposome dispersions with unsaturated (from eggs) and saturated fatty acid chains were studied. Trehalose was added as a lyoprotectant (17). Interestingly, trehalose turned out not only to be a good cryoprotectant and lyoprotectant, but also a radical scavenger. Degradation kinetics was strongly influenced by the presence of trehalose: degradation reduced significantly in the presence of trehalose. Oxidative damage for egg-derived phospholipids also decreased in the presence of this sugar
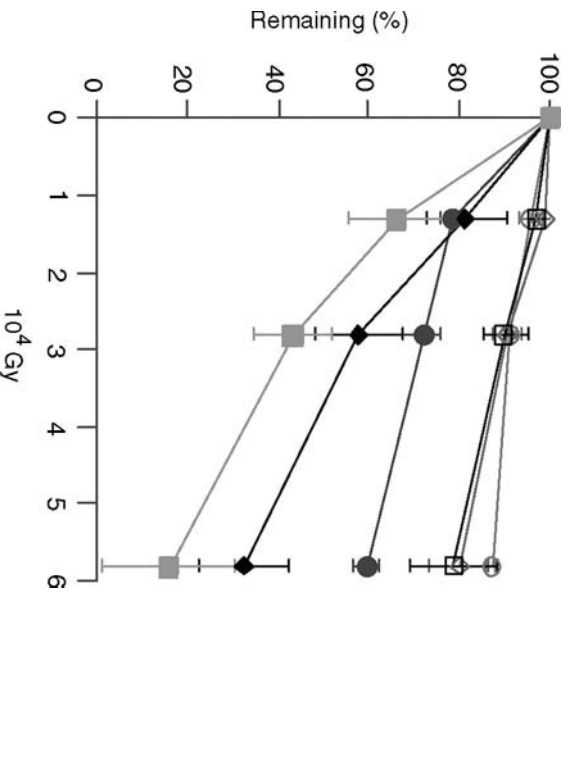
Figure 2 Percentage of DPPC and DPPG versus irradiation dose upon gamma irradiation of nonsized (O and ●, respectively), 0.18 μm (◇ and ◆, respectively) 0.10 μm (□ and ■, respectively) DPPC/DPPG 10/1-liposomes (22 mM) in phosphate buffer (pH 7.4) and 0.13 M NaCl. Vertical bars denote S.D. of triplicate determinations. *Source:* From Ref. 24.

and the changes in DSC profiles of saturated phospholipids were minimal. Unfortunately, trehalose degraded in the radical scavenging process, meaning that other options had to be explored. Nitroxides were studied as radical scavengers and showed irradiation protection (26). Later, the effect on the effect of irradiation on solid and lyophilized phospholipids was continued by Stensrud et al. (27).

CONCLUDING REMARKS

Because the liposomes were proposed as drug delivery systems, questions have been raised about the stability of liposomes as pharmaceutical formulations. Liposome stability and shelf life depend on a number of factors such as size and chemical composition. Liposomal drug products have to be stable for over two years at a minimum. Both in physical and chemical terms, little deviation from the specifications of the fresh product are tolerated. More information on the view of Food and Drug Administration on liposome drug products can be found in the "Guidance for Industry on some Drug Products" issued August 2002 (28). It suffices to say th

the last decade (since the publication of the second edition of "Liposome Technology"), a lot of progress has been made in determining and understanding hydrolysis processes in pharmaceutical liposome products, and the present chapter has reviewed these new insights.

REFERENCES

1. Grit M, Zuidam NJ, Crommelin DJA. Analysis and hydrolysis kinetics of phospholipids in aqueous liposome dispersions. In: Gregoriadis G, ed. Liposome Technology. 2d ed. Boca Raton, FL: CRC Press, 1993; 1:455.
2. Zuidam NJ, Van Winden E, de Vrueh R, Crommelin DJA. Stability, storage and sterilisation of liposomes. In: Torchilin VP, Weissig V, eds. Liposomes. 2d ed. Oxford University Press, 2003:149.
3. Zuidam NJ, Lee SSL, Crommelin DJA. Sterilization of liposomes by heat treatment. Pharm Res 1993; 10:1591–1596.
4. Zuidam NJ, de Vrueh R, Crommelin DJA. Characterization of liposomes. In: Torchilin VP, Weissig V, eds. Liposomes. 2d ed. Oxford University Press, 2003:31.
5. De Miguel I, Roueche A, Betbeder D. Separation of dipalmitoylcholine, cholesterol and their degradation products by high performance liquid chromatography on a perfluorinated bonded phase. J Chromatogr A 1999; 840:31–38.
6. Sas B, Peys E, Helsen M. Efficient method for (lyso)phospholipid class separation by high-performance liquid chromatography using an evaporative light-scattering detector. J Chromatogr A 1999; 864:179–182.
7. Vernooij EAAM, Kettenes-van den Bosch JJ, Crommelin DJA. Rapid determination of acyl chain position in egg phosphatidylcholine by high performance liquid chromatography/electrospray mass spectrometry. Rapid Commun Mass Spectrom 1998; 12:83–86.
8. Schiller J, Suss R, Arnhold J, et al. Matrix-assisted laser desorption and ionization time-of-flight (MALDI-TOF) mass spectrometry in lipid and phospholipid research. Prog Lipid Res 2004; 43:449–488.
9. Shmeeda H, Even-Chen S, Honen R, Cohen R, Weintraub C, Barenholz Y. Enzymatic assays for quality control and pharmacokinetics of liposome formulations: comparison with nonenzymatic conventional methodologies. Methods Enzymol 2003; 367:272–292.
10. Grohganz H, Ziroli V, Massing U, Brandl M. Quantification of various phosphatidylcholines in liposomes by enzymatic assay. AAPS Pharm Sci Tech 2003; 4:E63.
11. Nag A, Mitra G, Ghosh PC. A colorimetric estimation of polyethyleneglycol-conjugated phospholipid in stealth liposomes. Anal Biochem 1997; 250:35–43.
12. Vernooij EAAM, Gentry CA, Herron JN, Crommelin DJA, Kettenes-Van den Bosch JJ. 1H NMR quantification of poly(ethylene glycol)-phosphatidylethanolamine in phospholipid mixtures. Pharm Res 1999; 16:1658–1661.
13. Vernooij EAAM, Kettenes-van den Bosch JJ, Crommelin DJA. Fourier transform infrared spectroscopic determination of the hydrolysis of poly(ethylene glycol)–phosphatidylethanolamine-containing liposomes. Langmuir 2002; 18: 3466–3470.

14. Zuidam NJ, Crommelin DJA. Chemical hydrolysis of phospholipids. J Pharm Sci 1995; 84:1113–1119.
15. Grit M, Crommelin DJA. The effect of surface charge on the hydrolysis kinetics of partially hydrogenated egg phosphatidylcholine and egg phosphatidylglycerol in aqueous liposome dispersions. Biochim Biophys Acta 1993; 1167:49–55.
16. Grit M, Crommelin DJA. The effect of aging on the physical stability of liposome dispersions. Chem Phys Lipids 1992; 62:113–122.
17. Zuidam NJ, Lee SSL, Crommelin DJA. Gamma-irradiation of non-frozen, frozen and freeze-dried liposomes. Pharm Res 1995; 12:1761–1768.
18. Zhang JA, Pawelchak J. Effect of pH, ionic strength and oxygen burden on the chemical stability of EPC/cholesterol liposomes under accelerated conditions. Part I: lipid hydrolysis. Eur J Pharm Biopharm 2000; 50:357–364.
19. Zuidam NJ, Gouw HKME, Barenholz Y, Crommelin DJA. Physical (in)stability of liposomes upon chemical hydrolysis: the role of lysophospholipids and fatty acids. Biochim Biophys Acta 1995; 1240:101–110.
20. Vernooij EAAM, Kettenes-van den Bosch JJ, Underberg WJM, Crommelin DJA. Chemical hydrolysis of DOTAP and DOPE in a liposomal environment. J Control Rel 2002; 79:299–303.
21. Saetern AM, Skar M, Braaten A, Brandl M. Camptothecin-catalyzed phospholipid hydrolysis in liposomes. Int J Pharm 2005; 288:73–80.
22. Shin J, Shum P, Thompson DH. Acid-triggered release via dePEGylation of DOPE liposomes containing acid-labile vinyl ether PEG-lipids. J Control Rel 2003; 91:187–200.
23. Tardi C, Drechsler M, Bauer KH, Brandl M. Steam sterilization of vesicular phospholipid gels. Int J Pharm 2001; 217:161–172.
24. Zuidam NJ, Versluis C, Vernooy EAAM, Crommelin DJA. Gamma-irradiation of liposomes composed of saturated phospholipids. Effect of bilayer composition, size, concentration and absorbed dose on chemical degradation and physical destabilisation of liposomes. Biochim Biophys Acta 1996; 1280:135–148.
25. Zuidam NJ. Stability of Liposomes, Thesis, 1994 (ISBN 90–292–0535-8).
26. Samuni AM, Barenholz Y, Crommelin DJA, Zuidam NJ. Gamma-Irradiation damage to liposomes differing in composition and their protection by nitroxides. Free Radical Biol Med 1997; 23:972–979.
27. Stensrud G, Redford K, Smistad G, Karlsen J. Effects of gamma irradiation on solid and lyophilised phospholipids. Rad Phys Chem 1999; 56:611–622.
28. FDA 2002. http://www.fda.gov/ohrms/dockets/98fr/02d-0337-gdl0001-vol1.PDF.

15

Process Development and Quality Control of Injectable Liposomal Therapeutics

**Gerard M. Jensen, Tarquinus H. Bunch,
Ning Hu, and Crispin G. S. Eley**
Gilead Sciences, Inc., San Dimas, California, U.S.A.

INTRODUCTION AND PERSPECTIVE

The commercial realization of the therapeutic potential of liposomal drugs rests, in part, on the ability to produce batches in a commercial setting that have reproducibly the same quality attributes as those used during nonclinical and clinical development. Part of this is obviously related to formulation—both composition and the basic manner in which drug containing liposomes are produced—and literature discussing liposomal drugs is naturally dominated by these aspects. The purpose of this chapter is to contrast the role of the details of process parameters and technology, raw material quality, and quality control testing, versus a simple focus on formulation. Examples given below highlight the fact that differences in the process of manufacturing liposomes can, in many cases, be of equal importance.

Liposomal dispersions are not true solutions, although ideally they behave like them macroscopically. There is, at the microscopic level, a noncovalent molecular assembly whose structural elements may be critical to the desired functional aspects. These systems rely on the physics and chemistry of multiple components, and the physical assembly of many thousands
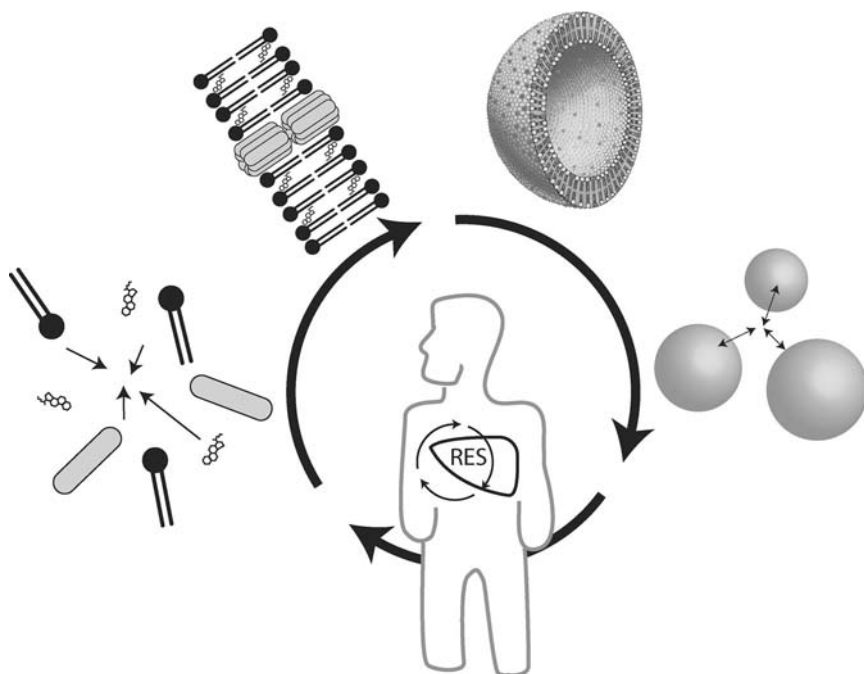
Figure 1 Liposomes: the third dimension. *Abbreviation*: RES, reticuloendothelial system.

of molecules. Figure 1 shows in cartoon format the structural elements at play. Clockwise from the left is illustrated the noncovalent assembly of the structural moieties, the assembled bilayer with a hypothetical pore structure formed, the canonical small unilamellar vesicle (SUV) liposome structure (cut away view), and the interaction of SUVs. These revolve around the human subject with an implied impact on reticuloendothelial system (RES) clearance, just as an example (see below). Among the many elements of this assembly that may be functionally critical are the size and the distribution of size, the level to which the drug is entrapped or encapsulated in the liposome interior or bilayer, or at the interfaces of these, etc.

Figure 2 illustrates a series of stresses and potential consequences. In the illustration, they are not meant to be paired up, nor are they meant to represent a comprehensive list. On the left side are examples of stresses applicable to most liposome products: filtration, for example sterile filtration during production, or filtration at the pharmacy or bedside; refrigeration during storage—one notes that for colloidal properties, lower rather than higher temperatures may represent the "stress" condition; freeze-drying, as is often desired to extend shelf life based on chemical instability; Brownian collisions, which are the result of their natural motion in the
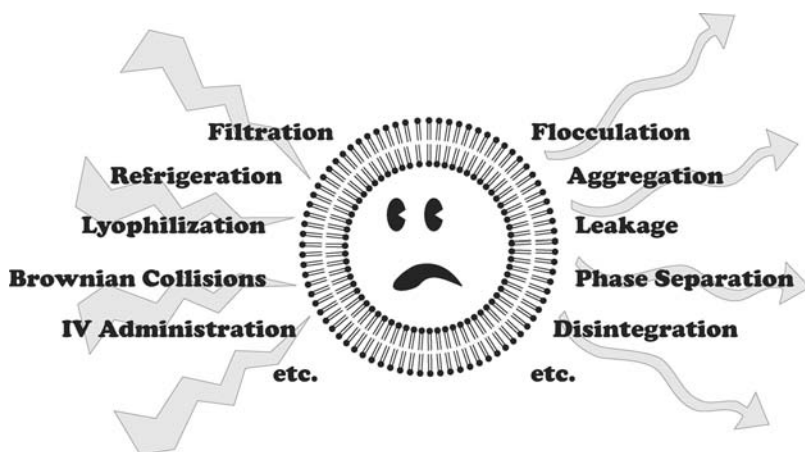
Figure 2 Liposomes: stress and consequences.

bottle; and intravenous administration—including dilution in infusion diluents (e.g., dextrose and saline) and use with giving sets. On the right are illustrations of consequences that, depending on how a liposome is assembled, can be the result of applied stresses. These include flocculation or aggregation of the particles; leakage of contents or alteration of release rate of drug; phase separation either macroscopically evident or microscopically present; disintegration of the liposome itself; etc.

Once a liposomal formulation has been achieved, which has desired properties and promising nonclinical or clinical data, the product must be reproducible from lot to lot. The therapeutic index enhancement must be maintained, whatever that is, whether on the efficacy or on the toxicity side, or both, for every batch. One must have a stable formulation with a commercially viable shelf life, and commercially viable storage and handling criteria. Again, most of the published literature describing these aspects, especially for particular liposomal products, involve composition, lamellarity, and the basic class of the liposome (e.g., SUV and large unilamellar vesicle). What we emphasize below, with selected examples, is that it is equally critical to achieve precision assembly—how it is all put together—and with that, sufficient raw material quality, and product and process characterization.

PROCESS VS. FORMULATION

What follows are examples where liposomal preparations of similar or identical formulation, and of common basic design, have very different quality attributes, owing to differences in raw material quality and/or details of the production process.

Pharmacokinetics of "Conventional" Liposomes

Figure 3A reproduces a figure from the literature (1) that, in a variety of incarnations, is often shown in articles or presentations about liposomes. What is typically shown are comparisons of pharmacokinetic plasma or blood decay curves (in this case, blood levels of liposome-encapsulated ^{67}Ga in rats) contrasting liposomes composed of phosphatidylcholine (PC) and cholesterol

(A)

(B)
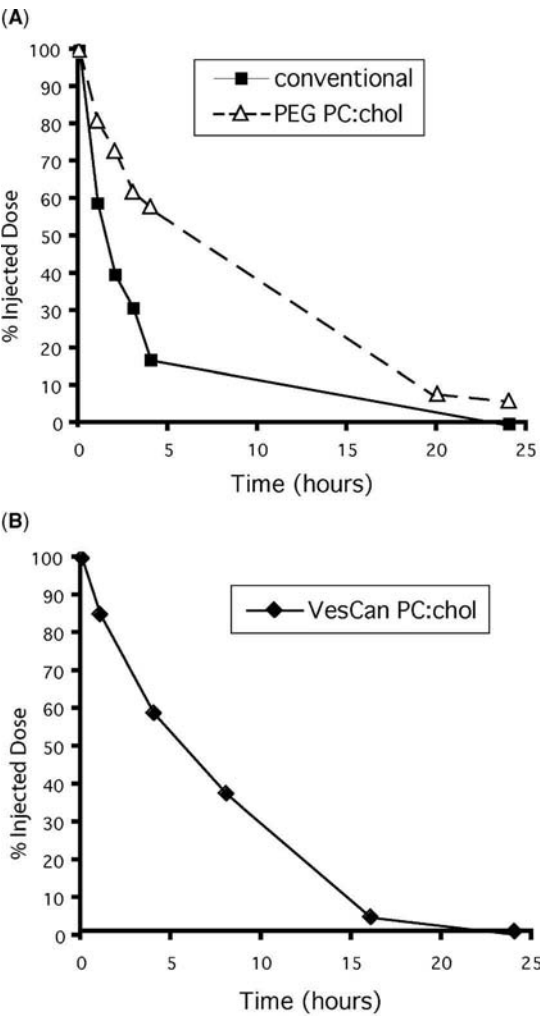
Figure 3 (**A**) Rat pharmacokinetics of conventional PC:chol and PEG PC:chol. (**B**) Rat pharmacokinetics of VesCan. *Abbreviations*: PEG, polyethylene glycol; PC, phosphatidylcholine; PC:chol, phosphatidylcholine:cholesterol; PEG PC:chol, polyethylene glycol PC:chol liposomes. *Source*: From Ref. 1.

(chol)—so-called "conventional" liposomes—and those that include decoration with polyethylene glycol derivatized lipids—so-called "pegylated" liposomes. The clear message from such figures is that the inclusion of pegylation can afford enhanced stability in blood or plasma, with increased circulation time/reduced clearance. All things being equal, this is typically true, well established, and has been used to good effect, e.g., in the commercially approved liposomal doxorubicin (DOX) product, Doxil. The implication of the figure, however, is that without polymer shrubbery, conventional liposomes would clear very rapidly. In the late 1980s, Vestar Inc., a company founded on the basis of science developed by the California Institute of Technology and the City of Hope, developed an imaging agent (2) based on liposome-encapsulated ^{111}In^{3+}. This agent, named VesCan, together with the gamma-ray–perturbed angular correlation spectroscopy technique to examine liposome integrity, was envisioned as a broadly applicable in vivo tumor diagnostic agent. Although not ultimately commercialized, the agent was used to successfully image a variety of tumors, and was evaluated in late-stage clinical trials. VesCan was developed as a long-circulating, RES-avoiding (at least in a relative sense) liposome, composed of distearoylphosphatidylcholine and chol (mole ratio, 2:1). Early on, in addition to process breakthroughs in the manufacture of the product by high-shear homogenization, came a substantial emphasis on the use of high purity phospholipids and chol (2). Figure 3B shows the clearance of encapsulated ^{111}In in rat blood after a single injection of VesCan. Thus, a conventional PC:chol liposome produced more than 15 years ago was shown to possess substantial stability in vivo.

More recently, conventional liposomes of substantial stability after injection have been developed. Rat pharmacokinetic data are shown in Figure 4 for a clinical development product, liposomal amikacin (MiKasome) (3), which has been shown to exhibit a 100-plus hour elimination half-life in man. Also shown in this figure are data for pegylated liposomal doxorubicin (Doxil), and data for a conventional [2:1 hydrogenated soy phosphatidylcholine (HSPC):chol] liposomal doxorubicin (L-DOX), which contains no pegylation but was prepared using gradient loading with 600 mM ammonium sulfate (i.e., which has a comparable drug retaining gradient to Doxil). The data for the two doxorubicin injections are very similar. This information is not meant to imply that these two liposomal formulations are bioequivalent in a strict sense; however, this data, and data like it [for example, for liposomal GW1843U89, a passively encapsulated, membrane impermeable thymidylate synthase inhibitor in a 2:1 HSPC:chol SUV (4–6) with a reported elimination half-life in man of ~70 hours], does indicate that extended stability and long elimination half-lives can be exhibited by so-called conventional liposomes properly made.

Aspects of Particle Size Distribution

To provide an example of the importance of quality control, we focus here on the aspects of particle size determination. Figure 5 displays the typical
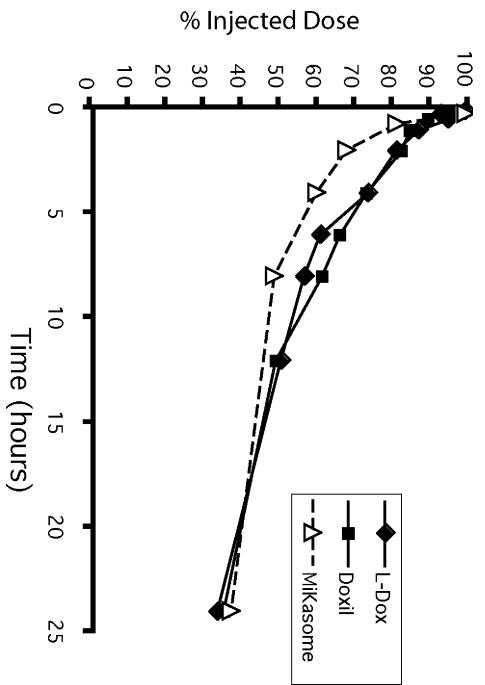
Figure 4 Plasma concentration versus time curves for single bolus intraven[ous injec]tion of rats for MiKasome (50 mg/kg), Doxil (1 mg/kg), and nonpegylated [liposomal] doxorubicin (L-DOX) (1 mg/kg) as indicated.

output of a commercial dynamic light scattering particle size appa[ratus.] a liposomal dispersion produced by high-shear homogenization. For t[he unit] in question, the volume-weighted median and mean sizes provide a[...] [when correlated to National Institute of Standards and Technolog[y...]
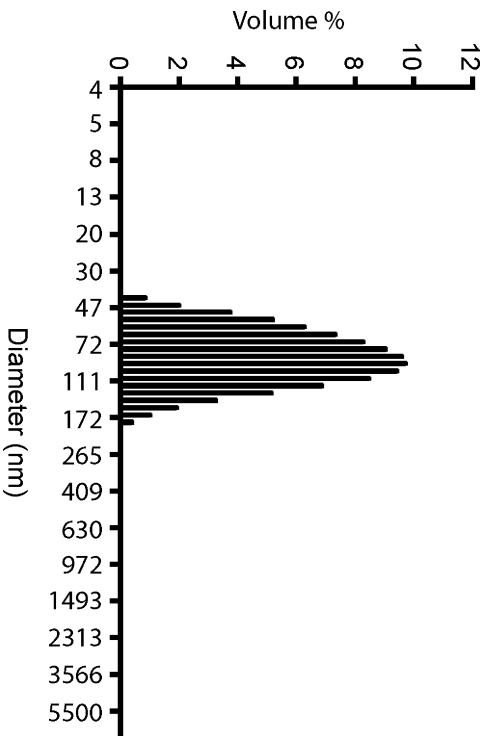
Figure 5 Dynamic light scattering size distribution for a liposome disp[...] typical rendering of the data by a commercial instrument.

traceable bead standards or to electron micrograph data, for example] and good operational precision—about 3.5% relative standard deviation (RSD).

However, it is obvious that liposome dispersions in fact exhibit a distribution of sizes. The quality control question is: do we have the sensitivity in this technique to detect a "change" in that distribution, and most importantly, detect small subpopulations, for example, of larger particles (formed via aggregation, flocculation, fusion, etc.). Figure 6 presents the same data shown in Figure 5, but on a linear scale. From this, one can get a more realistic picture of the nature of the size distribution. The evidence in this figure is a "tail" to larger size, which is at least of heuristic value. The importance of that tail can affect a number of different areas. It is well known that, all things being equal, liposomes of greater than 100 nm will be accumulated by Kupffer cells in the liver, and those smaller than 100 nm generally will not. Thus, a growing tail to larger size can have a biodistribution consequence. Another example is illustrated in Figure 6 with a plot of the shell (bilayer) to interior (aqueous) volume ratio. Across the size distribution, it can be seen that smaller liposomes are dominated volumetrically by the lipid portion, and for larger liposomes, by the aqueous portion. This can affect the structural architecture alluded to in the introduction above, with consequence for drug loaded in the interior or in the bilayer.
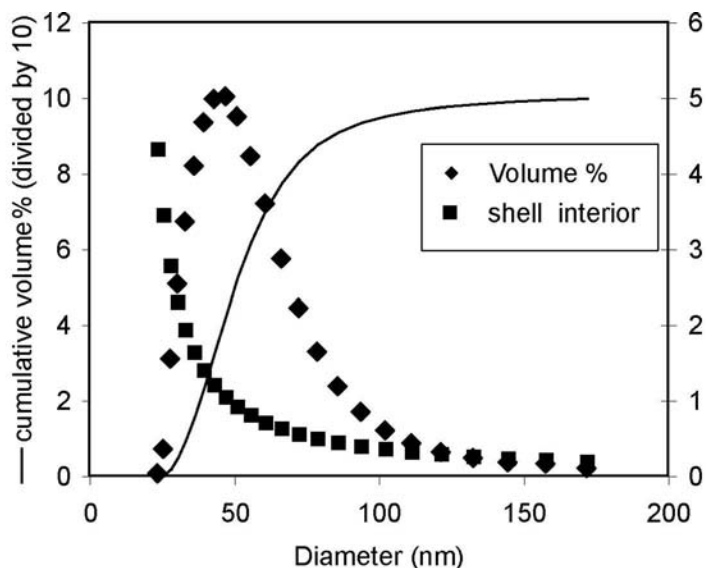
Figure 6 Dynamic light scattering size distribution for a liposome dispersion (*diamonds*), the cumulative volume percentage (*the line*), and the shell-to-interior volume ratio (*squares*) for the given diameter.

Can a dynamic light scattering apparatus provide sensitive information on the existence of a growing population of particles above 100 nm in a SUV dispersion? To mimic the effect of this potential aggregation/flocculation scenario, and to study the effect of large-sized liposome subpopulations, sizing experiments were carried out using mixtures of electrostatically stabilized [carrying a negative charge and, therefore, ostensibly noninteraction; 2:1: 0.1 mole ratio DSPC:chol:distearoylphosphatidyl glycerol (DSPG)] liposomes of small (~40 nm) and large (~230 nm) size. The large-sized liposomes were made by extrusion through polycarbonate filter membranes, and a median diameter of 230 nm was measured by dynamic light scattering and confirmed by freeze fracture electron microscopy. The small liposomes were made using the same formulation by probe sonication. Size was confirmed by dynamic light scattering. The larger liposomes were spiked into a dispersion of the small vesicles at up to 41.3 wt% to simulate flocculation or aggregation (76.4% by volume and 2.1% by number, calculated based upon measured lipid concentrations, mean diameter, and the assumption of a 5-nm bilayer thickness). Results are shown in Figure 7 for the corresponding 90%, 95%, and 100% (the median) passing diameters for these samples. For the whole of the titration of larger particles into the SUV dispersion, the median (100%) diameter value is unaltered and is thus insensitive. The 90% and 95% passing diameter values do reveal some sensitivity to the titration. However, this sensitivity is not evident for up to 8% by weight of added large liposomes and is a much less precise parameter (greater than 10% RSD vs. 3.5% for the 100% median diameter value). An alternate, more sensitive approach is therefore required.

Experienced laboratory personnel who make SUVs on a daily basis can see by eye if their preparations are substantially "contaminated" with
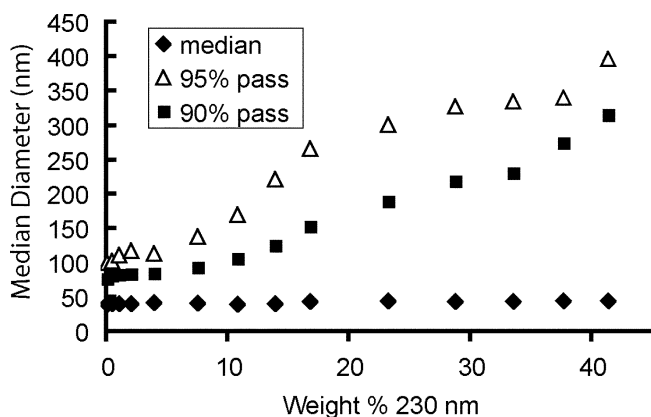
Figure 7 Ninety to 100% passing diameter dynamic light scattering data for a liposome dispersion of 40-nm median diameter after titration with 230-nm liposomes of the given final wt%.
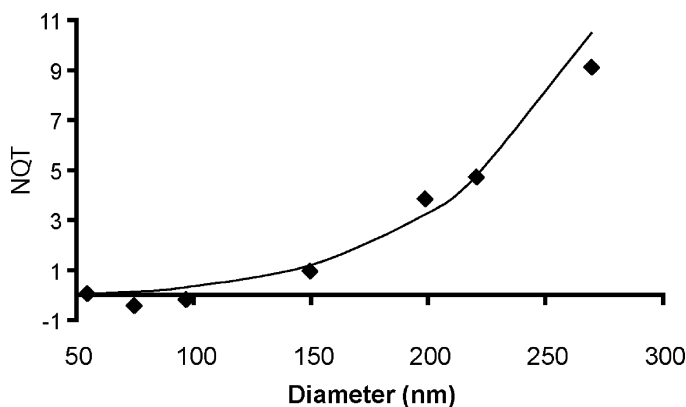
Figure 8 NQT data for NIST bead standards of given diameter 54, 74, 96, 149, 198, 220, and 269 nm. Fit is to a sixth-power dependence in diameter. *Abbreviation*: NQT, normalized quantitative turbidity.

particles above 100 nm in size. This is due to the sixth-power dependence on diameter of Rayleigh scattering in visible light. A turbidimetric analytical assay was developed, normalized for lipid concentration, and termed normalized quantitative turbidity (NQT). Figure 8 shows this sixth-power dependence of NQT for NIST bead standards in the size range 50 to 300 nm. Note that there is no signal in NQT for particles below 100 nm, i.e., the bulk of the lipsome SUV dispersion is "invisible" in the NQT technique. Figure 9A and C shows dynamic light scattering data for "developmental" (pre-process optimization for key process steps) and "commercial" (9A) or "clinical" (9C) (post-process optimization for key process steps) for two different liposomal products. The observed median diameter, monitored on stability at 5°C, shows no sensitivity to the process optimization. In contrast, in Figure 9B and D, the corresponding NQT data are provided. For the first case (9B), a steady linear change in NQT is evident before process optimization. Likewise in 9D, a dramatic change during the early storage period is evident before process optimization. NQT, thus, provided a key quality-control parameter for both of these products. Products of identical formulation, but made using different processing conditions can exhibit meaningfully different size distribution on stability, revealed only by properly sensitive methods.

Intermediate Quality Attributes

A brief example is provided for a lipid intermediate. In many cases, lipids, and sometimes drug as well, are solubilized in an organic medium to make an ostensibly molecular solution, and this solution is evaporated to leave a film (for example) of the desired lipid composition. This film is then available for hydration to form liposomes. In Figure 10, two dried lipid intermediate
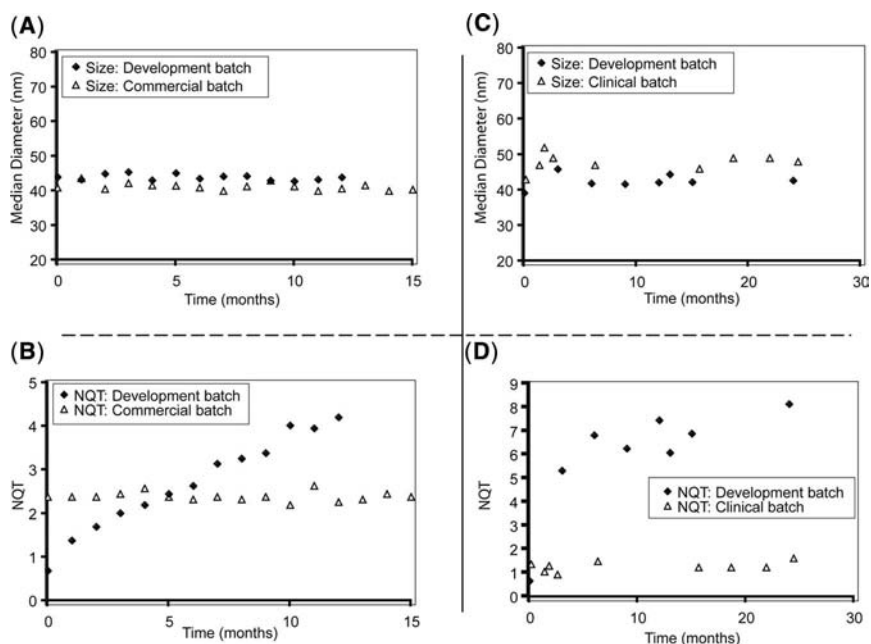
Figure 9 Results for preprocess optimization ("developmental") and postprocess optimization ("commercial" or "clinical") for median size by dynamic light scattering (**A**, **C**) and NQT (**B**, **D**) and for two different liposomal formulations (**A**, **B** and **C**, **D**). *Abbreviation*: NQT, normalized quantitative turbidity.

samples, containing in both cases 2:1:0.1 mole ratio HSPC:chol:DSPG, are examined by differential scanning calorimetry. The two materials, of identical composition, ostensibly produced from a true solution, nevertheless exhibit altered heat capacity as a function of temperature, and thus altered phase transition behavior. The two preparations had consequently altered hydration and subsequent sizing propensities.

In Vitro Stability Assessment

There are cases for liposome product quality control where, rather than a chemical or physical measurement, an analytical assay under a biological stress condition is warranted. An example is provided from a red cell–based assay developed around the liposomal amphotericin B product AmBisome (7). The assay is quite simple in principle: a titration of amphotericin B is carried out in rat blood and, after incubation at 37°C and centrifugation, potassium is measured in the incubate supernatant reflective of amphotericin B mediated potassium release from the red cell. Figure 11 illustrates this method, comparing the performance of a deoxycholate-amphotericin B suspension (the "free drug" formulation) and AmBisome. For a four-hour incubation,
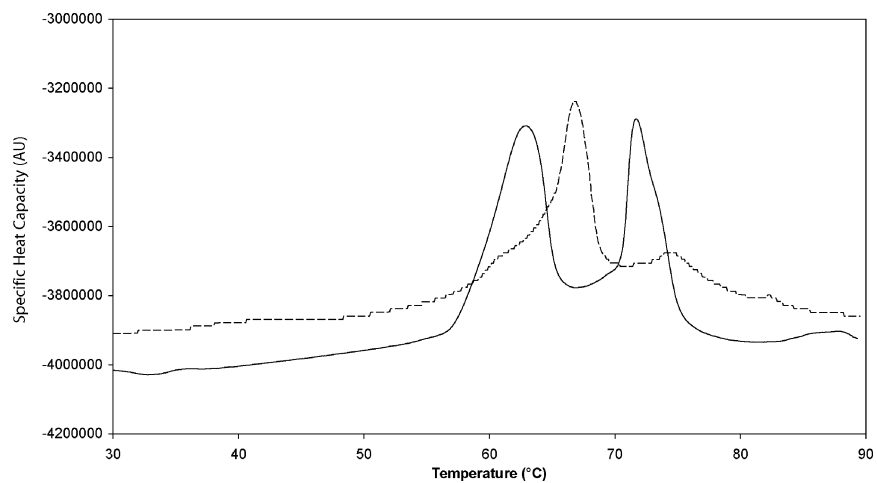
Figure 10 Differential scanning calorimetry results for two preparations of identical lipid composition.
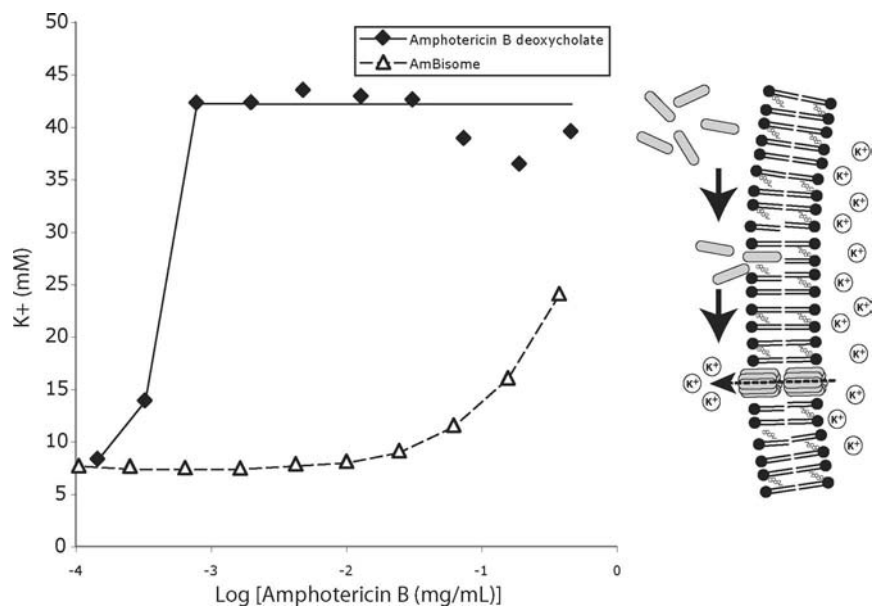
Figure 11 Titration of amphotericin B deoxycholate or AmBisome, as indicated, in washed rat blood, incubated for four hours at 37°C. *Source*: From Ref. 7.
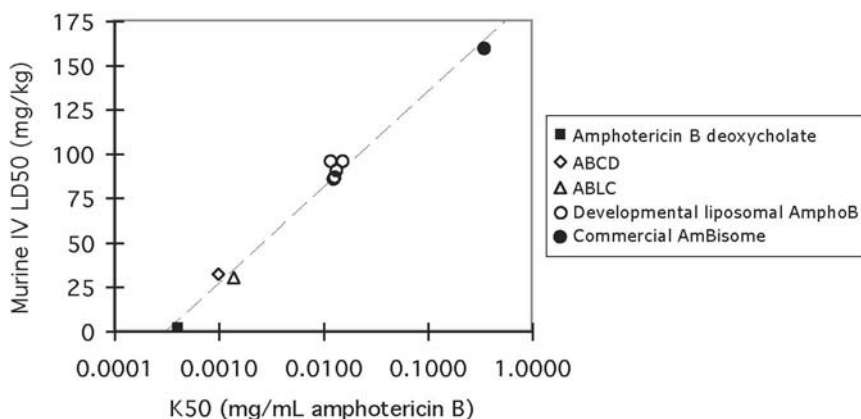
Figure 12 Plot of murine LD50 versus K50 for titrations of various samphotericin B formulations, as indicated, in washed rat blood, incubated for four hours at 37°C. The curve is a linear regression line for the data log(K50) versus LD50. *Abbreviations*: ABCD, amphotericin B colloidal dispersion; ABLC, amphotericin B lipid complex; IV, intravenous. *Source*: From Ref. 7.

a dramatic shift (~1000-fold) in concentration needed to induce potassium leakage is evident; this is a measure of how tightly held the drug is in AmBisome relative to the deoxycholate formulation. Developed into a quality control assay, the method affords a precision of ~10% RSD.

Figure 12 shows K50 data, wherein K50 is the concentration of amphotericin B needed to achieve 50% release of the total red cell potassium content. This K50 is plotted against an LD50, the murine lethal dose determined for the same preparations. Shown are results for the four available commercial preparations of amphotericin B (deoxycholate, the lipid complex, the cholesteryl sulfate colloidal dispersion, and the AmBisome liposome). Good correlation between K50 and LD50 is demonstrated. The focus here, for our purpose, is the cluster of data just below 100 mg/kg LD50 in the plot and the corresponding K50 values. These lots were made with a different process, but using an identical formulation, to AmBisome. The shift to higher toxicity is basically the result of those different processing conditions. As evidenced by the in vitro analysis, these preparations, chemically identical, exhibit a lower level of entrapment of the amphotericin B relative to the commercial process AmBisome.

CONCLUSIONS

The key to successful commercialization of liposome technology does not require magic, but it must be emphasized that choice of basic composition and liposome formation method are not sufficient. A focus on high-quality,
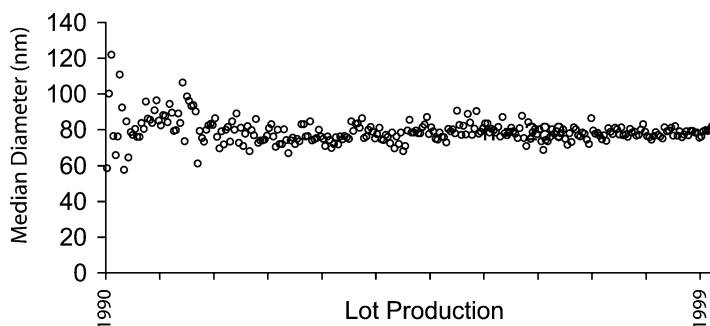
Figure 13 Median diameter by dynamic light scattering for AmBisome produced from 1990 to 1999.

well-controlled components, precision assembly, and rigorous quality testing and control is required. This requires the appropriate pharmaceutical infrastructure.

As an example, Figure 13 exhibits median particle size data over an approximately 10-year span of AmBisome production from 1990 to 1999. Over the last 180 batches in the plot, the median size variation exhibits an RSD that is within assay precision. It is an achievable reality.

ACKNOWLEDGMENTS

REFERENCES

1. Storm G, Crommelin DJA. Liposomes: quo vadis? Pharma Sci Technol Today 1998; 1:19 (and references therein).
2. Baldeschwieler JD, Schmidt PG. Liposomal drugs: from setbacks to success. Chemtech 1997; 27:34 (and references therein).
3. Fielding RM, Mukwaya G, Sandhaus RA. Clinical and preclinical studies with low-clearance liposomal amikacin (MiKasome®). In: Long Circulating Liposomes: Old Drugs, New Therapeutics. Berlin: Springer-Verlag and Landes Bioscience, 1998:213.
4. Ashvar CS, Chiang SM, Emerson DL, Hu N, Jensen GM. Liposomal benzoquinazoline thymidylate synthase inhibitor formulations. United States Patent 6,689,381 (2004).
5. Desjardins J, Emerson DL, Colagiovanni DB, Abbott E, Brown EN, Drolet DW. Pharmacokinetics, safety, and efficacy of a liposome encapsulated thymidylate

synthase inhibitor, OSI-7904L (S)-2-5-(1,2-dihydro-3-methyl-1-oxobenzofquinazolin-9-yl)methylamino-1-oxo-2-isoindolynl-glutaric acid in mice. J Pharmacol Exp Therapeut 2004; 309:894.

6. Beutel G, Glen H, Schoffsski P, et al. Phase I study of liposomal thymidylate synthase inhibitor (TSI) OSI-7904L in patients with advanced solid tumors. Proc Am Soc Clin Oncol 2003; 22:140.

7. Jensen GM, Skenes CR, Bunch TH, et al. Determination of the relative toxicity of amphotericin B formulations: a red blood cell potassium release assay. Drug Deliv 1999; 6:81.

Index

Pharmaceutical Technology

about the book . . .

Liposome Technology, Volume I: Liposome Preparation and Related Techniques, Third Edition, is a thoroughly updated and expanded new edition of a classic text in the field. Including step-by-step technical details, *Volume I* illustrates numerous methods for liposome preparation and auxiliary techniques necessary for the stabilization and characterization of liposomes. This source also offers critical discussions of the methodologies of each technology described so that readers can examine the benefits and limitations and compare it to other approaches.

Addressing major developments in the field, this title is one of three volumes of the only book that provides complete and comprehensive coverage of liposome research...showcases methods of testing stability for hydrolysis of phospholipids in liposomes...takes into account the importance of the delivery system when generating liposomes...discusses applications in gene therapy and scale-up...provides numerous examples for methods of putting liposomes into powder form...considers industrial aspects for process development and quality control...and includes chapters written by leading international experts.

about the editor . . .

GREGORY GREGORIADIS is Emeritus Professor and former Head of the Center for Drug Delivery Research (1990-2001) at The School of Pharmacy, University of London, UK. He is the founder of Lipoxen PLC, a drug delivery company based in London, of which he is also a director and the chief scientific officer. Professor Gregoriadis received his undergraduate degree in chemistry from the University of Athens, Greece and the M.Sc. and Ph.D. degrees in biochemistry from McGill University, Montreal, Quebec, Canada. He has carried out research in diverse fields and since 1970 has worked, published, and lectured extensively on the targeting of drugs and vaccines with liposomes. One of his major achievements was in 1992 with the introduction of polysialic acids as a means to improve the stability and pharmacokinetics of protein and peptide drugs. Professor Gregoriadis founded the ongoing Gordon Research Conference series *Drug Carriers in Medicine and Biology* in 1978, of which he was the first chairman, and the NATO Advanced Studies Institute (ASI) series *Targeting of Drugs* and *Vaccines* in 1981 and 1988, respectively, of which he was the director until 1999. The editor of numerous books and fifteen NATO ASI volumes on drug targeting and vaccines, Professor Gregoriadis received the Controlled Release Society Founder's Award in 1994, the A.D. Bangham FRS Life Achievement Award in 1995, fellowship status in the American Association of Pharmaceutical Scientists in 1998, and the D.Sc. award from the University of London in 2001. He is currently President of the International Liposome Society.

Printed in the United States of America

Liposome image courtesy of David McCarthy and Annie Cavanagh, The School of Pharmacy, University of London, London, U.K.

DK8821